Allen G. Shepherd, Jr.

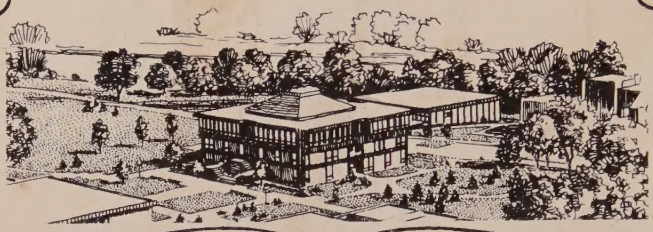

ROGER WILLIAMS COLLEGE
LIBRARY

This volume has been acquired through the generosity of

Allen G. Shepherd, Jr.

1986

RWBB ROGER WILLIAMS COLLEGE LIBRARY
TN690 .W6
Woldman, Norman Em
Physical metallurgy laboratory manual
3 1953 00036 3688

WITHDRAWN
FROM THE
ROGER WILLIAMS UNIV
LIBRARY

DATE DUE

GAYLORD PRINTED IN U.S.A

PHYSICAL METALLURGY

PHYSICAL METALLURGY

LABORATORY MANUAL

BY

NORMAN E. WOLDMAN, PH.D.

Formerly Head of the Department of Metallurgy and Chemistry, Postgraduate School, United States Naval Academy. Research Metallurgical Engineer, Westinghouse Electric and Manufacturing Company.

NEW YORK

JOHN WILEY & SONS, INC.

LONDON: CHAPMAN & HALL, LIMITED

1930

ROGER WILLIAMS COLLEGE LIBRARY

TN
690
W6

Copyright, 1930,
By NORMAN E. WOLDMAN

Printed in U. S. A.

Printing
F. H. GILSON CO.
BOSTON

Composition and Plates
TECHNICAL COMPOSITION CO.
CAMBRIDGE

Binding
STANHOPE BINDERY
BOSTON

PREFACE

This volume is the result of a purpose on the part of the author to meet a growing demand for a well illustrated laboratory manual and reference book in the metallography and heat-treatment of ferrous and non-ferrous metals and alloys. It is the outgrowth of the physical metallurgy and metallography courses given to the student officers of the Postgraduate School of the United States Naval Academy.

It is believed that this book is especially suited to those schools and colleges which are giving courses in physical metallurgy and metallography and which lack, nevertheless, adequate equipment and apparatus for the proper performance of the laboratory experiments.

The book is divided into groups of experiments according to the class of alloys to be studied, as: irons, steels, brasses, bronzes, aluminum alloys, bearing metals, and general non-ferrous alloys. These experiments are preceded by eight experiments on the study of the microscope, preparation and microscopic examination of alloy specimens, preparation of photomicrographs, cooling curves and thermal equilibrium diagram, macroscopic examination of metals and alloys, eutectic and eutectoid structures, calibration of a noble metal thermocouple, and thermal critical points in steel. In addition there are included experiments in carburizing and nitriding of steels, welding, brazing and soldering, defects and failures in metals, high-power metallography and X-ray metallography. Appendix I gives a list of etching reagents used. In Appendix II is found the theory of the Leeds & Northrup potentiometer pyrometer. Appendix III gives some properties of most of the common metals.

Each photomicrograph is discussed as completely as possible relative to history, microstructure, chemical analysis, physical properties and uses. Following each class of alloys are given the corresponding thermal equilibrium diagram and the physical property curves.

Owing to the many sources from which detailed information, photomicrographs and special alloy specimens were obtained in the preparation of this book, a complete acknowledgment is difficult. The material and photomicrographs were gradually accumulated in the development of the metallography courses given to the student officers of the Postgraduate School of the United States Naval Academy, and an accurate record was not kept of the sources. It is therefore hoped that the

author will be forgiven where proper acknowledgment is not made. Free use was made of standard books on metallurgy and metallography, and thanks are due to the authors of these. Thanks are due to Dr. V. O. Homerberg of Massachusetts Institute of Technology, Professor Van Wert of Carnegie Institute of Technology, Dr. F. F. Lucas of the Bell Telephone Laboratories, Dr. H. H. Lester of Watertown Arsenal, Dr. G. L. Clark of the University of Illinois; to The Naval Gun Factory, The Naval Experiment Station, The Bridgeport Brass Co., The American Brass Co., The Scovill Manufacturing Co., The Aluminum Company of America, The International Nickel Co., The Curtiss Aeroplane & Motor Co., The Duriron Co., The Ludlum Steel Co., The Leeds & Northrup Co., The Bausch & Lomb Co., and E. Leitz & Co.

Especial thanks are due to Mr. H. V. Tydings, laboratorian, for his aid in the preparation of many of these photomicrographs.

To Dr. William Campbell of Columbia University I wish to express my appreciation and gratitude for the knowledge and training he has given to me through his lectures and through personal contact.

Note: The second volume entitled "Theoretical Physical Metallurgy" to be used as a classroom text in conjunction with this laboratory manual, will be published shortly. This second volume will consider the theoretical aspects of physical metallurgy and will deal strongly with the development and interpretation of the thermal equilibrium diagrams.

CONTENTS

		PAGES
Introduction.	The Structure of Metals and Alloys	1–2
EXPERIMENT		
1.	The Microscope	3–13
2.	Preparation and Microscopic Examination of Alloy Specimens	14–18
3.	Preparation of Photomicrographs	19–22
4.	Cooling Curves and Thermal Equilibrium Diagram for a Series of Binary Alloys	23–28
5.	Macroscopic Examination of Metals and Alloys	29–47
6.	Eutectic and Eutectoid Structures	48–52
7.	Calibration of a Noble Metal Thermocouple	53–56
8.	Thermal Critical Points in Steel	57–63
9.	Pure Iron, Wrought Iron and Steel	64–74
10.	Cast Iron	75–80
11.	Heat-Treated Steels	81–95
12.	Alloy Steels	96–105
13.	Case-Hardening — Carburizing and Nitriding	106–117
14.	Brasses: Copper-Zinc Alloys, Effect of Composition	118–125
15.	Brasses: Effect of Mechanical Working and Heat-Treatment	126–130
16.	Alloy Brasses	131–134
17.	Bronzes: Copper-Tin Alloys, Effect of Composition	135–142
18.	Bronzes: Effect of Heat-Treatment	143–145
19.	Alloy Bronzes	146–151
20.	Aluminum and Its Alloys	152–160
21.	Effect of Heat-Treating Duralumin	161–166
22.	Bearing Metals	167–172
23.	General Non-Ferrous Alloys	173–177
24.	Welding, Brazing and Soldering	178–183
25.	Defects and Failures in Metals	184–195
26.	High-Power Metallography	196–212
27.	X-ray Metallography	213–236
APPENDIX		
I.	Etching Reagents	237–238
II.	Theory of the Potentiometer	239–245
III.	Some Properties of the Common Metals	246

PHYSICAL METALLURGY

INTRODUCTION

THE STRUCTURE OF METALS AND ALLOYS

Metallography deals with the constitution and structure of metals and alloys and their relations to the physical, mechanical and chemical properties.

Alloys may contain as structural elements or constituents: (1) pure metals; (2) solid solutions of one metal in another, or of a compound in a metal; (3) intermetallic compounds or compounds of a metal and a non-metal; (4) eutectics or eutectoids of pure metals, solid solutions or compounds. These different constituents have definite properties associated with them.

In general, the pure metals range from the very soft to hard and brittle ones; the compounds have generally high melting points, and are hard and brittle; solid solutions are usually strong, hard and tough; eutectics and eutectoids have high strength and toughness but have comparatively low melting points. All of the above constituents may be present in the various alloys, either singly or together.

A solid solution is defined as a chemically and physically homogeneous mixture of which the composition, within certain definite limits, can undergo continuous variation. It consists of a single phase which contains two or more kinds of atoms but retains the space lattice arrangement of the solvent. Solid solutions are the materials in which softness, ductility and low tensile strength have been modified by alloying to give harder and stronger materials.

A chemical compound is the union of two or more metals or non-metals with each other in certain, definite, simple proportions to form new bodies, which have properties distinct from those of either of the component metals.

The " eutectic " is the alloy with lowest melting point that solidifies sharply as a mechanical mixture at constant temperature. It is the alloy of maximum fusibility. The " eutectoid " is the alloy with the lowest transformation point in the solid. Both the eutectic and eutectoid consist of a mechanical mixture of two or more phases.

The structure of alloys* varies with chemical constitution and physical treatment. Alloys may be considered (1) as cast; (2) after heat-treatment; (3) after mechanical working; (4) after both mechanical working and heat-treatment. The cast condition of the alloy will depend upon whether the alloy is cast with rapid cooling as in metal molds or with slow cooling as in sand molds. In a number of cases the structure after heat-treatment will depend upon temperature of heat-treatment, duration of time during which the alloy is held at that temperature and especially on rate of cooling to room temperature. The structure after mechanical working will depend upon whether it has been cold-worked or hot-worked.

Annealed and heat-treated alloys show equiaxed, uniform, homogeneous grains. Cold-worked or cast metals and alloys show an inhomogeneous and non-uniform structure. Dendrites and cored structures are characteristic of castings. A dendrite (branching figure) is a crystal or grain that has grown most rapidly from a nucleus along some line which bears a simple relation to the symmetry of the crystal. A cored crystal or grain is a non-homogeneous solid solution in which the concentrations of the component elements vary from the center to the outer portions of the grains.

* Dr. William Campbell, Columbia University.

EXPERIMENT I

STUDY OF THE MICROSCOPE

References: Sauveur: Heat Treatment and Metallography of Iron and Steel, Appendix II.
Greaves and Wrighton: Practical Microscopical Metallography, Chapter III.
E. Leitz & Co., Catalogs.
Bausch & Lomb Optical Co., Catalogs.

Theory: The microscope is the instrument used in the study of the characteristic details of the microstructure of metals and their alloys, and in the correlation of their microstructure with their physical and mechanical properties. Chemical analysis gives information as to the composition of metallic substances, but indicates very little relative to the manner in which the various elements and phases are related to each other in a metallic aggregate. The microscope reveals the constituents, their size, shape, distribution, etc. By microscopic analysis one can follow the most systematic investigation of the physical properties of metals and their alloys, and the characteristic changes under thermal and mechanical treatment. Furthermore, the microscope points the way towards improving the structural details of metals and the control of their proper thermal and mechanical treatment. This is due to the fact that there is in general a definite relation between the microstructure and the physical and mechanical properties. Therefore by a careful microscopic examination it is possible to determine with an almost unbelievable degree of accuracy the chemical composition, the physical and mechanical properties, and the mechanical and heat treatment which the specimen has received.

The metallurgical microscope or micrometallograph is of the reflecting type in which the illumination is communicated to the specimen through the objective lens by means of a vertical or oblique illuminator and the illuminated image of the specimen is reflected back through the objective lens to the ocular and the eye of the camera. (Fig. 1.)

A microscope is made up of the stand, the stage, the observation tube, the illuminating apparatus, and the optical components which are the image-forming system of the microscope. The optical system consists of two compound lenses, one near the object (known as the ob-

jective) and the other (the eyepiece or ocular) at a distance of from 6 to 10 inches from the objective. The objective produces an enlarged real image of a portion of the object under examination. For visual examination, the ocular is arranged to give a further enlarged virtual image of that produced by the objective; for photomicrography the ocular is arranged to project a further enlarged real image onto the screen or photographic plate.

The objective may be achromatic (partially color-corrected) or apochromatic (fully color-corrected). Apochromatic objectives, though giving the more perfect resolution and definition in the center of the field,

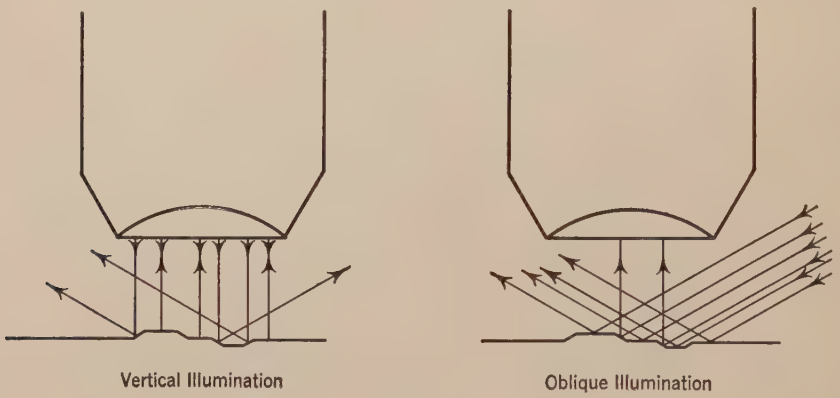

FIG. 1

generally suffer to a greater extent than the achromatic objectives from curvature of field, and from flare set up in them. An objective should be corrected for spherical and chromatic aberration. In spherical aberration, the rays passing through the outer edge of the lens and those coming through the center do not come to a focus at the same point along the optical axis. The outer edge of the image appears blurred and colored while the central part may be in sharp focus. Chromatic aberration is due to the dispersion of light in passing through the lens, with the result that light of different wavelengths comes to a focus at different points along the optical axis so that the images are not coincident. Also color fringes are often obtained due to inequality in the size of the images. The fluorite apochromatic objective offers a high efficiency and correction in regard to color and resolving power due to the fluorite in its construction. Fluorite is characteristic through: high degree of transparency, low refractive index, and most favorable conditions in its dispersion properties. Apochromatic objectives are so constructed as to bring the colors in focus at the same plane.

Fig. 2 is a detail drawing of a Leitz apochromatic 1.32 short mounted objective and an achromatic 14 mm. objective. One-half of the housing is cut away to show the lens construction. Fig. 3 is a photographic view of the Bausch & Lomb 16 mm., 4 mm., and 1.9 mm. objectives.

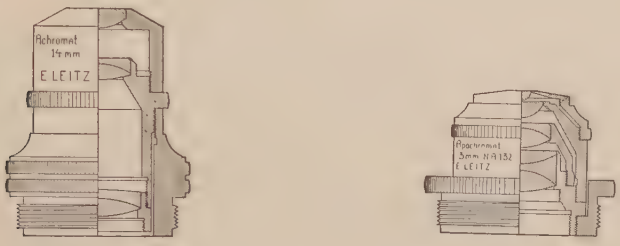

Fig. 2. Leitz Objectives

The eyepieces generally are of the Huygenian and of the compensating types. The Huygenian eyepiece will produce color fringes at the outer edges if used with an apochromatic objective. A compensating eyepiece, which will correct this defect, should be used with the

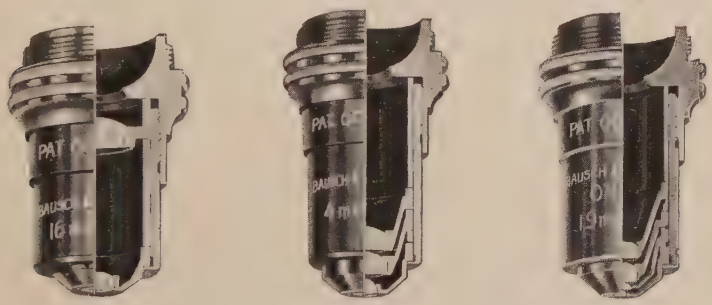

Fig. 3. Bausch and Lomb Objectives

apochromatic objective. The usual Huygenian eyepiece consists of the two achromatic plano-convex lenses with a diaphragm for limiting the field between them.

Fig. 4 shows a detailed drawing of the Huygenian form of eyepiece or ocular. Fig. 5 is a sketch of the positive compensating type of eyepiece. Fig. 6 is a detailed drawing of the 5-diameter and the 10-diameter Huygenian eyepiece.

For the study of structure, a surface of the metal specimen is ground down flat, then highly polished, and finally chemically etched. It is then examined by reflected light. For low-power work a ray of light

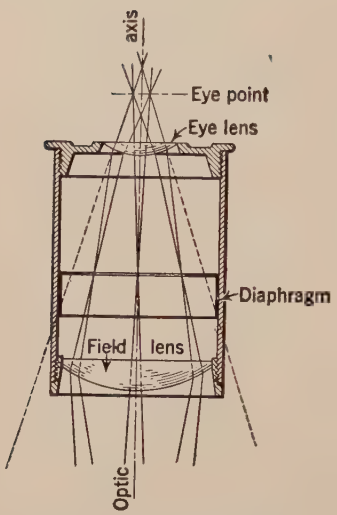

FIG. 4. Huygens Eyepiece

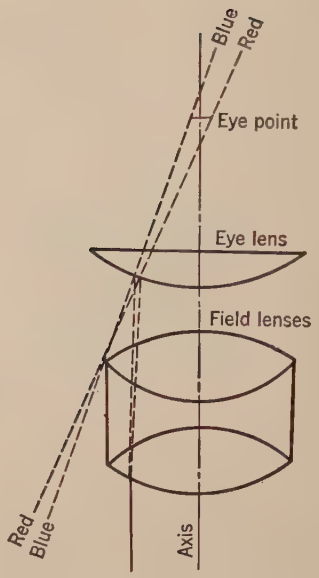

FIG. 5. Compensating Eyepiece

Huygens Eyepiece, 5×

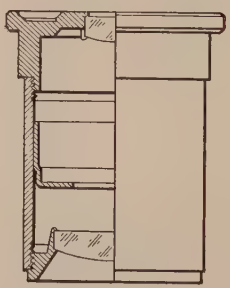

Huygens Eyepiece, 10×

FIG. 6

is directed obliquely upon the metallic surface by means of a condenser. The brighter parts of the surface which have been attacked very little, or not at all, by the etching reagent, reflect the light away from the tube and so appear dark to the observer. The parts which are corroded on account of their rough surface, cause scattering of the light to take place, with the result that some of the scattered rays pass up the microscope tube, and these parts of the specimen appear relatively bright.

For high-power work the distance between the objective and the specimen becomes too small to allow for oblique illumination, and an appliance is used which will direct the light vertically upon the face of the metal, the light being reflected again vertically from the polished surface up the microscope tube. This attachment, called a vertical illuminator, is made in several forms and consists essentially of a small cell which contains either a right-angled glass prism or a thin circular cover glass. The objective is screwed into the lower end of the vertical illuminator. A beam of light from a condenser is directed to the side aperture, and by turning the prism or the plate about its axis, which is at right angles to both the axis of the aperture and the optic axis of the microscope, the illuminating ray may be reflected down upon the face of the specimen; the light is again reflected from the specimen up the microscope tube to the eyepiece. With this method of illumination the unattacked parts of the specimen appear bright, since they reflect almost the whole of the incident light, whereas the etched parts appear relatively dark, on account of the scattering due to the roughened surface; thus the appearance of the metal under oblique illumination is often reversed with vertical illumination (Fig. 1).

For very high magnifications of 1000 diameters or over an oil-immersed objective is used, a thin film of cedar-wood oil being introduced between the specimen and the objective. This increases the resolving power, or the ability of a lens to make visible the fine details of a structure, by permitting a wider angle of rays to be collected and brought to a focus.

A vertical illuminator is shown in Fig. 7. It is provided with a society thread by which it attaches to the tube of all standard microscopes. The illuminator itself is equipped with a simplified objective-clutch by means of which the objectives, provided with adapter collars, are held in place and can be easily interchanged. A total reflecting prism and a reflecting glass plate are simultaneously mounted to a bar. The bar, fully inserted into the illuminator housing, places the total reflecting prism within the optical rays and when the bar is withdrawn to its extreme stop, the reflecting glass plate is within the optical rays. The use of either depends upon the nature of the specimen and the objective

employed. This vertical illuminator is also equipped with a condensing lens and iris diaphragm, by means of which the light rays can be stimulated for proper contrast.

The Leitz Workshop Microscope "Model — MS," shown in Fig. 8, consists of the upper portion of a compound microscope, mounted to a vertical column and the latter supported by a horse-shoe foot of large

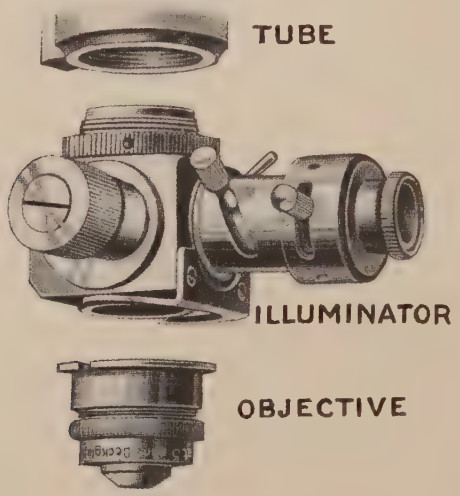

Fig. 7. Vertical Illuminator

dimensions, providing ample space for movement of the tube or specimen, respectively. The microscope tube is clamped to the vertical upright rod and consequently allows for an adjustment in height. As the illustration shows, the horse-shoe foot rests on three sharp points, two of which are provided with leveling screws. It is provided with rack and pinion for coarse focus and ball micrometer-screw for fine adjustment. The vertical illuminator is of the type shown in Fig. 7.

The Bausch & Lomb Metallurgical Microscope is shown in Fig. 9. The body of the microscope is of fixed optical length and takes standard size eyepieces and objectives. The body tube is adjustable for focusing both for coarse and fine adjustment movements. The stage is adjustable vertically by means of a rack and pinion, so that the specimen may be brought into focus without moving the position of the body tube. For illumination the body tube is provided with a vertical illuminator which serves to direct a horizontal beam of light down through the objective and onto that portion of the specimen under observation. The side tube on the vertical illuminator is provided with condensing lens,

filter and iris diaphragm for controlling the incident beam. The lamp of special design is mounted on the body tube in alignment with the side tube of the vertical illuminator.

For low powers the binocular microscope for sterioscopic observation is used. It consists of two adjacent microscopes whose axes are some-

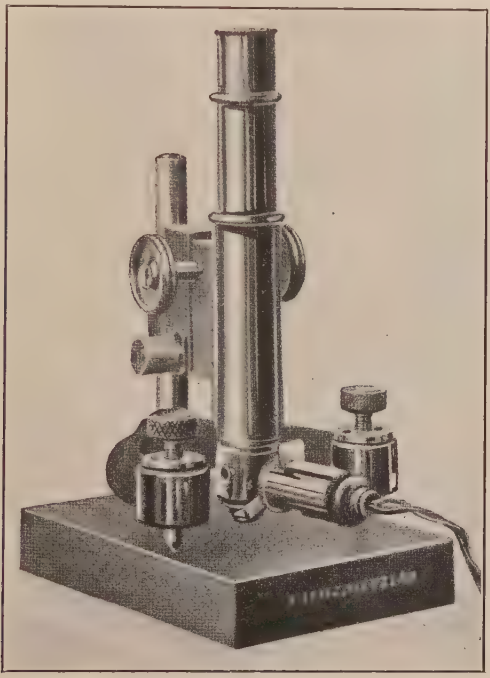

Fig. 8. Leitz Microscope, "Model MS"

what inclined to the vertical, the distance between them diminishing toward the objective. The distance between the two eyepieces is adjusted to fit the eyes of the observer by turning the cylinders in which the eyepieces are eccentric. The two microscopes are so arranged that the image is not reversed. The great advantage of the instrument is that the image appears in relief, as in a stereoscope. Fig. 10 is a photograph of the Bausch & Lomb Binocular Microscope.

The Micrometallograph is used for photographing the microstructure of the various materials for permanent record. The essential parts of a photomicrographic outfit consists of a microscope, the vertical illuminator, the illuminating system, the camera, the optical bench and the optical equipment. In this unit the ocular of the microscope is made to serve as the lens of an ordinary bellows-pattern camera.

The microscope is generally of the inverted type. The camera is attached to the microscope by means of a light-tight connection. The image of the specimen is focused onto a ground-glass plate, final focusing being done with the light filter in position and with the aid of a focusing glass. The illuminant is generally an arc light, in which the carbons are fed automatically or by hand. It is necessary to use a

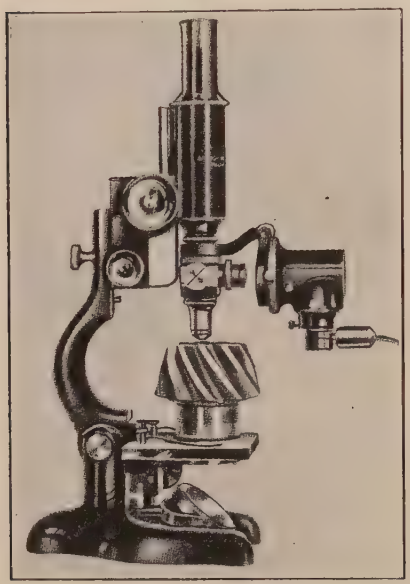

Fig. 9. Bausch & Lomb Microscope

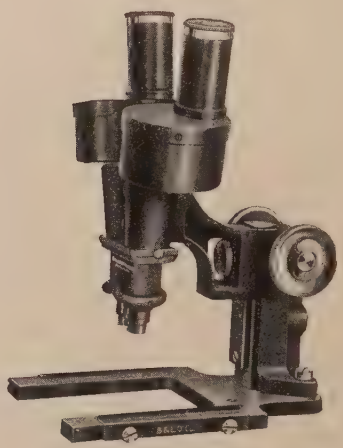

Fig. 10. Bausch & Lomb Binocular Microscope

most intense source of light in conjunction with a system of condensing lenses to collect the rays of as wide a pencil of light as possible and concentrate them into the microscope.

Monochromatic light should be used in photomicrography, since the correction for chromatic aberration is never perfect even with apochromatic objectives. Such light is obtained by using variously colored glass filters thereby preventing the passage of undesirable rays.

The Leitz Micro-Metallograph (Fig. 11 and Fig. 12) consists of the inverted microscope with vertical illuminator and mechanical stage, the illuminating system (arc) with collimator lens unit, the camera, the vibration (shock) absorber and the supporting table. The microscope embodies the general principles of the Le Chatelier microscope, whereby the microscope stage, being provided with two mechanical motions at right angles to each other, supports the metal specimen with its polished surface downward. Coarse adjustment is made by means of a rack and

pinion, thereby moving the stage and specimen toward the objective. Fine adjustment is made by a micrometer-screw which acts directly upon the objective and thereby functions entirely independent of the specimen support or coarse focusing device, respectively. The object stage is cast with the vertical column support in one solid heavy piece to which the rack and pinion movement is attached. And since the stage with specimen focuses toward the objective, it follows that the vertical illuminator with objective remains stationary, whereby a permanent adjustment of the illuminating rays to the optical center of the

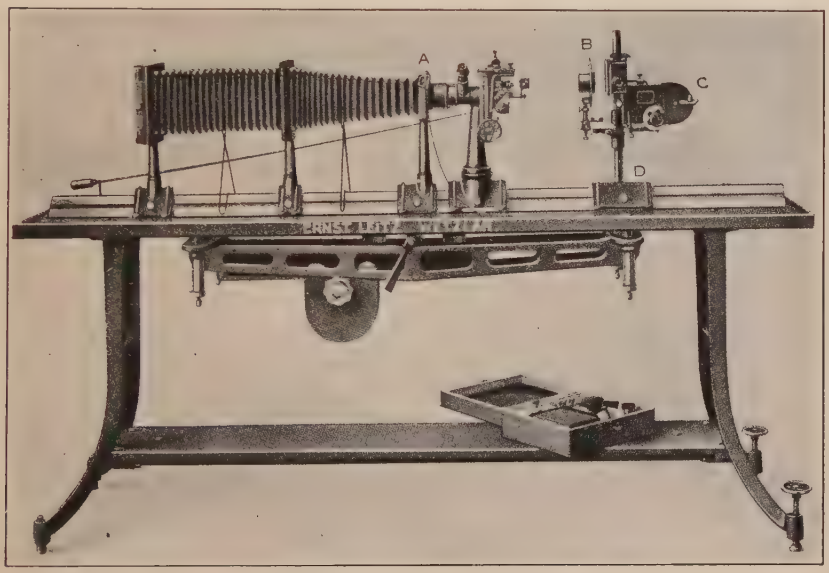

FIG. 11. Leitz "Micro-Metallograph"

Complete with Microscope, Camera, Illuminant, Table Support and Vibration Absorber

A — Indirect Observation Window
B — Collimator Lens System
C — Automatic Arclamp
D — Illuminator Support

microscope is always maintained. The object is placed upon the glass diaphragm of the stage and, therefore, automatically becomes oriented in a plano-parallel position to the objective.

Microscope tubes are both mounted to a central tube, attached to the vertical column support. The horizontal tube serves for photomicrography, whereas the tube mounted at right angles to the vertical column support is utilized for visual observation. In pulling out this tube, the prism clears the horizontal tube for the rays to pass centrally

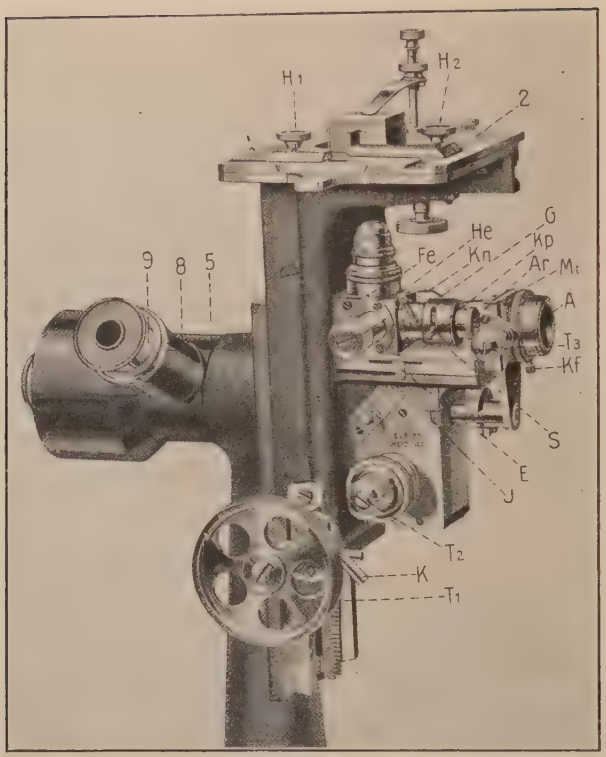

FIG. 12

Designation of Numbered Parts

2 — Object stage;
5 — Microscope tube cast in one piece with supporting stand;
8 — Adjustable microscope tube for visual observation;
9 — Draw tube controlling the position of prism "R";
A — Iris-diaphragm mounted to rack and pinion carrier;
Ar — Sliding adapter with protecting glass plate, preventing entrance of dust;
E — Lever to clamp vertical illuminator in place;
Fe — Clamping flange to hold objective in place;
G — Objective adapter handle;
H_1 and H_2 — Adjustable arms to orient specimen;
He — Handle for focusing condensing lens;
J — Indication lines for position of fine adjustment;
K — Lever for clamping coarse focusing device;
Kf — Handle for iris-diaphragm with eccentric movement;
Kn — Handle for the manipulation of total reflecting prism and reflecting plate of vertical illuminator;
Kp — Handle for operating iris-diaphragm of vertical illuminator;
Mt — Graduation at iris-diaphragm to gauge opening of same;
S — Dove-tailed slider for vertical illuminator;
T_1 — Rack and pinion wheel for coarse focus;
T_2 — Knob for micrometer screw;
T_3 — Pinion acting upon rack for displacing iris-diaphragm obliquely.

towards the focusing screen or plate, respectively, projecting the image for photomicrography.

The vertical illuminator is provided with two tubes, one sliding into the other. The one tube carries an iris diaphragm whereby the illuminating rays can be suitably stimulated and adjusted in their aperture to meet the conditions of objectives and specimen. The other tube is equipped with a focusable illuminating lens to concentrate the pencil of rays to suit the requirements of the different objectives employed. The illuminator carries a sliding rod, to which are mounted a total reflecting prism and a reflecting glass plate. This rod, fully inserted, places the total reflecting prism within the optical rays and, if withdrawn to its extreme stop, the reflecting glass plate. A metal mirror reflects the rays, received from the specimen, through the objective to the tubes for either visual observation or photomicrography.

The automatic arc lamp is designed so that the carbons are fed by means of a clock-work mechanism. The carbons are moved in exact accordance to their consumption and, therefore, a central crater is permanently maintained.

EXPERIMENT II

PREPARATION AND MICROSCOPIC EXAMINATION OF ALLOY SPECIMENS

Purpose: To become familiar with methods of preparing metal specimens for microscopic examination.

References: (*a*) Sauveur: Metallography and Heat Treatment of Iron and Steel, pp. 456–474.

(*b*) Gulliver: Metallic Alloys, pp. 2–9.

(*c*) Williams and Homerberg: Principles of Metallography, pp. 22–56.

(*d*) E. Leitz & Co., Catalog 1092.

Materials: 0.15% Carbon Steel; Wrought Iron; Muntz Metal Brass.

Theory: The three important operations (*d*) in the preparation of metal specimens for microscopic study of their internal structure are grinding, polishing and etching. Grinding is the removal of surface metal by the cutting action of the abrasive particles in order to make the surface as optically flat as possible. Polishing is the slight cutting and wiping of this finely abrased surface, resulting in very little metal being removed, but merely causing the solid to flow as a result of the polishing action. This produces a superficial glazed surface, necessary for obtaining a uniform etching action. Etching is the corrosion, erosion, or both, of parts of the polished surface, causing the constituents to appear in relief under light, due to differences in chemical and physical conditions of these constituents.

Procedure: The specimens are first ground down to a rather flat surface either by files of suitable fineness or by emery or hard silicon carbide wheels. If a file is used the specimen is rubbed on the file, which is held between the jaws of a vise. The coarse file marks or emery wheel marks are next removed by rubbing the specimens on different grades of progressively finer emery paper. The specimens should be so held that the new emery markings would be at right angles to the former. With mechanical polishing this can be done on finer grades of emery wheels, or disks covered with strong, fine canvas and armed with emery powders of progressively finer grades.

A metal disk covered with fine canvas cloth rotating on a vertical

disk at from 750 to 1000 r.p.m. is moistened from a wash-bottle with distilled water carrying levigated emery. Considerable pressure may be at first applied to the sample on the wheel in order that the polishing film penetrates the troughs of the deepest abrasions. It is best to rotate the specimen 90 degrees at intervals during the polishing in order to make it easy for the operator to discern when all of the previous abrasions have been removed. This is then followed by polishing with levigated tripoli on a broadcloth polishing disk. The specimen is rotated 90 degrees frequently and the pressure gradually diminished until the surface takes on a polished appearance. Following this the specimen is given its final polish with levigated alumina. The specimen is then washed well under the tap, and dried with alcohol and a warm-air blast. This must be done immediately or the polished surface will oxidize.

The specimens are now examined with the naked eye and with the microscope for inclusions, such as graphite particles, slag, oxides, sulfides, silicates, blowholes, scratches, cavities, flaws and cracks.

In the preparation of specimens the object is to learn the true structure of the material. In many cases this varies with the location of the specimen. In cast material, sections should be cut perpendicular to the cooling surface, from the outside to the center of the ingot or casting. In rolled or forged material the sections should be parallel to the direction of rolling or forging, because a cross-section alone is often misleading.

To develop the structure the usual method is by etching. Care must be taken to avoid overetching or the specimen must be repolished and re-etched. Wrought iron is usually etched by immersing the polished surface in a 5% picric acid-alcohol solution for a couple of minutes, and then washing in tap water and drying with alcohol and the hot-air blast. To develop the grain boundaries, a three-second immersion in a 5% nitric acid-alcohol solution is recommended. Steel is etched in the same manner as wrought iron. However, to differentiate between cementite and ferrite in steel (both constituents are not colored by picric acid and appear white under the microscope), boiling sodium picrate which darkens the cementite and not the ferrite, must be used. Brass is etched with ferric chloride solution or with ammonium hydroxide plus hydrogen peroxide. The latter solution is applied to the polished surface by rubbing gently with a small wad of absorbent cotton until the structure appears. (See Appendix I.)

PHOTOMICROGRAPHS

The various stages in polishing and etching the 0.15% carbon steel sample are shown in the photomicrographs on Plate I, Figs. 1 through 5. All photomicrographs are shown at 100 magnifications. Fig. 1 shows the surface structure after the first stage in polishing with emery cloth. Fig. 2 shows the surface structure after the second stage in polishing with levigated emery powder. Fig. 3 shows the surface structure after the third stage in polishing with levigated tripoli. Fig. 4 shows the surface structure after the fourth and final stage in polishing with levigated alumina. Here it is observed that the scratches have been eliminated and that the surface is covered with a thin layer of very finely divided (amorphous) metal. In Fig. 5 is shown the surface crystalline structure after etching with picric acid solution. The structure shows equi-axed, polyhedral grains of ferrite (white) and angular grains of pearlite (black).

In Plate II are shown photomicrographs of the polished and etched surfaces of the wrought iron and brass specimens. In Fig. 6 are seen the black non-metallic inclusions and gray slag particles in the white structureless ferrite matrix of the wrought iron. Fig. 7 is similar to Fig. 6, except that the etching has brought out the grain structure of the white ferrite matrix. Figs. 8 and 9 show respectively the polished (unetched) and etched surfaces of the brass specimen. In Fig. 8 small black specks of the non-metallic impurities are seen in the structureless brass matrix; while in Fig. 9 is seen the true structure of the brass, namely, the brown buff alpha solid solution in the lighter golden yellow beta solid solution matrix.

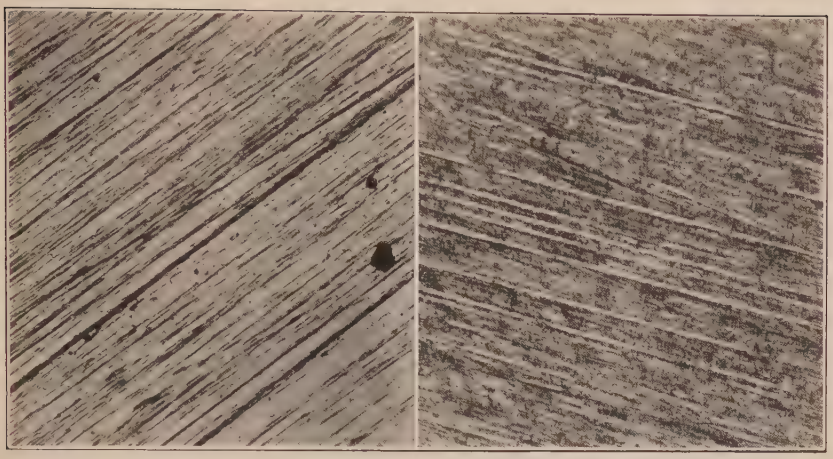

FIG. 1

FIG. 2

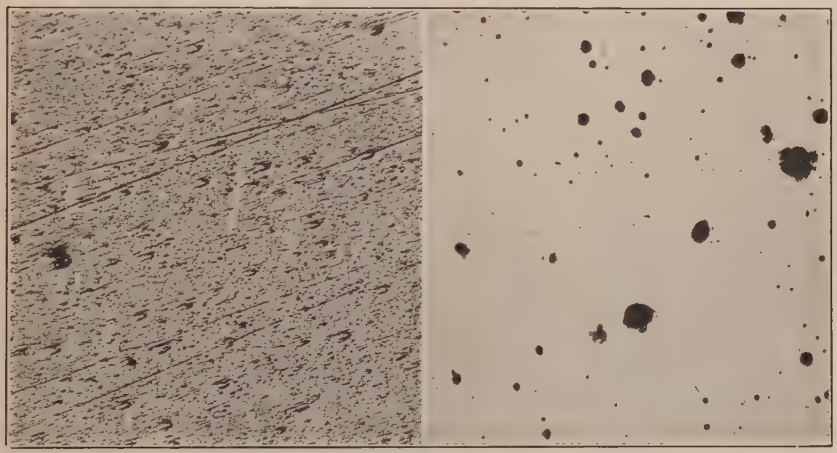

FIG. 3

FIG. 4

FIG. 5

FIG. 6 FIG. 7

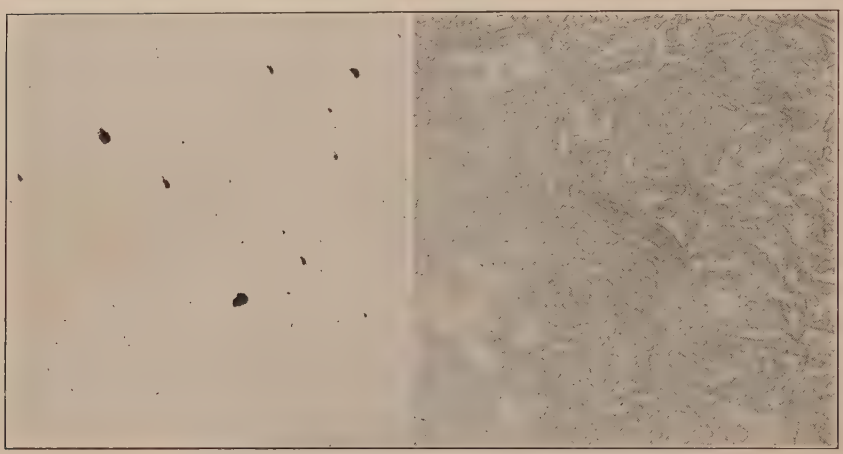

FIG. 8 FIG. 9

EXPERIMENT III

PREPARATION OF PHOTOMICROGRAPHS

Purpose: To learn how to make photomicrographs of metals and alloys and to become acquainted with the metallographic equipment.

References: (*a*) Sauveur: Metallography and Heat Treatment of Iron and Steel, pp. 518–524.

(*b*) Williams and Homerberg: Principles of Metallography, Chapter II.

Materials: Metal specimens as supplied, dry plates, photographic paper, developer for plates, developer for paper, hypo fixing solution.

Apparatus: Micrometallograph with accessories including objectives, eyepieces, ground glass, focusing glass, plate holders, Wratten filters, clock, photographic dark room equipment, polishing and etching equipment, etc.

Procedure: (1) *Preparation of Specimens.* Prepare all specimens to be photographed by the methods indicated in Experiment II.

(2) *Preparation of Developing and Fixing Solutions.*

(*a*) Contrast developer for plate negatives

Eastman Kodak Formula D-11 (Stock solution)

Hot water (125° F.)	200 cc.
Elon	4 grams
Sodium sulfite	300 grams
Hydrochinon	37.5 grams
Potassium carbonate	97.5 grams
Potassium bromide	22 grams
Water to make one gallon	about 4000 grams

(*b*) Print developer for Velox, Azo, Bromide paper and lantern slides

Eastman Kodak Formula D-67 (Stock solution)

Hot water (about 125° F.)	500 cc.
Elon	3 grams
Sodium sulfite	45 grams
Hydrochinon	9 grams
Sodium carbonate	75 grams
Potassium bromide	1 gram

Cold water to make a liter of solution.

For Velox paper dilute 1 to 1
For Azo and lantern slides dilute 1 to 2
For Bromide paper and softer results on lantern slides dilute 1 to 4.

(c) Fixing bath

Hypo solution (sodium thiosulfate) of specific gravity 1.1. To this solution add liquid hardener (potassium chrome alum) in proportion of one part liquid hardener to eight parts hypo solution. Liquid hardener stock solution consists of 32 parts H_2O, two parts potassium chrome alum, $\frac{1}{4}$ part conc. H_2SO_4.

(3) *Making Negatives.* Before opening the box of photographic plates in the dark room, see that Wratten Safe Light No. 2 is available for use. See also that you have the plate holders nearby and a camel's hair brush. Then turn out all lights except the safe light. Open the box of plates, remove a plate and dust it on both sides with the camel's hair brush. Then place it on the plate holder with the *shiny side next the back,* and close the holder. In the same manner load all the plate holders available.

Place the specimen on the stage of the metallograph and select, by viewing through the side observation tube, the most suitable spot to photograph. Secure the specimen by means of the spring clip. For this visual examination No. 3 objective and No. 4 eyepiece should be used (if Leitz Metallograph is used).

Next see that No. 2 eyepiece is in the observation tube next the camera. Then draw up camera close to observation tube. Set rear of camera at 36 to 38 cm. on the optical bench. This combination of objective, eyepiece and bellows extension gives a magnification on the ground glass of approximately 100×. Place a Wratten filter (B) in holder between source of light and condenser. Insert ground glass in back of camera. Drawn out side observation tube. Turn on light, so adjusting that the light from the crater in the horizontal carbon is not obstructed by the vertical carbon. It is desirable to use the automatic clock-work feed for this work. The image of the specimen should now be seen on the ground glass. If not clear, adjust the focus until it is perfectly clear when viewed through the focusing glass.

Next close the shutter, remove the ground glass and insert loaded plate holder. Draw slide in plate holder and, by means of shutter, expose plate for about 60 to 90 seconds depending upon character of the surface to be photographed and the kind of plates being used (see references).

After making exposures, take loaded plate holders to dark room to develop plates.

With lights as described above, remove plates and, after marking

on lower edge of sensitized side in pencil the *specimen number, the time of exposure,* and *magnification,* immerse in developer with sensitized side up for about $1\frac{1}{2}$ to 2 minutes, that is, until the white side begins to darken. Next rinse in water and then place in the hypo and leave there for about 15 minutes or until white no longer shows on the unsensitized side. Then wash in water for about one hour and dry.

(4) *Making Positives.* When negatives are thoroughly dry, place in printing frame and, when all lights in dark room are out except the Safe light with Wratten filter Series O inserted, place either Azo, Velox or Cyko printing paper as supplied, in frame with sensitized side next negative. Clamp on back and place over printing light. Turn on printing light and print for from 5 to 20 seconds. (This will vary with the density of the negative.) Remove paper from printing frame and put between black paper sheets and in a drawer while other prints are being made. Make three prints from each negative, varying the time, and mark the time on each print.

Place paper sensitized side down in developer and when completely wet, turn sensitized side up. Keep in developer for from about 40 seconds to $1\frac{1}{2}$ minutes or until fully developed. Rinse in water and then allow to fix in the hypo for about 15 minutes. Wash in clear water for about 30 minutes and dry.

Make at least two prints of each negative.

Report: The report will consist of the submission of the photomicrographs mounted on the form supplied, together with a record of all the information called for on that form insofar as it is available. Under remarks should be recorded any noteworthy observations with reference to the method of making the photomicrograph or with reference to the structure itself.

REPORT OF METALLOGRAPHIC TESTS

Manufacturer.....

Kind of Material.....

Use — Object.....

CHEMICAL ANALYSIS

PHYSICAL TESTS

Tensile Strength	Yield Point	Elongation Per cent in 2 in.	Per cent Reduction	Hardness

Card No. ...Diameters.... Etched in.....

Heat-Treatment:.....

.....

Structure:.....

.....

Remarks:.....

.....

EXPERIMENT IV

COOLING CURVES AND THERMAL EQUILIBRIUM DIAGRAM FOR A SERIES OF BINARY ALLOYS

Purpose: To prepare a series of binary alloys; to get their cooling curves and to plot the equilibrium diagram for the series.

References: (*a*) Gulliver: Metallic Alloys, pp. 12, 13, 23, 24, 36–48.
(*b*) Williams and Homerberg: Principles of Metallography, pp. 1–21.
(*c*) Appendix II.

Apparatus: Electric furnace, thermocouple-potentiometer, graphite crucibles, balance and weights, casting molds, graphite flakes, lead and antimony.

Theory: The binary alloys of lead and antimony represent a series of alloys soluble in each other in the liquid state and insoluble in each other in the solid state. Pure lead freezes at 327° C. and pure antimony freezes at 631° C. However, the addition of antimony to lead or the addition of lead to antimony lowers the freezing point progressively. In the series there is an alloy of a definite composition with the lowest freezing point. This alloy, called the "eutectic" alloy, consists of $87\frac{1}{2}\%$ lead and $12\frac{1}{2}\%$ antimony, and freezes at 247° C.

Those alloys of lead and antimony containing less than $12\frac{1}{2}\%$ of antimony will consist of primary grains of lead surrounded by secondary crystals of the eutectic, namely, a mechanical mixture of fine crystals of lead and antimony; and those alloys containing more than $12\frac{1}{2}\%$ antimony will consist of primary grains of antimony surrounded by the fine lead-antimony eutectic.

When a pure metal solidifies the temperature of the metal remains fairly constant until the whole metal has become solid due to the evolution of the latent heat of solidification; and vice versa, when a pure metal melts the temperature again remains fairly constant, until the whole metal has liquified due to the absorption of the latent heat of fusion. However, when an alloy of two metals freezes, it does so, not at a constant temperature, but through a temperature range. There is only one exception, namely, the eutectic, which also freezes at a constant temperature. Therefore, the cooling curves (temperature-time curves) of such a series of binary alloys, (pure metals and eutectic

alloy excepted) will show two breaks; first, at the temperature where solidification (freezing) begins, and second, at the temperature where solidification is complete. The pure metals and the eutectic will each freeze at a constant temperature. (Chemical compounds also freeze at a constant temperature.)

Procedure: Weigh out the lead and antimony to make 100 grams of each of the following eight alloys: (1) 100% lead, (2) 92% lead plus 8% antimony, (3) 87.5% lead plus 12.5% antimony, (4) 75% lead plus 25% antimony, (5) 50% lead plus 50% antimony, (6) 25% lead plus 75% antimony, (7) 10% lead plus 90% antimony, (8) 100% antimony.

To prepare the alloys used in this exercise, it will be sufficient to mix the two metals and melt them together. Consult reference (*a*) for precautions that must be observed when preparing certain other alloys.

After placing the mixture in the crucible, add a thin layer of graphite, cover with the crucible cover and place in the furnace. Insert the thermocouple so that the hot junction will be at about the center of the mass of molten metal. When the mixture is well melted, shut off the heat and begin taking time-millivolt readings by taking the time reading for each $\frac{1}{10}$ mv. change in temperature. Stir the mixture as well as possible with the thermocouple tube while taking these readings.

When it is certain that all critical points on the cooling curve have been determined, reference (*b*), start heating the alloy again. Take readings while heating also.

When the metal is molten, remove the thermocouple, stir thoroughly and quickly pour into the mold. When cold, remove the ingot, clean off slag and weigh.

Test the ingot for malleability by hammering it when clamped in a vise.

Polish a small specimen of each ingot, etch carefully with a 5% HNO_3 in alcohol solution, and examine the microstructure under the microscope.

Report: Convert millivolt readings into temperature readings by using the calibration curve supplied for the particular thermocouple used.

From the data obtained plot time versus temperature cooling curves for the alloys studied.

Locate the critical points on the cooling curves and the critical points for other alloys of the series and plot the thermal equilibrium diagram for the series of lead-antimony alloys.

Discussions: Select any alloy in the series and referring to the equilibrium diagram briefly discuss all the steps it passes through in cooling from the liquid to the solid condition.

Explain what is meant by liquidus, solidus and eutectic.

Addendum: In Fig. 1, Plate III, is shown the thermal equilibrium diagram for the lead-antimony series of alloys. This graph shows complete solubility in the liquid state, zero solubility in the solid state and a eutectic at the minimum temperature.

In Fig. 2, Plate III, are shown typical cooling curves for the lead-antimony series. The first curve is typical of the cooling of a pure metal. The metal solidifies at a constant temperature as shown by the horizontal part of the curve. The second curve is typical of the cooling of a pure metal plus a eutectic. The third curve shows the freezing of a eutectic at a constant temperature, similar to that of a pure metal.

Fig. 3 shows how a thermal equilibrium diagram is obtained from the cooling curves. In plotting a constitution diagram all of the points for a given alloy must be plotted in the proper composition vertical, one above the other.

Plate IV shows the photomicrographs of the eight alloys of the lead-antimony series prepared (100×).

Fig. 1 — 100% lead — showing large equi-axed grains of lead.

Fig. 2 — Pb 92% + Sb 8% — showing primary lead grains surrounded by the lead-antimony eutectic.

Fig. 3 — Pb 87.5% + Sb 12.5% — showing all eutectic, a mechanical mixture of very fine grains of pure lead and pure antimony. See Plate XIII, Fig. 6.

Fig. 4 — Pb 75% + Sb 25% — showing primary grains of antimony surrounded by the lead-antimony eutectic.

Fig. 5 — Pb 50% + Sb 50% — similar to Fig. 4, except there is more primary antimony and less eutectic.

Fig. 6 — Pb 25% + Sb 75% — similar to Fig. 5, except there is more primary antimony and less eutectic.

Fig. 7 — Pb 10% + Sb 90% — showing practically all antimony with a small amount of eutectic at the grain boundaries.

Fig. 8 — Antimony 100% — showing grains of pure antimony.

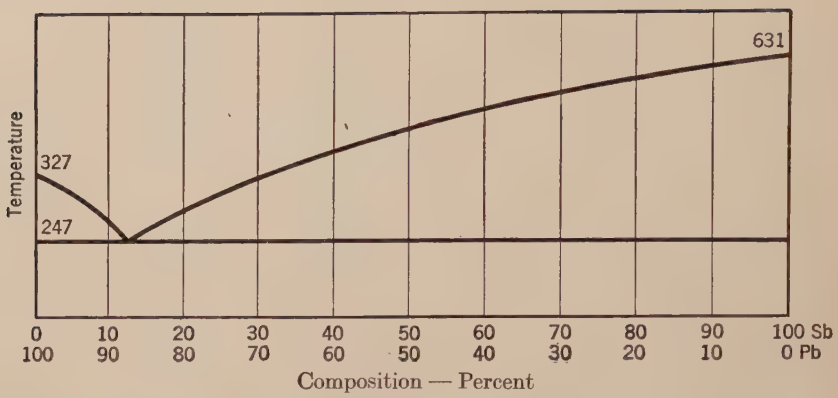

FIG. 1

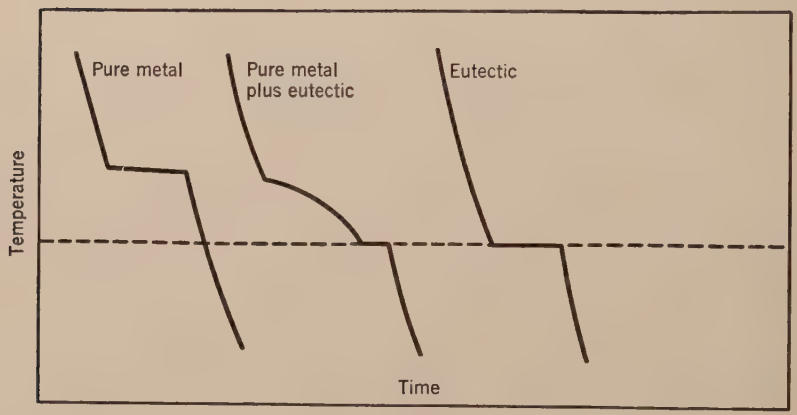

FIG. 2

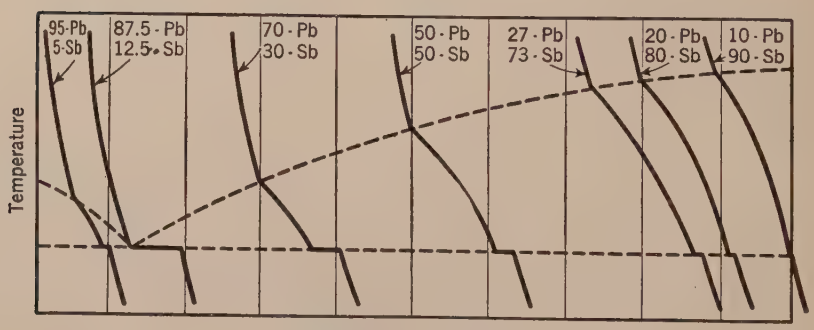

FIG. 3

PLATE IV

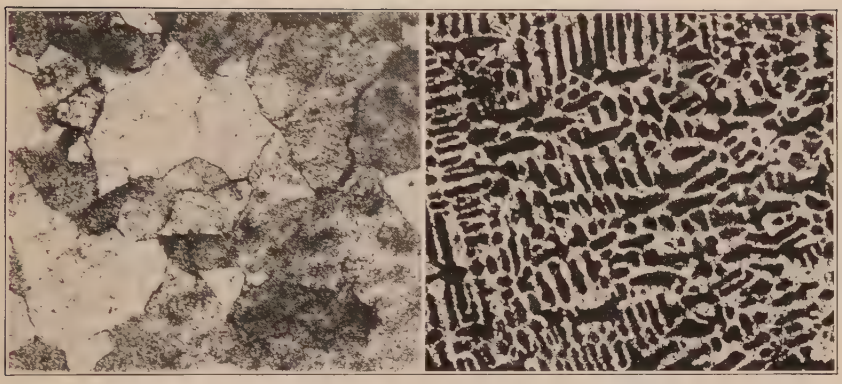

FIG. 1 FIG. 2

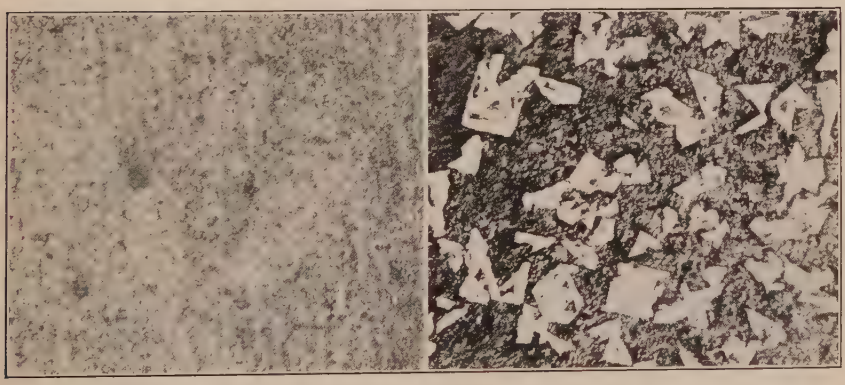

FIG. 3 FIG. 4

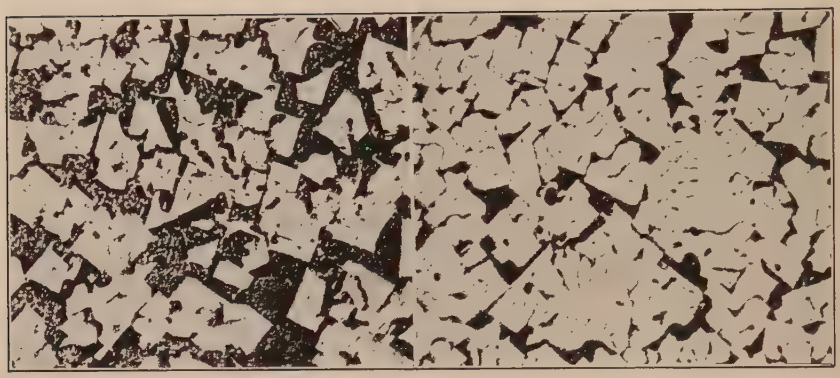

FIG. 5 FIG. 6

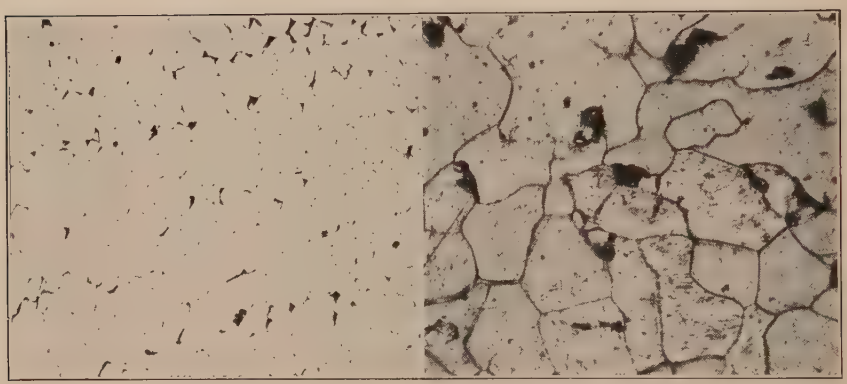

FIG. 7 FIG. 8

EXPERIMENT V

MACROSCOPIC EXAMINATION OF METALS AND ALLOYS

Purpose: To become familiar with characteristic macrostructures of metals and alloys.

References: (*a*) Gulliver: Metallic Alloys, Chapter VII.
(*b*) Desch, Metallography, Chapter IX.
(*c*) Guillet and Portevin: Metallography and Macrography, Chapters VI and VII.

Materials: Prepared specimens as provided.

Apparatus: Magnifying glass and binocular microscope.

Principles: A *macroscopic examination* consists in the investigation, as a whole, of one or more sections of a metal or an alloy, with the naked eye or under very low magnifications after simple polishing and suitable etching. The purpose is to determine if the specimen has a uniform chemical and structural composition and to judge if it will also have similar mechanical properties throughout its mass. It differs from a microscopic examination in that large surfaces are examined and minute details overlooked. From such an examination, deductions can be made regarding:

(A) Crystalline Heterogeneity.
(B) Mechanical Heterogeneity.
(C) Chemical Heterogeneity.

Procedure: 1. This examination is made with the eye alone and with a low-powered microscope. Record what is revealed.

2. Examine each of the specimens that have been prepared for macroscopic examination and study it in connection with its "History." On one page, for insertion in the report, make sketches as listed below, labeling each sketch and show in a few words, the correlation between the structures and the physical properties:

(*a*) A typical dendritic structure.
(*b*) The crystalline formation in a slowly cooled casting.
(*c*) The crystalline heterogeneity at a welded or brazed joint.
(*d*) A typical structure showing mechanical heterogeneity.
(*e*) A typical structure showing chemical heterogeneity.

NOTES ON STRUCTURES — CRYSTALLINE HETEROGENEITY

Crystalline Heterogeneity depends upon the method of crystalline growth. When a molten pure metal is cooled to its freezing temperature, minute crystals are formed in various centers and these rapidly grow in size. They usually grow in certain axial directions and from these axes arms grow and sometimes still other branches are formed. These " crystallites " or " crystal skeletons " often look very much like a pine tree and hence are called " dendrites." These dendrites often form on the surface of slowly cooled metals. In most metals the crystals are too small to be seen with the eye alone or under low magnification, but bismuth is an exception. Samples of bismuth are easily prepared to show that the crystals have definite geometric shapes.

Crystalline growths from various centers must eventually meet. This causes definite boundary lines between crystalline growths starting from the different centers. If the cooling is *very* slow the metal crystallizes along so many branches from a given center that a section through this growth will be nearly, if not quite, homogeneous. Such a crystalline growth is called a **grain.** The boundaries of these grains of pure metal are not crystalline faces but are due to interference during grain growth.

The grain structure of a pure metal or alloy is made visible by etching with a suitable reagent, often a weak acid. If etched deeply, adjacent grains in a pure metal differ in color. This is due to the fact that the etching reagent eats along the cleavage planes of the crystals and produces a kind of nap or minute facets on the surface of the grains. These facets vary in orientation from grain to grain. When the light so strikes them that it is reflected toward the observer, they appear bright. Otherwise they appear dark, varying in shade with the angle of reflection of the light.

PHOTOMICROGRAPHS

Fig. 1 — Bismuth Crystals (3×).

This specimen was prepared by melting bismuth and after it had started to freeze it was suddenly chilled. Note that the crystals caught in the chilled liquid have a definite geometric form, cubic. Note also how some have attached themselves to others, this being the beginning of a crystal skeleton, or dendrite.

Fig. 2 — Lead Dendrites (3×).

This specimen was prepared in the same manner as the bismuth specimen. In this case, however, the individual crystals cannot be seen but many almost perfect tree-like formations, or dendrites, can be seen caught in the chilled liquid.

Fig. 3 — Antimony Surface (2×).

When cast metals cool slowly, crystals are formed at the surface, this being slightly cooler than the walls of the mold or any other part of this metal, and as the branches are formed, the liquid metal drops down and leaves the pattern of the crystal skeleton on the surface of the ingot. Note the tree-like formations in this specimen.

Fig. 4 — Aluminum Surface (3×).

Note the dendrites on the surface of this metal also.

Fig. 5 — Zinc Surface (3×).

Note the dendrites.

Fig. 6 — Antimony Fragment (2×).

Examine the fracture and note how the cleavage planes are parallel to each other in any given crystalline growth or dendrite but have different inclinations from those in other dendrites.

Fig. 7 — Cast Brass (3×).

Etched for 5 seconds in acidified ferric chloride. Examine with the eyes alone, then with the magnifying glass and finally with the binoculars. Note the size and shape of the grains. Observe that the general grain formation for an alloy may be the same as for pure metals. The grains grow in at right angles to the walls of the casting mold.

Fig. 8 — Cast Zinc (3×).

Etched for 5 seconds in a solution of acidified ferric chloride. The unetched polished surface showed no structure at all. Examine with eye alone and also with the binoculars. Note how the etching has developed the definite grain structure. This is pure zinc, yet note how different the adjacent grains appear. Note that the grain-boundaries are fine lines. Note also that the grains all point toward the center. The grain growth began at the circumferential surface, where the metal began to cool, and grew in the direction toward the hottest part of the mass.

Fig. 9 — Cast Tin (3×).

Examine with the binoculars. Note the grain formation and variations in colors as for cast zinc.

Fig. 10 — Brazed Joint in Brass (15×).

Etched with HNO_3. Before etching the polished surface, the joint could not be detected. Note how the etching has clearly exposed the joint and note the difference in grain size and orientation of the grains in the weld and those in the plates. The weld (right) has a true casting structure. Observe the dendrites.

Fig. 11 — Brazed Joint in Boiler Plate (15×).

Etched with HNO_3. Compare the grain size in the plate at this joint with that at the joint in the welded plate. Note that the grain

size has not been affected in this case because the heat was not so great. This joint will not be so strong, however, because it cannot be stronger than the strength of the brazing metal. Brazing brass is in the center.

Fig. 12 — Welded Joint in Boiler Plate (15×).

Etched in HNO_3. Before etching this joint could not be detected in the polished section. It is a fusion weld made by the oxyacetylene method. Note the variation in the grain size and shape in the weld and in the plate near the weld and also at some distance from it. The heat has increased the grain size.

Fig. 13 — Welded Link of Chain (15×).

Etched in iodine solution for about 10 minutes. Note that the grains are not large and are irregular in size. This is due to the fact that the metal was worked (hammered) while hot. This broke up the large grains. Before etching, this joint could not be detected in the polished surface.

Fig. 14 — Welded Wrought Iron Joint (3×).

Etched in iodine solution (10 gr. iodine, 20 gr. potassium iodide, 100 cc. H_2O) for about 10 minutes. Note that the heterogeneity of the grains is not so pronounced as in a fusion weld. This is due to the breaking up of the grains by hammering. Oxide particles form, however, and sometimes prevent a perfect joint as in this case.

PLATE V

FIG. 1

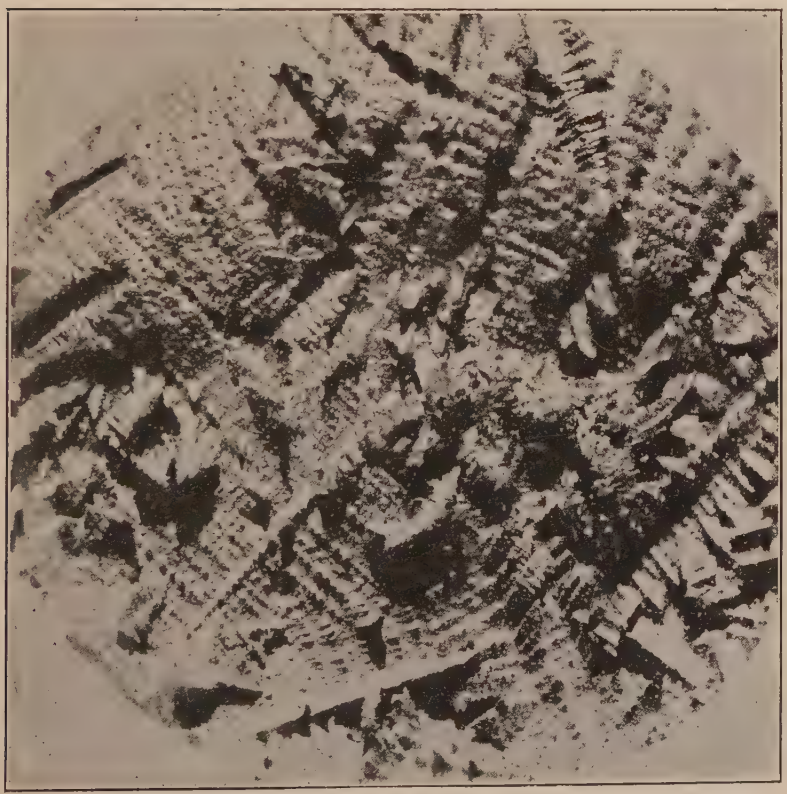

FIG. 2

PLATE VI

FIG. 3

Fig. 4

PLATE VII

Fig. 5

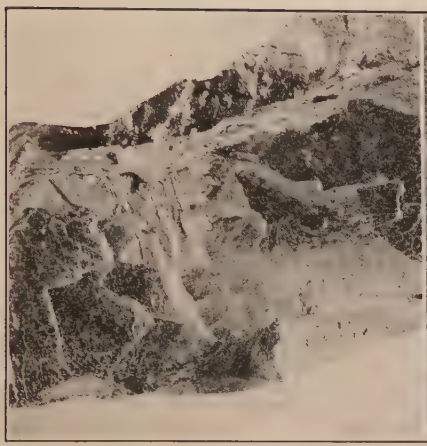

FIG. 6

FIG. 7

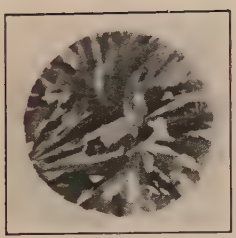

FIG. 8

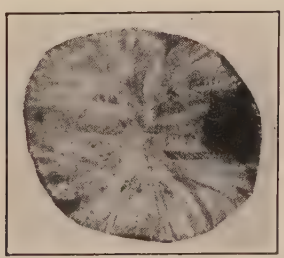

FIG. 9

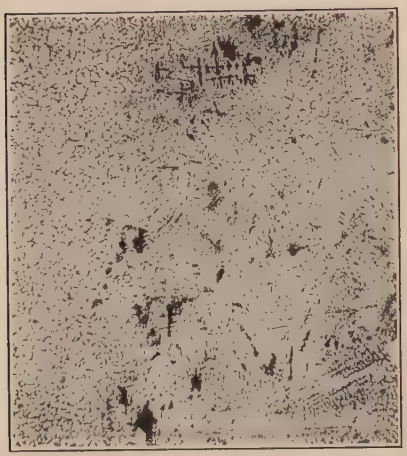

FIG. 10

FIG. 11

FIG. 12

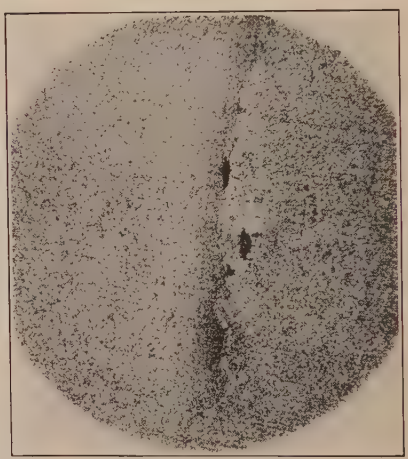

FIG. 13

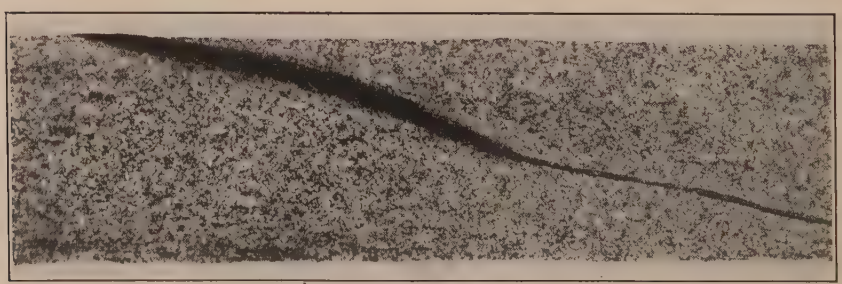

FIG. 14

NOTES ON STRUCTURES — CHEMICAL HETEROGENEITY

Chemical Heterogeneity results from impurities in the metal or alloy. This part of macroscopic examination is, no doubt, the most important of all. The origin of chemical heterogeneity may have been intentional as in case-hardened or cemented steel or it may have been unintentional and due to the method of cooling from the molten condition. When a metal cools from the molten state, it *contracts* and the last bit of liquid solidifies near the top center of the ingot. This causes a *pipe*. Because most impurities are more soluble in the molten metal than in the solid, the impurities tend to remain in that part of the mass that remains molten the longest. Consequently, slowly cooled metals often have segregated impurities around the pipe and near the top of the ingot. If cooled too fast, impurities often segregate and become frozen in other parts of the metal. Because of this phenomenon, risers are provided in castings and the top of the ingot is cropped off before the ingot is worked to finished shapes.

PHOTOMICROGRAPHS

Fig. 15 — Zinc Ingot (3×).

Etched with acidified ferric chloride for about 5 seconds. Note the size and location of the pipe. Note also how the impurities and spongy metal are near the top and around the pipe. Note also the heterogeneity of the grain structure and observe the way the grains have grown.

Fig. 16 — Zinc-Lead Ingot (Zn 95%; Pb 5%) (3×).

Etched with acidified ferric chloride. Note that the zinc and lead are insoluble when solid and that there is a distinct line of separation. Note the position and size of the pipe and the size and arrangement of the grains. The excess lead is on the bottom of the ingot.

Fig. 17 — Magnolia Metal Ingot (Pb 78%; Sb 16%; Sn 6%) (3×).

Etched in 5% picric acid for about 10 seconds. Note how the antimony has segregated and, being lighter, has floated to the top. This ingot is decidedly segregated.

Fig. 18 — Wrought Iron, Bent (3×).

Etched with iodine solution for about 20 minutes. Note how the etching reagent has attacked the slag and left decided grooves. This slag is in all puddled iron and makes a fracture fibrous. Puddled wrought iron is chemically heterogeneous due to this slag.

Fig. 19 — Case-hardened Steel (3×).

Etched in 5% picric acid for about 5 minutes. Examine with the eye alone and also under the binoculars. This is a 0.14% carbon steel that was packed in a mixture of 60% wood charcoal and 40% $BaCO_3$

and heated to about 1750° F. and held at that temperature for 8 hours. It was then allowed to cool slowly in the furnace. Note that at the surface the steel is high in carbon and this varies, getting less, as the center is approached. The carbon content of the central portion has not been changed. Fig. 19*a* shows the uncarburized surface; and Fig. 19*b* shows the carburized specimen surface.

FIG. 15

Fig. 16

FIG. 17

FIG. 18

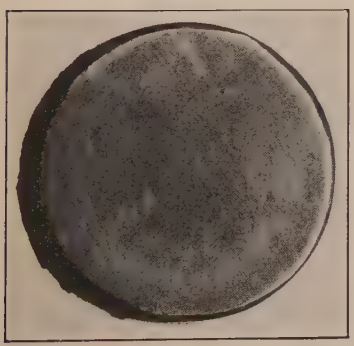

FIG. 19a

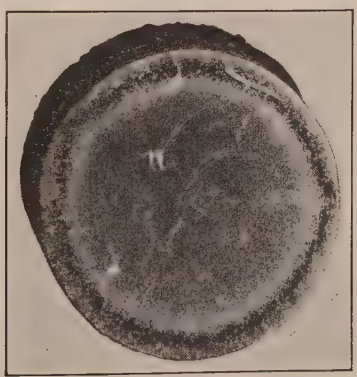

FIG. 19b

NOTES ON STRUCTURES — MECHANICAL HETEROGENEITY

Mechanical Heterogeneity results when a metal has been cold-worked or has been put in a strained condition by any method. Any metal or alloy is more readily attacked by a reagent when in a strained or hardened condition. This type of heterogeneity can occur only in strained material and hence does not often occur in cast metals. Any irregular or local hardening will be detected by variations in the etching. In a similar manner the porous sections and the welding lines are more readily attacked.

Fig. 20 — Sheared Steel (3×).

Etched in iodine solution for about 20 minutes. Note the flow-lines of the metal resulting from the over-strain while cold.

Fig. 21 — Twisted Steel (3×).

Etched in iodine solution for about 20 minutes. Note how the etching reagent has attacked the outer fibers more than those nearer the center of the rod. They were more severely strained than the ones along the axis.

Fig. 22 — Bolt Head (2×).

Mild steel etched with iodine solution for about 20 minutes. Note how the mechanical work on the metal has distorted it, introducing locations under internal strain. Material strained like this is difficult to machine to accurate dimensions due to the internal strains.

Fig. 23 — Rivet Head (2×).

Mild steel etched with iodine solution for about 20 minutes. Same sort of structure as in bolt head.

Fig. 24 — Section of I-Beam (2×).

Structural steel, etched for about 10 hours in 5% picric acid in alcohol followed by about 20 minutes in iodine solution. Note the flow-lines. These may be segregation of impurities in the steel but are probably due to internal stresses introduced when the metal was rolled. Some evidence of crystalline heterogeneity may be seen also.

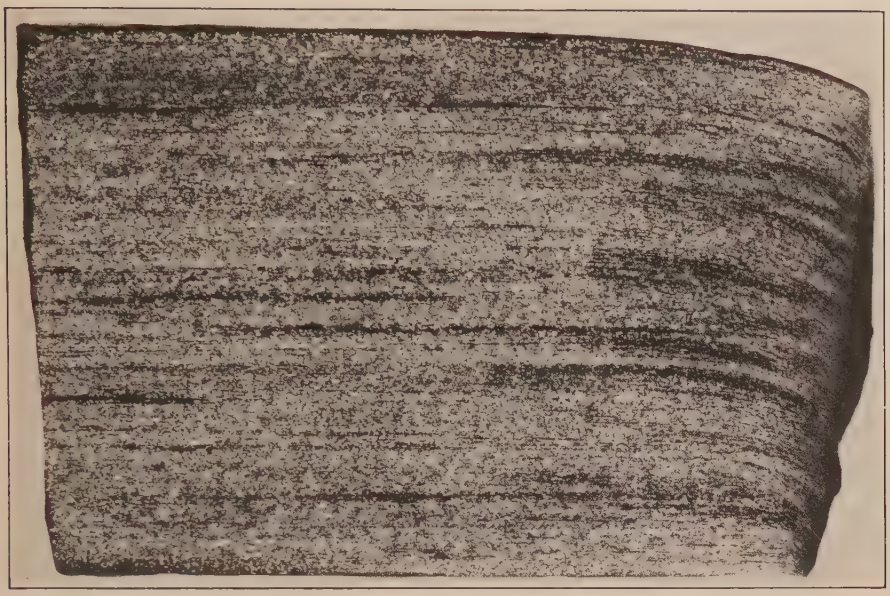

FIG. 20

FIG. 21

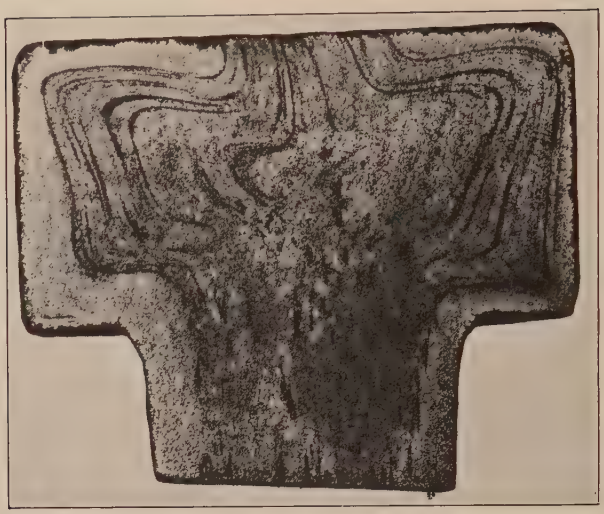

FIG. 22

FIG. 23

PLATE XIII

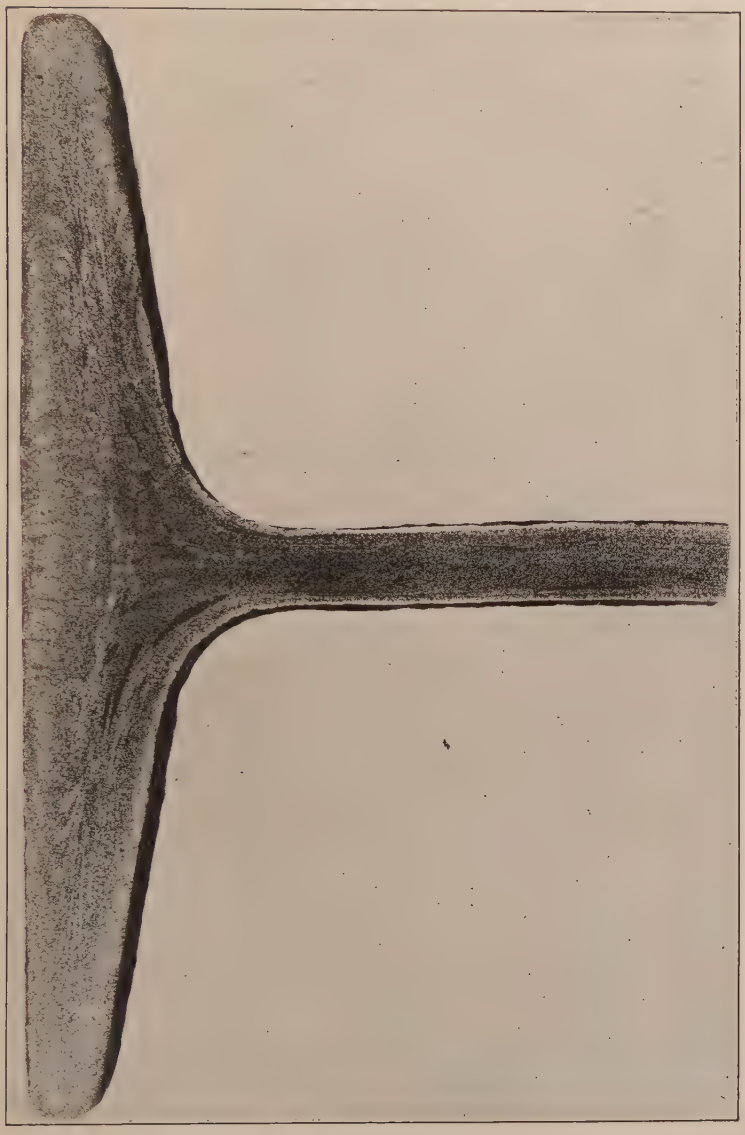

FIG. 24

EXPERIMENT VI

STRUCTURES — EUTECTICS AND EUTECTOIDS

Purpose: To study the microstructures of eutectics and eutectoids in alloys.

References: Jeffries and Archer: The Science of Metals.
H. L. Brady: Journal Inst. of Metals **28**, 369 (1922).
A. M. Portevin: Journal Inst. of Metals **29**, 239 (1923).
C. H. Green: Am. Inst. Min. and Met. Eng. J., Feb. 1925.

Theory: The term " eutectic " meaning " lowest melting " is applied to alloys of maximum fusibility. It is generally understood to mean the alloy having the lowest melting point of any series of alloys of the same two or more phases. The eutectic contains its components in definite proportions, but usually not in simple atomic or formula weight proportions. The solid eutectic is an intimate physical mixture of two or more phases, which may be (*a*) pure metals or metalloids, (*b*) solid solutions, or (*c*) chemical compounds. The eutectic freezes and melts at a constant temperature.

The eutectoid is the alloy of maximum transformation in the solid state at the lowest temperature. It is the disintegration of a solid solution into its components. The eutectoid is very similar to the eutectic but the transformation is more sluggish.

PHOTOMICROGRAPHS

Fig. 1 — Lead-Tin Eutectic (Pb 38%; Sn 62%) (250×).

Etched in 10% HNO_3 solution. Photomicrograph shows fine laminated eutectic of pure tin and tin-lead solid solution. Tin is partially soluble in lead in the solid state, but lead is insoluble in tin. This alloy melts sharply at 182° C.

Fig. 2 — Bismuth-Tin Eutectic (Bi 58%; Sn 42%) (250×).

Etched in concentrated HCl. Photomicrograph shows laminated eutectic of bismuth rich solid solution and tin rich solid solution. Bismuth and tin are each partially soluble in each other in the solid state. This alloy melts sharply at 137° C.

Fig. 3 — Bismuth-Lead Eutectic (Bi 57.5%; Pb 42.5%) (250×).

Etched in concentrated HNO_3. Photomicrograph shows laminated eutectic of bismuth rich solid solution and lead rich solid solution.

Bismuth and lead are each partially soluble in each other in the solid state. This alloy melts sharply at 125° C.

Fig. 4 — Tin-Zinc Eutectic (Sn 91.5%; Zn 8.5%) (250×).

Etched in 10% HNO_3. Photomicrograph shows fine eutectic of pure tin and pure zinc. Tin and zinc are insoluble in each other in the solid state. This alloy melts sharply at 197° C.

Fig. 5 — Cadmium-Tin Eutectic (Cd 32.5%; Sn 68.5%) (250×).

Etched in 10% HNO_3. Photomicrograph shows laminated eutectic of cadmium rich solid solution and tin rich solid solution. Cadmium and tin are each partially soluble in each other in the solid state. This alloy melts sharply at 178° C.

Fig. 6 — Lead-Antimony Eutectic (Pb 87.5%; Sb 12.5%) (500×).

Etched in 5% HNO_3. Photomicrograph shows granular eutectic of pure lead and pure antimony. Lead and antimony are each insoluble in each other in the solid state. This alloy melts sharply at 247° C.

Fig. 7 — Pearlite Eutectoid (0.85% Carbon Steel) (500×).

Etched in picric acid. Photomicrograph shows laminated eutectoid of ferrite and cementite. The pearlite grains vary in orientation as shown by the different directions of the lamellar structure.

Fig. 8 — Bronze Delta Eutectoid (Cu 73%; Sn 27%) (500×).

Etched in ferric chloride solution. Photomicrograph shows large dark grains of alpha bronze with the speckled white delta eutectoid. The black specks in the eutectoid are fine particles of alpha bronze embedded in white delta bronze. This photograph was taken from a bronze containing 15% tin.

Fig. 9 — Iron Phosphide Eutectic (Fe 89.8%; P 10.2%) (100×).

Etched slightly in picric acid. Photomicrograph shows fine eutectic mixture of iron and iron phosphide surrounded by the white cementite. This photomicrograph was taken from a sample of commercial pig iron high in phosphorus. The eutectic consists of about 61% Fe_3P and 39% of the saturated solution of Fe_3P in iron.

Fig. 10 — Aluminum-Zinc Bronze (500×).

Etched in ferric chloride. Photomicrograph shows fine alpha-delta eutectoid and free alpha grains with isolated crystallites of iron-bearing constituent. This specimen was sand-cast. The bronze analyzed Cu 78.97%, Fe 2.95%, Al 8.55% and Zn 9.53%.

Fig. 11 — Aluminum-Bronze Eutectoid (Cu 87%; Al 13%) (500×).

Etched in ferric chloride solution. Photomicrograph shows lamellar alpha-delta eutectoid between the large alpha grains. This photomicrograph was taken from an aluminum bronze containing 10.2% of aluminum and the balance copper.

Fig. 12 — Aluminum-Silicon Eutectic (Al 90%; Si 10%) (100×).
Etched in ferric chloride solution. Photomicrograph shows clear areas of primary aluminum surrounded by the fine aluminum-silicon eutectic. There is a slight tendency toward dendritic structure. This photomicrograph was taken from an aluminum-silicon alloy containing 12.50% silicon, 0.013% copper, 0.04% iron and the balance aluminum.

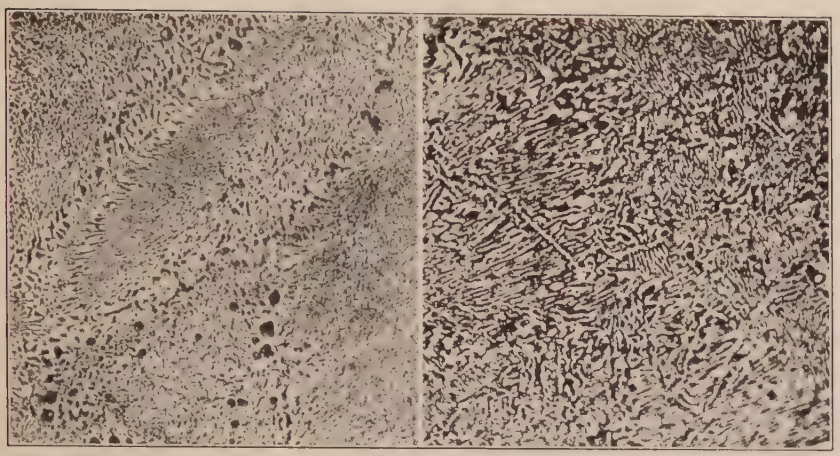

FIG. 1 FIG. 2

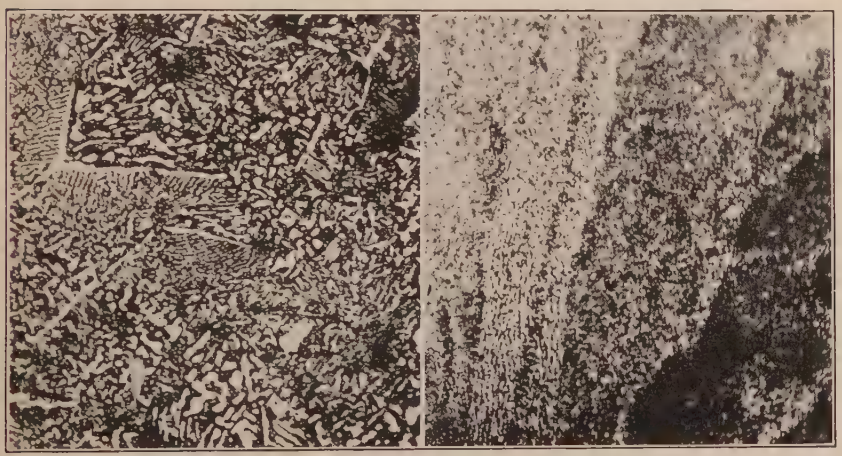

FIG. 3 FIG. 4

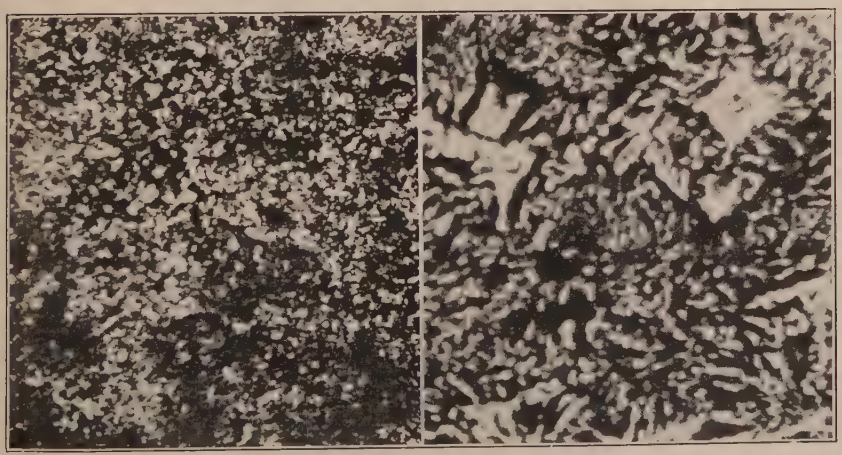

FIG. 5 FIG. 6

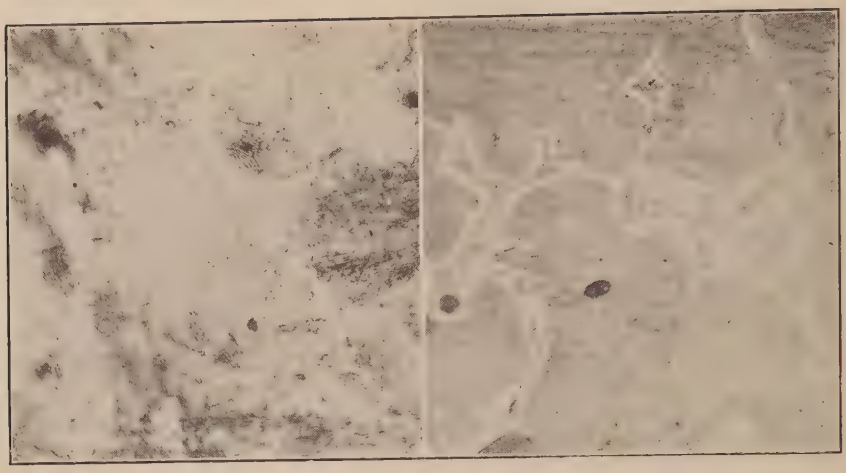

FIG. 7 FIG. 8

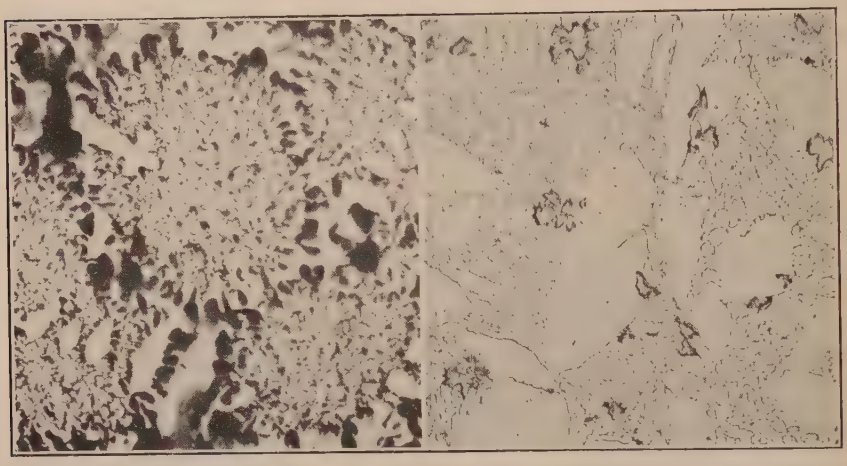

FIG. 9 FIG. 10

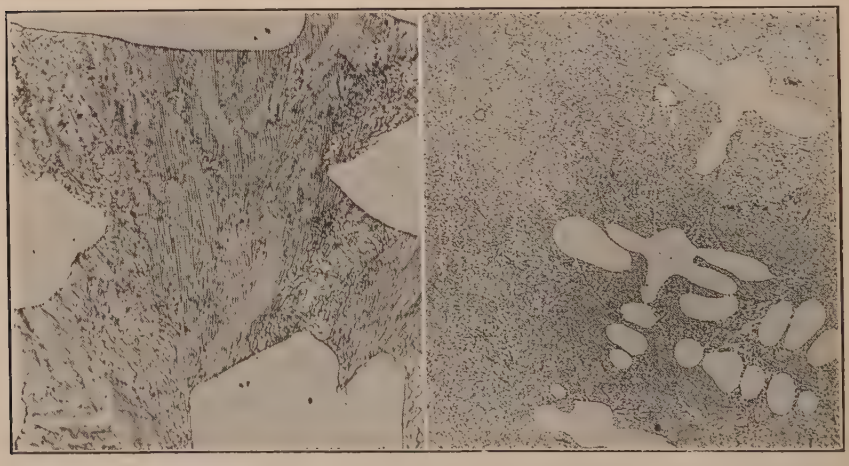

FIG. 11 FIG. 12

EXPERIMENT VII

CALIBRATION OF A THERMOCOUPLE

Purpose: To calibrate a noble metal (Pt, Pt-Rh) thermocouple.

References: (*a*) "Pyrometer Testing and Heat Measurements," Bureau of Standards Circular 7.

(*b*) "Pyrometric Practice," Bureau of Standards, Tech. Paper 170.

(*c*) Burgess: High Temperature Measurements.

Apparatus: Electric Resistance Furnace; noble metal thermocouple, potentiometer, crucibles, tongs, graphite, molds, watch, jar of ice, graphite or quartz protection tube for thermocouple.

Materials: Samples of pure metals as supplied.

Theory: A thermoelectric pyrometer consists of a thermoelectric couple in connection with a millivoltmeter or a potentiometer to indicate electromotive force between the hot and cold junctions. The fundamental principle underlying the use of a thermoelectric pyrometer is that a definite relation exists for any particular couple between the electromotive force and the temperature difference of the hot and cold junctions. For the range 300° C. to 1100° C., the following equation is well suited:

$$E = a + bt + ct^2,$$

where E is the electromotive force expressed in millivolts for a temperature difference of $t°$ C. between the hot and cold junction, while a, b and c are constant quantities for the given couple.

(*Note:* A base metal thermocouple may be similarly calibrated.)

To obtain numerical values of the constants it is only necessary to obtain the e.m.f.'s corresponding to only three known temperatures lying within the range. Definitely known and easily produced temperatures are most satisfactorily obtained by the freezing points of metals and compounds. And if these values are substituted in the equation, three simultaneous equations will be obtained, the solving of which will give the numerical values of the three constants. Knowing the values of these constants and substituting them in the equation, the e.m.f. for any desired temperature can be calculated. And in this manner the

e.m.f.-temperature curve can be extrapolated or extended somewhat beyond the range of the actual measurements.

Some of the metals and compounds used for the standardization are: tin (232° C.), bismuth (270° C.), lead (327° C.), zinc (419° C.), antimony (630° C.), sodium chloride (800° C.), barium chloride (950° C.), silver (961° C.), copper (1083° C.) and nickel (1452° C.).

Procedure: The apparatus is set up by properly connecting up the thermocouple with the potentiometer and the furnace.

The graphite crucible containing the substance freezing point of which is to be determined is placed in the electric pot furnace and the heating current is adjusted. After the metal is melted, the hot junction of the thermocouple insulated by a quartz tube is inserted in the molten metal and the current supply is cut off. While the metal is cooling, time-millivolt readings are taken at every 0.1 millivolt change until the metal has solidified. The current is then again cut in and the check readings of time versus millivolts are taken during the melting of the metal.

In the same manner the melting and freezing points of at least two other substances are taken, and from the data obtained the cooling and heating curves are plotted and the electromotive forces corresponding to the freezing points obtained. The calibration curve is then plotted with the freezing points as ordinate and the corresponding electromotive forces as abscissa.

Data:

Experimental:

Metal	*Temperature*	*Electromotive Force, Millivolts*
Tin	232° C.	1.8
Lead	327° C.	2.45
Zinc	419° C.	3.1
Antimony	630° C.	4.6
Copper	1083° C.	8.5

Calculated Values:

Temperature	*Electromotive Force, Millivolts*
100° C.	0.84
500° C.	3.37
800° C.	5.74
1000° C.	7.52
1200° C.	9.49
1500° C.	12.77

Numerical Value of Calculated Constants:

$a = 0.32$

$b = 0.005$

$c = 0.0000022$

Calculations:

Metal	*Temperature*	*Millivolts*
Tin	232° C.	1.6
Zinc	419° C.	3.3
Antimony	630° C.	5.4

(1) $E = a + bt + ct^2$

Substitute the values above in equation (1)

(2) $1.6 = a + b(232) + c(232)^2$
(3) $3.3 = a + b(419) + c(419)^2$
(4) $5.4 = a + b(630) + c(630)^2$

Simplify equations (2), (3) and (4) by multiplying out

(5) $1.6 = a + 232b + 53824c$
(6) $3.3 = a + 419b + 175561c$
(7) $5.4 = a + 630b + 396900c$

Multiply equation (5) by 419 and equation (6) by 232

(8) $670.4 = 419a + 97208b + 22552256c$
(9) $765.6 = 232a + 97208b + 40730152c$

Subtract equation (9) from equation (8)

(10) $-95.2 = 187a - 18177896c$

Multiply equation (5) by 630 and equation (7) by 232

(11) $1008 = 630a + 146160b + 33909120c$
(12) $1252.8 = 232a + 146160b + 92080800c$

Subtract equation (12) from equation (11)

(13) $-244.8 = 398\ a - 58171680c$

Multiply equation (10) by 398 and equation (13) by 187

(14) $-37889.6 = 74426a - 7234802608c$
(15) $-45777.6 = 74426a - 10878104160c$

Subtract equation (14) from equation (15)

(16) $-7888 = -3643301552c$
$c = 0.0000022$

Substitute the numercial value of c in equation (13)

(17) $-244.8 = 398a - (58171680)\ (0.0000022)$
(18) $a = 0.32$

Substitute the numerical values of a and c in equation (5)

(19) $1.6 = 0.32 + 232b + (53824)\ (0.0000022)$
$b = 0.005$

The electromotive force values for the temperatures of 100° C., 500° C., 800° C., 1000° C., 1200° C., and 1500° C. are obtained by substituting the numerical values for the constants a, b, and c and for the temperature t in equation (1):

$E_{100} = 0.32 + 0.005(100) + 0.0000022(100)^2 = 0.84$
$E_{500} = 0.32 + 0.005(500) + 0.0000022(500)^2 = 3.37$
$E_{800} = 0.32 + 0.005(800) + 0.0000022(800)^2 = 5.74$
$E_{1000} = 0.32 + 0.005(1000) + 0.0000022(1000)^2 = 7.52$
$E_{1200} = 0.32 + 0.005(1200) + 0.0000022(1200)^2 = 9.49$
$E_{1500} = 0.32 + 0.005(1500) + 0.0000022(1500)^2 = 12.77$

Addendum: Fig. 1 shows the calibration curve for the platinum, platinum-rhodium thermocouple in which the temperature in degrees Centigrade is plotted as the ordinate and the electromotive force in millivolts is plotted as the abscissa. The points on the curve enclosed in circles are the experimental values whereas the other points enclosed in triangles are the calculated values. It will be observed that the experimental and the calculated values check very closely, indicating that equation (1) holds for this thermocouple calibration for extrapolation.

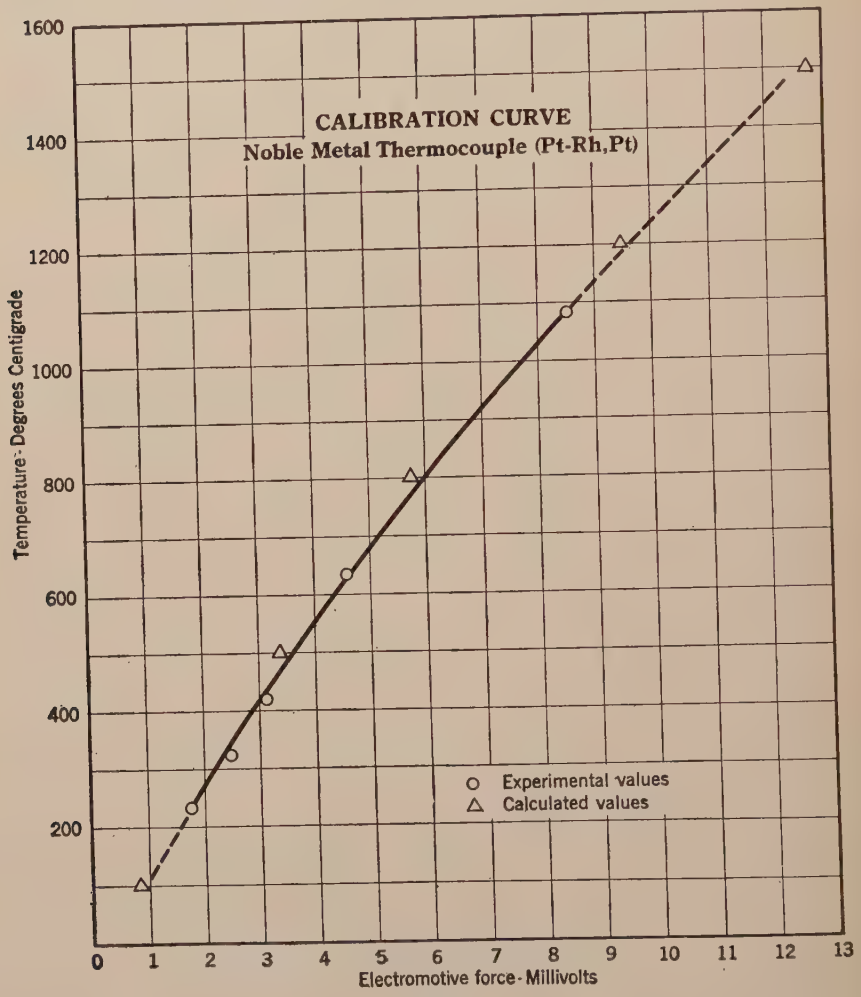

FIG. 1

EXPERIMENT VIII

THERMAL CRITICAL POINTS OF STEEL

Purpose: To determine the thermal critical points in a low carbon steel.

References: (*a*) Sauveur: Metallography and Heat Treatment of Iron and Steels, Chapters VII, VIII, IX.

(*b*) Leeds and Northrup: Bulletin 866-A.

(*c*) Appendix II.

Material: Specimens of carbon steel as supplied.

Apparatus: Electric resistance furnace, platinum and platinum-rhodium thermocouple, nickel neutral body, potentiometer, wall galvanometer, and Leeds & Northrup double thermocouple holder.

Theory: The physical properties and the structure of steels depend upon the temperatures at which they are mechanically worked and heat-treated. And due to the close relationship between treatment and structure on the one hand and structure and physical properties on the other hand, it is very important that one shall thoroughly understand the transformations, chemical and physical changes, taking place at well defined temperatures. The temperatures at which these changes occur are termed "transformation points" or "critical points," also "retardations."

If a sample of steel is heated at a uniform rate in a furnace, a marked absorption of heat will occur at nearly a definite temperature marking a retardation in the rise of the temperature of the specimen. In reverse order if a sample of steel is cooled from an elevated temperature (about 1000° C.), a marked liberation of heat will occur at nearly a definite temperature marking a retardation in the cooling of the specimen. Those transformations occurring while the sample is being heated are termed decalescence points (Ac), and those occurring while it is being cooled are termed recalescence points (Ar).

The methods generally applied for the location of such transformation points depend upon the fact that the changes in the chemical or physical state are accompanied by absorption or evolution of heat. This absorption or evolution of heat can be observed by the "direct time-temperature method" in which the temperature is measured at definite time intervals, or by the "inverse rate method" in which the inverse

rate of temperature change is plotted against temperature of the specimen, or by the " difference method " in which the difference in temperature between the specimen to be tested and a neutral body, as nickel, is plotted against temperature of the furnace.

METHOD USED IN THE LEEDS & NORTHRUP TRANSFORMATION POINT APPARATUS

(Reference b)

Leeds & Northrup apparatus embodies a method that is more sensitive and reliable than the " temperature-time " method. The sample under test and a body which will heat at a uniform rate (that is, a body having no transformation points) are heated in close contact, one with the other. Two thermocouples are employed. One measures the temperature of the sample the other the temperature-difference between the sample under test and the neutral body. Temperatures are plotted as one ordinate and the corresponding temperature differences as the other. So long as both sample and neutral body heat uniformly there will be no change in the temperature-difference ordinate; when, however, the temperature of the sample remains stationary or lags behind the temperature of the sample holder, due to a transformation in the steel, the temperature-difference ordinate, formerly approximately zero, undergoes a large percentage change, even though the actual change in temperature difference is small.

The means used in the Leeds & Northrup apparatus for detecting the difference between sample temperature and neutral body temperature is a special thermocouple. This couple, called the " difference couple," is composed of two pieces of platinum joined by a short piece of platinum-iridium alloy. One of the junctions of the couple is in contact with the sample and the other in contact with the neutral body. The platinum-iridium couple develops a high electromotive force, which changes with temperature at a nearly uniform rate and is therefore well adapted for the purpose.

For indicating the changes in the electromotive force due to these transient differences in temperature between sample and sample holder a sensitive reflecting galvanometer is employed.

Simultaneously with the measurements of temperature difference, the temperature of the sample must be determined accurately in order that the results may be relied upon for controlling commercial heat-treating operations. For this purpose a platinum, platinum-rhodium thermocouple is employed in connection with a potentiometer. The potentiometer is the device used when high precision is required in measuring electromotive forces and is therefore employed as the meas-

uring device for use with the couple employed to measure the temperature of the sample.

Procedure: A small hole about $\frac{1}{8}$ in. in diameter is drilled through the center of the steel specimen which is placed in the end of the neutral body in the double couple holder. Both the steel specimen and the nickel neutral body are in contact with the hot junctions of the double thermocouple. The cold junction is placed in an ice bath and the double thermocouple holder is placed in the furnace. The Pt-Rh,Pt thermocouple in contact with the steel sample is connected to the potentiometer, while the Pt,Pt-Ir,Pt thermocouple (difference couple) in contact with both the steel specimen and the nickel neutral body is connected to the "difference galvanometer."

The temperature of the furnace is brought up to about 500° C. and readings of potentiometer millivolts versus galvanometer scale millimeter divisions are taken. Readings on the "difference galvanometer" are taken for each 0.1 millivolt change as indicated by the potentiometer. When the furnace temperature has reached about 1000° C. the supply of heat to the furnace is discontinued and similar readings are taken while the specimen cools in the furnace to a temperature of about 500° C.

Report: Plot "difference curves" for both heating and cooling. Transform the millivolt readings at the critical points into temperature readings from the calibration curve for the thermocouple.

Record the critical temperature found for both heating and cooling conditions.

Consult the iron-carbon equilibrium diagram and note how critical points found check with the diagram.

Discussion: The slower the rate of heating and cooling of the specimen the smaller the gap between the Ac and Ar critical points and the nearer the two points will approach each other. Due to hysteresis the critical points on heating are somewhat above and on cooling are somewhat below the true critical points. The difference in temperature between the Ac and Ar points is known as the hysteresis gap.

Addendum: Table I gives the potentiometer millivolt readings and temperatures (°C.) for the corresponding galvanometer deflections in millimeters for a 0.6% carbon steel.

Fig. 1 shows the transformation point curves for the 0.6% carbon steel. For steel of this composition the A_2 and A_3 points coinside.

Fig. 2 shows representative transformation point curves obtained with the Leeds & Northrup apparatus from carbon steels, arranged in order of increasing carbon content.

Fig. 3 shows the cross-section of the Leeds & Northrup sample holder, with sample and thermocouples in place.

Fig. 4 shows the diagram of the Leeds & Northrup potentiometer circuit with double thermocouple in place.

TABLE I

DATA

Potentiometer e.m.f., Millivolts	Temperature, °C.	Galvanometer Deflection, Millimeters	Potentiometer e.m.f., Millivolts	Temperature, °C.	Galvanometer Deflection, Millimeters
3.888	468	3.0	7.444	815	2.5
4.642	549	5.0	7.444	815	1.0
4.891	573	6.5	7.200	794	−2.0
5.646	646	7.5	6.909	765	−5.5
5.735	653	8.0	6.806	755	−7.0
6.373	710	9.5	6.728	747	−9.0
6.546	731	14.0	6.330	710	−12.0
6.558	732	20.0	6.205	699	−15.0
6.578	734	25.5	6.204	699	−21.0
6.634	740	30.5	6.204	699	−25.0
6.634	740	28.0	6.204	699	−28.0
6.634	740	25.0	6.204	699	−30.0
6.634	740	20.0	6.190	698	−34.0
6.830	760	13.0	6.189	698	−34.5
6.910	765	10.0	6.122	690	−26.0
6.993	774	9.5	6.077	685	−22.0
7.064	780	9.0	6.051	684	−18.0
7.156	790	9.0	5.866	665	−15.0
7.157	790	8.0	5.346	615	−14.0
7.444	815	4.5	5.000	580	−13.0

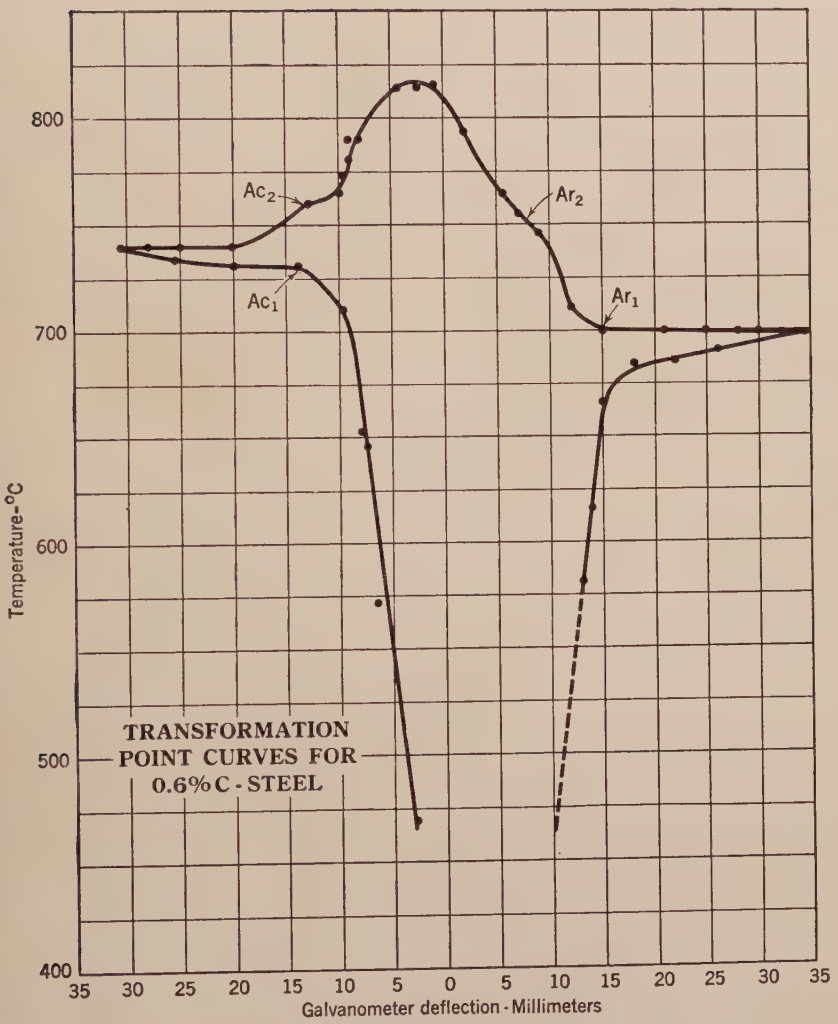
800
700
600
500
400
Temperature-°C
Ac2
Ac1
Ar2
Ar1
TRANSFORMATION
POINT CURVES FOR
0.6%C-STEEL
35 30 25 20 15 10 5 0 5 10 15 20 25 30 35
Galvanometer deflection-Millimeters

FIG. 1

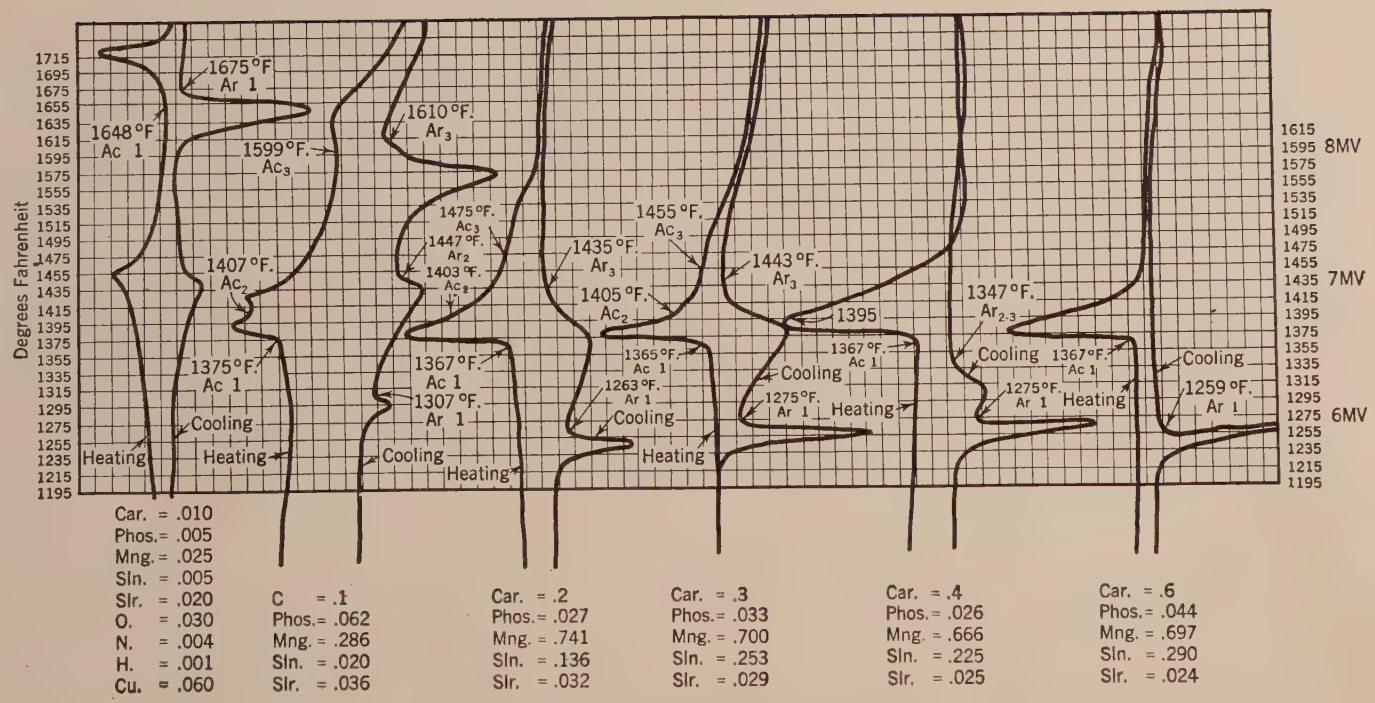

FIG. 2 (Leeds & Northrup)

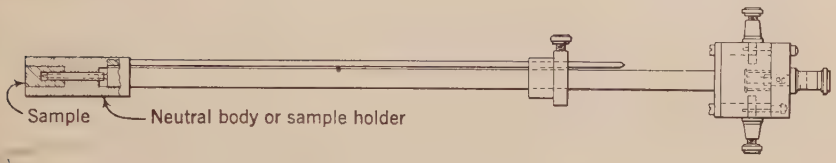

FIG. 3 (Leeds & Northrup)

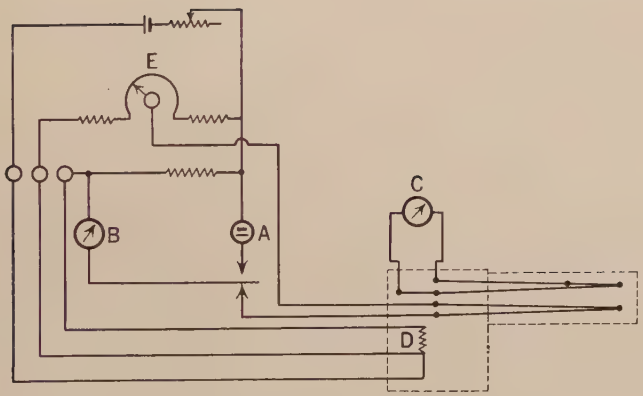

FIG. 4 (Leeds & Northrup)

EXPERIMENT IX

WROUGHT IRON — PURE IRON — STEEL

Purpose: To study the microstructures of Wrought Iron, Pure Iron and Steels.

References: Sauveur: Metallography and Heat Treatment of Iron and Steel, Chapters III, IV, V.

Bullens: Steel and Its Heat Treatment, Chapter II.

Guillet and Portevin: Metallography and Macrography, pp. 127–152.

Williams and Homerberg: Principles of Metallography, pp. 123–137.

WROUGHT IRON (Plate XVI)

Wrought iron is a slag-bearing, malleable iron, which does not harden materially when suddenly cooled.

Fig. 1 — Wrought Iron — Longitudinal Section — Unetched (100×).

Note the amount and shape of the dark areas which are slag particles composed chiefly of oxides, phosphides and silicates. The white matrix is iron (ferrite). Note that the slag particles extend in the direction of the rolling.

Fig. 2 — Wrought Iron — Longitudinal — Etched (100×).

Etched in 5% picric acid in alcohol for 4 minutes. Structure shows bright, nearly white, grains of ferrite or alpha iron (carbonless iron) separated from each other by fine black lines. If deeply etched, some grains of the ferrite will darken. Some grains are larger than others. The size of the grain depends upon the amount of hot-work the metal has received and the temperature at which the hot-work was stopped. In general, the higher the temperature above the upper end of the critical range, the larger the grain size. Iron with larger grains will not be as strong as with fine uniform grains. Note that the slag streaks are still visible. If small dark areas appear at the corners of grains, this may be pearlite due to carbon. Too much of this gives the metal a hardening power that is undesirable in wrought iron. The best grade of wrought iron will contain practically no pearlite.

Fig. 3 — Wrought Iron — Cross-section — Unetched (100×).

Bright matrix of ferrite. Note the small dark spots. These are cross-sections of the slag streaks.

Fig. 4 — Wrought Iron — Cross-section — Etched (100×).

Etched in 5% picric acid in alcohol for 4 minutes. Bright, nearly white, grains are of ferrite. Note that the cross-sections of the slag streaks are still visible.

Fig. 5 — Slag in Wrought Iron — Unetched (500×).

Structure at 500 magnifications shows a slag streak surrounded by ferrite. Inside the dark gray iron silicate can be seen particles of iron oxide and phosphide.

Fig. 6 — Slag in Wrought Iron — Etched (500×).

Etched in 5% picric acid. The ferrite grains are here developed.

IRON (Plate XVII)

There are two commercial grades of pure iron, namely, Electrolytic Iron and Armco Iron. Electrolytic iron is obtainable of a degree of purity frequently exceeding 99.95% iron. The product of the open-hearth furnace, known as " American ingot iron " or " Armco " iron, generally contains more than 99.90% iron.

Fig. 7 — Electrolytic Iron — Unetched (100×).

The few dark particles are non-metallic impurities in a white matrix of ferrite.

Fig. 8 — Electrolytic Iron — Etched (100×).

Etched with 5% picric acid in alcohol for 3 minutes. This metal is found to be composed, like other pure metals, of allotriomorphic crystals in the form of crystalline grains. Bright, nearly white, polyhedral grains of ferrite separated by black hair-line boundaries are observed.

Fig. 9 — Armco Iron — Unetched (100×).

The few dark particles are non-metallic impurities in a white matrix of pure amorphous iron.

Fig. 10 — Armco Iron — Etched (100×).

Etched with 5% picric acid in alcohol for 3 minutes. Bright, nearly white, grains of ferrite. Same as Electrolytic Iron, except more non-metallic impurities are present.

STEELS (Plates XVII, XVIII, XIX)

A steel is an iron-carbon alloy which is malleable at least in some one range of temperature, and in addition is either (*a*) cast into an initially malleable mass; or (*b*) is capable of hardening greatly by sudden cooling; or (*c*) is both so cast and so capable of hardening. In this definition of steel the first sentence (" is malleable at least in some one range of temperature ") distinguishes steel from cast iron and pig iron; the second sentence (" is cast into an initially malleable mass ") distinguishes

it from malleable cast iron; and the third sentence (" is capable of hardening greatly by sudden cooling ") distinguishes it from wrought iron. (Stoughton.)

Fig. 11 — Soft Steel (C 0.15%) — Unetched (100×).

The few dark particles are non-metallic impurities in a white matrix of ferrite.

Fig. 12 — Soft Steel (C 0.15%) — Etched (100×).

Etched in 5% picric acid in alcohol for 5 minutes. White areas are ferrite grains, dark areas are pearlite particles. Pearlite is the eutectoid alloy of the iron-carbon series. It contains about 0.85% carbon and is a mixture of ferrite (Fe) and cementite (Fe_3C). When steel containing it is allowed to cool very slowly, it has a laminated appearance. Its appearance is sometimes likened to finger prints. In this condition it is called laminated pearlite. If cooled more rapidly but not too rapidly, it looks granular and is then called sorbitic pearlite. These structures may be better seen in steels having a greater amount of carbon or observed at higher magnifications.

Since pearlite has a much greater tensile strength than ferrite, the strength of steels will increase as the pearlite increases. Hence these steels will be stronger than ingot iron and somewhat stronger than wrought iron. Soft steels are used for boiler plates and tubes, rivets and bolts, and when containing less than 0.2% carbon, they may be case-hardened readily. Soft steels are also used for structural purposes.

Fig. 13 — Mild Steel (C 0.3%) — Etched (100×).

Etched in 5% picric acid in alcohol for 5 minutes. As the carbon increases the pearlite increases likewise so that in the higher-carbon steels it predominates. In these steels the grains are of pearlite (dark) and of ferrite (white). As the amount of pearlite increases in steel, so the hardening power of steel increases. Hence steels in this range can be hardened more than soft steels. Steels in this range are used for reinforcing bars for concrete, rails, axles, shafts, gun-jackets, steel castings, some tools, gears, dies, wire, etc.

Fig. 14 — Medium Steel (C 0.5%) — Etched (100×).

Etched in 5% picric acid in alcohol for 5 minutes. The structure is similar to the previous specimen, but shows more pearlite and less ferrite. It has similar uses as mild steel. It is especially used for parts which are to be subjected to shock and heavy reversals of stresses as in axles and crank pins.

Fig. 15 — Semi-Hard Steel (C 0.8%) — Etched (100×).

Etched in 5% picric acid in alcohol for 5 minutes. As the composition gets close to the eutectoid composition, the major part of the microstructure is pearlite. Hypo-eutectoid steels (less than about

0.85% C) show small white areas of ferrite surrounding dark pearlite grains. Steel of eutectoid composition is of maximum strength and also has the maximum hardening power. Some rails contain as much as 0.7% carbon. Tool steel falls in this range as does also spring steel. It is also used for dies, car wheels, punches and drills.

Fig. 16 — Hard Steel (1.0%) — Etched (100×).

Etched in 5% picric acid for 5 minutes. This structure is that of hyper-eutectoid steel. The major part of the microstructure is pearlite, which is surrounded by thin envelopes of the hard, brittle cementite at the grain boundary. This steel is too hard for many machine parts and is too brittle for many structural uses. It is used for tools for lathes, springs, dies, drills, reamers, files, etc.

Fig. 17 — Very Hard Steels (C 1.4%) — Etched (100×).

Etched in 5% picric acid in alcohol for 5 minutes. Steels in this range are very hard and brittle due to the additional free cementite. Since cementite is very low in tensile strength (about 5000 lb. per sq. in.) this steel is not as strong in tension as that of eutectoid composition. Cementite is the hardest natural constituent of steel, hence this steel is harder than eutectoid steel. An examination of the microstructure shows pearlite grains (dark) surrounded by cementite (white). These hard cementite membranes of low tensile strength make the steel extremely brittle. By certain methods of heat-treating these hard cementite membranes may be prevented and in this case the steel is not so brittle. The cementite, in the latter case, occurs as small white particles rather uniformly distributed. It is called "spheroidal" cementite. In this form steel has excellent wearing properties because the cementite is very hard and is embedded in a softer matrix. Furthermore, the steel is more easily machined in this condition than when the cementite occurs as hard membranes at the grain boundaries.

Very hard steel around this composition is used for drills, general lathe work, dies for wire drawing, special tools, etc.

Fig. 18 — Extra Hard Steels (C 1.7%) — Etched (100×).

Etched in picric acid in alcohol for 5 minutes. Steels in this range are extremely hard and brittle. The structure is similar to the specimen above but shows more cementite at the grain boundary of the pearlite. This steel is used for steel cutting saws, wire drawing dies, and special tools.

Fig. 19 is the same as Fig. 16 but shows the 1.0% carbon steel at 500 magnifications. Note the laminated structure of the grains of pearlite.

Fig. 20 is the same as Fig. 17 but shows the 1.4% carbon steel at 500 magnifications. Note the hard cementite surrounding the laminated grains of pearlite.

Fig. 21 shows the iron-carbon thermal equilibrium diagram, including the steels and cast irons.

Fig. 22 gives the curves showing the change in the physical properties of the normal iron-carbon alloys with increase in carbon content.

CONSTITUENTS OF STEELS

Ferrite. — Ferrite in iron and steel is not pure iron but rather iron holding in solid solution small amounts of silicon, phosphorus, and other impurities. It is soft, ductile and relatively weak. It has a tensile strength about 40,000 to 50,000 lb. per sq. in. and an elongation about 40% in 2 in. It is highly magnetic, has high electric conductivity, but no hardening power. In slowly cooled irons and steels, ferrite crystallizes in the body-centered cubic lattice. The polygonal grains of ferrite therefore consist of a large number of little cubic crystals.

Cementite. — In slowly cooled steels the carbon is always combined with a definite amount of iron to form a " carbide of iron," corresponding to the chemical symbol Fe_3C. This compound consists of 6.67% carbon and 93.33% iron, and is micrographically known as " cementite." It is an extremely hard and brittle substance with a very low tensile strength. In those steels containing less than 0.85% carbon, it exists as irregular-shaped laminated plates along with ferrite, but with higher percentages of carbon it is present in the massive form. The tensile strength of cementite is about 5000 lb. per sq. in. Its hardness is about 272 times that of ferrite.

Pearlite. — Pearlite is not a simple substance, but consists of two constituents, namely, interstratified layers or plates (lamellae) of ferrite and cementite in the proportion represented by the eutectoid point. It is formed on very slow cooling through the critical range and consists of about 87% ferrite and about 13% cementite. The field of a true pearlite area contains about 0.85% carbon. Its tensile strength is between 125,000 and 130,000 lb. per sq. in. and its elongation is about 10% in 2 inches. Pearlite has maximum hardening power.

Eutectoid Steels. — Steel made up exclusively of pearlite is called " eutectoid " steel. It contains about 0.85% carbon. Steel containing less than 0.85% carbon or thereabout, and in which, therefore, some free ferrite is present, is called " hypo-eutectoid," while steel containing more than 0.85% carbon, that is, more highly carburized than eutectoid steel, is called " hyper-eutectoid." Hyper-eutectoid steels contain free cementite.

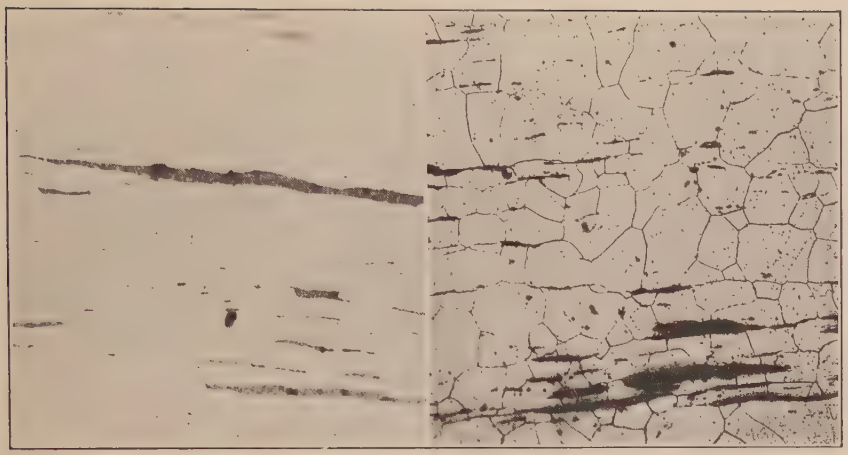

FIG. 1 FIG. 2

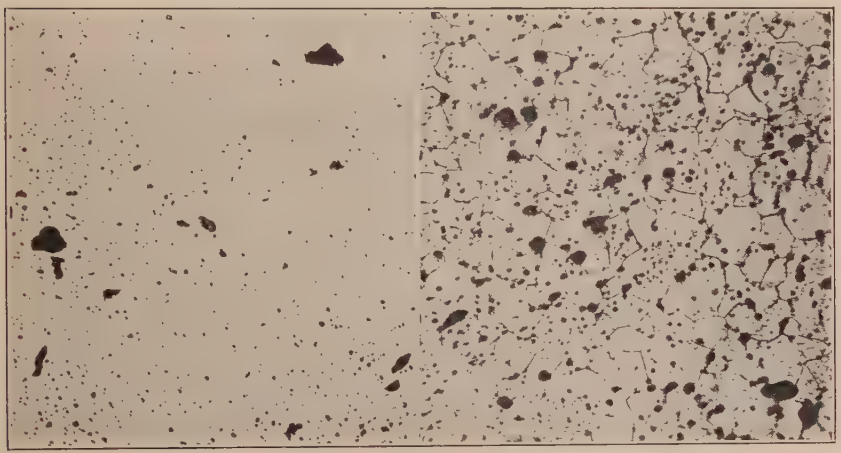

FIG. 3 FIG. 4

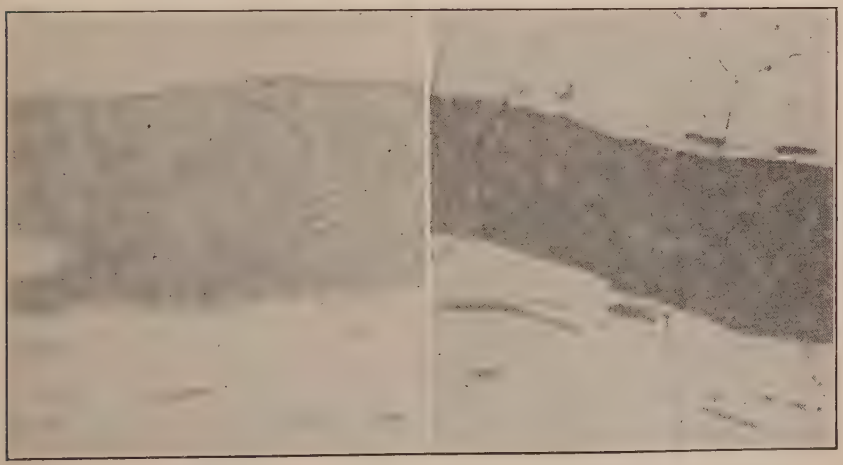

FIG. 5 FIG. 6

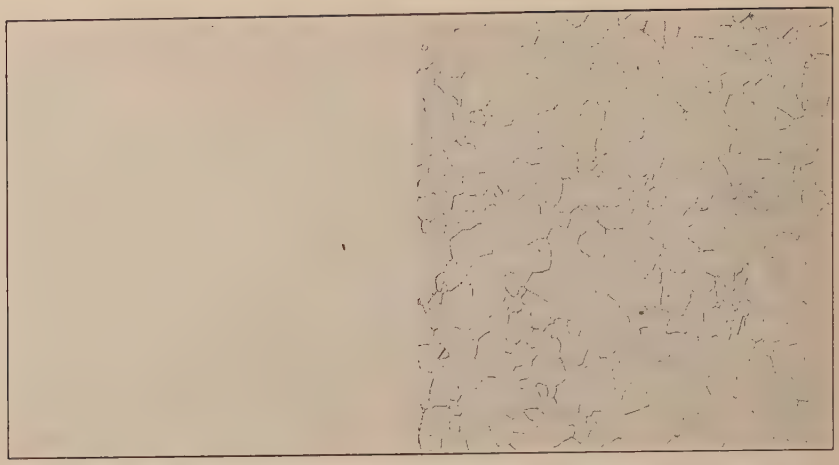

FIG. 7 FIG. 8

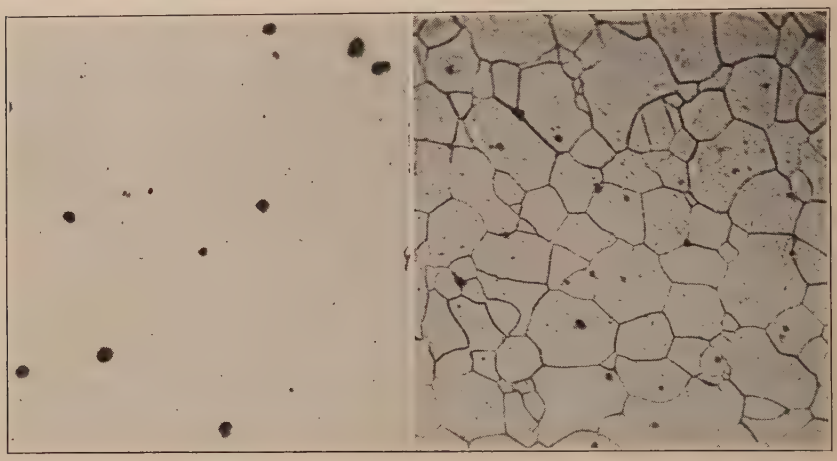

FIG. 9 FIG. 10

FIG. 11 FIG. 12

FIG. 13

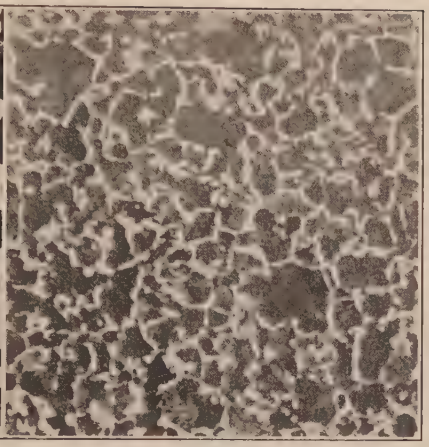

FIG. 14

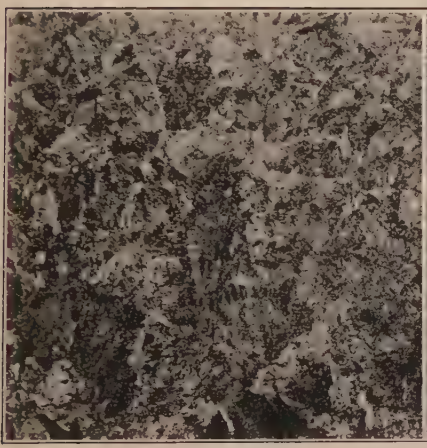

FIG. 15

FIG. 16

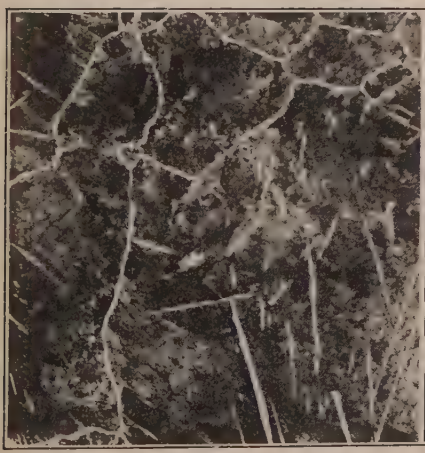

FIG. 17

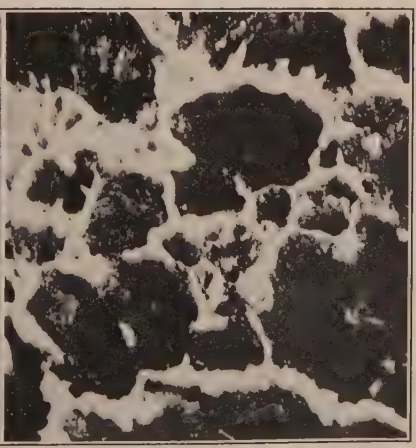

FIG. 18

PLATE XIX

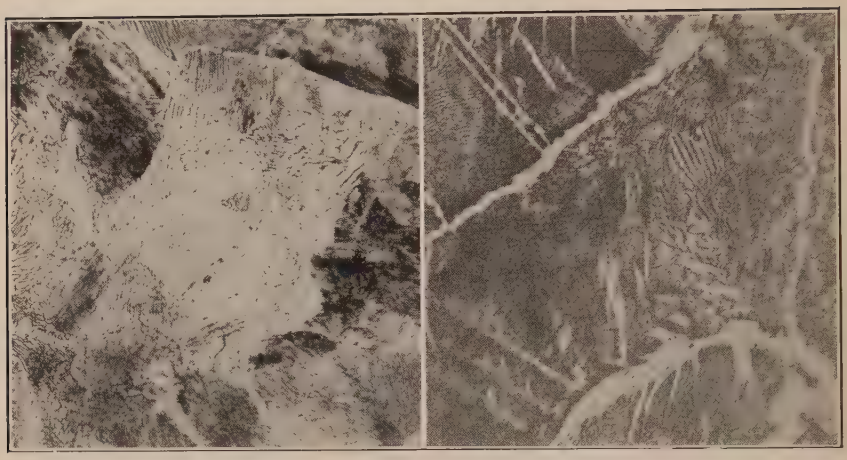

FIG. 19 FIG. 20

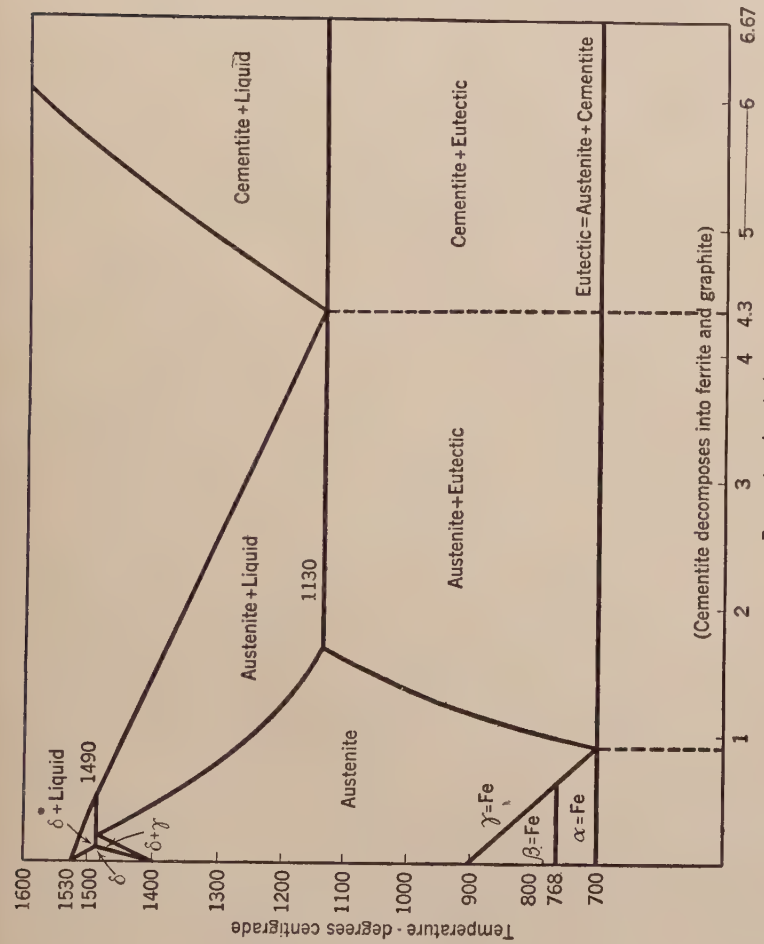

FIG. 21 Iron-Carbon Thermal Equilibrium Diagram (International Critical Tables, II)

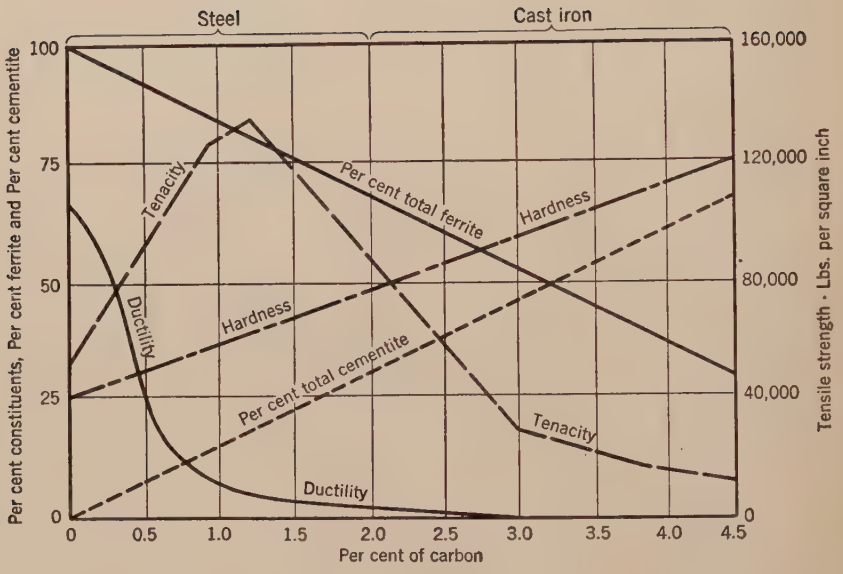
Steel
Cast iron
Per cent constituents, Per cent ferrite and Per cent cementite
Tensile strength - Lbs. per square inch
Per cent of carbon
100
75
50
25
0
160,000
120,000
80,000
40,000
0
0
0.5
1.0
1.5
2.0
2.5
3.0
3.5
4.0
4.5
Tenacity
Ductility
Hardness
Per cent total ferrite
Hardness
Per cent total cementite
Tenacity
Ductility

FIG. 22 (Howe)

EXPERIMENT X

CAST IRONS

Purpose: To study the microstructures of pig iron, gray cast iron, white cast iron and malleable cast iron.

References: Sauveur: Metallography and Heat Treatment of Iron and Steel, Chapters XXI and XXIII.

Guillet and Portevin: Metallography and Macrography, pp. 154–156.

Williams and Homerberg: Principles of Metallography, pp. 174–182.

Theory: Cast iron is a carbon-iron alloy in which the total carbon content ranges from 2.5 to 5.0%. The high carbon content deprives the alloy of malleability and it is this property which distinguishes the cast irons from the steels. The carbon present in cast iron may be wholly in the graphitic condition, wholly in the combined condition as iron carbide (Fe_3C), or partly in the graphitic condition and partly in the combined condition.

There are three classes of true cast irons, namely, white cast iron, gray cast iron and malleable cast iron. Pig iron is an impure gray cast iron cast from the blast furnace, while mottled cast iron is a grade of cast iron that is midway between a white cast iron and a gray cast iron. The latter two irons are usually not included in the classification.

White cast iron has all the carbon in the combined state as iron carbide and it is consequently very hard and brittle. It is machined with the greatest difficulty and resists wear by abrasion very effectively. It has a tensile strength of 15,000 to 30,000 lb. per sq. in. White cast iron has very few uses. It is employed chiefly in the making of gray and malleable cast irons, and also as a hard surface on the outside of gray iron castings. It is called " white cast iron " due to its white, brilliant and highly metallic fracture.

Gray cast iron is graphitic cast iron. It lacks malleability and ductility due to the presence of the soft, friable and porous graphite which causes discontinuity in the metal. In gray cast irons the carbon is present in both the graphitic and the combined states. Its tensile strength varies from 15,000 to 40,000 lb. per sq. in., its crushing strength

is as high as 90,000 to 120,000 lb. per sq. in., while its ductility is exceedingly small. Gray cast iron is used for castings of all kinds.

In malleable cast iron the carbon is present entirely in the uncombined state as temper carbon. It is made by the long annealing of white cast iron until the brittle iron carbide is completely dissociated into ferrite and amorphous carbon. This dissociation of the hard, brittle cementite converts the non-malleable cast iron into a soft, malleable, easily machinable metal called " malleable cast iron." It has a tensile strength between 35,000 and 60,000 lb. per sq. in., an elastic limit between $2\frac{1}{2}$ and $7\frac{1}{2}\%$ in 2 in., and a reduction in area of $2\frac{1}{2}$ to 8%. Thus it has good strength and high toughness. It is used for automobile parts, railway equipment, pipes, pipe fittings, valves and for general agricultural equipment.

PHOTOMICROGRAPHS — (Plates XX–XXI)

Fig. 1 — Pig Iron (C 3.5%) — Unetched (100×).

White areas are unetched polished surface of iron. Black areas are plates of uncombined carbon in the form of graphite. In pig iron these are usually large. They break up the uniformity of the iron and are the principal cause of its weakness and brittleness. Not all of the carbon is uncombined; some of it is in the combined state as Fe_3C.

Fig. 2 — Pig Iron (3.5% total C) — Etched (100×).

Etched in 5% picric acid in alcohol for 5 minutes. Note the black areas of uncombined carbon or graphite. The dark laminated areas are pearlite particles and the white areas may be ferrite or cementite, depending on whether the composition of the matrix is hypo-eutectoid or hyper-eutectoid. In this specimen the white areas are ferrite and some iron carbide (cementite). Silicon promotes the graphitization of cementite, that is, the formation of free graphite. Hence, if the iron is high in silicon, more carbon occurs as free graphite and less remains as cementite (Fe_3C). Such iron will very likely have its matrix hypo-eutectoid. When phosphorus is high in the iron, it may often be detected as a eutectic of $Fe + Fe_3P$ in the matrix. It appears as a light area with dark spots in it having somewhat the appearance of lace.

Fig. 3 — Gray Cast Iron — Unetched (100×).

Note that the carbon occurs in smaller plates, more uniformly distributed and more kinky than in the pig iron. The iron is thereby better interlocked and has somewhat better strength than pig iron. Specimen shows white surface of iron with black graphite plates and particles of non-metallic impurities

Fig. 4 — Gray Cast Iron — Etched (100×).

Etched in 5% picric acid in alcohol for 6 minutes. Jet black areas

are graphite, dark laminated areas are pearlite, and white areas are ferrite plus a small amount of undissociated cementite. Etching with sodium picrate will darken the cementite and leave the ferrite white. By this means the cementite can be differentiated from the ferrite.

Fig. 5 — White Cast Iron — Unetched (100×).

Relatively few small black areas. These are non-metallic inclusions — some slag, dirt and possibly some free carbon, but very little. Dove gray globules indicate manganese sulphide. Brownish ones indicate iron sulphide. White cast iron is produced by quick cooling of low-silicon iron. Since the temperature conditions (cold iron) in the smelting zone of the furnace that produce a low-silicon iron also produce a high-sulphur iron, and since manganese has great affinity for sulphur, white cast iron is very likely to contain iron and manganese sulphide. The white matrix is finely divided iron on the surface of the specimen due to polishing.

Fig. 6 — White Cast Iron — Etched (100×).

Etched in 5% picric acid in alcohol for 6 minutes. White areas are cementite. Dark areas are pearlite. This is produced by quick cooling. The quicker the cooling, the more cementite will be obtained and the harder the iron will be. Slow cooling from the freezing temperature to the critical temperature (700° C.) promotes the formation of free graphite from cementite thus:

$$Fe_3C + \text{heat} = 3\,Fe + C$$

This produces mottled iron if the rate of cooling is moderate and gray iron if the rate of cooling is very slow. The great hardness of white cast iron is due to the large amount of cementite it contains.

Fig. 7 — Malleable Cast Iron — Unetched (100×).

This specimen is Black Heart Malleable Cast Iron. White areas are unetched polished surfaces. Black areas are temper carbon. Malleable iron is made from white cast iron by annealing at a high temperature (about 1400° F.) for a considerable time (about 15 days). This promotes the formation of free graphite from the cementite (Fe_3C) in the iron. This free graphite collects in spongy masses within the iron. Some of it near the surface is practically burned out. In this form, the carbon does not injure the tensile strength of the iron nearly so much as it does when in the form of plates as in pig and gray iron.

Fig. 8 — Malleable Cast Iron — Etched (100×).

Etched in 5% picric acid in alcohol for 4 minutes. This is Black Heart Iron as above. White areas are ferrite grains with hair-line boundaries. Black areas are temper carbon. Practically all the cementite in the original white cast iron has been converted into ferrite

and temper carbon. This explains why malleable cast iron has the tensile strength of wrought iron and a high ductility as exhibited in the curling test. Malleable cast iron has remarkable shock resisting qualities.

PLATE XX

FIG. 1

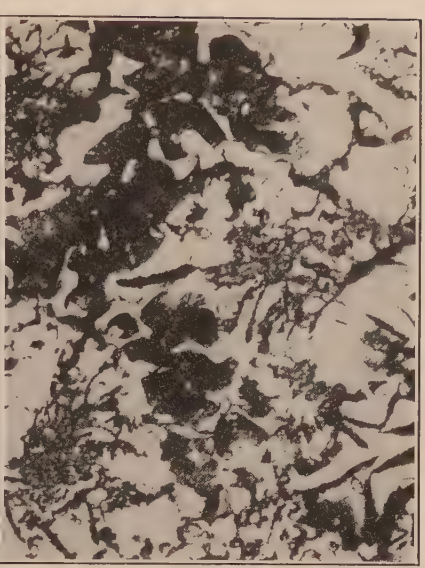

FIG. 2

FIG. 3

FIG. 4

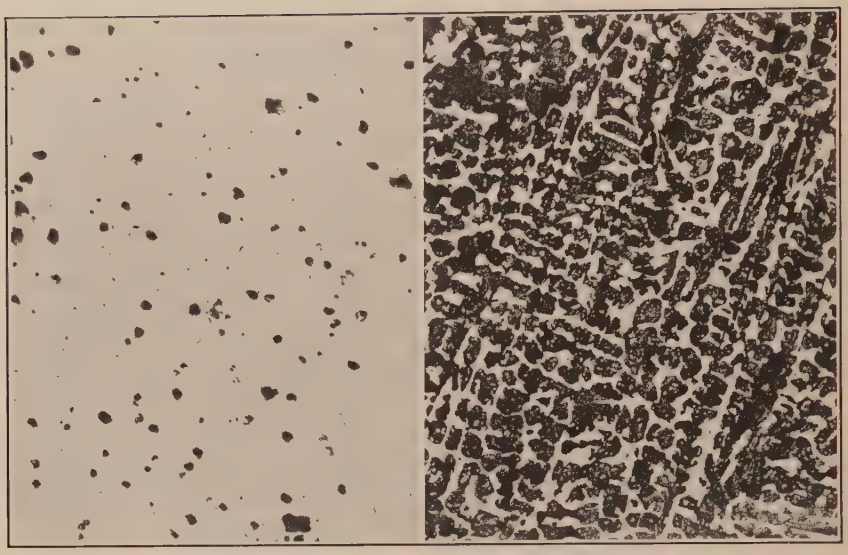

FIG. 5 FIG. 6

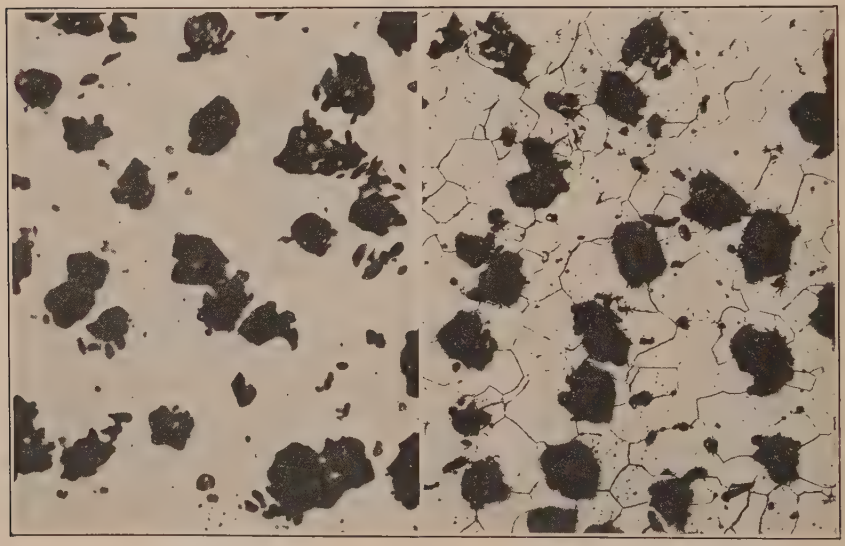

FIG. 7 FIG. 8

EXPERIMENT XI

METALLOGRAPHY OF HEAT-TREATED STEELS

Purpose: To study the effect of heat-treatment on grain size and structure of steels.

References: Sauveur: Metallography and Heat Treatment of Iron and Steel, Chapters XII and XIII.

Bullens: Steel and its Heat Treatment, Chapters III, V and VI.

Part A

EFFECT OF WATER QUENCHING REHEATED ANNEALED STEEL SPECIMEN FOR HEAT TREATMENT

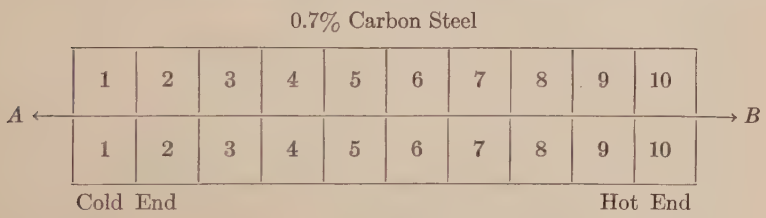

Heat-Treatment. — Heated uniformly to 1000° C., maintained at that temperature for 10 minutes, and air-cooled. Then the end numbered 10 was placed in the forge and raised to a very high temperature, practically burnt, while the end numbered 1 was kept at nearly room temperature with cold water. An effort was made to keep the temperature uniformly varying from the hot to the cold end. The piece was then completely quenched in cold water and broken with a hammer along the length *A–B*. The upper half was cut into the squares for microscopic study and the lower half was kept intact for macroscopic study at low magnifications.

Macroscopic Examination of Fracture (Plate XXVII, Fig. 26). — The broken surface of the specimen clearly shows, macroscopically, the effect of temperature on grain size of steel. Note that there is no apparent change in the fracture from the cold end (No. 1) up to about No. 6, then the fracture gets decidedly finer for a short distance and thereafter the grains increase in size as the hot end is approached, being the largest and coarsest at the hottest end. No appreciable change in

grain size occurs in steel heated for a short time below the critical range (700° C.), but when heated through the critical range grain refinement results, and on further heating above the critical range pronounced grain growth and coarsening of the steel take place.

Microscopic Examination of Fracture (Plates XXII–XXIII). — One half of the above specimen was cut into squares as numbered. The fractured edge of each piece was polished and etched for 5 minutes with 5% picric acid in alcohol. All photomicrographs are at 150 diameters.

Fig. 1 — No. 1. Cold end of specimen. Quenched at room temperature. White areas are pro-eutectoid ferrite. Dark areas are of sorbitic pearlite. Examination at high magnifications shows that this contains laminated pearlite also. The grain size is large due to the heating to 1000° C. and slow cooling therefrom.

Fig. 2 — No. 2. Quenched at about 100 to 200° C. Structure and grain size about same as No. 1.

Fig. 3 — No. 3. Quenched at about 200 to 350° C. Structure and grain size about same as No. 1 and No. 2.

Fig. 4 — No. 4. Quenched at about 350 to 475° C. Structure and grain size about same as No. 1, No. 2 and No. 3.

Fig. 5 — No. 5. Quenched at about 475 to 600° C. Structure and grain size about same as above.

Fig. 6 — No. 6. Quenched at about 600 to 675° C. Structure and grain size about same as above.

Fig. 7 — No. 7. Quenched at about 700 to 800. This specimen has been heated and quenched within the critical region. Light areas are regions of martensite, dark areas (many in the form of sections through nodules) are of troostite. This specimen varies in structure from ferrite and sorbite at the left end to troostite and martensite at the right end. (500×.)

Fig. 8 — No. 8. Quenched at about 800 to 1000° C. This specimen had been heated and quenched from a temperature above the critical range. Structure shows martensite and troostite. Troostite (black) is in the martensite matrix and at the grain-boundaries.

Fig. 9 — No. 9. Quenched at about 1000 to 1200° C. Structure shows all martensite with traces of troostite.

Fig. 10 — No. 10. Quenched at about 1200 to 1400° C. Structure shows austenite-martensite and pure martensite. The grains have increased in size and coarsened enormously. Specimen shows some cracks and oxide inclusions where the steel was actually burnt. Deep etching has brought out the sliver-like structure of the martensite.

From No. 1 through No. 10 the structure varies from ferrite and pearlite in the regions below the critical range to sorbitic pearlite, granu-

lated sorbite, black troostite and then to martensite when heated and quenched within and above the critical range. Where the troostite is alone, it is very dark, somewhat mottled but without any very definite structure. When martensite begins to appear, it usually appears as small, nearly white, irregular, sharp-pointed masses, which on deeper etching will show a sliver-like structure. At the hotter end of the specimen the martensite and austenite predominate. (A more drastic quench would have snown all austenite in No. 9 and No. 10, and perhaps in part of No. 8.)

When steel is cooled from a temperature above the critical range, various transition products may form. If cooled very suddenly, martensite, sliver-like in appearance, probably will form. This is the hardest transition product. If cooled quickly, but somewhat slower than required to produce martensite, troostite will form. In its first stages of formation, troostite appears as rounded dark spots, somewhat specked. They are sometimes described as sections through nodules. When the production of troostite has proceeded farther, these spots join and at first form grain-boundaries around martensite, and on further growth, become grown entirely together producing a dark, somewhat specked mass of indefinite structure. When etched with 5% HNO_3 or 5% picric acid, areas rich in troostite are noticeably darkened. This transition product is very hard and strong but not so hard as martensite.

Note that there is a decided change in grain size as the critical temperature on heating is passed.

Summary: The above series shows that no marked change in grain structure nor grain size occurs in annealed steel when heated to any temperature below its critical range, but as soon as the temperature exceeds the critical range a very marked change occurs. Furthermore the higher the temperature above the critical range, the *coarser* will be the structure. If the temperature is sufficient to start melting the steel, it is said to be burnt. Oxide particles form between grain-boundaries, and the steel is ruined. Sudden cooling from above the critical range produces martensite and troostite, both very hard. Slow cooling through the critical range produces pearlite or sorbite and free ferrite (if less than 0.85% C), all of which are comparatively soft and ductile. Sorbite is tougher than pearlite.

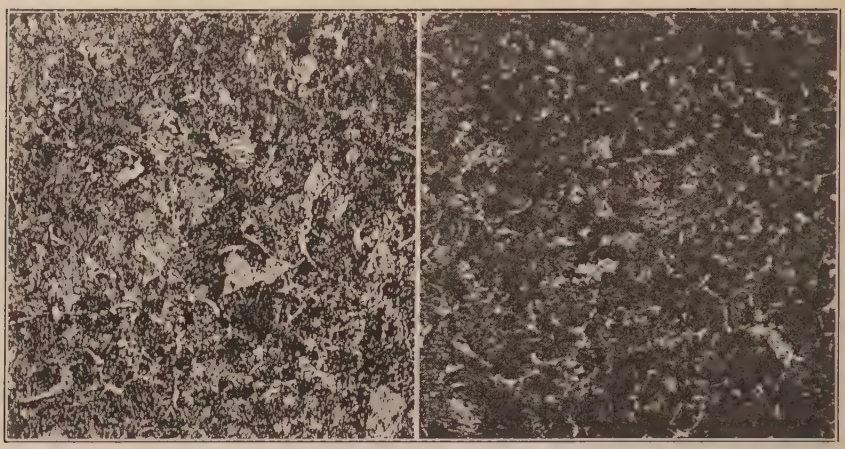

FIG. 1 FIG. 2

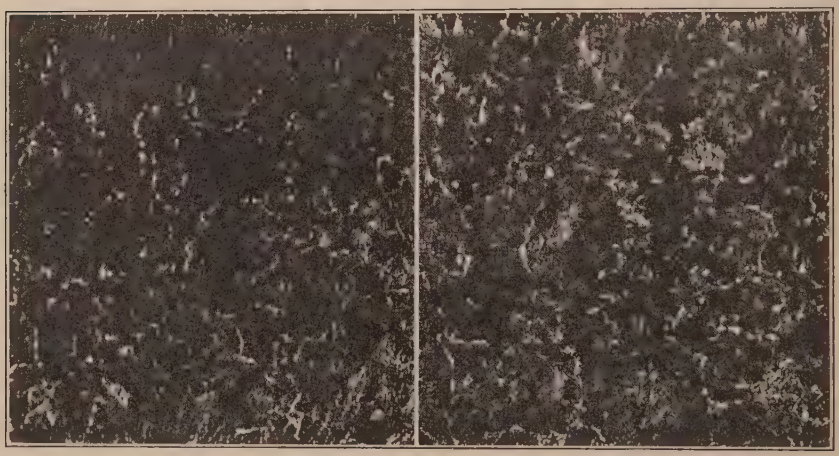

FIG. 3 FIG. 4

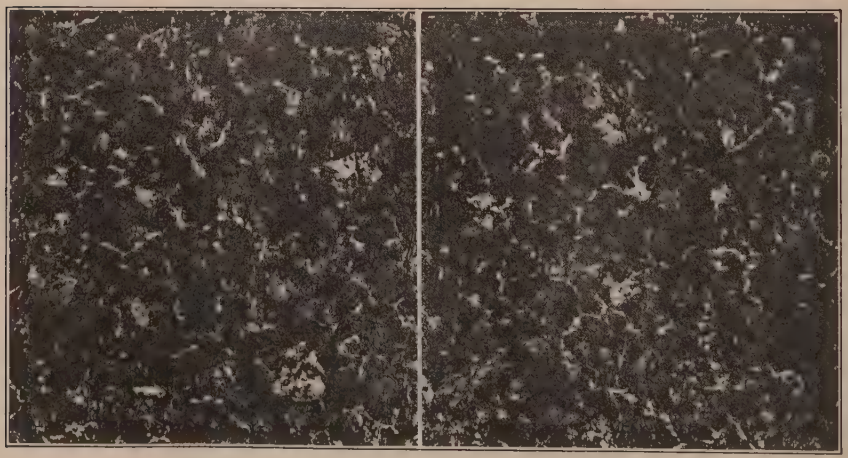

FIG. 5 FIG. 6

PLATE XXIII

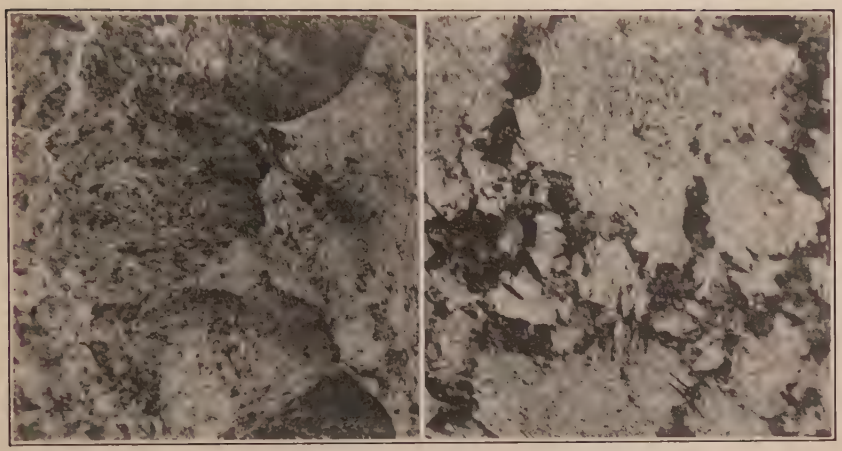

FIG. 7 FIG. 8

FIG. 9 FIG. 10

Part B

EFFECT OF REHEATING HARDENED STEEL — (Plates XXIV–XXV)

The following specimens, numbered from 1 to 10, were taken from a rod of 0.83% carbon steel about 10 in. long that was first uniformly heated to about 900° C. and then quenched in cold water, thereby hardening it uniformly throughout its length. Then one end of the rod, about 4 in. beyond No. 10, was placed in the gas forge and reheated to a temperature of about 1000° C. while the No. 1 end was left in the air and kept cold by pouring cold water over it. After heating for 5 minutes in this way, the temperature of the rod varied uniformly from about room temperature at No. 1 to a bright red heat at No. 10. Thus, the originally hardened rod was reheated to various temperatures up to and through the critical range. The whole rod was then quenched in cold water. Thus was produced in one rod steel that was *hardened*, steel that was *tempered* and steel that was *drawn* to such an extent that it was *toughened*.

Before breaking into small specimens, the Rockwell hardness numbers were taken throughout the length. These are recorded. Note the effect on the hardness of reheating hardened steel. All specimens were etched in 5% picric acid solution and shown at 150 magnifications.

Fig. 11 — No. 1. Cold end, as hardened. Quenched at room temperature. Structure is fine, sliver-like and typical of martensite, the hardest form in which the steel may be put by heat-treatment. Traces of black troostite are seen at the grain-boundaries.

Fig. 12 — No. 2. Quenched at about 100° C. Structure is similar to Fig. 1, but more black troostite can now be seen at the grain-boundary of the martensite.

Fig. 13 — No. 3. Quenched at about 200° C. Structure is similar to Fig. 2, but more troostite is present at the grain-boundaries.

Fig. 14 — No. 4. Quenched at about 300° C. Structure shows very much troostite and a small amount of untransformed white martensite.

Fig. 15 — No. 5. Quenched at about 400° C. Structure shows practically all troostite with traces of the old martensite and new sorbite. The structure would be expected to be all troostite where the steel had been reheated to about 400° C. At the end of the specimen that was at the highest temperature, sorbite, a speckled structure coarser than troostite, is found. Troostitic steels are tempered steels. Tempering is reheating a hardened steel to the troostitic structure.

Fig. 16 — No. 6. Quenched at about 500° C. Structure shows fine troostite and sorbite. This specimen is partially drawn.

Fig. 17 — No. 7. Quenched at about 600° C. Structure shows sorbite. Traces of troostite are still present. This specimen is a drawn steel having the tough sorbitic structure.

Fig. 18 — No. 8. Quenched at about 675° C. Structure shows the ductile sorbitic-pearlite. This specimen is a partially annealed steel.

Fig. 19 — No. 9. Quenched at about 750° C. Structure shows troostite with traces of sorbite and martensite. Reheating and quenching from a temperature above the critical range has reconverted the pearlite and ferrite to sorbite, then to troostite and finally to martensite.

Fig. 20 — No. 10. Quenched at about 900° C. Structure again, as in Fig. 1, shows martensite with some troostite at the grain-boundary. This specimen was deeply etched to develop the martensitic sliver-like structure.

Summary: These specimens have shown that steel that is *hardened* by quick cooling from above the critical range shows *martensite*; that reheating this at temperatures below the critical range first changes the martensite to troostite which is somewhat softer and then to *sorbite* which is still softer and tougher. To temper steel, it is first hardened and then reheated to a low temperature to draw out some of the hardness. The microstructure shows martensite or troostite or both. To *toughen* hardened steel, it should be reheated to a temperature near but somewhat below the lower end of the critical range. This reheating of hardened steel to temperatures below the critical temperature also lowers the hardness as is shown by the Rockwell hardness numbers.

Rockwell Hardness:

No. 1 — 59
2 — 58
3 — 58
4 — 57
5 — 59
6 — 41
7 — 38
8 — 39
9 — 59
10 — 60

Steel Structural Transitions (on Reheating) (approximate temperatures):

Austenite ——— up to 200° C. ——→ Martensite ——— up to 400° C. ——→ Troostite

Troostite ——— up to 600° C. ——→ Sorbite ——— up to 650° C. ——→ Pearlite

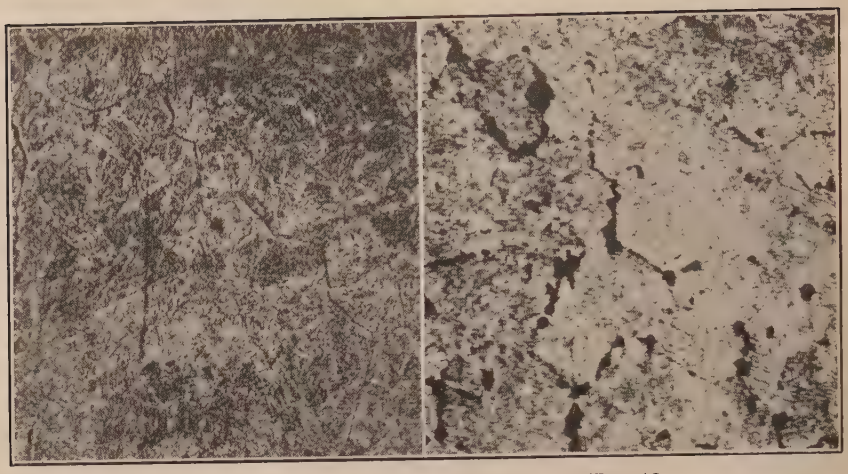

FIG. 11 FIG. 12

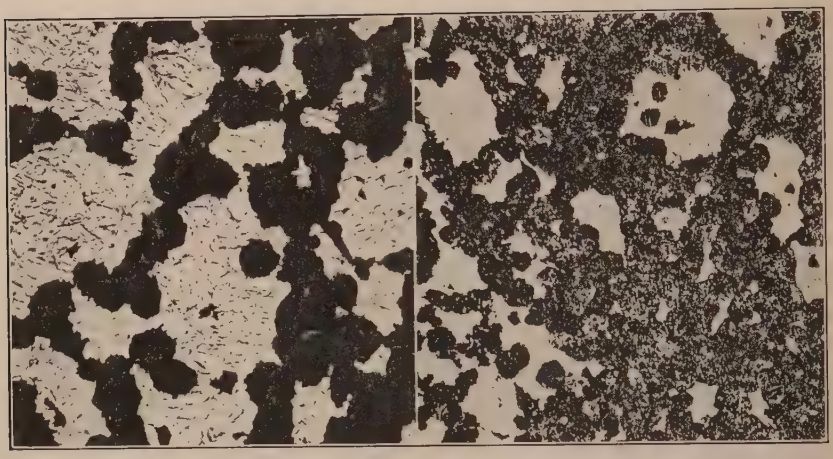

FIG. 13 FIG. 14

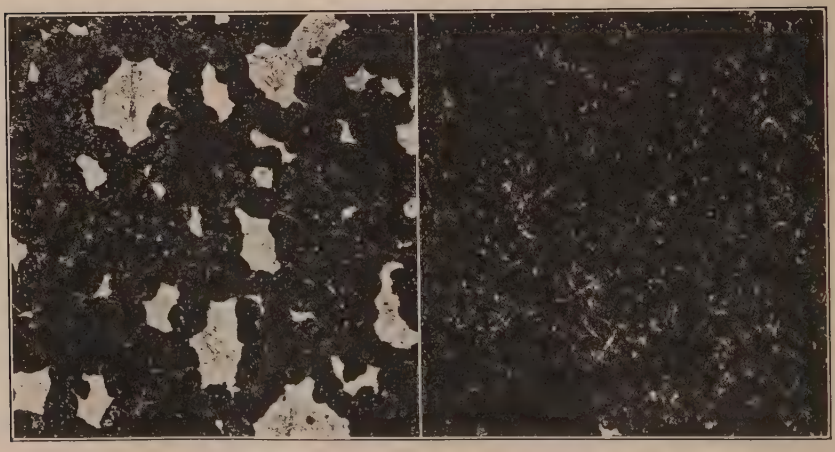

FIG. 15 FIG. 16

PLATE XXV

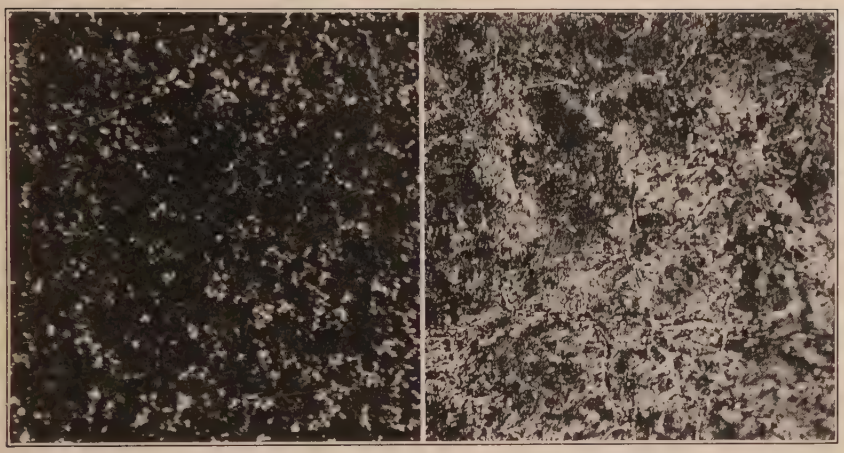

FIG. 17 FIG. 18

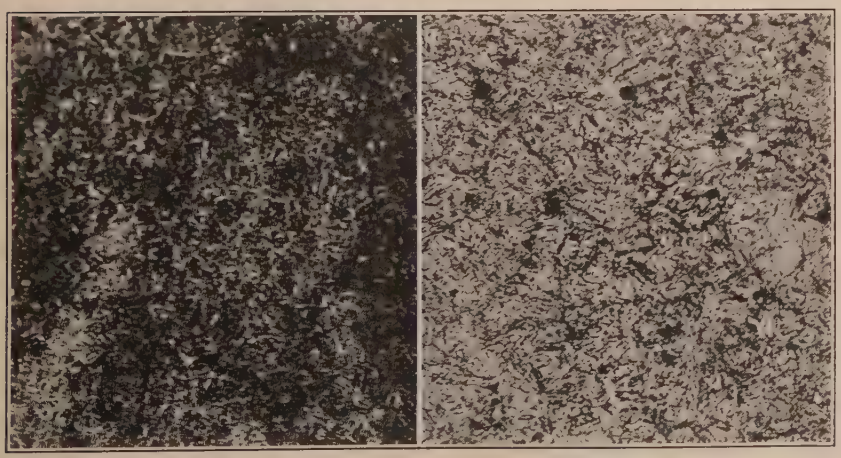

FIG. 19 FIG. 20

Part C

EFFECT OF RATE OF COOLING THROUGH CRITICAL RANGE— (Plate XXVI)

The following five specimens were taken from a piece of 0.60% carbon steel that had been hot-rolled. One specimen shows the structure as hot-rolled. The other four were heated to about 900° C. and cooled in various ways as indicated (500 magnifications).

Fig. 21 — No. 1. As received. Etched in 5% picric acid in alcohol for 5 minutes. Bright areas are ferrite. Dark areas are of pearlite. Pearlite predominates due to the composition. Grain size is rather small and nearly uniform.

Fig. 22 — No. 2. Quenched in *ice water* from 900° C. Etched in 5% HNO_3 for 3 seconds and 5% picric acid for 1 minute. Structure shows bright areas containing small dark sliver-like streaks in several directions. This is the characteristic structure of *martensite*, which is the first transition product formed when austenite is transformed into pearlite at the critical temperature. Martensite is produced by quickly cooling steel from temperatures well above the critical range.

Fig. 23 — No. 3. Quenched in oil from 900° C. Etched as No. 2. Bright areas are martensite. Dark areas, some having the appearance of sections through nodules, are troostite, the second transition product formed when austenite is transformed to pearlite. Troostite etches very quickly and the surface of the specimen is noticeably darkened where the troostite is plentiful. Deeper etching will develop the martensite into its characteristic appearance. Troostite is not so hard as martensite and is more ductile and tough. Oil quenching is not so harsh as ice water and hence the steel does not so easily crack when quenched in oil.

Fig. 24 — No. 4. Cooled in the *air* from 900° C. Etched in 5% picric acid in alcohol for 5 minutes. Bright areas are ferrite. Dark areas are sorbite and pearlite. Sorbite is somewhat speckled. Pearlite is laminated and looks somewhat like a finger print. This is best observed at high magnifications. The grain size in this is not very uniform but in no place is it larger than in No. 1. Sorbite is the third transition product formed in cooling austenite. It is softer and tougher than troostite.

Fig. 25 — No. 5. Cooled in and with the *furnace* from 900° C. Etched as No. 4. Bright areas are ferrite. Dark areas are pearlite.

That the pearlite is laminated is best observed at high magnifications. Pearlite is the softest form that austenite can be transformed into and is the product sought when steel is given a dead soft anneal. Due to the length of time that the steel is at temperatures above the critical range when it is given a dead soft anneal, the grain size will be somewhat large.

Summary: These five specimens have shown that very pronounced differences in structure are produced by varying the rate of cooling through the critical range. When these typical microstructures are properly correlated with the physical properties of the steel, it is possible to tell the physical properties of a given steel quite closely by an examination of the microstructure only. Furthermore, when the conditions necessary to produce these typical structures are thoroughly understood, a microscopic examination alone will reveal what sort of heat-treatment the steel has undergone. This is often very valuable in determining the cause of failure in steel that has failed in service.

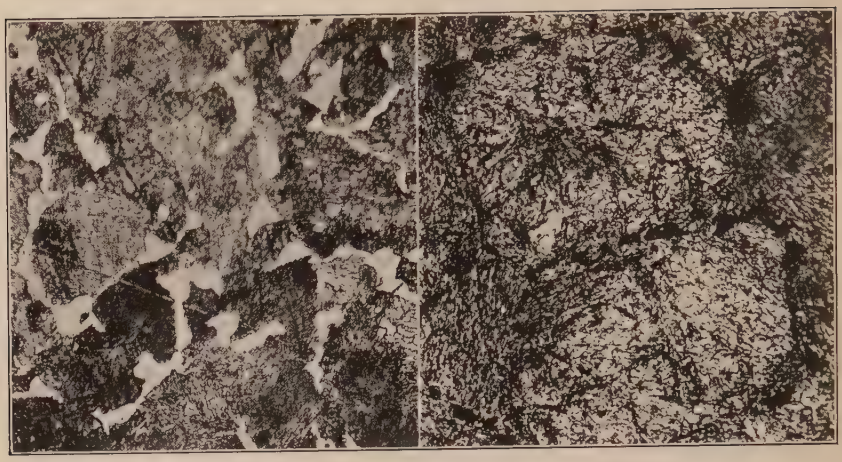

FIG. 21 FIG. 22

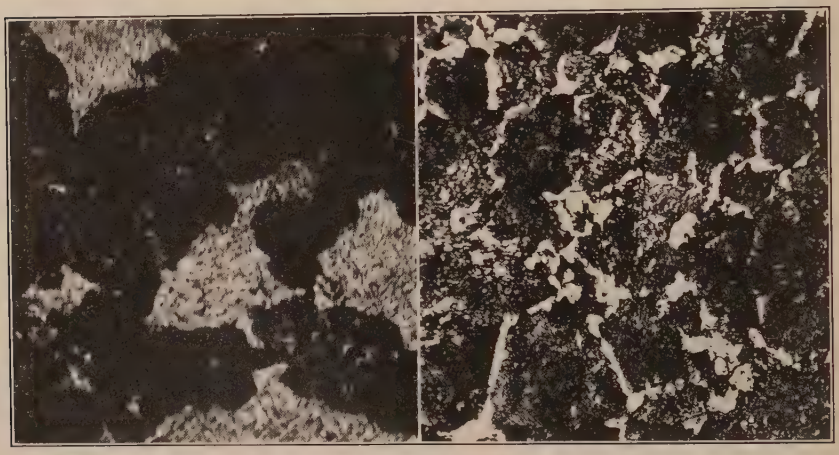

FIG. 23 FIG. 24

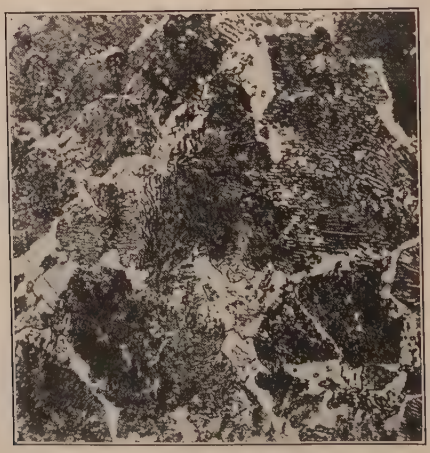

FIG. 25

PLATE XXVII

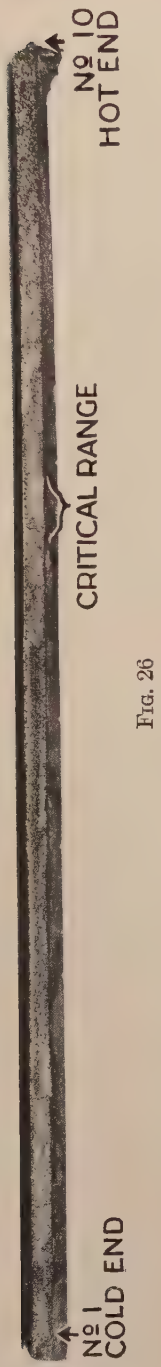

FIG. 26

CONSTITUENTS OF HEAT-TREATED STEELS

Austenite. — Austenite is a solid solution of finely dispersed carbon or iron carbide in gamma iron. It is obtained only in carbon steels containing upwards of 1.0% carbon by very rapid quenching from temperatures above 1000° C. and in special alloy steels with less drastic quenching. Austenite is usually associated with more than 30% martensite in carbon steels. It is non-magnetic. The iron atoms (gamma iron) have the face-centered cubic lattice. Austenite is relatively soft and ductile as compared to martensite.

Martensite. — Martensite is obtained by quenching carbon steels from temperatures above their highest recalescence point, when the whole of the carbide is in solid solution. Martensite usually does not form in steels of less than 0.15% carbon. It has an interlacing needle-like structure, the markings of which are often disposed in triangular formation. The structure is fine-grained, submicroscopic in size. The iron atoms in martensite have the body-centered cubic lattice (alpha iron). Martensite is the hardest and also the most brittle, having extremely high tensile strength with little or no ductility. Martensite is magnetic. It is considered as a decomposition of austenite along the octahedral crystallographic planes.

Troostite. — Troostite is an emulsion of small cementite particles in fine-grained alpha iron. It is obtained in any steel regardless of carbon content by modifying temperature of quenching or rate of cooling. It is also obtained in " tempering," that is, by heating martensite or austenite to 400° C. or by cooling to the temperature of liquid air. Troostite is rather soft and more ductile than martensite of the same carbon content.

Sorbite. — Sorbite is a finer form of " pearlite," often called Sorbitic-Pearlite. It is regarded as the transition stage between troostite and pearlite. Sorbite is an emulsion of cementite particles in alpha iron, the particles of which, however, are larger than in troostite. Sorbite, although it is slightly less ductile than pearlite for a given carbon content, has such high tenacity and elastic limit that a higher combination of these three properties can be had in sorbitic than in pearlite steels. Steels that are so treated as to contain sorbite are often called " toughened steels." Sorbite may be considered as granulated pearlite.

For contrast with the normal and heat-treated steels, there are shown, in Plate XXVIII, Figs. 27, 28, 29 and 30, photomicrographs at 30 diameters of a 0.40% carbon steel in the as cast condition. It will be observed that the structure is very coarse with irregular, interlocking grains of ferrite and pearlite. Steel in the cast condition has a decreased ductility.

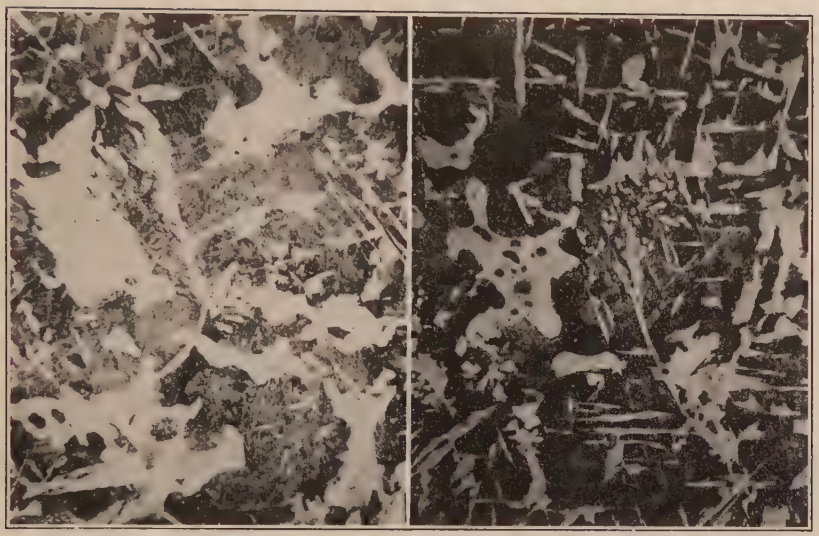

FIG. 27 FIG. 28

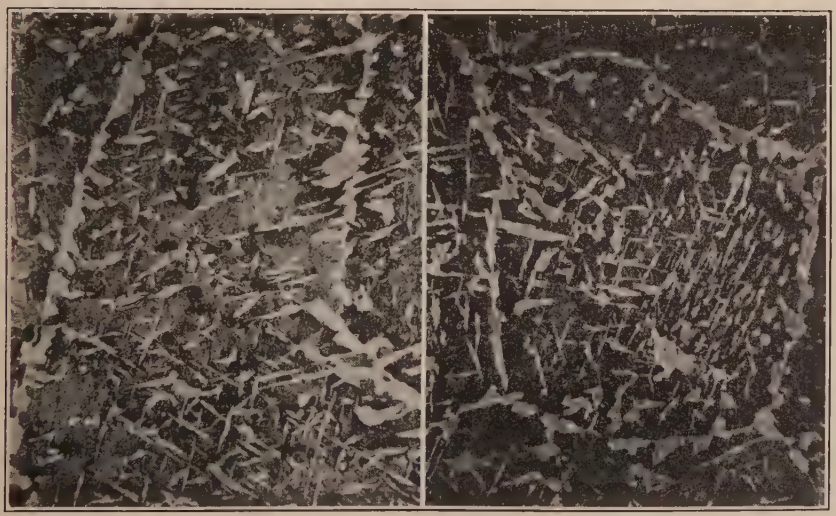

FIG. 29 FIG. 30

EXPERIMENT XII

ALLOY STEELS

Purpose: To study the microstructure of alloy steels in comparison with straight carbon steels.

References: Sauveur: Metallography and Heat Treatment of Iron and Steel, Chapters XIX and XX.

Bullens: Steel and its Heat Treatment, Chapters IX through XXI.

Williams and Homerberg: Principles of Metallography, pp. 163–173.

Theory: In addition to the elements sulphur, phosphorus, silicon and manganese always found in commercial steels, other metals are added to give further or improved properties to the steels. Normalized carbon steels owe their properties chiefly to the proportion of carbon present, whereas, normalized alloy steels owe their properties in a marked degree to the presence of special elements. The most important special elements used are nickel, chromium, manganese, copper, silicon, vanadium, tungsten, molybdenum, cobalt and a few others. Some of these metals, like nickel, silicon and copper, dissolve in the ferrite to strengthen and toughen the matrix; whereas others like chromium, tungsten, manganese and vanadium form double carbides with the iron greatly increasing the hardness.

Nickel dissolves completely in the ferrite and consequently increases the hardness and tensile strength with a slight decrease in ductility. This means a tougher steel. The high-nickel steels of 25% to 35% nickel are extremely tough and dense, have a high resistance to shock and a low coefficient of expansion, and in particular are little subject to corrosion.

Chromium forms complex carbides with iron, producing hard and strong steels with high elastic limit and little loss in ductility and toughness. It has a marked effect with proper carbon-chromium ratio upon magnetic properties and resistance to corrosion. It is usually used with nickel in the ratio of $2\frac{1}{2}$ parts of nickel to 1 part of chromium to combine the improvement of ductility and toughness conferred by nickel with the increased strength and hardness conferred by chromium. It is also used with vanadium and other elements.

Manganese is twice as effective as nickel and produces increased strength, hardness and toughness. It partly dissolves in the ferrite and partly forms complex carbides. High-manganese steels have remarkable resistance to cutting and abrasion.

Copper dissolves in the ferrite, strengthening the steel and increasing its resistance to corrosion.

Silicon dissolves in the ferrite as iron silicide (FeSi) up to its saturation value and accelerates the formation of graphitic carbon.

Vanadium improves the steel through its powerful deoxidizing and scavenging effect and as an alloying element, producing a high combination of tensile strength, elastic limit, ductility and great resistance to wear, shock and alternate stresses. Vanadium chiefly forms carbides with iron, but partly dissolves in the ferrite.

Tungsten forms carbides with iron, greatly increasing the hardness, strength, toughness and resistance to abrasion at high speeds.

Molybdenum has an influence on steels similar to that of tungsten, but several times more intense. It produces greater ductility and toughness for a given elastic limit, and a higher ratio of elastic limit to tensile strength. Molybdenum steels have remarkable resistance to impact and are easily worked and easily machined.

PHOTOMICROGRAPHS — (Plates XXIX through XXXII)

Fig. 1 — Charcoal Iron (100×).

C 0.04%; S 0.019%; Mn 0.042%; Si 0.008%; P 0.044%.

Etched in nitric acid. Structure shows grains of ferrite, slag and other non-metallic inclusions. This structure is characteristic of wrought iron. The grain size is moderate. A considerable amount of slag, occurring principally in streaks is present. This metal has a tensile strength of 50,750 lb. per sq. in., a proportional limit of 28,000 lb. per sq. in., an elongation of 43.0% in 2 in. and a reduction in area of 59.5%.

Fig. 2 — Nickel Iron (100×).

C 0.045%; Mn 0.17%; S 0.020%; P 0.017%; Si 0.01%; Ni 2.08%.

This photomicrograph shows the structure of a 13-in. × 13-in. bloom, forged to 9 in. round, normalized at 900° C. for 9 hours and air-cooled. The physical properties of this alloy are: tensile strength 52,500 lb. per sq. in., yield point 38,700 lb. per sq. in., elongation in 2 in. 33.0%, reduction in area 74.0% and Brinell hardness 112. Microstructure shows uniform grains of the nickel-iron solid solution with faint traces of pearlite at the grain-boundary.

Fig. 3 — Copper-Molybdenum Steel (100×).

C 0.04%; Mn 0.32%; S 0.020%; P 0.012%; Cu 0.44%; Mo 0.14%.

This photomicrograph shows the structure of a 13-in. × 13-in. bloom, forged to 9 in. round, normalized 900 °C. for 9 hours, air-cooled. The tensile strength is 50,950 lb. per sq. in., the yield point is 30,100 lb. per sq. in., the elongation is 35% in 2 in., the reduction in area is 60.3% and the Brinell hardness is 97. Structure shows uniform grains of the copper-molybdenum-iron solid solution with pearlite at the grain-boundary.

Fig. 4 — Transformer Iron-Silicon Alloy (100×).

C 0.07%; Mn 0.14%; S 0.022%; P 0.020%; Si 4.04%.

This photomicrograph shows the structure of 24 gage transformer sheet stock, showing Neumann lines and recrystallization along slip planes. The grains of the iron-silicon solid solution are rather coarse but uniform.

Fig. 5 — Nickel-Chrome-Molybdenum Steel (100×).

C 0.349%; Mn 0.99%; S 0.034%; P 0.018%; Si 0.22%; Cr 0.20%; Ni 1.40%; Mo 0.20%.

This photomicrograph shows the structure of a billet forged to $2\frac{3}{4}$ in. round and normalized at 900° C. It has a tensile strength of 115,500 lb. per sq. in., a yield point of 97,900 lb. per sq. in., an elongation of 18.5%, a reduction in area of 53.3% and a Brinell hardness of 241. Structure shows very small uniform grains of the nickel-molybdenum-iron solid solution with the black pearlite at the grain boundary.

Fig. 6 — Nickel-Vanadium Steel (100×).

C 0.52%; Mn 0.81%; S 0.035%; P 0.018%; Si 0.15%; Cr 0.09%; V 0.20%; Ni 0.20%.

This photomicrograph shows the structure of a bloom forged to $2\frac{3}{4}$ in. round, and normalized at 900° C. It has a tensile strength of 121,000 lb. per sq. in., a yield point of 77,300 lb. per sq. in., an elongation of 17.0%, a reduction in area of 35.7% and a Brinell hardness of 217. Structure shows small white grains of nickel-vanadium-iron solid solution and small black grains of pearlite (sorbitic pearlite).

Fig. 7 — Low Manganese Steel (100×).

C 0.485%; Mn 0.66%; S 0.03%; P 0.016%; Si 0.11%.

This photomicrograph shows the structure of an ingot forged to $2\frac{1}{2}$ in. round, heated to 845° C. for 3 hours, air-cooled, reheated to 705° C. for 3 hours and furnace-cooled. It has a tensile strength of 84,300 lb. per sq. in., a yield point of 45,000 lb. per sq. in., an elongation in 2 in. of 27.0%, a reduction in area of 51.9% and a Brinell hardness of 163. Structure shows white ferrite and laminated black pearlite.

Fig. 8 — Nickel-Manganese Steel (100×).

C 0.20%; Mn 0.62%; S 0.022%; P 0.018%; Si 0.15%; Ni 3.40%.

Photomicrograph shows the structure of a billet forged to 6 in.

round, normalized at 900° C. for 6 hours, air-cooled. It has a tensile strength of 84,800 lb. per sq. in., a yield point of 58,900 lb. per sq. in., an elongation of 23.0% in 2 in., a reduction in area of 43.4% and a Brinell hardness of 156. Structure shows white ferrite and laminated pearlite. The manganese is in the pearlite as manganese carbide.

Fig. 9 — Stainless Iron (500×).

C 0.08%; Mn 0.40%; P 0.025%; S 0.025%; Si 0.40%; Cr 14.0%.

Etched in saturated solution of ferric chloride in HCl plus small amount of HNO_3. Structure shows grains of ferrite plus black particles of sorbite and specks of carbide.

Fig. 10 — Stainless Iron (toughened) (100×).

C 0.08%; Mn 0.40%; P 0.025%; S 0.025%; Si 0.40%; Cr 14.0%.

Etched in saturated solution of ferric chloride in HCl plus small amount of HNO_3. Specimen was heated to 980° C., held for 20 minutes and quenched in oil. It was then tempered at 650° C. for 30 minutes. Structure shows all sorbite with traces of ferrite.

Fig. 11 — Stainless Steel (500×).

C 0.37%; Si 0.37%; S 0.011%; P 0.015%; Mn 0.54%; Ni 0.22%; Cr 14.71%.

Etched in aqua regia. This steel was forged, annealed at 800° C. for one hour and furnace-cooled. Photomicrograph shows a martensitic structure with the carbide non-uniformly distributed.

Fig. 12 — Stainless Steel (500×).

C 0.37%; Si 0.37%; S 0.011%; Mn 0.54%; Ni 0.22%; Cr 14.71%; Cu 0.08%; V 0.04%.

Etched in dilute aqua regia. Alloy was heat-treated by heating to 870° C., cooling in furnace, then reheated to 1000° C. for $\frac{1}{2}$ hour and cooled in oil. Structure shows particles of the complex chromium-iron carbides in ground mass of extremely fine martensite. This alloy has a tensile strength of 262,500 lb. per sq. in.; a yield point of 106,900 lb. per sq. in.; an elongation in 2 in. of 10.0% and a reduction in area of 21.5%.

Fig. 13 — Corrosion Resisting Steel (500×).

C 0.42%; Si 1.77%; S 0.015%; Mn 0.78%; Ni 20.75%; Cr 6.80%; Cu 1.52%.

Etched in dilute HNO_3. Structure shows the precipitation of the complex iron-chromium carbide in the nickel-chromium-gamma iron solid solution matrix. This steel was heat-treated by holding at 980° C. for 4 hours and air-cooling. It has a tensile strength of 96,000 lb. per sq. in., an elongation of 35.8% in 2 in., a reduction in area of 58.2% and a Brinell hardness of 159.

Fig. 14 — Aero-Valve Steel (100×).

C 0.32%; Si 1.11%; S 0.031%; Mn 0.61%; Ni 19.90%; Cr 6.96%.

Etched in ferric chloride. Structure shows twinned grains of the nickel-iron solid solution with free carbide particles. This alloy has a tensile strength of 105,600 lb. per sq. in.; an elongation of 24.3% in 2 in. and a reduction in area of 65.0%.

Fig. 15 — Silicon-Zirconium Steel (500×).

C 0.52%; Si 1.44%; S 0.023%; P 0.024%; Mn 0.66%; Ni 0.12%; Cr 0.16%; Cu 0.06%; V 0.30%; Zr 0.1%.

Etched in 2% alcoholic nitric acid. Specimen is a 1 in. round bar forged from 4-in. × 6-in. billet. Specimen was heated ½ hour at 955° C., water-cooled to 27° C., reheated to 565° C. for 1 hour and quenched in oil. Structure shows extremely fine sorbite on the patterns of the original martensite. Note at left and at right inclusions and zirconium nitride crystals embedded in crystal of zirconium sulfide. This alloy has a tensile strength of 173,900 lb. per sq. in.; a proportional limit of 140,600 lb. per sq. in.; an elongation in 2 in. of 14.0%; and a reduction in area of 37.0%.

Fig. 16 — Silicon-Zirconium Steel (500×).

C 0.52%; Si 1.44%; S 0.023%; P 0.024%; Mn 0.66%; Ni 0.12%; Cr 0.16%; Cu 0.06%; V 0.30%; Zr 0.1%.

Etched in 2% alcoholic nitric acid. Specimen is a 1-in. round bar forged from a 4-in. × 6-in. billet. Specimen was heated to 845° C. for ½ hour, air-cooled, reheated to 565° C. for 1 hour and cooled in oil. Structure shows grains of sorbite and ferrite, typical of shallow-hardening medium-carbon alloy steels. Note crystals of zirconium nitride and zirconium sulfide. This alloy has a tensile strength of 122,200 lb. per sq. in.; a proportional limit of 66,200 lb. per sq. in.; an elongation in 2 in. of 22.5%; and a reduction in area of 47.9%.

Fig. 17 — Duriron (500×).

Si 14.50%; Mn 0.50%; P 0.05%; S 0.05%; temper carbon 0.80%; Fe balance.

Etched in glycerol 2 parts, 30% HF 2 parts, and nitric acid 1 part. This is a sand-cast acid resistant metal. Structure shows primary grains of the alpha solid solution of FeSi in iron and the eutectic of alpha solid solution and iron silicide (FeSi). It has a tensile strength of 18,000 lb. per sq. in. It is practically impossible to obtain a yield point on this material, and there is practically no reduction in area. Duriron is very brittle.

Fig. 18 — Duriron (500×).

Si 14.50%; Mn 0.50%; P 0.05%; S 0.05%; temper carbon 0.80%; Fe balance.

Etched in glycerol 2 parts, 30% HF 2 parts, and nitric acid 1 part.

This is a medium chill Duriron specimen. Structure shows large grains of the alpha solid solution and the fine Fe-FeSi eutectic.

Fig. 19 — Nickel Cast Iron (500×).

Temper carbon 3.61%; combined carbon 0.62%; Si 1.48%; Ni 1.23%; Fe balance.

Etched in 2% Nital. Structure shows small particles of ferrite in a fine sorbitic pearlite matrix, with evenly-distributed graphite flakes. This is a typical nickel alloyed cast iron possessing high strength and a very good machineability as well as hardness. It has a tensile strength of 31,860 lb. per sq. in.; a transverse strength of 4510 lb. per sq. in.; and a Brinell hardness of 192.

Fig. 20 — Nickel-Chrome Cast Iron (500×).

Temper carbon 3.04%; combined carbon 0.75%; Si 1.39%; Ni 0.96%; Cr 0.33%; Fe balance.

Etched in 2% Nital. Structure shows small patches of free cementite in a sorbitic-pearlite matrix, with a few graphite flakes. The ratio of nickel to chromium has served to increase the strength and hardness without forming an excessive amount of cementite. This structure represents a very good wear-resistant, strong and close-grained iron. It has a tensile strength of 43,000 lb. per sq. in.; a transverse strength of 4570 lb. per sq. in.; and a Brinell hardness of 234.

PLATE XXIX

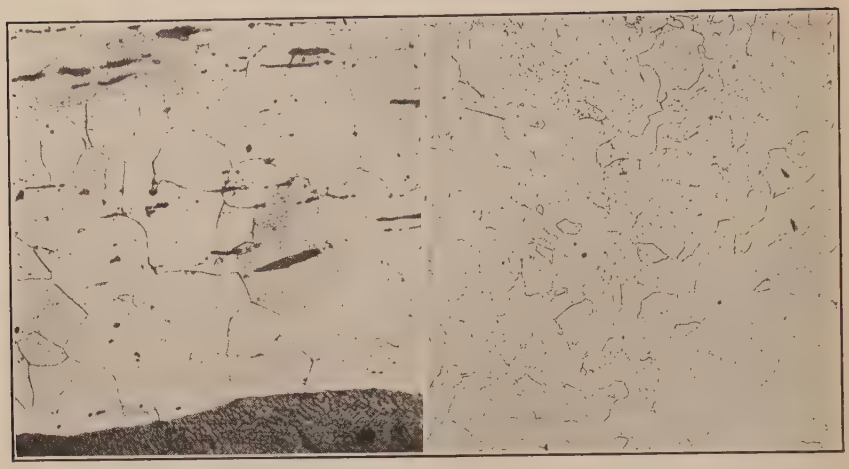

FIG. 1 FIG. 2

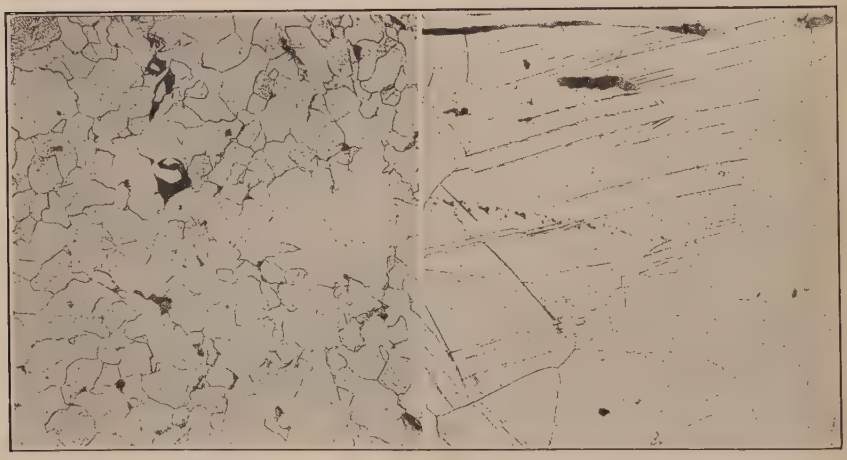

FIG. 3 FIG. 4

PLATE XXX

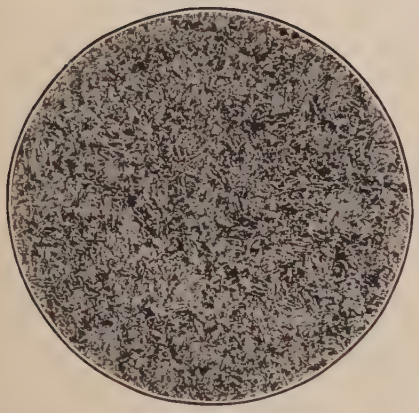

FIG. 5

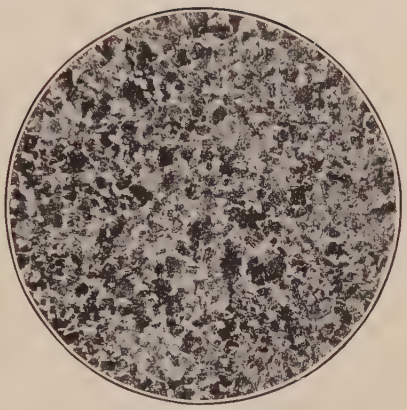

FIG. 6

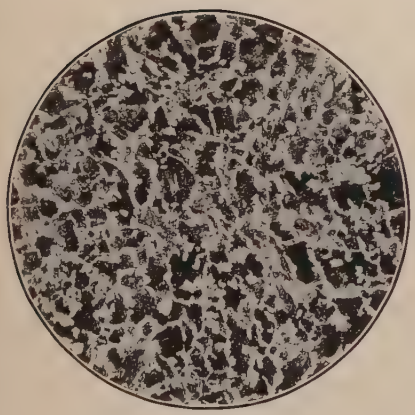

FIG. 7

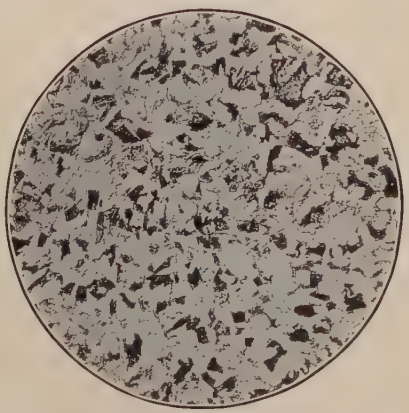

FIG. 8

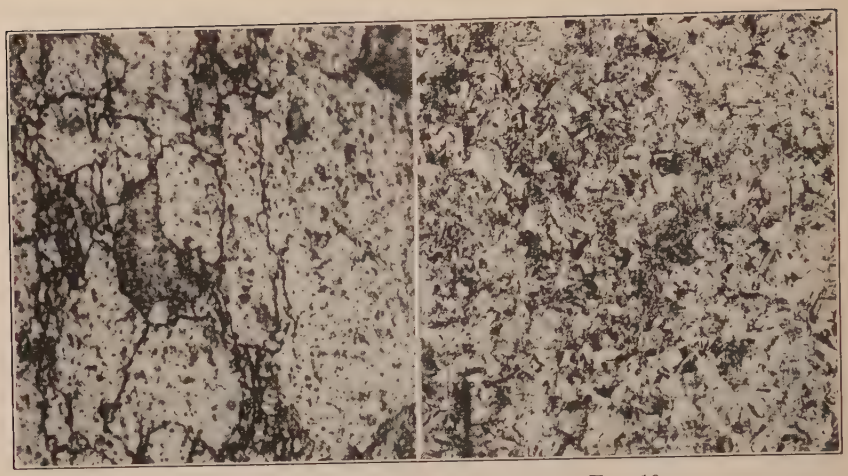

FIG. 9 FIG. 10

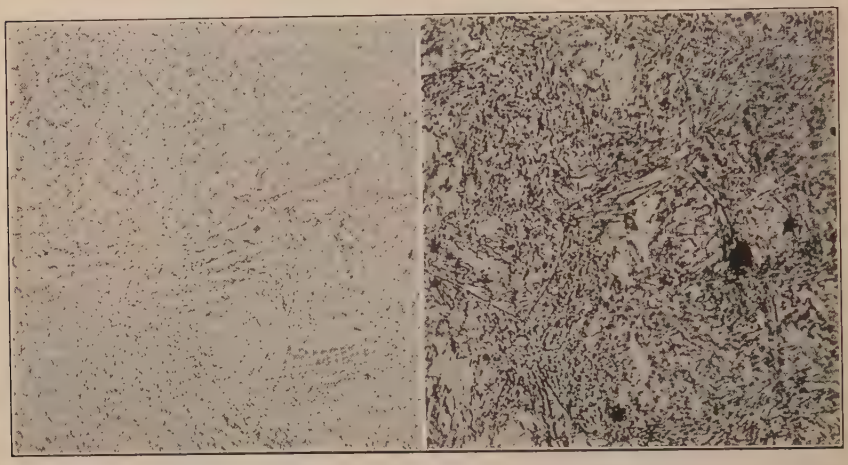

FIG. 11 FIG. 12

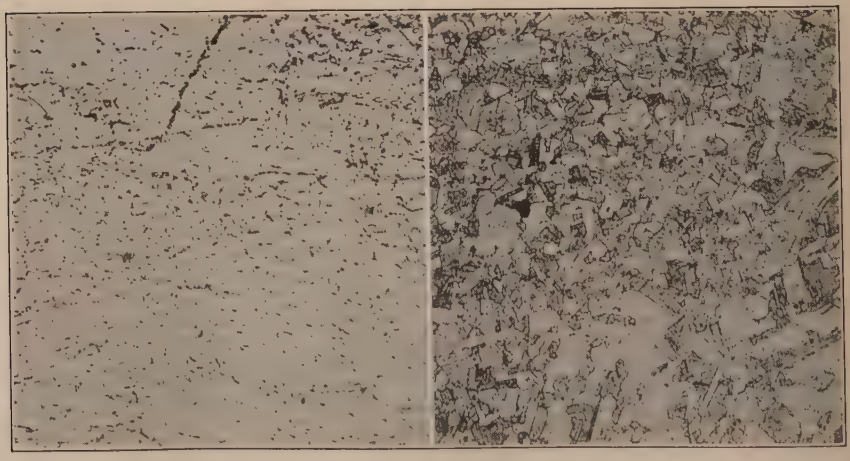

FIG. 13 FIG. 14

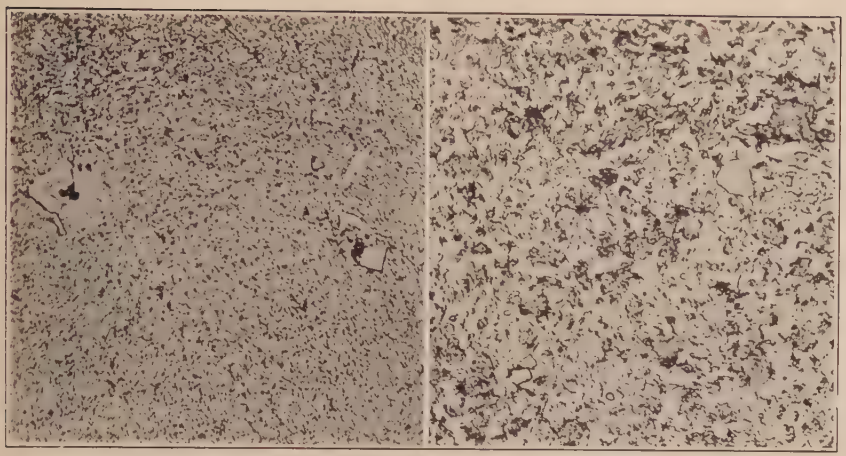

FIG. 15 FIG. 16

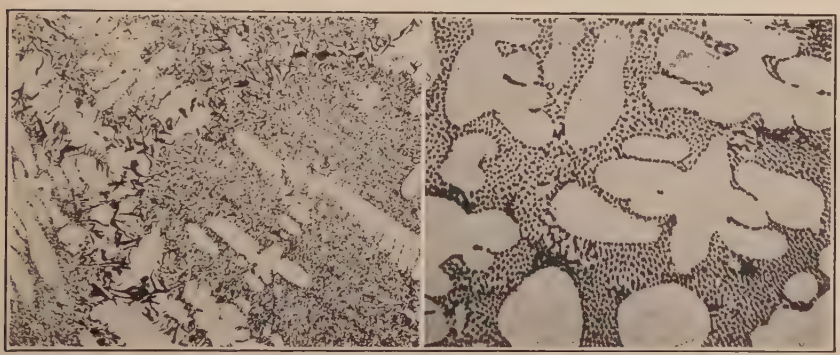

FIG. 17 FIG. 18

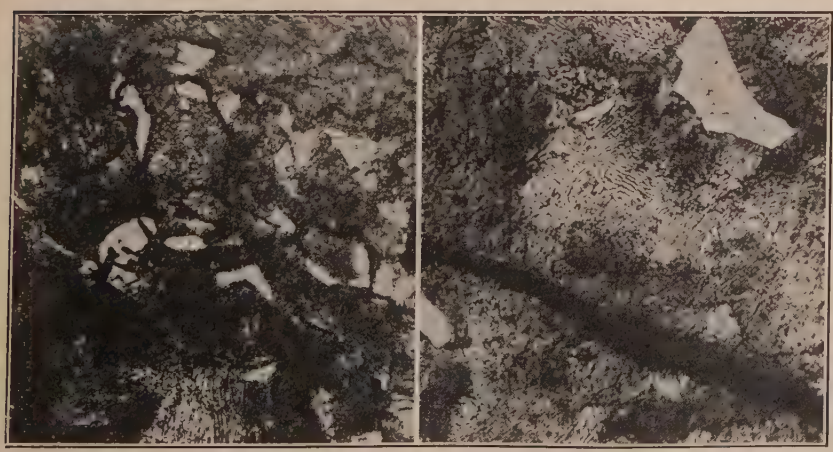

FIG. 19 FIG. 20

EXPERIMENT XIII

CASE-HARDENING

Part A

CARBURIZING STEEL

Purpose: To study the method and results of the cementation and the case-hardening of steel.

References: (*a*) Sauveur: Metallography and Heat Treatment of Iron and Steel, Chapter XVIII.

(*b*) Bullens: Steel and its Heat Treatment; Chapters VII and VIII.

Materials: Seven specimens of low-carbon steel (not over 0.2% C) as supplied, charcoal and barium carbonate.

Apparatus: Electric furnace, graphite crucibles with covers, metallographic polishing and etching outfit, metallographic microscope, Brinell hardness testing machine, Shore scleroscope hardness testing machine.

Theory: The object of case-hardening or partial cementation (carburization) is the production of a hard exterior wearing surface (the "case") on low-carbon steel, and, at the same time, the retention or increase of the toughness of the interior (the "core") of the metal. The process may be divided into two distinct periods: first, the carburization or impregnation of the surface by which the carbon content is raised sufficiently to give a steel capable of taking on very great surface hardness; second, suitable heat treatment to develop the properties of both "case" and "core." Briefly, the aim is to get a steel which shall possess minimum fragility and a maximum surface hardness.

The affinity of iron for carbon is so great that when heated to a sufficiently high temperature in contact with some suitable carbonaceous matter the iron readily absorbs some of that element. The proportion of carbon in the outer layer, and the depth to which it penetrates, will depend chiefly on the temperature and the time of contact between the steel and the carbonaceous matter.

Procedure: (*a*) *Effect of Carburizing Mixture on Depth of Case.*

Heat a sample of the steel of carbon content not over 0.2% in a mixture of 60% charcoal and 40% barium carbonate in the covered graphite crucible for at least 2 hours at 1000° C.

Likewise heat another specimen of the same steel in 100% charcoal for the same time and at the same temperature.

At end of specified time, furnace-cool each specimen.

PHOTOMICROGRAPHS — (Plate XXXIII)

Fig. 1 — As Received (100×).

Etched in 5% picric acid. White areas are grains of free ferrite. Small black areas at grain-boundaries are grains of pearlite. At high magnifications the pearlite is seen to be laminated.

Fig. 2 — Case-Hardened in 100% Charcoal (100×).

Etched in 5% picric acid. Photomicrograph shows the case of maximum carburization. Structure shows grains of pearlite plus envelopes of ferrite at the left nearer the core and 100% pearlite at the extreme outer fiber of the case at the right of the photomicrograph. The case-hardening increased the carbon content at the outer fibers of this specimen from 0.15% to 0.85%.

Fig. 3 — Case-Hardened in Charcoal — $BaCO_3$ Mixture (100×).

Etched in 5% picric acid. Photomicrograph shows case of maximum carburization. Structure at left shows pearlite plus envelopes of ferrite and at the right the structure shows pearlite plus envelopes of cementite. The case-hardening increased the carbon content at the outer fibers of this specimen from 0.15% to about 1.0%.

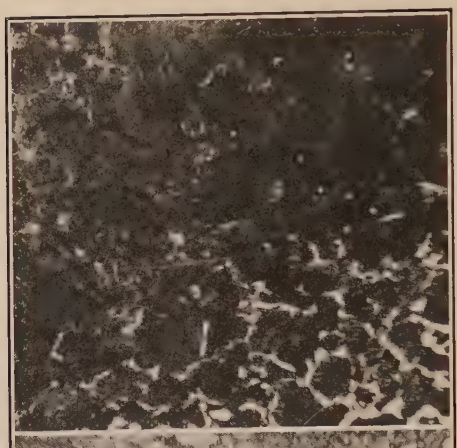

FIG. 3

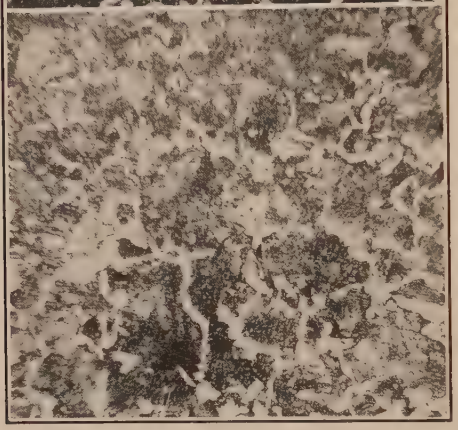

FIG. 2

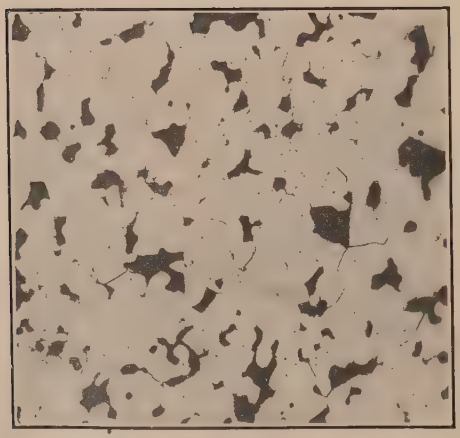

FIG. 1

(*b*) *Effect of Time on Depth of Case.*

Heat 4 samples of the steel in a mixture of 60% charcoal and 40% barium carbonate in 4 covered graphite crucibles at 1000° C. Remove specimen No. 1 at the end of the first hour, specimen No. 2 at the end of the second hour, specimen No. 3 at the end of the third hour and specimen No. 4 at the end of the fourth hour. Cool each specimen in a bed of sand.

PHOTOMICROGRAPHS — (Plate XXXIV)

Fig. 4 — As Received (100×).

Etched in 5% picric acid. White areas are grains of free ferrite. Small dark areas at grain-boundaries are regions of pearlite.

Fig. 5 — Case-Hardened for One Hour (100×).

Etched in 5% picric acid. Photomicrograph shows the outer case or maximum carburization of the specimen at the end of the first hour of case-hardening. Structure shows large, coarse grains of pearlite surrounded by thick membranes of ferrite. The case shows a maximum of about 0.65% carbon content.

Fig. 6 — Case-Hardened for Two Hours (100×).

Etched in 5% picric acid. Photomicrograph shows the outer case or maximum carburization of the specimen at the end of the second hour of case-hardening. Structure shows large, coarse grains of pearlite with thin envelopes of cementite. The case shows a maximum of about 1.0% carbon content.

Fig. 7 — Case-Hardened for Three Hours (100×).

Etched in 5% picric acid. Photomicrograph shows the outer case or maximum carburization of the specimen at the end of the third hour of case-hardening. Structure shows large, coarse grains of pearlite with long needles and envelopes of white cementite. The case shows a maximum carburization of about 1.2% carbon content.

Fig. 8 — Case-Hardened for Four Hours (100×).

Etched in 5% picric acid. Photomicrograph shows the outer case or maximum carburization of the specimen at the end of the fourth hour of case-hardening. Structure shows large, coarse grains of pearlite surrounded by thick membranes of cementite. The case shows a maximum of about 1.4% carbon content.

Fig. 4

Fig. 5

Fig. 6

Fig. 7

Fig. 8

The following 6 photomicrographs (Figs. 9 through 14) (Plate XXXV) show the change in microstructure of case-hardened alloy steels as the carbon penetrates through the outer fiber of the specimens to the core.

Case-Hardening of a Chrome-Vanadium Alloy Steel, Figs. 9, 10, 11.

C 0.15/0.25%; Mn 0.50/0.80%; S 0.04%; P 0.04%; Cr 0.80/1.10%; V 0.18%; Fe balance.

Carburized at 1650° F. for 6 hours and furnace-cooled.

Fig. 9 — Core (100×).

Structure shows uniform grains of ferrite (white) and pearlite (black) in the core or non-carburized zone

Fig. 10 — Hypo Zone (100×).

Photomicrograph shows a section midway between the core and the outer fibers of the case. The carbon content increases gradually from the core to the outer fibers. Structure shows increasing amount of pearlite and decreasing amount of ferrite as we proceed from the core to the case. At the extreme right of the photomicrograph the structure shows 100% pearlite, that is, 0.85% carbon steel.

Fig. 11 — Hyper Zone — Case (100×).

Photomicrograph shows the outer fibers of the specimen, that is, the case itself, where maximum carburization has occurred. Structure shows a hyper-eutectoid steel, black grains of pearlite surrounded by thin envelopes of cementite.

Case-Hardening of a Nickel Alloy Steel, Figs. 12, 13, 14.

C 0.10/0.20%; Mn 0.30/0.60%; S 0.045%; P 0.04%; Ni 3.25/3.75%.

Carburized at 1690° F. for 6 hours and furnace-cooled.

Fig. 12 — Core (100×).

Structure shows uniform grains of ferrite (white) and pearlite (black) in the core or non-carburized zone.

Fig. 13 — Hypo Zone (100×).

Structure shows an increasing quantity of carbon (pearlite) from the core to the case.

Fig. 14 — Hyper Zone — Case (100×).

Photomicrograph shows the structure of the outer fibers or case, black, laminated grains of pearlite and white needles and envelopes of cementite.

Discussion: The barium carbonate-wood charcoal mixture produces about twice the carbon penetration that wood charcoal alone produces. This is due to the carbon monoxide formed which penetrates the steel deeper. Also, the amount of carburization taking place and the thickness of the case are directly proportional to the time and the temperature of case-hardening. However, as the carbon content of the case increases, the rate of carburization gradually decreases.

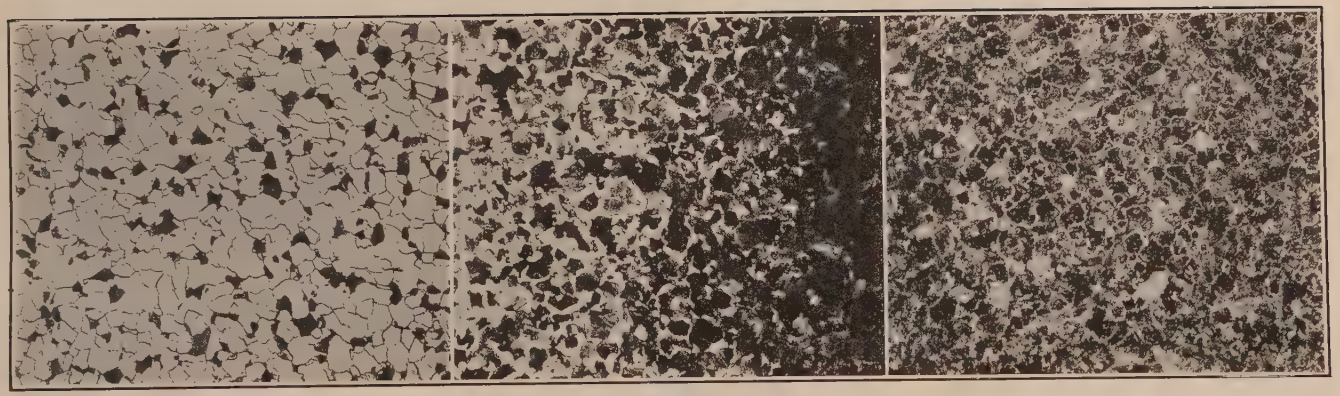

FIG. 9 FIG. 10 FIG. 11

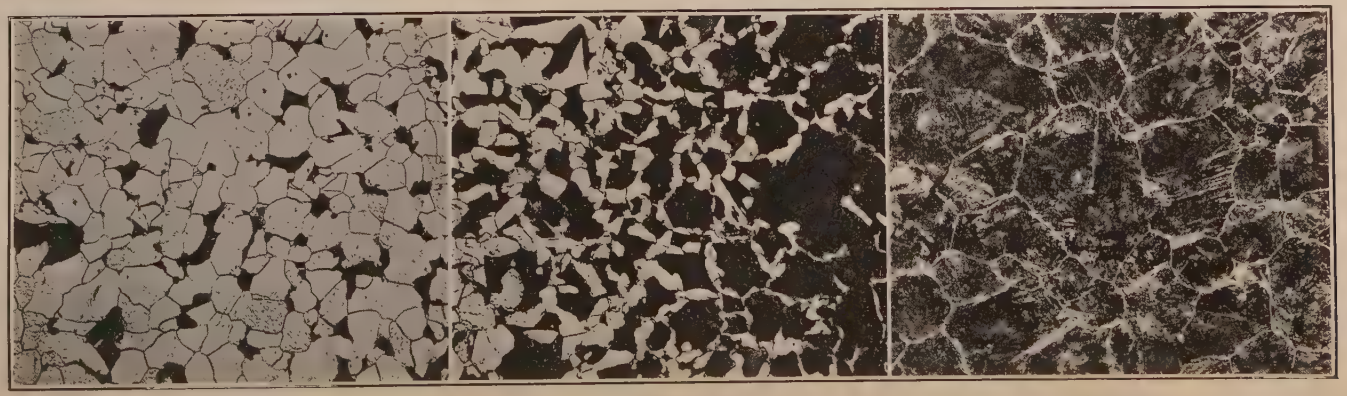

FIG. 12 FIG. 13 FIG. 14

Part B

NITRIDING

Purpose: To study the microstructures of different nitrided steels and to compare them to the case-hardened steels.

References: Williams and Homerberg: Principles of Metallography, pp. 158–163.

Adolph Machlet: American Gas Furnace Co.

Adolph Fry: Krupp Company of Germany.

Nitriding Symposium: Trans. Amer. Soc. Steel Treating, Nov. 1929.

Theory: When iron or steel is heated in an atmosphere of ammonia, above a temperature of 480° C. for a sufficient length of time, the iron or steel obtains a surface hardness which is file-hard and very resistant to corrosion. This process of increasing the surface hardness of steel by the addition of nitrogen to the outside portion is termed nitriding. The ammonia dissociates into atomic nitrogen, which combines with the iron forming iron nitride. The addition of aluminum, chromium, molybdenum and similar alloying elements to the steel greatly improves the process.

PHOTOMICROGRAPHS — (Plates XXXVI, XXXVII, XXXVIII)

Fig. 15 — Nitrided Steel (500×).

This photomicrograph shows the iron nitride needles in ferrite grains in a nitrided low-carbon steel.

Fig. 16 — Nitrided Steel (500×).

This photomicrograph shows the iron nitride needles in the ferrite grains of a medium-carbon steel.

Fig. 17 — Nitrided Steel (500×).

This photomicrograph shows the iron nitride needles in the ferrite grains of a high-carbon steel.

. . . . . .

The following 6 figures are photomicrographs of Nitralloy G, analyzing C 0.35%, Mn 0.52%, Si 0.40%, Cr 1.50%, Al 1.05%, Fe balance. These specimens were nitrided at 510° F. for 48 hours and etched in Nital.

Fig. 18 — Annealed Nitralloy (100×).

This photomicrograph shows the nitrides, ferrite and spheroidized carbides in the case, and ferrite and spheroidized carbides in the core.

Fig. 19 — Heat-Treated Nitralloy (100×).

Specimen was quenched in oil from 900° C. and drawn at 675° C.

The case shows nitrides (probably in solid solution) and sorbite. The core shows a sorbitic structure.

Fig. 20 — Annealed Nitralloy (500×).

Photomicrograph shows the nitrides (probably in solid solution), very fine network around grains, and spheroidized carbides in the case.

Fig. 21 — Annealed Nitralloy (500×).

Photomicrograph shows ferrite and spheroidized carbide in the core.

Fig. 22 — Heat-Treated Nitralloy (500×).

Specimen was quenched in oil from 900° C. and drawn at 675° C. Photomicrograph shows nitrided needles in solid solution in the sorbite of the case.

Fig. 23 — Heat-Treated Nitralloy (500×).

Specimen was quenched in oil from 900° C. and drawn at 675° C. Photomicrograph shows sorbitic structure of the core.

FIG. 15 (Van Wert)

FIG. 16 (Van Wert)

PLATE XXXVII

Fig. 17 (Van Wert)

FIG. 18 (Homerberg)

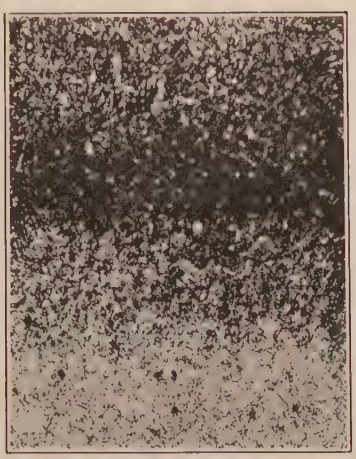

FIG. 19 (Homerberg)

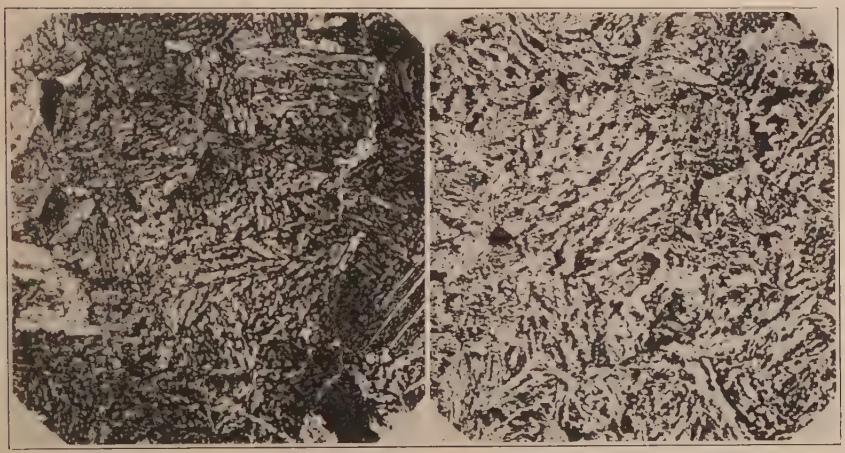

FIG. 20 (Homerberg)

FIG. 21 (Homerberg)

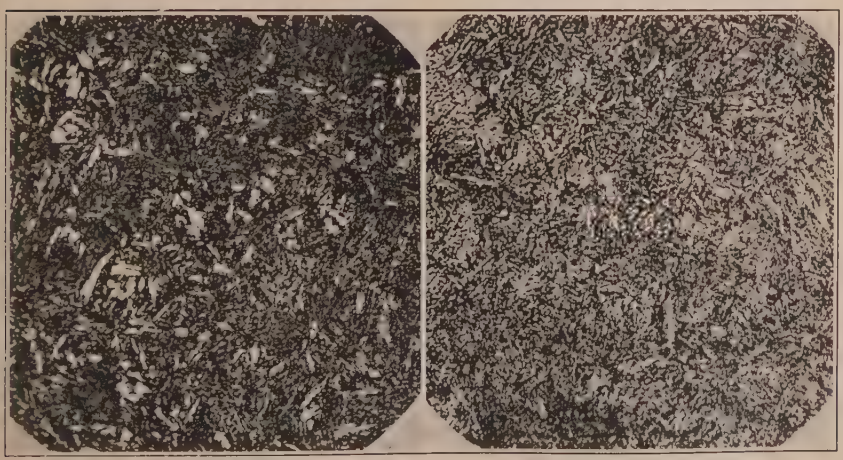

FIG. 22 (Homerberg)

FIG. 23 (Homerberg)

EXPERIMENT XIV

BRASSES (COPPER-ZINC ALLOYS)

EFFECT OF COMPOSITION

Purpose: To study the effect of composition on the microstructure and the physical properties of brasses.

References: Jeffries and Archer: The Science of Metals.
Guillet and Portevin: Metallography and Macrography, pp. 216–227.
Johnson: Materials of Construction, pp. 739–744.
Gulliver: Metallic Alloys, pp. 267–280.
Greaves and Wrighton: Practical Microscopical Metallography, pp. 99–107.

Character of Brasses. — Brasses are alloys of copper and zinc in which the zinc content varies from a minimum to about 60%. This covers the useful range and in it are included the malleable and ductile alpha and beta phases. The gamma phase is too brittle and lacks strength. By addition of tin the brasses are gradually merged in the tin bronzes, and many alloys of both groups contain essential elements foreign to their respective binary series. Usage has extended the term "bronze" to several brasses, as well as to certain copper aluminum alloys; but composition and treatment affect strength and ductility so profoundly that each alloy presents an individual range of properties to which the usual terminology is a poor guide.

PHOTOMICROGRAPHS — (Plates XXXIX–XL)

Fig. 1 — Copper — Etched (100×).

Etched in NH_4OH and H_2O_2. Annealed after cold-working. Structure shows grains (twinned) of nearly pure copper. The annealing twins are produced by cold-working followed by an anneal. Pure cast copper has a tensile strength of 25,000 lb. per sq. in., an elongation of 20% and a Brinell hardness of 80. The annealed copper has a tensile strength of 35,000 lb. per sq. in., an elongation in 2 in. of 50%, and a Brinell hardness of 42.

Fig. 2 — Zinc — Etched (100×).

Annealed after chill-casting. Etched for 20 seconds in a 5% nitric acid solution. The structure shows grains of pure zinc with black specks

of non-metallic impurities. This specimen was chill-cast and this was followed by an anneal. Before annealing, the structure showed Neumann bands within the zinc grains. Note how annealing caused recrystallization at the Neumann band borders. Cast zinc has a tensile strength of 5400 lb. per sq. in., a yield point of 4900 lb. per sq. in., an elongation in 2 in. of zero per cent and a Brinell hardness of 39. Annealed zinc has a tensile strength of 22,400 lb. per sq. in., a yield point of 10,700 lb. per sq. in., and an elongation of 38%.

Fig. 3 — Brass (Cu 90%; Zn 10%) — Cast, Etched (100×).

Cooled rather quickly. Etched in NH_4OH and H_2O_2. Dendritic or cored structure of one solid solution, alpha brass, is shown. Grains are large and somewhat inhomogeneous, due to the rate of cooling. All brasses (cast) that contain less than about Zn 37% show a similar structure, that is, they are made up of a single solid solution.

Fig. 4 — Brass (Cu 90%; Zn 10%) — Annealed, Etched (100×).

Etched in NH_4OH and H_2O_2. Structure shows uniform grains of alpha brass. Annealing destroyed the cored and heterogeneous structure.

Fig. 5 — Brass (Cu 80%; Zn 20%) — Annealed, Etched (100×).

Etched in NH_4OH and H_2O_2. Structure shows uniform grains of alpha brass. Much twinning is evident.

Fig. 6 — Brass (Cu 70%; Zn 30%) — Annealed, Etched (100×).

Etched in NH_4OH and H_2O_2. Structure shows uniform grains of alpha brass. Alloys of this composition have good tensile strength and ductility but cannot be worked while hot. Condenser tubes and cartridge shell are made of an alloy of about that composition.

Fig. 7 — Brass (Cu 60%; Zn 40%) — Cast, Etched (100×).

Cooled rather slowly. Etched in NH_4OH and H_2O_2. Brown rods and granules are of alpha solid solution and the golden yellow matrix is of beta solid solution. Due to the two different solid solutions in this alloy, it is more subject to corrosion than Alpha Brass or Admiralty Metal. The buff alpha grains are embedded in the golden yellow beta matrix.

Fig. 8 — Brass (Cu 52%; Zn 48%) — Cast, Etched (100×).

Cooled by quenching in water. Etched in NH_4OH and H_2O_2. Only one solid solution, beta, is shown. The grains are very large and coarse. The copper-zinc thermal equilibrium diagram indicates that this beta-solid solution will throw off some blue gamma compound. But this disintegration takes place very slowly in the quenched specimen and is more evident at the grain-boundaries.

Fig. 9 — Brass (Cu 50%; Zn 50%) — Cast, Etched (100×).

Cooled moderately slowly. Etched in NH_4OH and H_2O_2. Bright

areas are of beta solid solution. Dark (blue) areas are of gamma solid solution. Dark speckled areas are the eutectoid mixtures composed of beta and gamma. This alloy first solidified as the beta solid solution, then threw off gamma particles when the temperature dropped below 725° C. The gamma constituent makes this alloy hard and brittle.

Fig. 10 — Brass (Cu 45%; Zn 55%) — Cast, Etched (100×).

Slowly cooled. Etched in NH_4OH and H_2O_2. White areas are of beta solid solution. These are surrounded by matrix that is the eutectoid alloy of small particles of gamma and beta solid solutions. That the brass cooled rather slowly is evident since the eutectoid is laminated. Because of the gamma phase, this alloy is very brittle and is of no important technical use except for brazing rods.

Summary: These specimens of different brasses show clearly what marked changes occur in the structure of brass when changes are made in the composition. Because of this, the physical properties of brass vary greatly with its composition. Brasses of greatest technical importance contain about 40% zinc or less. Alloys of copper and zinc containing more than 60% zinc are not considered as brasses but rather as zinc-base bearing metals. Brasses containing 60 to 75% copper are used for sheets, tubes and wire. For castings brasses containing from 60 to 70% copper are used.

Fig. 11 shows the copper-zinc thermal equilibrium diagram.

Fig. 12 shows the physical property curves of cast brass for varying proportions of copper and zinc.

Relation between the properties and the microstructure which may be expressed in general terms:

1. The tensile strength increases with increase in zinc content, rises somewhat abruptly with the appearance of the beta, and reaches a maximum at a composition corresponding roughly to equal parts of the alpha and the beta; it falls off rapidly at the appearance of the gamma constituent.

2. Elongation rises to a maximum and begins to fall again before the composition reaches the limit of the alpha solid solution; it falls considerably as the amount of the beta increases, and is very small in the presence of the gamma.

3. The alpha constituent shows the greatest resistance to shock; this is diminished by the presence of beta, and the alloy becomes extremely brittle when gamma is present.

4. Hardness is greatly increased by the presence of beta and still further when gamma appears.

5. Alloys containing alpha only are especially suitable for working cold, and may be rolled hot or cold; those containing alpha and beta

will suffer very little deformation in the cold without rupture and may only be rolled hot. The beta constituent may also be forged, rolled or extruded hot, but alloys containing gamma should invariably be avoided for any mechanical treatment.

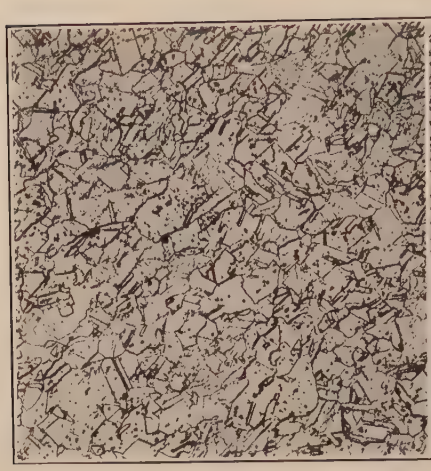

FIG. 1

FIG. 2

FIG. 3

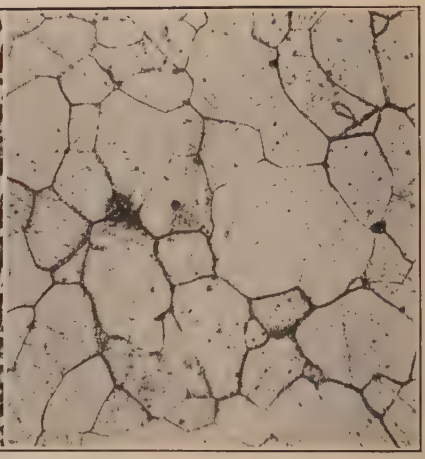

FIG. 4

FIG. 5

FIG. 6

PLATE XL

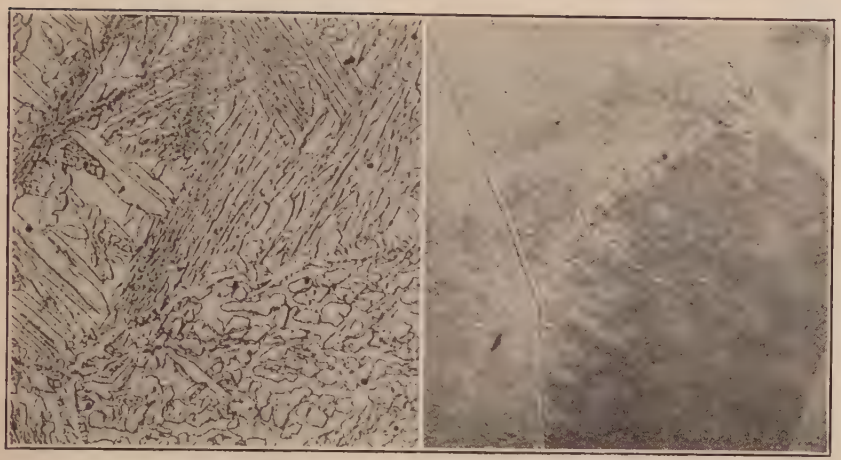

FIG. 7

FIG. 8

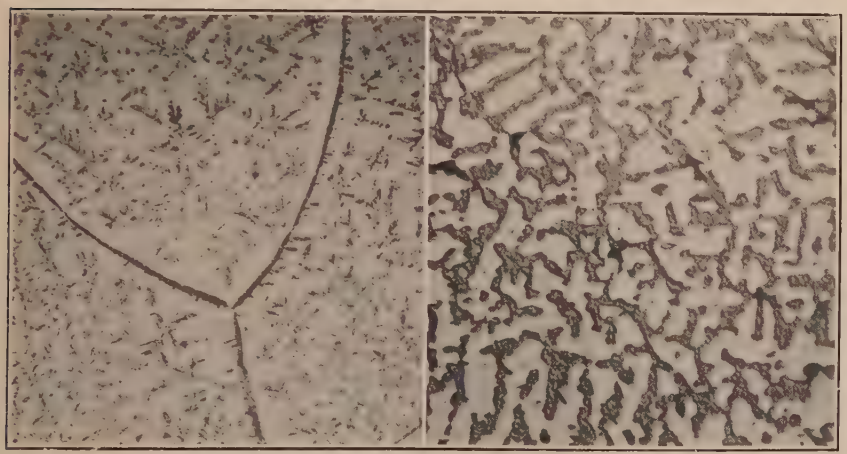

FIG. 9

FIG. 10

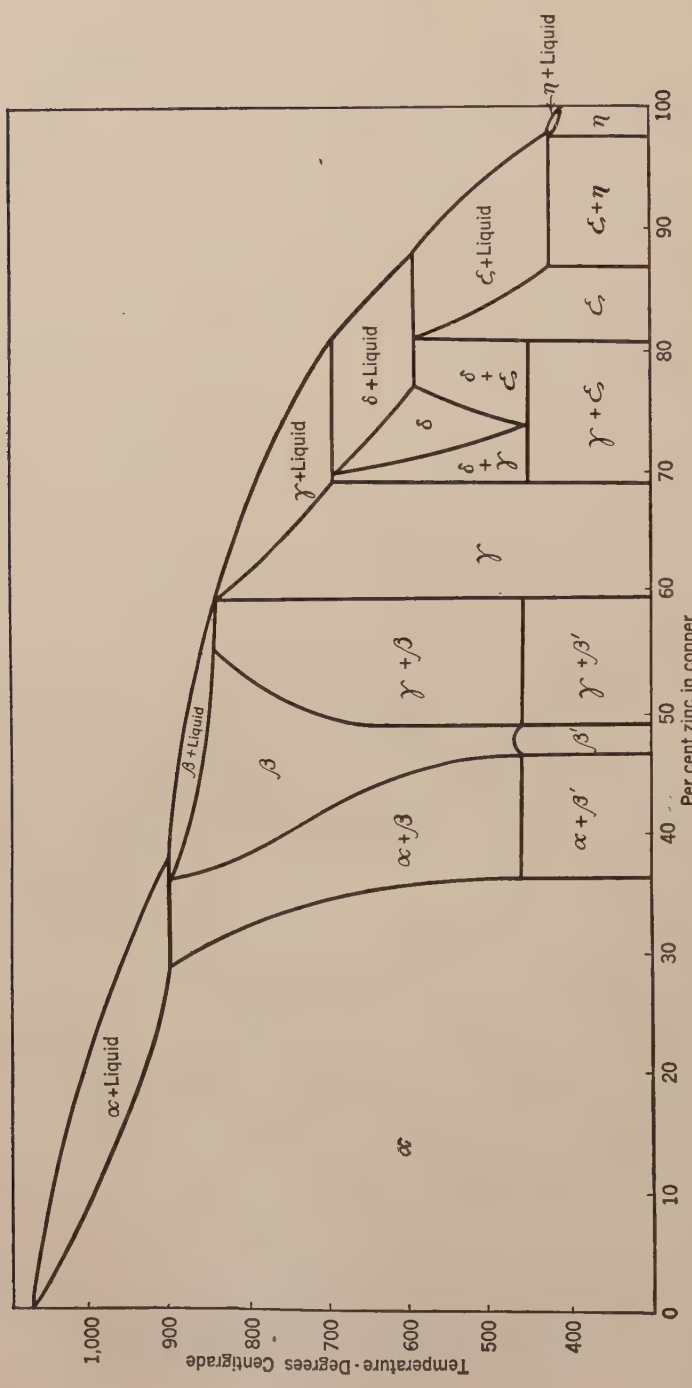

COPPER-ZINC THERMAL EQUILIBRIUM DIAGRAM

FIG. 11

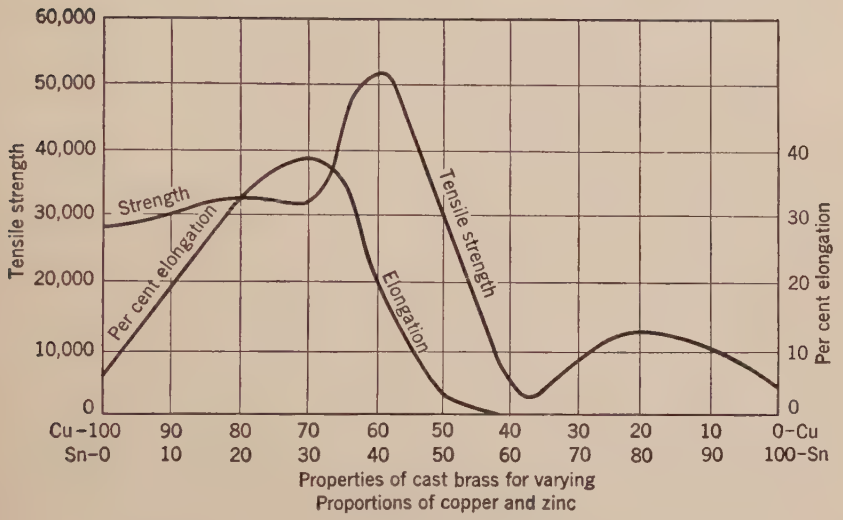
60,000
50,000
40,000
30,000
20,000
10,000
0
Tensile strength
40
30
20
10
0
Per cent elongation
Strength
Per cent elongation
Tensile strength
Elongation
Cu–100 90 80 70 60 50 40 30 20 10 0–Cu
Sn–0 10 20 30 40 50 60 70 80 90 100–Sn
Properties of cast brass for varying
Proportions of copper and zinc

Fig. 12

EXPERIMENT XV

BRASSES Cu-Zn ALLOYS

EFFECT OF HEAT-TREATMENT AND MECHANICAL WORKING *

Purpose: To become familiar with the microstructures and to study the effects of heat-treatment and the mechanical working of brasses.

References: Jeffries and Archer: The Science of Metals, pp. 190, 191, 356.

Williams and Homerberg: Principles of Metallography, pp. 113, 120.

Johnson: Materials of Construction, pp. 741–749, 767.

Price and Davidson: American Institute of Metals, September, 1916.

Part A

EFFECT OF ANNEALING ROLLED BRASS — (Plate XLI)

Cu 69.84%; Zn 30.16%

Fig. 1 — Hard Brass (72×).

Rolled from No. 5 to No. 8 B. & S. Etched in NH_4OH and H_2O_2. Structure shows deformed grains of alpha brass due to the cold-rolling.

Fig. 2 — Partly Recrystallized (72×).

The hard brass in Fig. 1 was annealed for $\frac{1}{2}$ hour at 350° C. Etched in NH_4OH and H_2O_2. Structure shows partial recrystallization due to the anneal. It has a tensile strength of 58,494 lb. per sq. in.; an elongation in 2 in. of 42.7%; and a Scleroscope hardness of 19.2.

Fig. 3 — Very Fine Grain (72×).

Annealed for $\frac{1}{2}$ hour at 500° C. Etched in NH_4OH and H_2O_2. Structure shows complete recrystallization and very fine grains. It has a tensile strength of 49,721 lb. per sq. in.; an elongation in 2 in. of 64.3%; and a Scleroscope hardness of 9.5.

Fig. 4 — Medium Grain (72×).

Annealed for $\frac{1}{2}$ hour at 592° C. Etched in NH_4OH and H_2O_2. Structure shows grain growth to a medium grain size. It has a tensile strength of 46,208 lb. per sq. in.; an elongation in 2 in. of 71.8% and a Scleroscope hardness of 8.0.

* With permission of W. P. Price, Metallurgist, Scovill Manufacturing Co.

Fig. 5 — Coarse Grain (72×).

Annealed for $\frac{1}{2}$ hour at 650° C. Etched in NH_4OH and H_2O_2. Structure shows coarse and twinned grains of alpha brass. It has a tensile strength of 44,910 lb. per sq. in.; an elongation in 2 in. of 74.8% and a Scleroscope hardness of 7.07.

Fig. 6 — Very Coarse Grain (72×).

Annealed for $\frac{1}{2}$ hour at 708° C. Etched in NH_4OH and H_2O_2. Structure shows an abnormal grain growth. Large coarse grains are present. Annealing twins are very evident. It has a tensile strength of 44,010 lb. per sq. in.; an elongation in 2 in. of 74.5%; and a Scleroscope hardness of 6.75.

PLATE XLI*

FIG. 1 FIG. 2

FIG. 3 FIG. 4

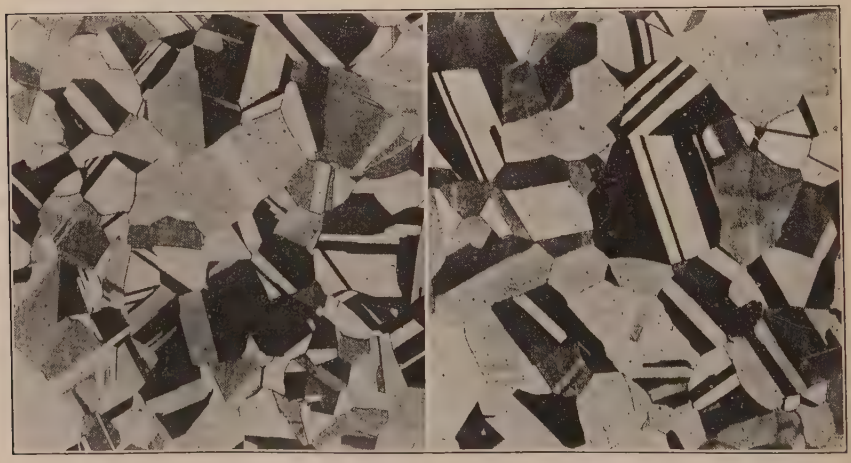

FIG. 5 FIG. 6

* Scovill Manufacturing Co.

PART B

EFFECT OF COLD ROLLING ANNEALED BRASS — (Plate XLII)

Cu 64.71%; Zn 35.27%; Fe 0.02%

Fig. 7 — Annealed Brass (72×).

Longitudinal section of brass alloy gage 0.256 in. finished on No. 2 B. & S. and given a regular mill anneal. Etched in NH_4OH and H_2O_2. Structure shows large grains of the twinned alpha brass. It has a tensile strength of 42,683 lb. per sq. in.; an elastic limit of 21,446 lb. per sq. in.; an elongation in 2 in. of 77.5%, a reduction in area of 76.6% and a Scleroscope hardness of 7.25.

Fig. 8 — Half Hard Brass (72×).

The above alloy was reduced 18% by rolling from 0.256 to 0.210 in. Etched in NH_4OH and H_2O_2. It has a tensile strength of 52,020 lb. per sq. in.; an elastic limit of 41,580 lb. per sq. in.; an elongation in 2 in. of 45.3%; a reduction in area of 70.1% and a Scleroscope hardness of 18.0.

Fig. 9 — Hard Brass (72×).

Reduced 35.5% by rolling from 0.256 to 0.165 in. Etched in NH_4OH and H_2O_2. It has a tensile strength of 67,340 lb. per sq. in.; an elastic limit of 65,983 lb. per sq. in.; an elongation in 2 in. of 16.0%; a reduction in area of 65.2%; and a Scleroscope hardness of 28.3.

Fig. 10 — Extra Hard Brass (72×).

Reduced 47.7% by rolling from 0.256 to 0.134 in. Etched in NH_4OH and H_2O_2. It has a tensile strength of 78,003 lb. per sq. in., an elastic limit of 78,003 lb. per sq. in., an elongation in 2 in. of 8.0%, a reduction in area of 61.2% and a Scleroscope hardness of 33.4.

Fig. 11 — Spring Temper Brass (72×).

Reduced 66.7% by rolling from 0.256 to 0.085 in. Etched in NH_4OH and H_2O_2. It has a tensile strength of 92,933 lb. per sq. in., an elastic limit of 92,933 lb. per sq. in., an elongation in 2 in. of 4.8%, a reduction in area of 49.8% and a Scleroscope hardness of 38.3.

FIG. 7

FIG. 8

FIG. 9

FIG. 10

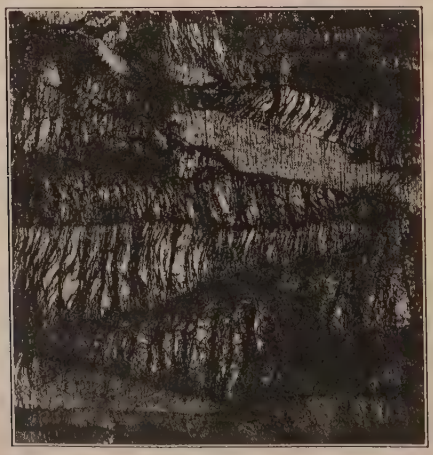

FIG. 11

* Scovill Manufacturing Co.

EXPERIMENT XVI

ALLOY BRASSES

Purpose: To study the effect of alloying elements on the microstructure and physical properties of brasses.

References: Guillet and Portevin: Metallography and Macrography: pp. 216–226.

Williams and Homerberg: Principles of Metallography: pp. 105–122.

Greaves and Wrighton: Practical Microscopical Metallography: pp. 99–107.

Gulliver: Metallic Alloys: pp. 275–280.

Theory: The usefulness of the copper-zinc alloys for certain purposes is augmented and intensified by the addition of small proportions of one or of two other elements. These elements are generally added for purposes for which increased strength, hardness, machinability or resistance to corrosion are required. The most important of these added substances are lead, tin, manganese, aluminum, iron and nickel. The general behavior of most of these on the microstructure of the brasses is much the same.

Lead is added to allow more easy machining. It diminishes, however, both the strength and the ductility of the metal.

Tin considerably increases the strength and the hardness of brass, but it decreases the ductility. Tin also increases the resistance to corrosion.

Manganese increases the strength of brass very sensibly, without causing any great diminution of ductility so long as its proportion does not exceed 4%. It increases the resistance to corrosion.

Aluminum causes a very appreciable increase in the strength of brass, but it rapidly diminishes the ductility when present in quantities over 3%.

Iron, up to 2% has comparatively little effect upon brass, slightly increasing its tensile strength and hardness.

Nickel increases the strength, toughness and resistance to corrosion of brass. It also makes the brass very malleable.

PHOTOMICROGRAPHS — (Plate XLIII)

Fig. 1 — Common Brass — Rolled (100×).

Cu 62%; Zn 35%; Sn 1.5%; Pb 3.5%.

Etched in NH_4OH and H_2O_2. Buff areas are of alpha solid solution. At the grain-boundaries of the alpha grains are small golden yellow particles of beta solid solution and black globules of lead. The grains are elongated showing the effect of rolling. This brass takes a good polish and is used for brass pipe, hand rails, and other places where strength and incorrodibility are not required.

Fig. 2 — Muntz Metal (100×).

Cu 60%; Zn 40%.

Etched in NH_4OH and H_2O_2. Brown buff areas are of alpha solid solution embedded in the golden yellow matrix of the beta solid solution. Muntz metal is used for fresh-water condenser tubes where strength is required. It has a tensile strength of 50,000 to 55,000 lb. per sq. in. and an elongation in 2 in. of 15 to 20%.

Fig. 3 — Naval Brass (100×).

Cu 60%; Zn 39%; Sn 1%.

Etched in NH_4OH and H_2O_2. Small quantities of iron and lead are allowed also as impurities. Brown buff areas are alpha solid solution. Yellow areas (matrix) are beta solid solution. This is similar to Muntz metal except tin has been added. This makes the alloy more resistant to corrosion. This is used in the form of bars, sheets, plates and rods and tubes. Naval brass has a tensile strength of 55,000 to 70,000 lb. per sq. in., an elongation in 2 in. of 30 to 45%, and an elastic limit of 24,000 to 27,000 lb. per sq. in.

Fig. 4 — Tobin Bronze (100×).

Cu 61%; Zn 38%; Sn 1%.

Etched in NH_4OH and H_2O_2. Small quantities of iron and lead as impurities. This is a patented alloy made by the American Brass Co. and is similar to Naval brass. The brown or buff areas are alpha solid solution and the lighter yellow areas are beta brass. Due partly to the tin, this alloy resists corrosion fairly well. It may also be given good tensile strength and ductility by suitable working. Tobin bronze has a tensile strength of 60,000 to 80,000 lb. per sq. in., an elastic limit of 40,000 to 55,000 lb. per sq. in., and an elongation in 2 in. of 30 to 35%.

Fig. 5 — Admiralty Metal (100×).

Cu 70%; Zn 29%; Sn 1%.

Etched in NH_4OH and H_2O_2. This alloy shows twinned grains of alpha solid solution. Admiralty metal is used for salt water condenser tubes where maximum resistance to corrosion is required. It has a tensile strength of 45,000 to 50,000 lb. per sq. in.

Fig. 6 — Manganese Bronze — Cast (100×).

Cu 55–60%; Zn 38–42%; Mn 0–1.5%; Al 0–1.5%; Fe 0–2.5%; Pb 0–0.2%.

Etched in NH_4OH and H_2O_2. This alloy is similar to Muntz metal and Naval brass except that the manganese has been added to act as a deoxidizer, thereby cleaning the brass and giving it greater strength. The iron also helps to improve the strength. Microstructure shows rods and grains of alpha brass in a light beta matrix. Small cubes of the iron-zinc compound are also present. Cast manganese bronze has a tensile strength of 70,000 to 80,000 lb. per sq. in., an elastic limit of 25,000 to 30,000 lb. per sq. in., and an elongation in 2 in. of 20 to 30%. This alloy resists corrosion well. It is used for castings requiring good strength and incorrodibility such as propeller hubs and blades, engine framing, gears, torpedo tube castings, gun-mount castings, condenser tubes, etc.

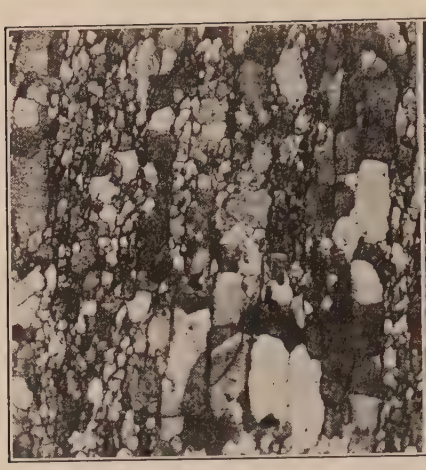

FIG. 1

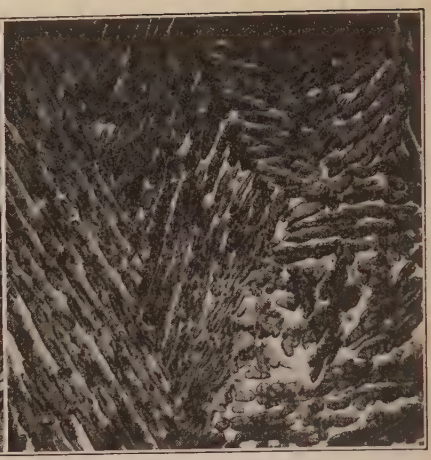

FIG. 2

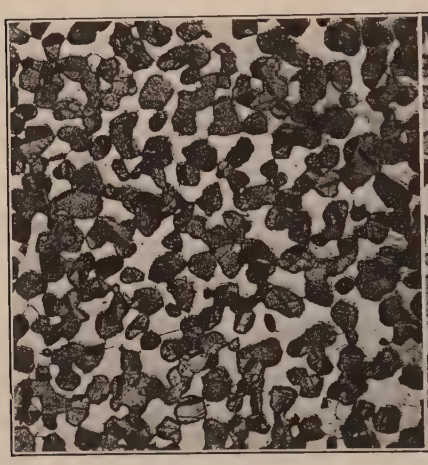

FIG. 3

FIG. 4

FIG. 5

FIG. 6

EXPERIMENT XVII

BRONZES Cu-Sn ALLOYS

EFFECT OF COMPOSITION

Purpose: To study the effect of composition on the microstructure and physical properties of bronzes.

References: Gulliver: Metallic Alloys, pp. 249–266.
Guillet and Portevin: Metallography and Macrography, pp. 227–235.
Jeffries and Archer: The Science of Metals, pp. 351–352.
Williams and Homerberg: Principles of Metallography, pp. 101–104.
Greaves and Wrighton: Practical Microscopical Metallography, pp. 108–111.

Theory: Bronzes are alloys of copper and tin. They are much more costly alloys than brasses, but are harder, stronger in compression, and much less corrosive. Bronzes are used for bearings, for parts where resistance to corrosion and resistance to wear are important, for bushings, gears, worn wheels, valves, pipe-fittings, etc.

PHOTOMICROGRAPHS — (Plates XLIV–XLV)

Fig. 1 — Bronze (Cu 95%; Sn 5%) — Cast, Etched (100×).
Rather quickly cooled. Etched in NH_4OH and H_2O_2. Dendritic cored structure showing only one component, the alpha solid solution. This is not completely homogeneous due to the rapid rate of cooling. Black areas are non-metallic inclusions. Bronzes in this region have a good tensile strength and are very ductile. The grains are very large and can be seen with the naked eye.

Fig. 2 — Bronze (Cu 95%; Sn 5%) — Annealed, Etched (100×).
Etched in NH_4OH and H_2O_2. Structure shows uniform grains of the alpha solid solution. Annealing removed the dendritic cored structure.

Fig. 3 — Bronze (Cu 85%; Sn 15%) — Cast, Etched (100×).
Cooled rather quickly. Etched in NH_4OH and H_2O_2. Dendritic structure characteristic of a casting is shown. Brown or buff areas are alpha solid solution, somewhat inhomogeneous, due to the quick cooling.

Surrounding the primary grains of alpha is the eutectoid mixture, consisting of a bluish-gray delta solid solution with small specks of alpha solid solution mixed in. Black areas indicate non-metallic inclusions, chiefly blow-holes. Bronzes of this composition and near it have good tensile strength, they can be hot-worked and can be given ductility by suitable heat-treatment. When slowly cooled they are brittle and are suitable for bells.

Fig. 4 — Bronze (Cu 73%; Sn 27%) — Cast, Etched (100×).

Cooled moderately slowly. Etched in NH_4OH and H_2O_2. This alloy is of the eutectoid composition of bronze. Referring to the copper-tin equilibrium diagram, it is seen that when first solidified, this alloy was practically all a beta solid solution. At about 500° C. this beta is saturated and, when cooling slowly through this critical temperature, it breaks up into a eutectoid which is a mixture of delta and alpha solid solutions, the delta predominating. The diagram shows that on further slow cooling, the alpha in the eutectoid gradually transforms into delta. If cooled slowly enough, then, this specimen should show practically all delta solid solution. The specimen shows considerable bright areas inside the grains and at the grain-boundaries, which is the finally transformed delta solid solution. The darker mottled areas or grains consist of particles of delta surrounded by the alpha plus delta eutectoid. The eutectoid mixture is very fine and seen to be a mixture only at high magnifications. The delta solid solution is very hard and brittle, therefore alloys of this composition have no important technical use.

Fig. 5 — Bronze (Cu 70%; Sn 30%) — Cast, Etched (100×).

Cooled moderately slowly. Etched in NH_4OH and H_2O_2. The copper-tin equilibrium diagram shows that for equilibrium this should be all delta solid solution. The microstructure is very similar to the previous specimen. The bright areas within the grains and at the grain-boundaries are delta solid solution and the darker speckled areas, best examined at high magnification, are the fine eutectoid mixture of alpha and delta, formed at about 500° C. that did not have the opportunity to transform entirely into delta solid solution. Since delta predominates, however, this is a *very* hard and brittle alloy and therefore of no important technical use. Annealing this specimen would convert the alloy entirely into the homogeneous delta solid solution.

Fig. 6 — Bronze (Cu 20%; Sn 80%) — Cast, Etched (100×).

Cooled moderately slowly. Etch in ferric chloride solution for 4 seconds. The copper-tin equilibrium diagram shows that when this alloy first begins to solidify from the molten condition, a chemical compound, Cu_3Sn, is formed. At about 400° C. this compound reacts

with the liquid solution, now of composition about Cu 8%, Sn 92%, to form a solid solution, *epsilon*, which, when first formed is of composition about Cu 40%, Sn 60%. On further cooling, at about 225° C., the remaining liquid solidifies, forming a eutectic alloy that is a mixture of a very small amount of epsilon solid solution and pure tin. The bright areas in the specimen have two shades. The grayish interior is slightly darker than the portion near the boundary. The interior is the Cu_3Sn compound and the almost white boundary is the epsilon solid solution. The specimen was not cooled slowly enough for the chemical compound Cu_3Sn to complete its transformation into epsilon solid solution at 400° C. The dark area is the eutectic mixture, black being fine tin and the small bright particles being the epsilon solid solution. Bronzes in this region have a very low tensile strength and poor ductility and hence are not commercially important. This alloy is really a tin-base bearing metal.

Fig. 7 — Delta Eutectoid in Bronze — Etched (500×).

This shows the structure of the delta eutectoid phase found in most bronzes. At 500 magnifications it is observed that the delta-eutectoid constituent is embedded in the alpha solid solution and consists of the irregular, bluish-gray delta phase occluding small black specks of the alpha phase.

Fig. 8 gives the copper-tin thermal equilibrium diagram showing the positions of the various phases.

Fig. 9 gives the tensile strength and per cent elongation curves for the copper-tin series of alloys. A discussion of the relation between the mechanical properties and microstructure of copper-tin alloys is also given.

Summary: These six specimens show clearly what pronounced changes occur in the structures of bronzes as the composition changes and explain why the physical properties change so abruptly when the composition is changed. Only bronzes that contain over 70% copper are of technical importance.

RELATION BETWEEN MECHANICAL PROPERTIES AND MICROSTRUCTURE OF COPPER-TIN ALLOYS

The mechanical properties of the various phases give an indication of the range of composition within which useful alloys may be expected.

Alpha solid solution is soft and ductile, increasing in strength and also in ductility as the proportion of tin increases. It is the softest of all the different constituents. It may be rolled or stamped cold, but hardens under treatment much more rapidly than alpha-brass.

Beta solid solution is stronger and harder than alpha, but much less ductile.

Gamma and **delta** solid solutions and the compound Cu_3Sn are hard, white, brittle bodies. The delta phase is almost pure Cu_4Sn and is capable of receiving a hard polish.

Epsilon solid solution is also brittle, but is not so hard as the gamma and delta phases.

The tensile strength of the chill-cast alloys increases regularly with increasing tin content up to 19% tin, but the ductility reaches a maximum at 8% tin, although the ductility of alloys containing higher proportions of tin can be raised by annealing and quenching in order to reduce the quantity of delta phase to a minimum.

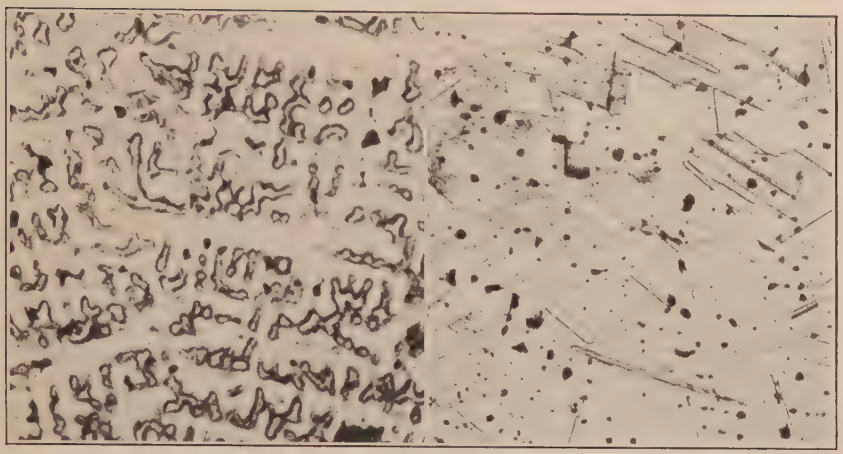

FIG. 1 FIG. 2

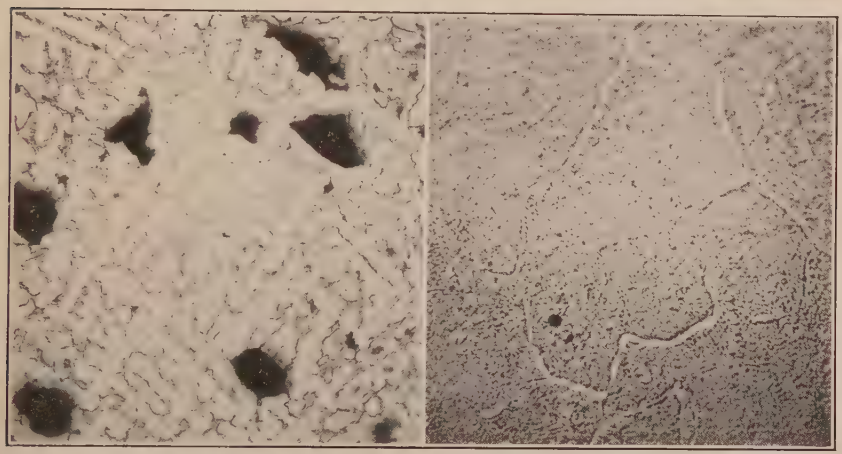

FIG. 3 FIG. 4

FIG. 5 FIG. 6

PLATE XLV

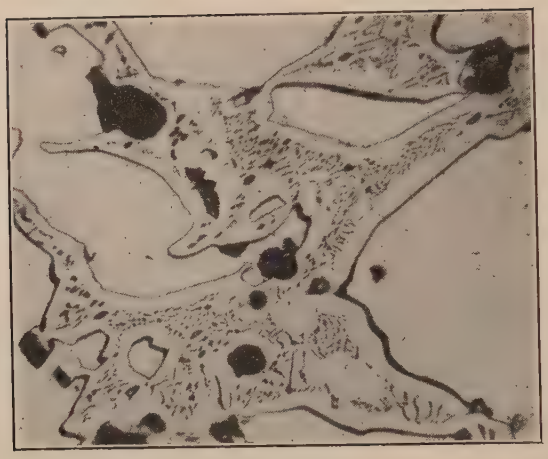

FIG. 7

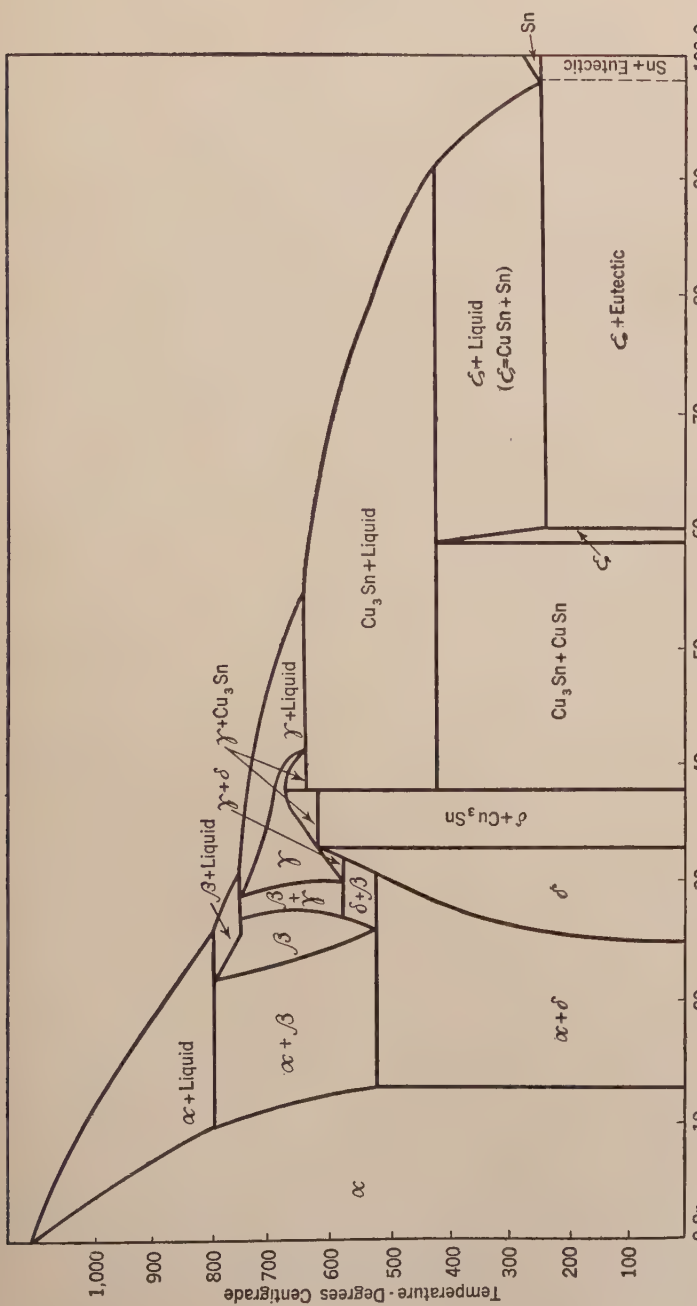

COPPER-TIN THERMAL EQUILIBRIUM DIAGRAM

FIG. 8

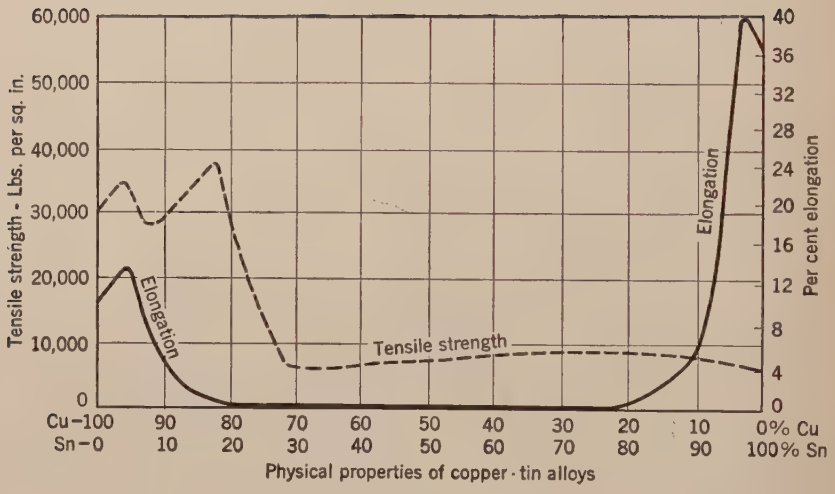
60,000
50,000
40,000
30,000
20,000
10,000
0
Tensile strength - Lbs. per sq. in.
40
36
32
28
24
20
16
12
8
4
0
Per cent elongation
Elongation
Tensile strength
Elongation
Cu–100 90 80 70 60 50 40 30 20 10 0% Cu
Sn–0 10 20 30 40 50 60 70 80 90 100% Sn
Physical properties of copper-tin alloys

FIG. 9

EXPERIMENT XVIII

BRONZES Cu-Sn ALLOYS

EFFECT OF HEAT-TREATMENT

Purpose: To study the effect of heat-treatment on the structure of bronzes.

References: Gulliver: Metallic Alloys, pp. 249–266.
Guillet and Portevin: Metallography and Macrography, pp. 227–235.

Specimens: The following five specimens are bronze of composition about Cu 80%, Sn 20%, all taken from one casting and subsequently heat-treated as indicated.

PHOTOMICROGRAPHS — (Plate XLVI)

Fig. 1 — As Cast. Rather quickly cooled. Etched in ferric chloride solution, for 2 seconds. A dendritic structure, characteristic of a casting, is shown. White areas are alpha solid solution. Surrounding the alpha, is the dark eutectoid mixture consisting of a bluish-gray delta solid solution in which are mixed small particles of alpha solid solution.

Fig. 2. Cast and then reheated to 450° C. and quenched in cold water. Etched in ferric chloride solution for 3 seconds. Structure not materially different from Fig. 1, since the critical temperature was not reached on reheating.

Fig. 3. Cast and then reheated to 500° C. and quenched in cold water. Etched as Fig. 2. Structure similar to Fig. 2. While it was reheated to the critical temperature at which the eutectoid dissolves into a homogeneous solid solution beta, it was not left at this temperature long enough for this transformation to take place. However, note that there is less of the dark delta eutectoid and more of the alpha solid solution than in Figs. 1 and 2.

Fig. 4. Cast and reheated to 750° C. and quenched in cold water. Etched in ferric chloride solution for 5 seconds. Light areas are alpha solid solution. Dark areas, brownish, are beta solid solution. Referring to the copper-tin equilibrium diagram, it is seen that the alloy of this composition, when in equilibrium at temperatures below about

500° C. is composed of primary alpha grains in a eutectoid mixture of the delta and alpha solid solutions, but when heated to temperatures above about 500° C. and not over 800° C., it is composed of two solid solutions, alpha and beta. Beta is formed from the eutectoid at about 500° C. when heating. Beta is much more ductile than delta and hence bronze of this composition is ductile when hot and may be hot-worked but is brittle when slowly cooled below 500° C. This is the reason why these bronzes are softened by heating to a cherry red color and quenching.

Fig. 5. Cast, reheated to 750° C., then cooled to 450° C. and quenched in water. Etched as Fig. 4. Bright buff areas are alpha solid solution. These are surrounded by a eutectoid mixture similar to Fig. 1. The beta solid solution shown in Fig. 4 is saturated at about 500° C., and when cooling through this temperature, it breaks up into a mixture of alpha and delta solid solutions, the delta predominating. In this form, the bronze is harder and more brittle than when like Fig. 4.

Summary: These five specimens have shown that there is a pronounced change produced in the microstructure of bronzes of this composition and thereabouts, when they are heated or cooled through a critical temperature. Upon heating, they have shown that a mixture of two solutions dissolves at a critical temperature, forming a single new homogeneous solution, beta. It can be shown that the beta solid solution is much more ductile than the mixture of alpha and delta; therefore in order to work (that is, forge or roll) bronze of this composition, it must be done at temperatures between 500° C. and 800° C. or else quenched from these temperatures and then worked cold. Quenching these bronzes from a temperature above the cherry red color produces a softer material which is just the reverse of what happens to steel when so treated.

FIG. 1 FIG. 2

FIG. 3 FIG. 4

FIG. 5

EXPERIMENT XIX

ALLOY BRONZES

Purpose: To study the microstructure and physical properties of alloy bronzes.

References: Williams and Homerberg: Principles of Metallography, pp. 101–103.

Greaves and Wrighton: Practical Microscopical Metallography, pp. 108–113.

Gulliver: Metallic Alloys, pp. 261–266.

Theory: A true bronze is an alloy of copper and tin, but common usage has applied the term to other alloys of copper with one or more special elements. The more general elements commercially used in alloying true bronzes are zinc, lead, silicon, manganese, aluminum, phosphorous arsenic, antimony and nickel.

The influence of the different alloying elements varies with the conditions imposed by the different combinations, but, in general, they greatly affect the physical properties of the bronzes relative to strength, hardness, toughness, conductivity, resistance to corrosion, and so forth. *Zinc* is used to close the grain by its fluxing action. Lead increases machinability, lowers the tensile strength and decreases the ductility. Manganese is a stronger deoxidizer, producing sound castings. In larger quantities it increases the tensile strength, hardness and toughness. Aluminum acts as a scavenger and also as an alloying element. It produces sounder ingots and increases the tensile strength. Phosphorus is a strong deoxidizing agent, increasing fluidity and producing sound castings. In larger quantities it acts as a hardener, thereby increasing tensile strength and decreasing the elongation. Nickel aids in forming a dense, close-grained structure. Antimony is also a hardener and produces a close-grained bronze with greater tensile strength.

PHOTOMICROGRAPHS — (Plates XLVII–XLVIII)

Fig. 1 — Bronze — Phono Electric Trolley Wire (75×).

Cu 98.74%; Sn 1.25%; Fe 0.008%.

Etched in NH_4OH and H_2O_2. Hard-drawn from hot-rolled section. Structure shows deformed grains of alpha solid solution of

copper and tin. It has a tensile strength of 74,000 lb. per sq. in., an elongation of 3.75% in 2 in. and a reduction in area of 70%.

Fig. 2 — Phosphor Bronze (75×).

Cu 94.31%; Sn 5.5%; Fe 0.04%; P 0.15%.

Etched in NH_4OH and H_2O_2. Rolled hard to size after final annealing operation. Structure shows solid solution of tin and phosphorus in copper. It has a tensile strength of 80,500 lb. per sq. in. and an elongation in 2 in. of 14.5%.

Fig. 3 — Bronze (Composition " G ") (100×).

Cu 85.41%; Sn 9.53%; Zn 1.24%; Fe 0.02%; Pb 1.53%; Ni 2.03%.

Etched in NH_4OH and H_2O_2. The photomicrograph shows cored alpha plus delta eutectoid plus lead globules. The dendritic arrangement of the crystals is due to the fact that this alloy has a wide solidification range of temperature. The dendritic cores, the first material to solidify, are richest in nickel and copper; the percentages of these elements decrease from the center to boundary of each core. Between the dendrites, the zinc-rich delta eutectoid is faintly visible. This alloy has a tensile strength of 38,750 lb. per sq. in., a yield point of 17,000 lb. per sq. in., an elongation in 2 in. of 15.5% and a reduction in area of 18.7%.

Fig. 4 — Bronze (Composition " G ") (50×).

Cu 88.4%; Sn 9.66%; Zn 1.90%; Fe 0.01%; Pb 0.03%.

Etched in chromic acid solution. Structure shows alpha solid solution of tin and zinc in copper and traces of delta eutectoid. This is the typical structure of Composition " G " as cast. The dark areas represent crystallite cores whose orientation is uniform throughout each grain. Portions of several grains can thus be distinguished in the field of view. At high magnifications, a few particles of the alpha-delta eutectoid are visible.

Fig. 5 — Zinc Bronze (100×).

Cu 80.24%; Sn 12.72%; Zn 5.97%; Pb 0.753%.

Etched in NH_4OH. This specimen was taken from a defective turbine gland ring. The structure shows cored alpha plus the delta eutectoid constituents. Pits and flaws are also seen as black spots. The eutectoid structure surrounds the cored alpha crystallites as a fine network thus making the metal brittle. The delta envelopes form a brittle boundary between the tougher alpha constituent.

Fig. 6 — Everdur Metal — Bronze (500×).

Cu 94.56%; Si 3.66%; Mn 1.18%; Fe 0.24%.

Etched in NH_4OH and H_2O_2. Structure at 500 magnifications shows twinned alpha grains.

Fig. 7 — Dawson " Hardened " Copper (100×).

Cu 81.82%; Sn 17.14%; P 0.17%; Ni 0.90%; Pb 0.01%.

Etched in chromic acid. Structure shows primary crystallites of alpha solid solution surrounded by the alpha-delta eutectoid. As shown by this photomicrograph, the hard, brittle eutectoid forms a continuous network surrounding the relatively soft solid solution of tin in copper. The large proportion of this eutectoid is due to the high percentage of tin in this alloy. This alloy has a tensile strength of 33,000 lb. per sq. in. and an elongation in 2 in. of 1%.

Fig. 8 — Aluminum Bronze (125×).

Cu 89.38%; Al 9.88%; Fe 0.20%.

Etched in ammonium persulphate. Specimen was heated to 1600° F. for 15 minutes and quenched in water. Structure shows grains of alpha in the alpha-gamma eutectoid. It has a tensile strength of about 80,000 lb. per sq. in.

Fig. 9 — Phosphor Bronze Rolled.

Cu 94%; Sn 3.5%; P 0.05%–0.50%; Zn, Fe and Pb as impurities.

Etched in NH_4OH and H_2O_2. The structure shows homogeneous grains of alpha solid solution. Some twinning is shown, indicating previous overstrain followed by an anneal. The small amount of phosphorus together with the work gives this bronze a tensile strength of over 80,000 lb. per sq. in. and an elongation in 2 in. of over 12% when worked to a diameter not over $\frac{1}{2}$ in. This is suitable for parts requiring good strength and incorrodibility.

Fig. 10 — Gun Metal — Cast (100×).

Cu 88%; Sn 10%; Zn 2%.

Etched in NH_4OH and H_2O_2. Buff cored areas are regions of the alpha solid solution. Bluish-gray angular areas containing small black specks are regions of the alpha and delta eutectoid. The delta solid solution is very hard and brittle so this makes a suitable material to take wear. It is used for bushings, bearings, large composition valves, etc. Gun metal has a tensile strength of 35,000 lb. per sq. in.; and an elongation in 2 in. of 16%.

Fig. 11 — Vanadium-Manganese Bronze (40×).

Sn 0.28%; Zn 38.51%; Cu 60.59%; Fe 0.09%; Al 0.75%; Mn trace; V trace.

Etched in NH_4OH and H_2O_2. Structure shows grains of alpha in the beta matrix. This alloy is really a brass, although it is called a bronze. The manganese and vanadium were added as scavengers and were removed with the slag. This alloy has a tensile strength of 62,600 lb. per sq. in., a yield point of 23,400 lb. per sq. in., and an elongation in 2 in. of 36.0%.

Fig. 12 — Tensilite (500×).

Cu 68.26%; Zn 21.04%; Mn 3.20%; Si 0.04%; Pb 0.14%; Al 4.80%; Fe 2.03%.

Etched in chromic acid and ferric chloride. Structure shows crystals of alpha solid solution in the beta solid solution matrix. The halftone crystals are probably a compound of iron. This alloy has a tensile strength of 103,200 lb. per sq. in., a yield point of 30,000 lb. per sq. in., an elongation in 2 in. of 21.0% and a reduction in area of 24.5%.

Fig. 13 — Alcumite — Chill — Cast (75×).

Cu 86.16%; Fe 2.02%; Ni 1.98%; Al 9.84%.

Etched in 10% chromic acid solution. Alcumite is a special aluminum bronze and an acid-resistant metal. Structure shows alpha plus beta solid solutions (alpha, light; beta, dark). Sand-cast Alcumite has a tensile strength of 82,800 lb. per sq. in., a yield point of 34,000 lb. per sq. in., an elongation in 2 in. of 10.0% and a reduction in area of 10.0%.

Fig. 14 — Alcumite — Annealed (200×).

Cu 88.16%; Fe 3.55%; Ni 0.68%; Al 7.61%.

Etched in 10% chromic acid solution. Structure shows alpha plus beta solid solutions. This alloy was annealed by heating to 1500° F. for 1 hour, and air-cooling. It has a tensile strength of 75,000 lb. per sq. in., a yield point of 25,000 lb. per sq. in., an elongation in 2 in. of 40.0% and a reduction in area of 45.0%.

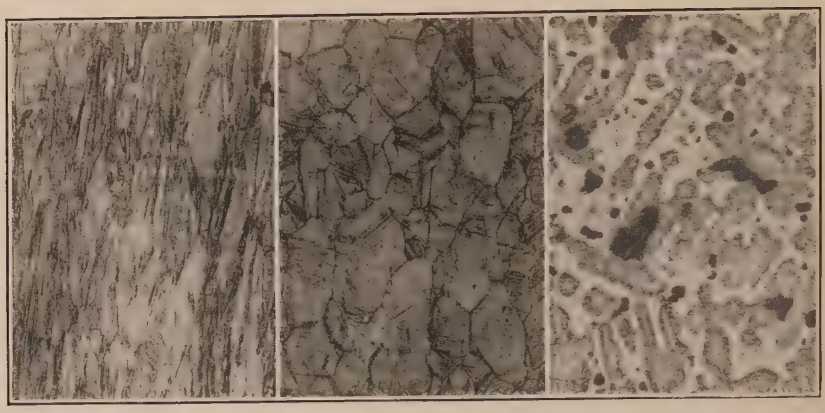

FIG. 1 FIG. 2 FIG. 3

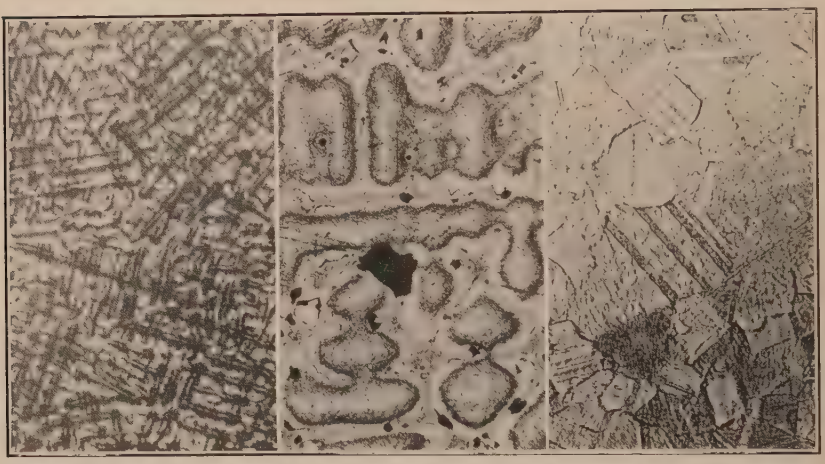

FIG. 4 FIG. 5 FIG. 6

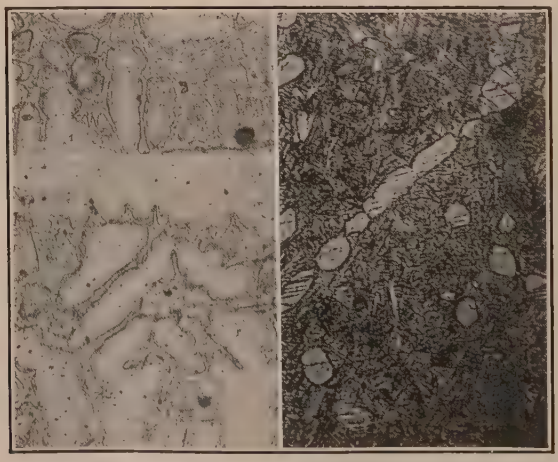

FIG. 7 FIG. 8

FIG. 9 FIG. 10

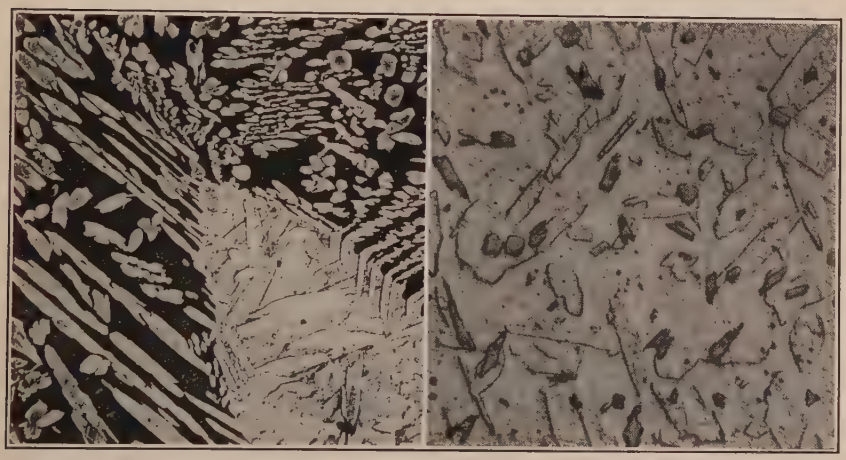

FIG. 11 FIG. 12

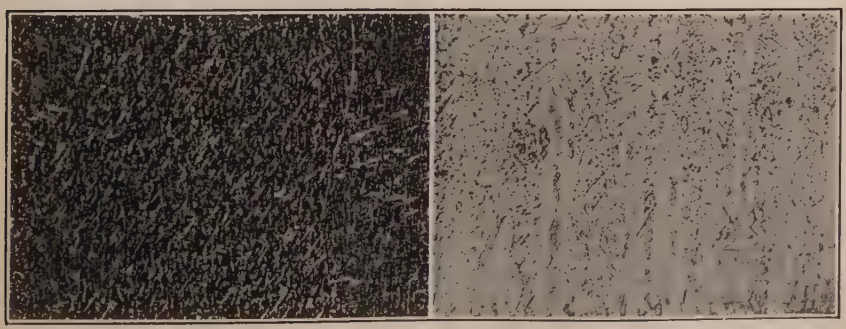

FIG. 13 FIG. 14

EXPERIMENT XX

ALUMINUM AND ITS ALLOYS*

Purpose: To study the microstructures of aluminum and its alloys.

Reference: (*a*) The Aluminum Company of America publications.

(*b*) Anderson: The Metallurgy of Aluminum and Aluminum Alloys.

(*c*) Williams and Homerberg: Principles of Metallography, pp. 89–95.

(*d*) Bureau of Standards Bulletin 76: "Aluminum and Its Light Alloys."

Theory: Commerical aluminum is from 98 to 99.5% pure, the impurities being usually copper, iron and silicon. The more definite and more useful alloys of aluminum include certain binary aluminum-copper, aluminum-zinc alloys, certain ternary aluminum-copper-zinc alloys, duralumin and its related alloys, the new silicon alloys and certain complex alloys.

For casting alloys the aluminum-zinc-copper or the aluminum-copper alloys have been most largely used, whereas, for forging and rolling the duralumins are preferred.

PHOTOMICROGRAPHS — (Plates XLIX, L, LI, LII)

Fig. 1 — Aluminum Ingot (100×).

Cu 0.12%; Fe 0.39%; Si 0.25%; Ti 0.02%; Al remainder.

Etched in ½% HF solution. This micrograph shows the typical cast network in a 99% aluminum ingot, consisting of Fe and Fe-Si constituents in the aluminum matrix.

Fig. 2 — Aluminum Ingot (500×).

Photomicrograph is of the same ingot as in Fig. 1, but at 500 diameters.

Fig. 3 — Aluminum — Rolled (100×).

Cu 0.10%; Fe 0.40%; Si 0.20%; Al remainder.

Etched in ½% HF solution. This micro-section was taken parallel to direction of rolling of a hard-rolled aluminum sheet. The structure shows the alignment of the constituent particles which are various combinations of aluminum with its metallic impurities. The line pattern in the aluminum matrix which has been revealed by etching is charac-

* Aluminum Company of America.

teristic of the rolled structure. This metal has a minimum tensile strength of 22,000 lb. per sq. in. and an elongation in 2 in. of 1–4%.

Fig. 4 — Aluminum — Rolled (500×).

Photomicrograph is of the same metal as in Fig. 3, but at 500 diameters.

Fig. 5 — Aluminum — Rolled (100×).

Etched in ½% HF. Aluminum sheet, half-hard, reduced four gage numbers in thickness subsequent to the final annealing treatment. This photomicrograph shows the entire cross-section of the aluminum sheet. Although rolled subsequent to the annealing operation, the new grains formed by recrystallization during this process are easily distinguished. This metal has a tensile strength of 16,000 to 20,000 lb. per sq. in. and an elongation of 3 to 7%.

Fig. 6 — Duralumin Sheet — Hard Rolled (100×).

Cu 4.0%; Fe 0.50%; Si 0.60%; Mn 0.56%; Mg 0.55%; Al remainder.

Etched in HF + HCl + HNO_3 solution. This photomicrograph shows the typical hard-rolled sheet structure. This sheet has a tensile strength of 39,800 lb. per sq. in., a yield point of 36,300 lb. per sq. in., an elongation of 4% and a Brinell hardness of 71.7.

Fig. 7 — Duralumin Sheet — Hard Rolled (500×).

Same as Fig. 6 but at a magnification of 500 diameters. The clear outlined particles are probably $CuAl_2$. The small particles of this compound have been precipitated by preheating and annealing during the rolling process. The particles darkened by etching are the Cu-Fe-Mn constituent characteristic of this alloy.

Fig. 8 — Duralumin Sheet — Annealed (100×).

Same alloy as in Fig. 6 but annealed after rolling. This photomicrograph shows the average structure illustrating recrystallized grains and alignment of the constituent particles. This annealed alloy now has a tensile strength of 26,545 lb. per sq. in., a yield point of 11,800 lb. per sq. in., an elongation in 2 in. of 19.4%; and a Brinell hardness of 44.8.

Fig. 9 — Duralumin Sheet — Annealed (500×).

Same as Fig. 8 but at a magnification of 500 diameters. The photomicrograph shows the annealed structure in greater detail and reveals the fine precipitate of $CuAl_2$ produced by preheating and annealing.

Fig. 10 — Duralumin (17ST) (100×).

Cu 4.07%; Fe 0.50%; Si 0.60%; Mn 0.56%; Mg 0.55%; Al remainder.

Etched in HF-HCl-HNO_3 mixture. This photomicrograph shows the average microstructure of heat-treated Duralumin Sheet, grains of aluminum solid solution and fine particles of copper aluminide precipitated out. This alloy has a tensile strength of 58,550 lb. per

sq. in., a yield point of 35,900 lb. per sq. in., an elongation in 2 in. of 19.1% and a Brinell hardness of 99.

Fig. 11 — Duralumin (17ST) (500×).

This alloy is the same as in Fig. 10 but at 500 magnifications. The structure is typical of duralumin at high magnification. The individual grains are easily distinguished, recrystallization having taken place during heat-treatment. The black particles of Cu-Fe-Mn compounds have been attacked by the etch and are relatively insoluble in solid aluminum. One or two outlined particles of $CuAl_2$ are visible, although most of this constituent exists as particles of submicroscopic dimensions, or in solid solution in the aluminum.

Fig. 12 — Aluminum Alloy — No. 122 (100×).

Cu 10.29%; Fe 1.12%; Si 0.18%; Mn 0.01%; Mg 0.22%; Al balance.

Unetched. Photomicrograph is a section of a permanent-mold-cast piston of Al-Cu-Mg alloy (No. 122 Alloy). Structure shows a eutectic network consisting principally of $CuAl_2$ and aluminum around the aluminum matrix.

Fig. 13 — Al-Mn Alloy (500×).

Cu 0.11%; Si 0.22%; Fe 0.52%; Mn 1.23%; Al balance.

Etched in $\frac{1}{2}$% HF. Photomicrograph is of an aluminum-manganese alloy sheet (350) annealed at 800° F. The principal microconstituent is $MnAl_3$, occurring both as large particles and as small dots in this micrograph. The latter particles have grown from a submicroscopic dispersion during the preheating of the original ingot. Particles of the Fe-Mn, Fe-Si, and Mn-Si constituents are also present. This alloy has a tensile strength of 16,050 lb. per sq. in., a yield point of 8145 lb. per sq. in., and an elongation in 2 in. of 32.7%.

Fig. 14 — Aluminum Alloy — No. 12 (100×).

Cu 8.03%; Fe 0.48%; Si 1.54%; Mn 0.06%; Al balance.

Etched in $\frac{1}{2}$% HF. This photomicrograph is of a sand-cast section of aluminum-copper alloy (No. 12 Alloy). Structure shows a eutectic network around the grains of aluminum. This alloy has a tensile strength of 18,000 to 23,000 lb. per sq. in. a yield point of 11,000 lb. per sq. in., an elongation in 2 in. of 1 to 3% and a Brinell hardness of 65. No. 12 Aluminum Alloy is used for automobile parts, as, for example, crankcases, oil pans, transmission housings. It is also used for boat propellers, etc.

Fig. 15 — Aluminum Alloy — No. 12 (500×).

Photomicrograph is of the same alloy as in Fig. 14, but at 500 magnifications. Two constituents are readily identified; these are $CuAl_2$, which is the light-colored constituent present in largest amount, and Si,

dark and associated with the $CuAl_2$. A third phase will be observed near the center of the field. It is apparently the alpha constituent, which contains Al, Fe and Cu.

Fig. 16 — Aluminum Alloy — No. 43 (100×).

Cu 0.17%; Fe 0.62%; Si 5.31%; Mn 0.01%; Ti 0.011%; Al remainder.

Unetched. Photomicrograph is of a sand-cast section of aluminum-silicon alloy (43 alloy). Structure shows primary grains of aluminum plus eutectic of aluminum and silicon. This alloy has a tensile strength of 17,000 to 22,000 lb. per sq. in., a yield point of 7,000 lb. per sq. in., an elongation in 2 in. of 3 to 7% and a Brinell hardness of 40.

Fig. 17 — Aluminum Alloy — No. 43 (500×).

This photomicrograph is of the same alloy as in Fig. 16, but at 500 magnifications. The cast structure of primary aluminum grains of aluminum plus the eutectic of aluminum and silicon is shown.

Fig. 18 — Al-Si Alloy (250×).

Cu 0.16%; Fe 1.05%; Si 12.20%; Al 86.5%.

Etched in dilute HF. Structure shows massive silicon with much finely divided silicon and thick plates of $FeAl_3$ in the aluminum solid solution. This alloy has a tensile strength of 20,300 lb. per sq. in. and an elongation in 2 in. of 1.8%.

Fig. 19 — Alclad 17ST Sheet (50×).

Etched in 1% HF. The photomicrograph shows the full cross-section of a duralumin sheet on both sides of which has been superimposed a thin layer of aluminum of the highest purity. The alloy base is deeply etched and the intermediate zone well revealed; whereas the pure aluminum surfaces have not been appreciably attacked by the etching. This intermediate zone between the pure metal and the alloy is due to the diffusion of the soluble constituents $CuAl_2$ and Mg_2Si from the duralumin into the pure aluminum during fabrication and heat-treatment and is clear evidence of the integral character of the product. Alclad is a new corrosion-resistant product.

Fig. 20 — Alclad 17ST Sheet (100×).

This photomicrograph is of the same alloy as in Fig. 19, but at 100 diameters. The strong alloy core (dark area) and the surface of pure aluminum will be noted.

Fig. 21 — Y-Alloy (350×).

Cu 3.50%; Mg 1.0%; Ni 1.75%; Al remainder.

Etched in 10% NaOH. Alloy was heated to 950° F., quenched in hot water, reheated to 210° F. for 16 hours, then air-cooled. Structure shows the network of the Cu-Mg-Ni-Al compounds at the grain-boundary of the aluminum solid solution. This alloy is used for pistons,

air-cooled cylinder heads and in airplane engines where high hardness and high yield point are required for aluminum alloys.

Fig. 22 — Al-Cu Alloy (No. 195 Alloy) (25×).

Cu 4.4%; Fe 0.57%; Si 0.75%; Mn 0.02%; Zn 0.25%; Al balance.

Etched in HF-HCl-HNO_3 mixture. Alloy was heated to 960° F. and water-quenched. This is a lower power photograph of a part of a cross-section of a sand-cast test bar of Al-Cu Alloy (No. 195 alloy), etched to produce a grain contrast. Structure shows grains of aluminum holding the chemical compounds in solid solution.

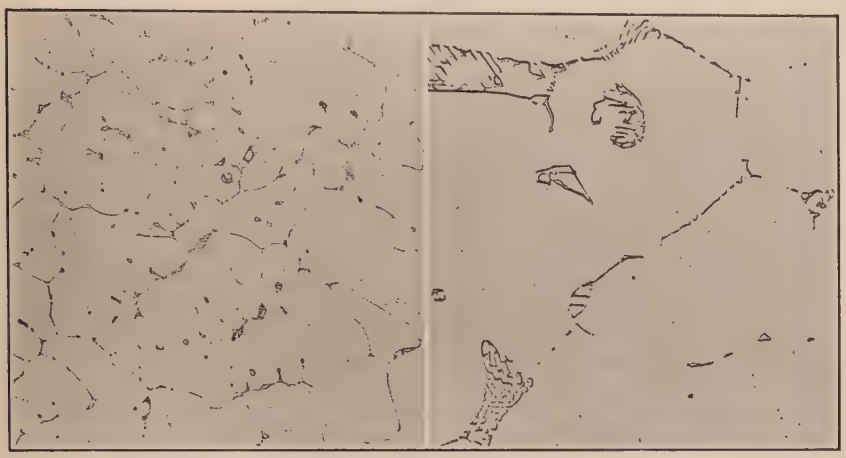

FIG. 1 FIG. 2

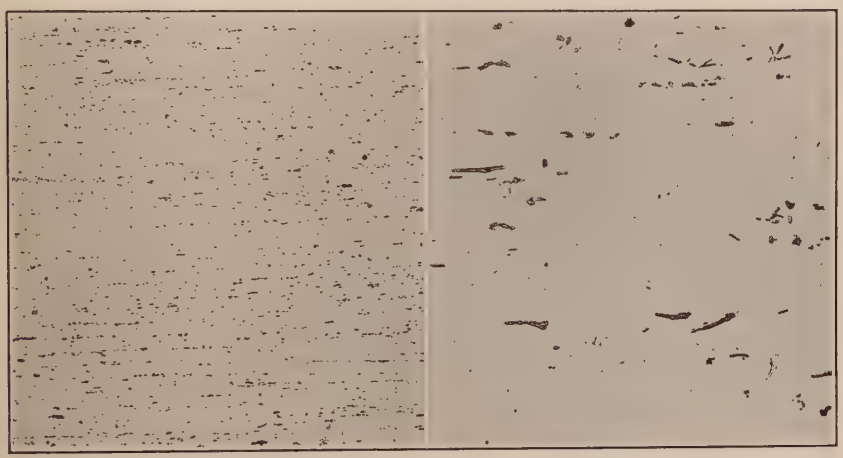

FIG. 3 FIG. 4

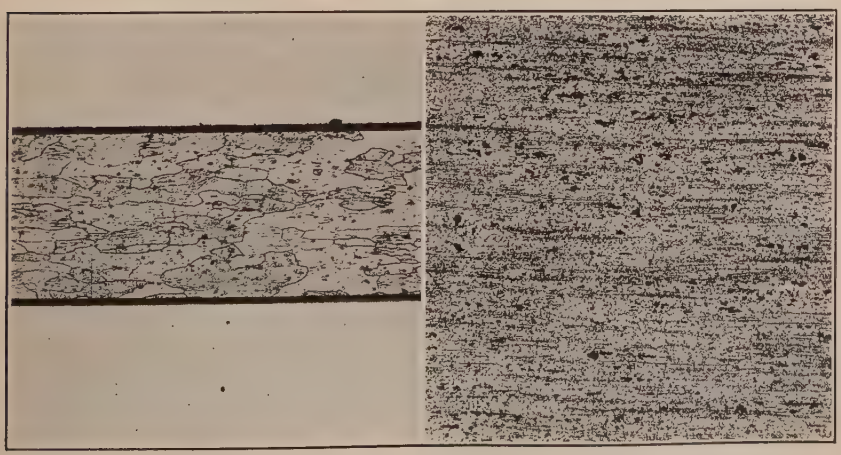

FIG. 5 FIG. 6

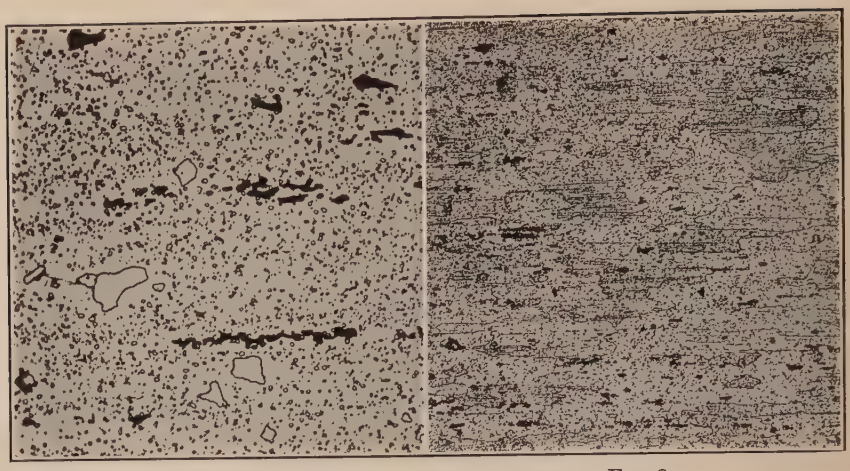

FIG. 7 FIG. 8

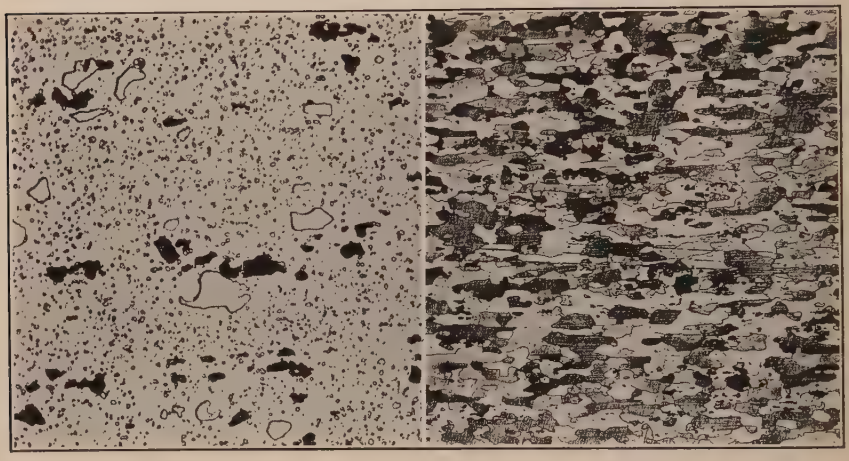

FIG. 9 FIG. 10

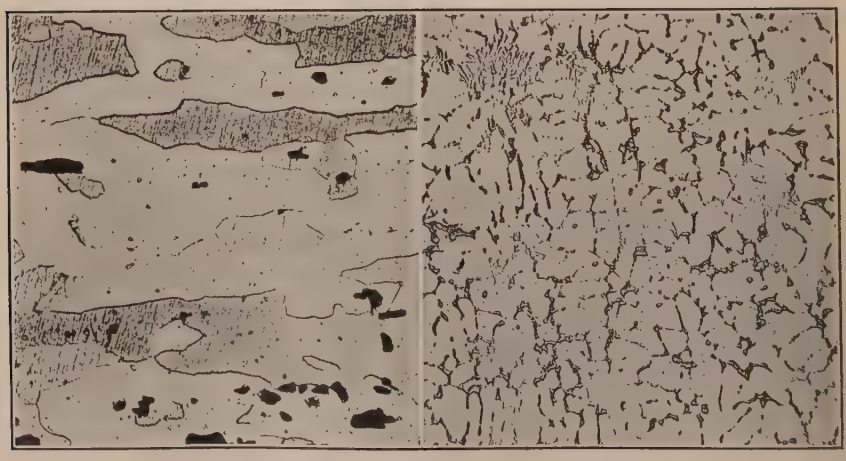

FIG. 11 FIG. 12

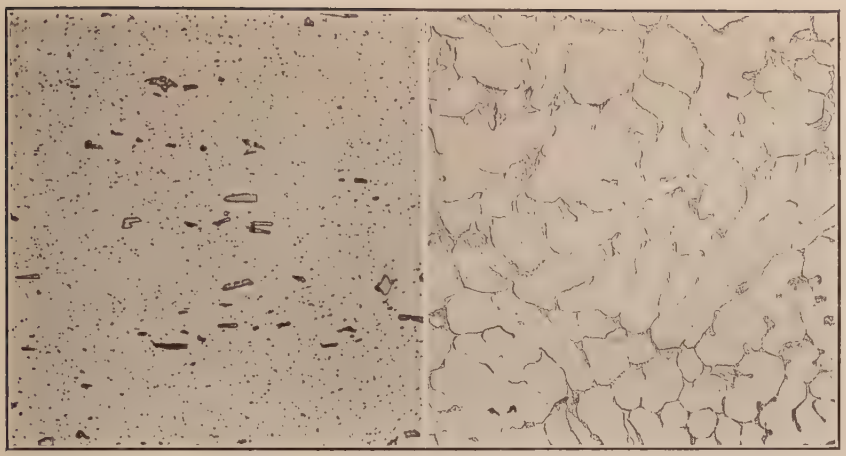

Fig. 13 Fig. 14

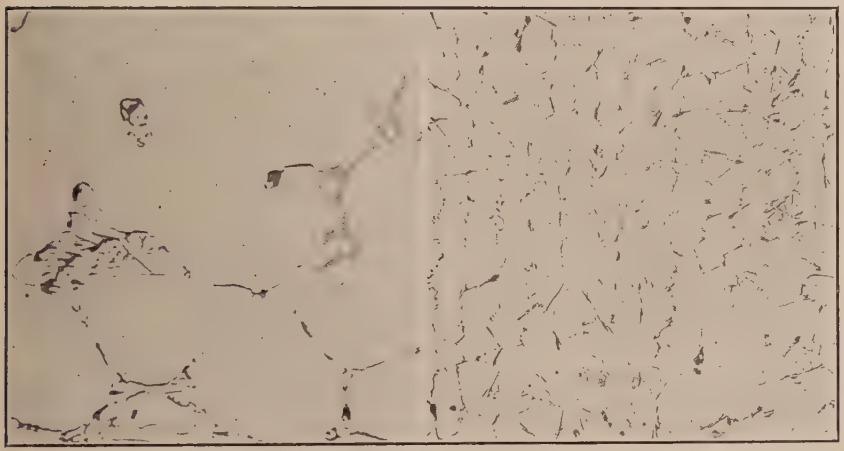

Fig. 15 Fig. 16

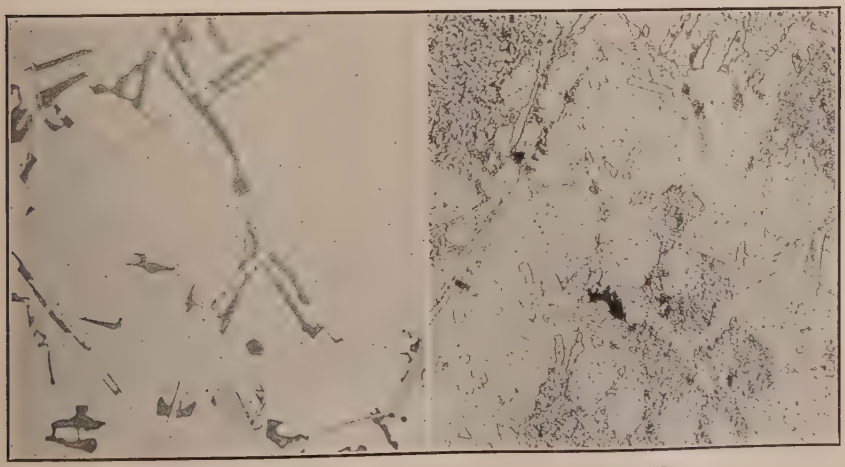

Fig. 17 Fig. 18

PLATE LII

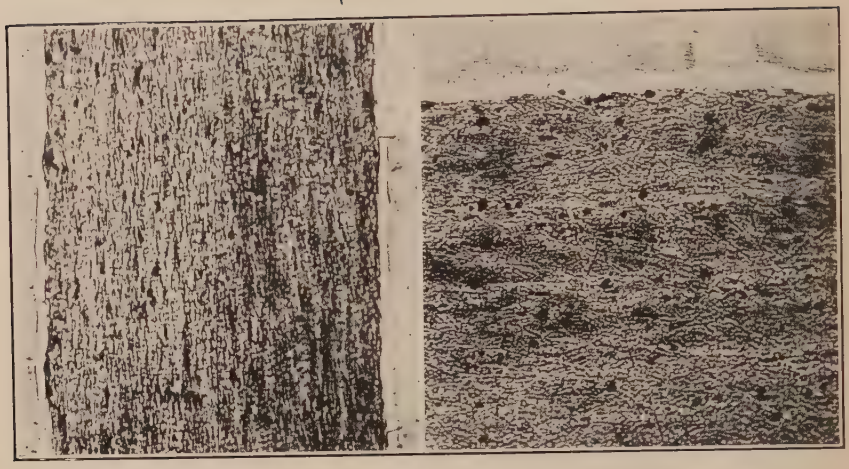

FIG. 19 FIG. 20

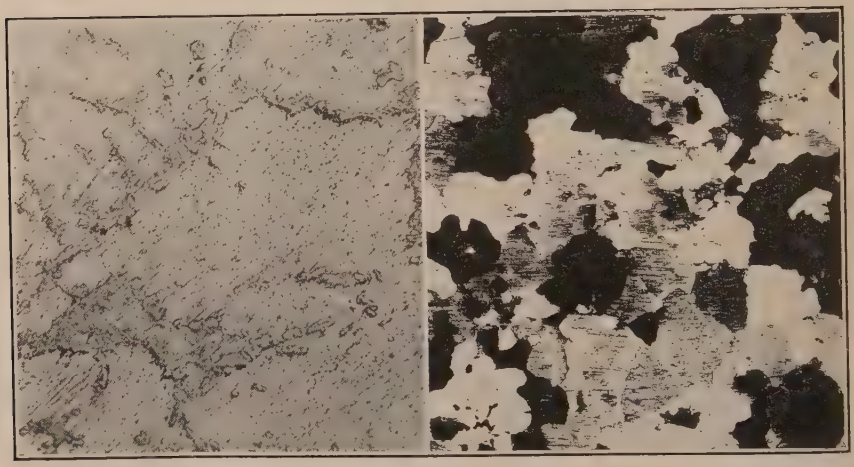

FIG. 21 FIG. 22

EXPERIMENT XXI

EFFECTS OF HEAT-TREATING DURALUMIN

Purpose: To study the effects on the physical properties of aging annealed and heat-treated duralumin.

References: (*a*) Anderson: The Metallurgy of Aluminum and Its Alloys.

(*b*) Bureau of Standards: "Heat Treatment of Duralumin," Scientific Paper 347.

(*c*) "Properties and Treatment of Duralumin in the Construction of Aircraft," Technical Note 136, Bureau of Aeronautics, Navy Department, dated July 10, 1924.

Material: 22 tension test specimens of Duralumin Sheet.

Analysis: { Cu 3.93% Mg 0.50% Si 0.33%
Mn 0.56% Fe 0.58% Al 94.08% ±.

Apparatus: Salt baths, thermocouples, pyrometer, steel stencils, tension testing machine, Shore Scleroscope and Rockwell hardness tester.

Character of Duralumin. — Duralumin is the commercial name given to any light aluminum alloy that is capable of being hardened by heat-treatment followed by aging. Duralumin is therefore not a definite alloy, but a class of alloys. The duralumins may, in general, be classified as simple duralumins, zinc duralumins and special duralumins. The most commonly used are the simple or ordinary duralumins.

The average chemical composition of the simple duralumins is as follows:

Copper	3.0–4.5%
Magnesium	0.4–1.0%
Manganese	0.0–1.0%
Iron (as impurities)	0.4–1.0%
Silicon	0.3–0.6%
Aluminum	Balance

Duralumin bears much the same relation to aluminum as alloy steel bears to soft iron or steel, and, like alloy steel, it must be suitably heat-treated to develop its best physical properties. Heat-treatment consists in raising to a certain elevated temperature and rapidly cooling,

as by quenching in water. Contrary to steel, duralumin is soft after quenching, but it attains its maximum hardness and strength after "aging" for several days at room temperature. This characteristic is very useful in fabrication. Like steel, duralumin can also be annealed, thus it will remain in a soft condition indefinitely, until given a hardening-heat treatment, and it can, like steel, have its hardness and strength increased by mechanical working, such as cold-rolling, but the ductility is correspondingly reduced.

To produce maximum tensile strength and hardness with increased ductility, duralumin must be heated to 500–515° C., quenched in water to 30–100° C. and aged at a temperature between 30 and 100° C. Quenching and aging at 100° C. produces the desired maximum properties within 4 to 5 days, whereas quenching in cold water and aging at room temperature produce approximately the same physical properties at the end of 15 to 30 days.

To produce soft and workable metal, duralumin is annealed by heating to 350–380° C. and quenching in warm water or cooling in air. Some increase in hardness and tensile strength of annealed duralumin takes place on aging.

The theory of hardening is very similar in one respect to that of steel. At the elevated temperatures the intermetallic compounds, $CuAl_2$, Mg_2Si, $FeAl_3$, are dissolved in the aluminum matrix. At lower temperatures this solid solution is supersaturated and there results a slow precipitation of these compounds in a highly dispersed state at the cleavage planes and crystal boundaries of the aluminum. This causes a keying action and an increased resistance to slip.

Procedure:

A. Heat-Treatment.

Stamp each end of each specimen with its proper mark as indicated below and proceed with the designated heat-treatment as follows:

(*a*) *Heat-Treatment for Maximum Strength and Hardness*

Mark	Heat to	Hold for	Quench in	Age at 100° C. for
		Minutes		
A — 1	500° C.	10	Boiling water	½ hour
A — 2	500° C.	10	Boiling water	1 day
A — 3	500° C.	10	Boiling water	2 days
A — 4	500° C.	10	Boiling water	3 days
A — 5	500° C.	10	Boiling water	4 days
A — 6	500° C.	10	Boiling water	5 days
A — 7	500° C.	10	Boiling water	6 days
A — 0	Untreated — to be used as standard			

(*b*) *Heat-Treatment for Strength and Hardness*

Mark	Heat to	Hold for	Quench in	Age at room temperature for
		Minutes		
B — 1	500° C.	10	Cold water	½ hour
B — 2	500° C.	10	Cold water	1 day
B — 3	500° C.	10	Cold water	2 days
B — 4	500° C.	10	Cold water	3 days
B — 5	500° C.	10	Cold water	4 days
B — 6	500° C.	10	Cold water	5 days
B — 7	500° C.	10	Cold water	6 days

(*c*) *Annealing for Maximum Softness*

Mark	Heat to	Hold for	Quench in	Age at room temperature for
		Minutes		
C — 1	370° C.	10	Cold water	1 hour
C — 2	370° C.	10	Cold water	1 day
C — 3	370° C.	10	Cold water	2 days
C — 4	370° C.	10	Cold water	3 days
C — 5	370° C.	10	Cold water	4 days
C — 6	370° C.	10	Cold water	5 days
C — 7	370° C.	10	Cold water	6 days

B. Physical Testing.

After heat-treating as specified, perform a commercial tension test to determine the yield point, maximum tensile strength, per cent elongation and reduction of area. Get also the Scleroscope hardness.

Curves. — Plot on one sheet of paper curves showing each physical property as a function of the time of aging (abscissa) for both the annealed and heat-treated specimens.

Table I shows the data, and Fig. 1 shows the tensile strength and hardness curves for the heat-treated duralumin. Table II gives the average general and mechanical properties of duralumin.

TABLE I

DATA

Heat-Treatment	Time of Aging, Hours	Tensile Strength, lb./sq. in.	Per cent Elongation in 2 in.	Scleroscope Hardness
(*a*) Heated to 500° C. for 10 minutes, quenched in boiling water and aged at 100° C.	½	57,330	12.5	17
	24	62,700	14.5	24
	48	64,000	18	25
	72	65,533	19	26.5
	96	65,700	20	27.5
	120	66,000	22	28.5
	144	66,800	25	29
(*b*) Heated to 500° C. for 10 minutes, quenched in cold water and aged at 25° C.	½	50,000	15	16
	24	57,000	19	22
	48	58,600	20	24
	72	59,800	20	25
	96	60,600	19	26
	120	61,200	21	28
	144	61,667	22	28
(*c*) Heated to 370° C. for 10 minutes, quenched in cold water and aged at 25° C.	1	36,700	6.2	14
	24	44,000	9.2	17
	48	46,200	14.2	18
	72	47,000	16.5	18.5
	96	48,800	17	18.5
	120	49,200	19	19
	144	51,900	19	19

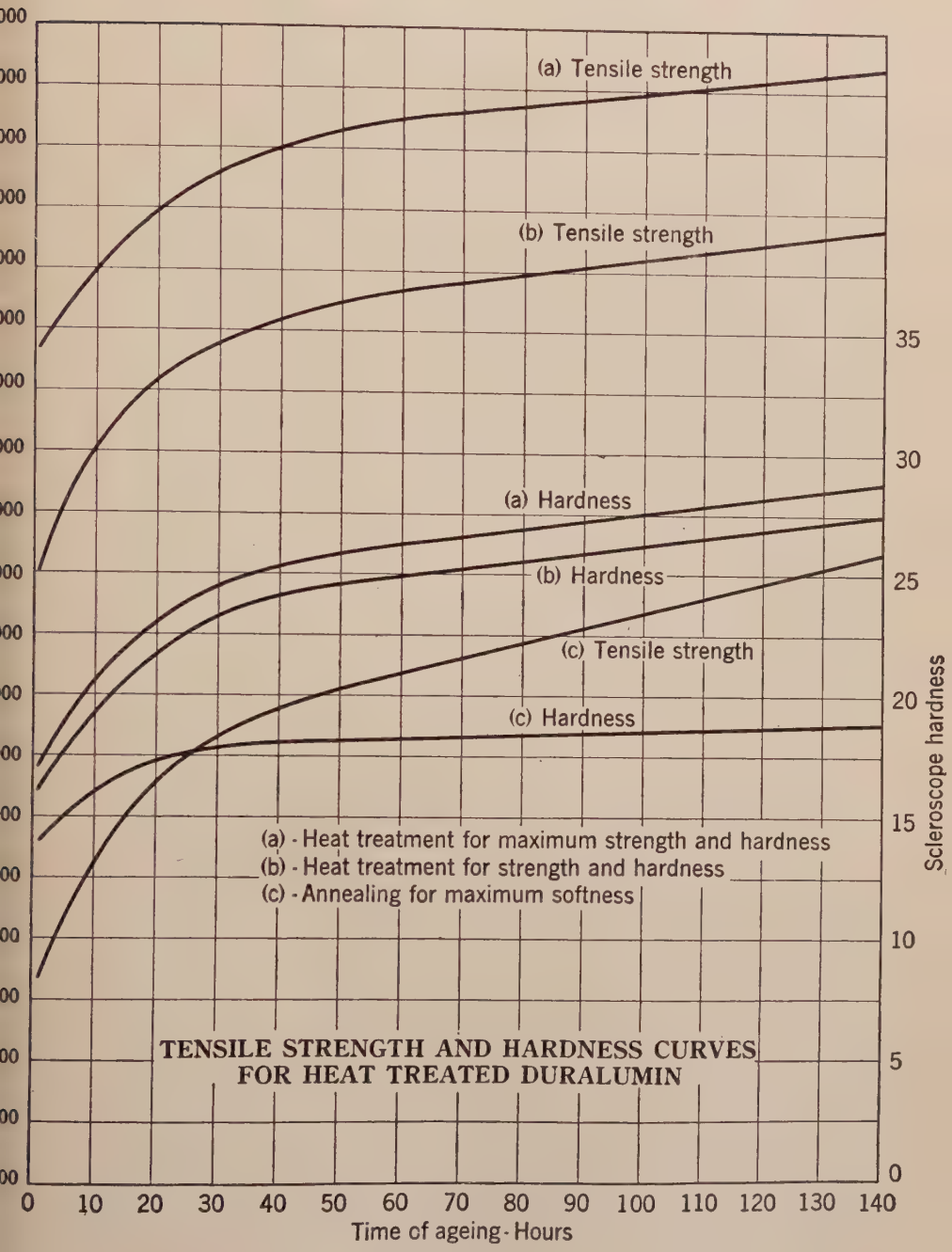
(a) Tensile strength
(b) Tensile strength
(a) Hardness
(b) Hardness
(c) Tensile strength
(c) Hardness
(a) - Heat treatment for maximum strength and hardness
(b) - Heat treatment for strength and hardness
(c) - Annealing for maximum softness
TENSILE STRENGTH AND HARDNESS CURVES FOR HEAT TREATED DURALUMIN
Time of ageing - Hours
Scleroscope hardness
0 10 20 30 40 50 60 70 80 90 100 110 120 130 140
35 30 25 20 15 10 5 0

FIG. 1

Discussion: Draw conclusions from the results of this test as to

(*a*) The effects of aging *annealed* duralumin.

(*b*) The effects of aging *heat-treated* duralumin.

(*c*) The difference in the physical properties resulting from the two temperatures used in heating the specimens.

Compare your results with those given in reference (*b*) and make any comments that this comparison suggests.

Addendum: Representative mechanical properties for material not over $\frac{3}{4}$ in diameter or thickness are given here (see also reference *c*).

TABLE II

PHYSICAL PROPERTIES OF DURALUMIN

General:

Specific gravity	2.80 to 2.85
Weight, pounds per cubic inch	0.100 to 0.102
Weight, pounds per cubic foot	173 to 176
Melting range	540° to 650° C.
Coefficient of linear expansion per degree Centigrade	0.0000226
Thermal conductivity (silver 100)	31
Specific heat	0.214

Duralumin is non-magnetic

Mechanical (lb./sq. in.)	Heat-Treated	Annealed	Hard-Rolled
Tensile strength	55,000 to 62,000	25,000 to 35,000	67,000 to 72,000
Yield point	30,000 to 36,000	.....	55,000 to 65,000
Elongation in 2 in.	18 to 25%	10 to 14%	3 to 8%
Brinell hardness	93 to 100	54 to 60	130 to 140
Scleroscope hardness	23 to 31	9 to 12	37 to 42

EXPERIMENT XXII

BEARING METALS

Purpose: To study the microstructures of various bearing metals.
References: Gulliver: Metallic Alloys, pp. 372–376.
Guillet and Portevin: Metallography and Macrography, pp. 243–251.

Theory: Bearing metals embrace a number of alloys in which binary compounds occur, but no ternary compounds are formed. The alloys used for bearings in all classes of machinery are of the same general type. They consist of a hard and a soft constituent, the function of the former being to resist wear and to provide a surface with a low coefficient of friction, and that of the latter to permit a uniform distribution of load, so as to prevent local heating and seizing. In other words the essential property of a bearing or of an antifriction metal is that it should consist of hard particles capable of resisting abrasion and bearing the load, embedded in a softer matrix which is capable of yielding slightly and adjusting itself to any local pressure. The alloy should have sufficient compressive strength at the temperature of working to withstand the load; it should not be brittle and must be easily workable. The melting point must not be too low and a high thermal conductivity is desirable. These and various other properties are mainly dependent on the chemical composition and the microstructure, which is greatly influenced by the casting temperature.

PHOTOMICROGRAPHS — (Plates LIII, LIV, LV)

Fig. 1 — Copper-Tin Bearing (Cu 20%; Sn 80%) — Cast (100×). Cooled moderately slowly. Etched in 5% HNO_3 in alcohol for 4 seconds. Bright shaft-like crystals are of two colors. The darker interiors are of composition Cu_3Sn and the almost white edges are of CuSn (or possibly a solid solution rich in CuSn). The darker area surrounding the light-colored crystals is the eutectic mixture of tin and CuSn.

In these copper-tin alloys the chemical compounds (crystals) Cu_3Sn and CuSn offer the hard wearing surface and the eutectic matrix of Sn and CuSn offer the plastic backing.

Fig. 2 — Antimony-Tin Bearing (Sb 30%; Sn 70%) — Cast (100×). Etched in 5% HNO_3 in alcohol. This alloy shows primary SbSn

crystals and Snα solid solution. The white squares and triangles are the SbSn crystals and the dark, almost black, areas are the tin-rich solid solution, Snα. The white specks in the dark area are small bits of SbSn that had not completely reacted with the liquid to form the tin-rich solid solution.

In the antimony-tin bearing metals the bearing qualities are due to the presence of the hard SbSn crystals (chemical compound) and to the plastic Snα solid solution matrix.

Fig. 3 — Lead-Antimony Bearing (Pb 75%; Sb 25%) — Cast (100×). Slowly cooled. Etched in 5% nitric acid in alcohol. White areas are primary grains of pure antimony; the dark speckled matrix is the eutectic alloy of lead and antimony. The quantity of pure antimony grains increases and the eutectic matrix decreases as the composition of the alloys gets richer in antimony.

The antifrictional qualities of lead-antimony bearing metals are due to the presence of the hard antimony crystals, while the eutectic forms a plastic matrix to support these crystals, and enables a proper bearing surface to be obtained.

Fig. 4 — Lead-Tin Bearing (Pb 90%; Sn 10%) — Cast (100×). Slowly cooled. Etched in 5% nitric acid. White specks are grains of pure tin thrown out of solid solution as the alloy cooled slowly. The matrix is the lead-tin solid solution containing about 7% tin in solution.

Fig. 5 — Lead-Tin Bearing (Pb 70%; Sn 30%) — Cast (100×). Slowly cooled. Etched in 5% nitric acid. Structure shows very small white grains of pure tin surrounded by the dark speckled eutectic of lead-tin solid solution and pure tin.

Fig. 6 — Lead-Tin Bearing (Pb 10%; Sn 90%) — Cast (100×). Slowly cooled. Etched in 5% nitric acid in alcohol. White areas are primary grains of pure tin. Dark speckled area at the boundaries of the primary grains is the eutectic alloy, the white specks being pure tin and the dark portion being lead-rich solid solution of lead and tin.

Fig. 7 — Babbitt (Sn 88.94%; Cu 7.38%; Fe 0.10%; Sb 3.58%) — Cast (100×). Slowly cooled. Etched with nitric acid. Skeleton network of copper-tin epsilon solid solution, white crystals of antimony-tin gamma solid solution, tin-rich ground-mass. The crystals of CuSn and SbSn offer the hard bearing surface embedded in the soft tin-rich matrix. The rather large white isolated square or triangular crystals are SbSn and the smaller irregular shaped white crystals are CuSn. Bearing metals of the above composition (approximately) are called Babbitts and also Navy antifriction metal.

Fig. 8 — Frary Bearing Metal (100×).

Ca 0.71%; Sn 0.26%; Ba 2.02%; Cu 0.04%; Pb 96.97%.

Etched in nitric and picric acids. The structure shows a white constituent which is $CaPb_3$, a compound of calcium and lead. It appears sometimes as elongated crystallites, sometimes as cubes. The gray constituent is a solid solution of calcium and barium in lead. The dark constituent is an eutectic of the calcium-barium-lead solid solution and the barium-lead compound. The eutectic was the last portion to solidify.

Fig. 9 — Plastic Bronze (100×).

Cu 77.32%; Sn 0.55%; Pb 21.69%; Zn 0.22%.

Etched in ferric chloride solution. The white and halftone areas represent a solid solution of tin and zinc in copper; the black areas represent lead.

Fig. 10 — Copper-Lead Bearing (100×).

Cu 73.80%; Pb 26.17%.

Etched in chromic acid. The white areas represent copper and the dark areas represent lead. Lead forms a network structure around the pure copper.

Fig. 11 — Navy Antifriction Metal (100×)

Cu 4.2%; Sb 7.8%; Sn 88%.

Etched in 5% HNO_3 in alcohol. Photomicrograph shows the cubic white crystals of SbSn and the small irregular shaped crystals of the copper-tin epsilon solid solution in the tin-rich matrix.

Fig. 12 — Steel Roller Bearing (500×).

Etched in picric acid. Photomicrograph shows the annealed structure of roller-bearing steel. Structure shows laminated pearlite grains surrounded by thin envelopes of cementite.

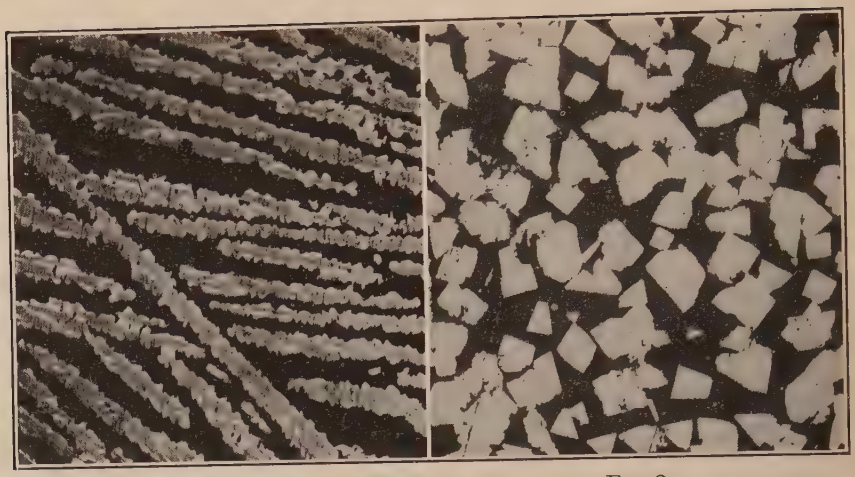

FIG. 1

FIG. 2

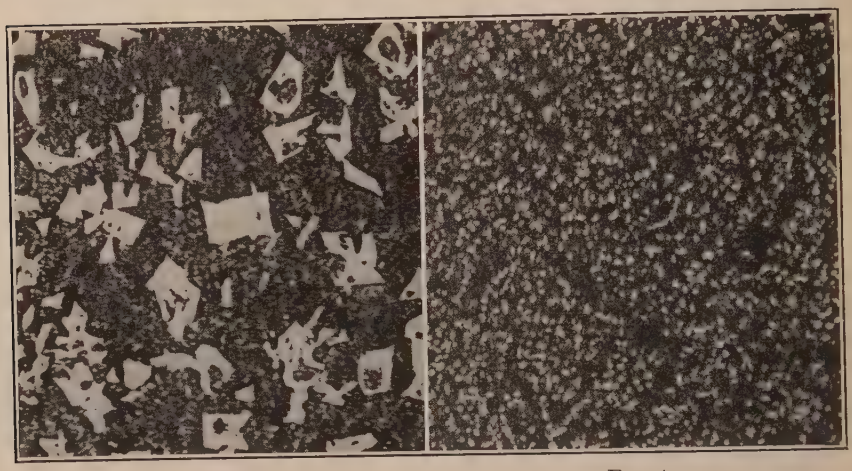

FIG. 3

FIG. 4

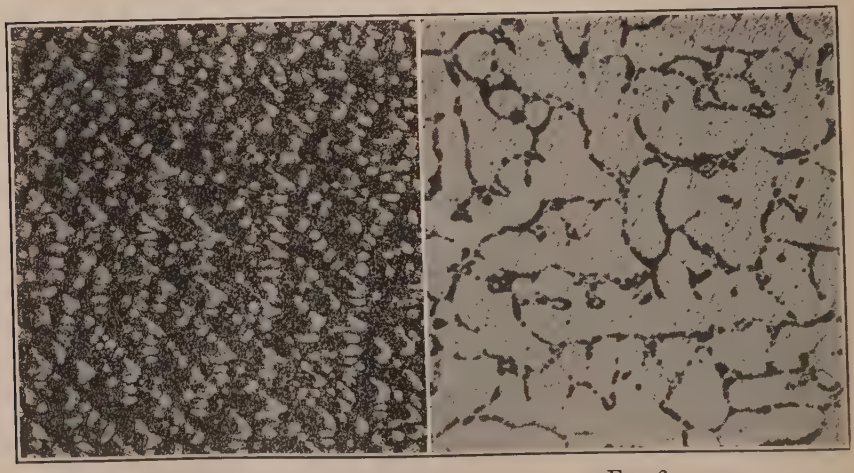

FIG. 5

FIG. 6

PLATE LIV

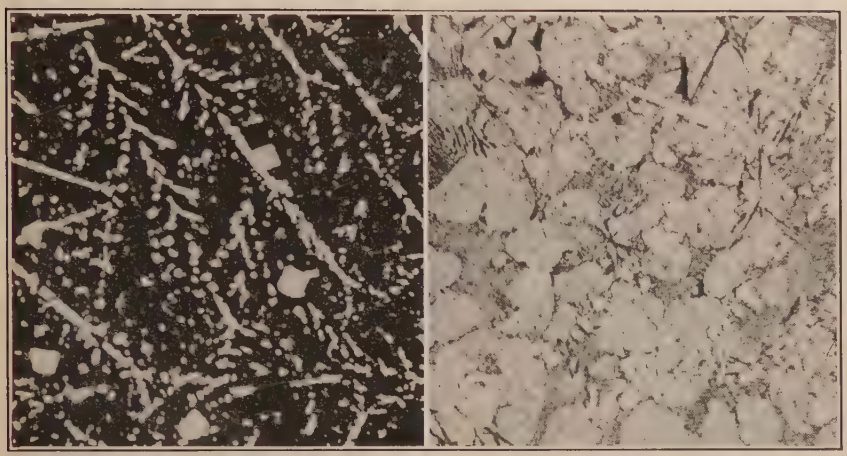

FIG. 7 FIG. 8

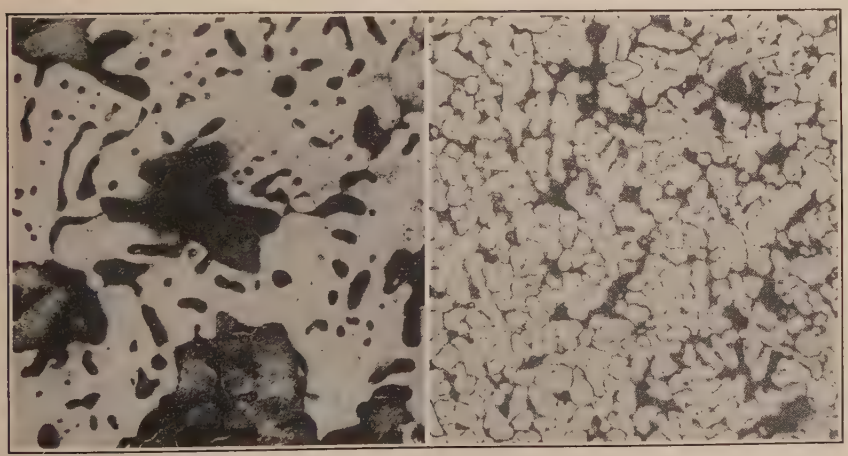

FIG. 9 FIG. 10

PLATE LV

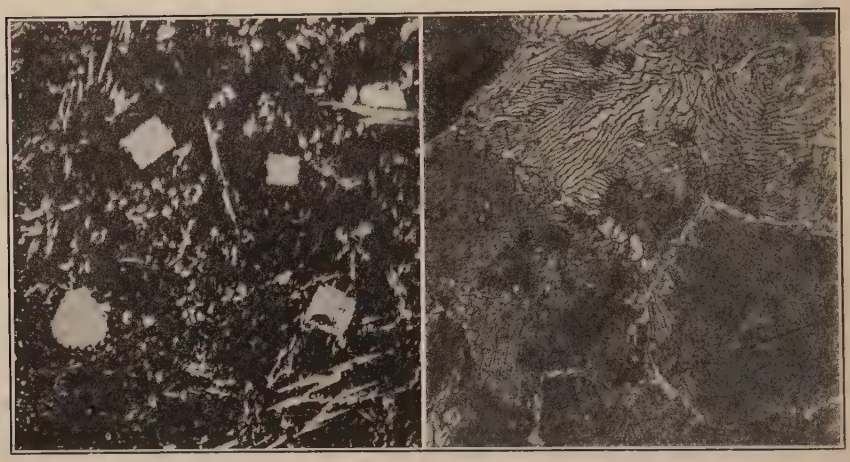

FIG. 11

FIG. 12

EXPERIMENT XXIII

GENERAL NON-FERROUS ALLOYS

Purpose: To study the microstructures of the general non-ferrous alloys.

References: Gulliver: Metallic Alloys.
Greaves and Wrighton: Practical Microscopical Metallography.
Williams and Homerberg: Principles of Metallography.
Jeffries and Archer: Science of Metals.
Guillet and Portevin: Metallography and Macrography.

PHOTOMICROGRAPHS — (Plates LVI–LVII)

Fig. 1 — Nickel — Rolled (100×).
98.99% pure.

Etched in nitric and acetic acids. Structure shows twinned grains of nickel and black spots of non-metallic impurities, chiefly nickel oxide.

Fig. 2 — Constantan — Cast (100×).
Cu 60%; Ni 40%.

Etched in solution containing 50% HNO_3 + 25% $HC_2H_3O_2$ + 25% H_2O. The inner boundary, being richer in nickel, gives a cored structure of an inhomogeneous solid solution of nickel in copper. Nickel greatly increases the electrical resistance of copper, the maximum resistance being obtained with 40% nickel. This alloy has a very low temperature coefficient. Constantan is used for electrical purposes and for thermocouples.

Fig. 3 — Monel Metal — Rolled (100×).
Cu 26%; Ni 72%; Fe 2%.

Etched in ferric chloride solution. This alloy had been rolled and followed by a partial anneal. Structure shows small twinned crystals of the copper-nickel-iron solid solution. Monel metal is characterized by its marked resistance to corrosion and by the fact that it retains its strength at high temperatures to a remarkable degree. After rolling and annealing it has a tensile strength of 65,000 lb. per sq. in., or better, with an elongation of 40%. Monel metal is used for valves, pump rods, pump liners, high-pressure steam fittings, etc.

Fig. 4 — Monel Metal — Cast (100×).
C 0.20%; Si 1.50%; Mn 0.35%; Fe 2.5%; Cu 28.0%; Ni 67.45%.

No. 1 was given a flat etch with HNO_3 and $HC_2H_3O_2$; and No. 2 was given a contrast etch with $FeCl_3$. Both photomicrographs show dendritic structure of the solid solution, characteristic of a casting.

Fig. 5 — White Metal (100×).

Pb 75%; Sb 25%.

Etched in 2% HNO_3. Structure shows white angular crystals of antimony surrounded by the fine lead-antimony eutectic.

Fig. 6 — Duralumin (100×).

Cu 3.9%; Mn 0.56%; Mg 0.50%; Si 0.33%; Fe 0.50%; Al balance.

Etched in 10% NaOH solution. This specimen was heat-treated and aged. The major portion of the structure is grayish-white and composed of an aluminum-rich solid solution. The dark particles are compounds of copper aluminide, $CuAl_2$, manganese silicide and iron aluminide embedded in matrix of aluminum containing soluble constituents in solution.

Commercial duralumin after proper heat-treatment has a tensile strength of 55,000 to 60,000 lb. per sq. in., a yield point of 35,000 to 37,000 lb. per sq. in., and an elongation in 2 in. of 12 to 18%.

Fig. 7 — Tin-Lead Solder Alloy (100×).

Sn 63.66%; Pb 36.34%.

Etched in HCl. Photomicrograph is a transverse section of a tin-lead alloy having the proportions of the eutectic. The structure consists almost entirely of the eutectic of pure tin and tin-lead solid solution. A few large white particles of pure tin are visible.

Fig. 8 — Tin — (99.9% pure) (100×).

Etched in HCl. Structure shows uniform grains of pure tin.

Fig. 9 — Manganese-Nickel (100×).

C 0.12%; S 0.005%; Si 0.05%; Fe 0.90%; Cu 0.20%; Mn 4.50%; Ni 94.20%.

Etched in 50% HNO_3 + 50% $HC_2H_3O_2$ solution. Alloy was hot-rolled. Structure shows uniform grains of the nickel-manganese solid solution. Some twinning is noticeable. This alloy has a tensile strength of 85,000 lb. per sq. in., a yield point of 40,000 lb. per sq. in., an elongation in 2 in. of 40% and a reduction in area of 65%.

Fig. 10 — Al-Mn-Mg Alloy (125×).

Al 4.36%; Mn 0.41%; Mg 94.97%.

Etched in 1% HNO_3. Structure shows primary grains of the Al-Mg-Mn solid solution surrounded by envelopes of the eutectic. This alloy, as cast, has a tensile strength of 18,000 lb. per sq. in., a yield point of 10,000 lb. per sq. in. and an elongation in 2 in. of 4%.

Fig. 11 — Al-Mn-Mg Alloy (525×).

This photomicrograph is of the same alloy as in Fig. 10, but at 525

diameters. Structure shows primary grains of the Al-Mg-Mn solid solution and the fine eutectic.

Fig. 12 — Copper-Magnesium Casting (525×)

Cu 13.22%; Mg 86.10%.

Etched in 0.5% HCl. Structure shows primary grains of magnesium and the fine eutectic of Mg_2Cu plus Mg.

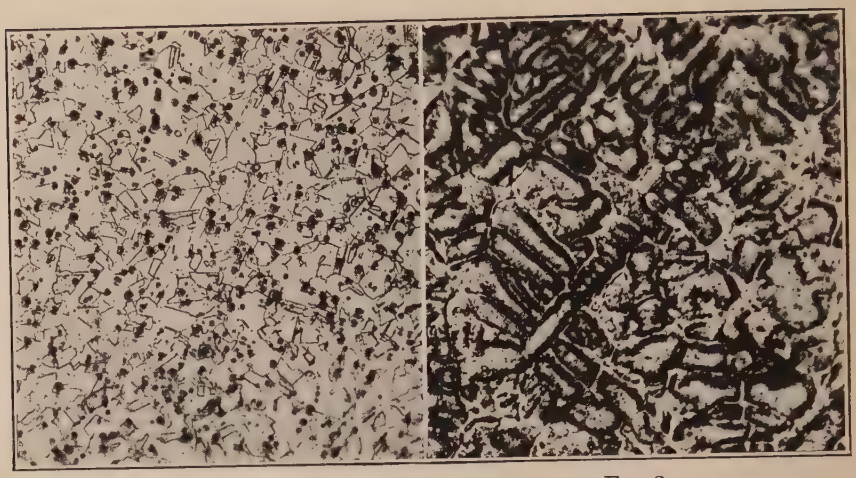

FIG. 1 FIG. 2

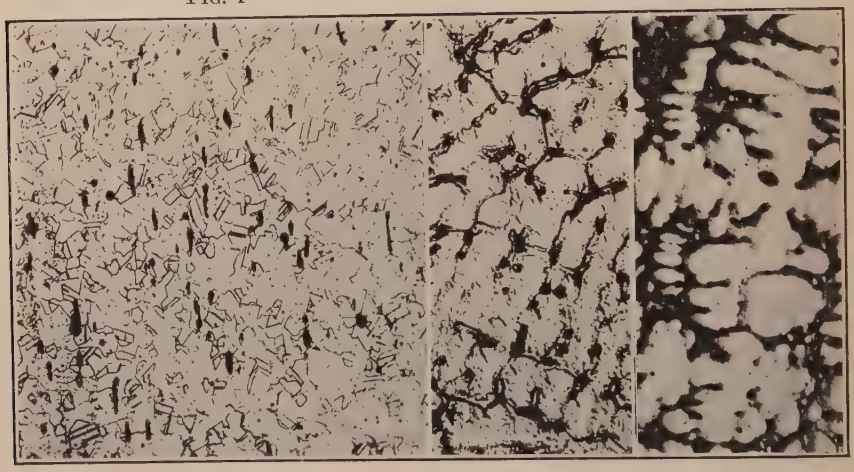

FIG. 3 No. 1 FIG. 4 No. 2

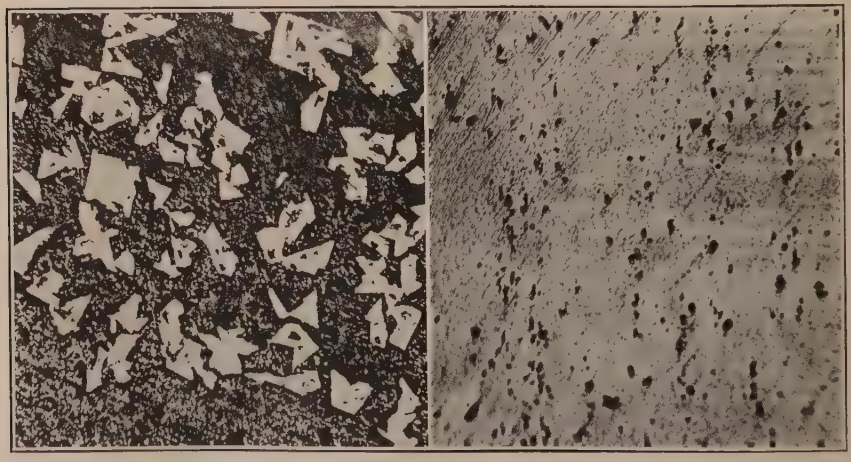

FIG. 5 FIG. 6

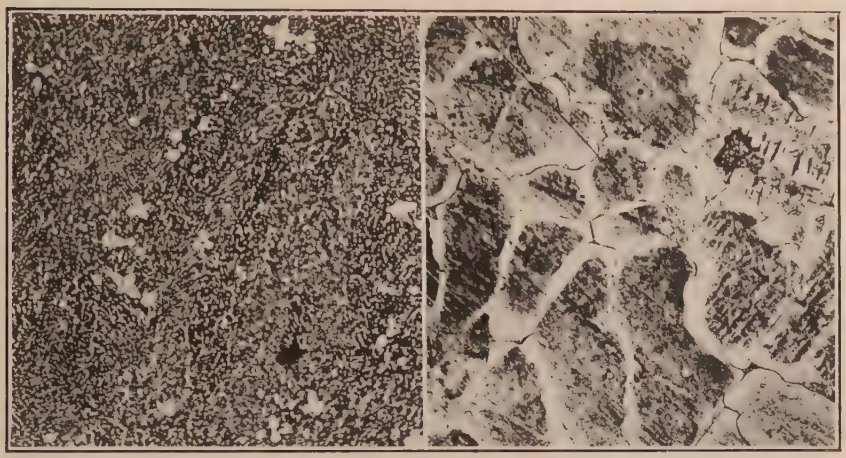

FIG. 7 FIG. 8

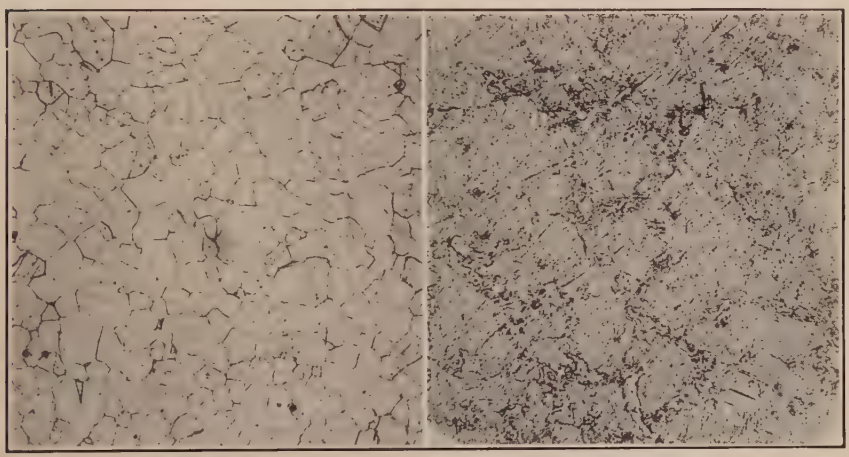

FIG. 9 FIG. 10

FIG. 11 FIG. 12

EXPERIMENT XXIV

WELDING — BRAZING — SOLDERING

Purpose: To study the microstructures of welded, brazed and soldered joints.

References: Gulliver: Metallic Alloys; pp. 21, 143, 276, 306, 385, 394, 395.

Stoughton and Butts: Engineering Metallurgy, pp. 132–147.

Theory: Welding is the joining of two metallic pieces by diffusion under pressure; whereas brazing and soldering are the joining of two metallic pieces by diffusion through chemical solution. Welding is usually divided into three main processes; forge, pressure and fusion welding. The principal difference between these processes is that in forge welding the weld is in general completed by the application of a hammer blow; in pressure welding, by means of mechanical pressure; and in fusion welding without any mechanical means.

There are three types of fusion welding: electric welding, gas welding and thermit welding. In electric welding the heat of the arc or the heat generated by the high resistance of the metal to the passage of the electric current is utilized. In gas welding, the heat of the oxy-acetylene, oxy-hydrogen or atomic hydrogen flame is used. Thermit welding depends upon the production of extreme hot metal and high temperatures by chemical reduction of iron oxide through aluminum: $Fe_2O_3 + 2Al = 2Fe + Al_2O_3 + 197{,}000$ calories. The liberated iron can be deposited in any location desired.

Brazing is the method of joining through the alloyable medium of non-ferrous alloys of copper base, reduced to a molten condition between the parts to be joined, whose melting point must be higher than that of the brazing material.

Soldering is much like brazing except that the soldering material is generally of comparatively low melting point, and that usually, omitting the case of some hard solders, it forms no alloy with the parts to be soldered. Soft solders include those of tin-lead or of tin-zinc base; hard solders have a much higher melting point, such as silver-copper-zinc solders.

PHOTOMICROGRAPHS — (Plates LVIII, LIX, LX)

Fig. 1 — Welded Lead-Antimony Alloy (100×).

Etched in 5% picric acid. Analysis above the weld is Pb 95.95%; Cu 0.05%; Sb 4.06%. Analysis below the weld is Pb 92.49%; Sb 7.53%; Cu 0.05%. The photomicrograph shows the line of weld of a lead storage battery positive plate hanging bar. The upper half of the view represents the structure of the hanging bar and the lower half represents the structure of the old electrode. The structure shows black crystallites of lead surrounded by the lead-antimony eutectic. The antimony content is proportional to the quantity of nearly white eutectic.

Fig. 2 — Welded Lead-Antimony Alloy (100×)

Etched in 5% picric acid. Structure in both halves of weld show primary lead crystallites surrounded by the lead-antimony eutectic. This photomicrograph shows a defective portion of the weld on a lead storage battery positive plate hanging bar. The antimony content above the weld analyzed 3.58% and below the weld 8.33%.

Fig. 3 — Brazed Condenser Tube (30×).

Etched in chromic acid. This photomicrograph shows the structure at the brazed joint of an Admiralty Metal Condenser Tube. The metal in the braze (center of photograph) contains an excess of slag or burned metal.

Fig. 4 — Brazed Condenser Tube (30×).

Etched in chromic acid. This photomicrograph shows the structure at the brazed joint of an unknown condenser tube. The metal in the braze is seen to have a fine dendritic structure, whereas the metal on either side is coarse grained and irregular. The large black spot in the braze is slag.

Fig. 5 — Welded Steel Plate (100×).

Etched in nitric acid. Photomicrograph shows the junction of weld metal and base metal on longitudinal section. The weld was made with the electric arc. The structure shows small grains of ferrite and pearlite.

Fig. 6 — Welded Steel (45×).

Etched in picric acid. The photomicrograph shows the weld of a low-carbon steel. On the right of the photograph, added weld metal is shown, but on the left the original metal is shown. The metal is coarsened by the heat of the process, but not to an excessive degree. The structure shows white grains of ferrite and dark grains of sorbitic pearlite and sorbite.

Fig. 7 — Welded Steel (27×).

Etched in picric acid. The black areas are cavities due to imperfect welding, the white areas are ferrite and the dark gray areas are sorbitic pearlite. This photomicrograph shows a longitudinal section of a

welded low-carbon steel. On the left is new metal from a melt bar; it has a very low-carbon content. On the right is the original metal altered by the heat of the process. Carbon arc weld.

Fig. 8 — Welded Steel (27×).

Etched in picric acid. The black areas are slag and cavities due to imperfect welding. The white areas are ferrite and the dark gray areas are sorbitic pearlite. This photomicrograph shows a longitudinal section of a welded low-carbon steel. On the left is the new metal and on the right is the original metal. Carbon arc weld.

Fig. 9 — Welded Steel (27×).

Etched in picric acid. The white areas are ferrite and the dark areas are sorbitic pearlite. This photomicrograph shows a longitudinal section of a welded low-carbon steel. The line between added metal on the left and the original metal on the right is clearly seen. Electric weld. Evidently the temperature was carefully regulated so that there has been no overheating of the metal.

Fig. 10 — Welded Steel (27×).

Etched in picric acid. The black areas are slag and cavities. The white areas are ferrite and the dark gray areas are sorbitic pearlite and sorbite. This photomicrograph shows a longitudinal section of a welded low-carbon steel. This piece was welded by the oxy-acetylene process. The view here shown is at the line of weld; the black areas are slag and holes due to imperfect welding. On the left is added metal and on the right is the original metal altered by the heat of the process. A sorbitic structure always indicates overheating.

Fig. 11 — Welded Steel (27×).

Etched in picric acid. The white areas are ferrite and the dark areas are sorbitic pearlite or sorbite. This photomicrograph shows a longitudinal section of a welded low-carbon steel. This weld was made by the oxy-acetylene process. The line along which the test piece broke is shown on the left. The grain size is very coarse due to the high temperature to which the metal was heated at this point. The grain size decreases as the distance from the line of weld increases.

Fig. 12 — Soldered Iron Joint (75×).

Etched in HNO_3. Structure shows small uniform grains of ferrite at both sides of the soldered joint.

Fig. 13 — Brazed Steel (75×).

The steel was etched in picric acid and the brazing brass was etched in ammonium hydroxide and hydrogen peroxide. Photomicrograph shows the grains of alpha and beta brass of the brazing material at the left and the small white grains of ferrite and black pearlite of the low-carbon steel at the right. The joint is in the center.

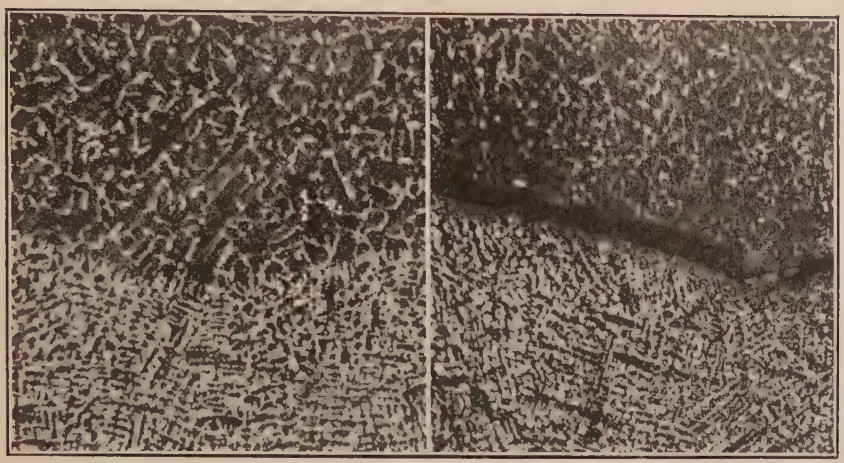

FIG. 1 FIG. 2

FIG. 3

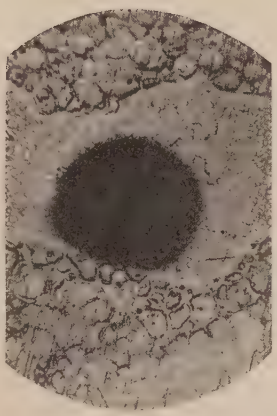

FIG. 4

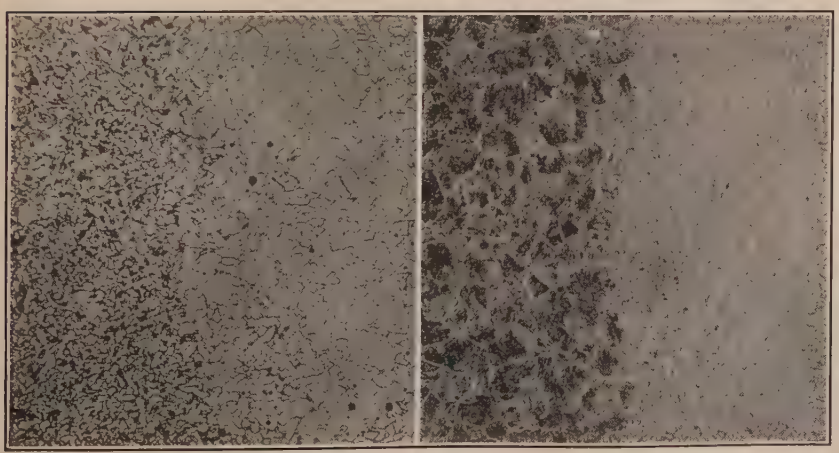

FIG. 5 FIG. 6

PLATE LIX

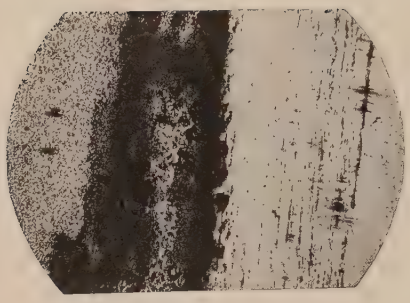

FIG. 7

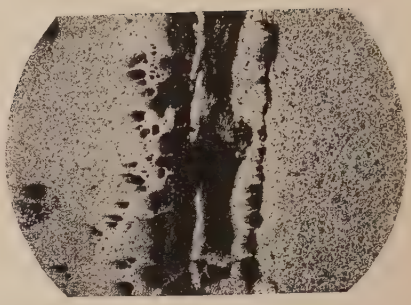

FIG. 8

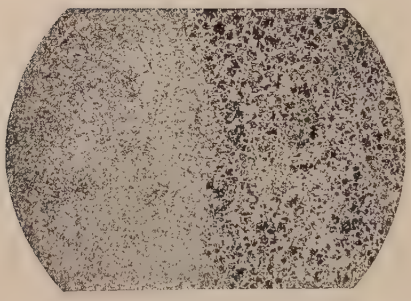

FIG. 9

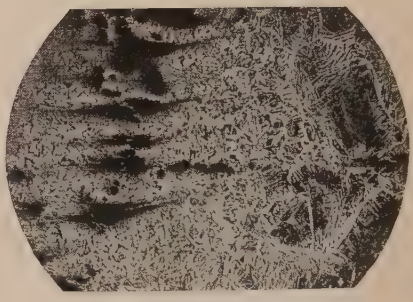

FIG. 10

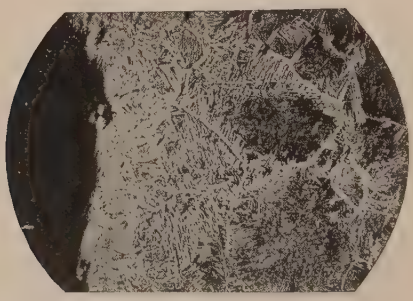

FIG. 11

PLATE LX

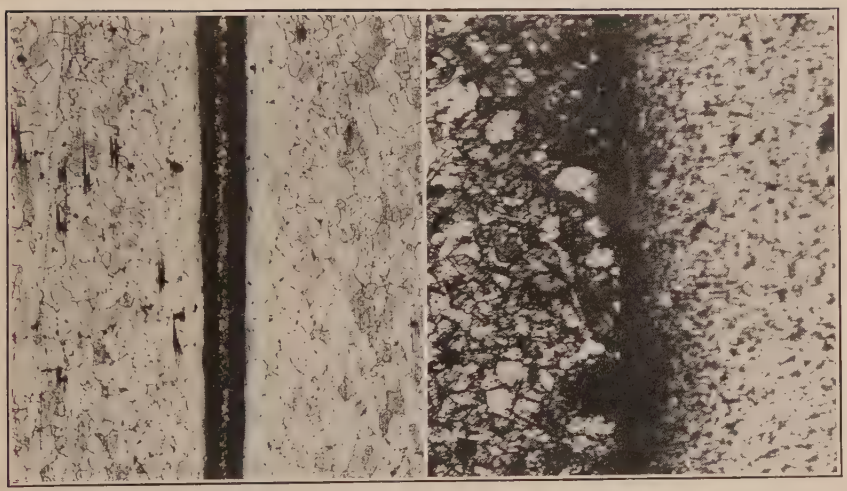

FIG. 12

FIG. 13

EXPERIMENT XXV

DEFECTS AND FAILURES IN METALS

Purpose: To study the causes of defects and failures in metals from their microstructures.

Reference: Rosenhain: Introduction to Physical Metallurgy; Chapter XIV.

Theory: The causes of defects and failures in metals are numerous. Faulty chemical composition may lead to unsuitable physical properties and to suspended or mechanically enclosed particles. This faulty chemical composition may be due to the original mixture or to actions occurring during the melting, such as loss through volatility, oxidation, absorption of gases, inadequate cleaning or skimming of the molten metal, etc. In the casting process, the metal may have been overheated causing excess volatilization, oxidation and absorption of gases. Improper casting may lead to segregation, seams, blow-holes, pipe, shrinkage cracks, ingotism and admixture of foreign matter from the mold.

Metals may fail during the process of mechanical working, such as rolling, forging, pressing and stamping. Fissures and cracks may result when working at too high a temperature. Severe strain-hardening and brittleness results when working at too low a temperature. The working into the surface of the metal of scale or other matter is deleterious.

Failure due to thermal treatment results when the heat-treatment is carried on at too high a temperature, leading to burning and overheating, decarburization of steel, volatilization and oxidation. Errors in rate of cooling from elevated temperatures result in wrong structure, cracking, warping, non-uniformity, different physical properties, etc. Abnormal grain growth or "germination" will cause failure.

In service metal may fail due to excess loads, corrosion, erosion, fatigue, etc., in addition to the causes outlined above.

PHOTOMICROGRAPHS — (Plates LXI, LXII, LXIII, LXIV, LXV, LXVI)

Fig. 1 — Nickel-Steel Propeller Shaft (100×).

C 0.44%; S 0.039%; Mn 0.62%; Si 0.30%; P 0.041%; Ni 3.32%.

Etched with picric acid. The white areas represent ferrite and the dark areas represent pearlite and non-metallic impurities. Though the grain structure is good, this material is defective on account of the

prominent ferrite streaks, containing long non-metallic inclusions of manganese sulfide.

Fig. 2 — Nickel-Steel Stern Tube Shaft (100×).

C 0.19%; S 0.024%; Mn 0.46%; Si 0.12%; P 0.04%; Ni 3.34%.

Etched with picric acid. Structure shows ferrite plus sorbitic pearlite plus non-metallic inclusions. Large particles of slag and non-metallic impurities caused this metal to fail.

Fig. 3 — Rivet-Steel (100×).

C 0.12%; S 0.04%; Mn 0.38%; Si 0.013%; P 0.007%; Ni 0.12%; Cr 0.03%.

Etched in picric acid. Structure shows ferrite plus pearlite. This is a longitudinal section of a specimen from annealed material. The grain size is somewhat large. The steel is annealed by maintaining at 1725° F. for ½ hour and cooling in the furnace. This slow cooling has allowed the pearlite to segregate along the lines of segregation of impurities insoluble in the ferrite. This annealed rivet steel has a tensile strength of 46,270 lb. per sq. in., a yield point of 26,830 lb. per sq. in., an elongation in 2 in. of 46.2% and a reduction in area of 71.8%.

Fig. 4 — Chrome-Nickel Steel-Turbine Blade (100×).

C 0.27%; S 0.034%; Mn 0.47%; Si 0.14%; P 0.006%; Ni 0.11%; Cr 0.63%; V 0.14%.

Etched in nitric acid. Structure shows ferrite and coarse sorbitic pearlite. This photomicrograph shows the structure at the tip of the turbine blade. The grain size is very coarse. This blade has evidently been overheated at the tip.

Fig. 5 — Steel — Airplane Engine Crankshaft (100×).

Etched in aqua regia. The structure shows ferrite, sorbitic pearlite and a streak of non-metallic impurities. This view shows a transverse section of the crankshaft, located near the fracture, and including a streak of non-metallic inclusions. The grain size is fine and the constituents are evenly distributed. Except for the non-metallic inclusions, this structure is considered good for this class of material. The broad band of non-metallic inclusion extends clear across the specimen. Such streaks of non-metallic inclusions constitute planes of weakness.

Fig. 6 — S.A.E. No. 1025 Steel (100×).

C 0.25%; Mn 0.65%; P 0.045%; S 0.05%.

Etched in 2% Nital. Banded structure of ferrite and sorbite. Note inclusions of manganese sulfide elongated in direction of rolling.

Fig. 7 — B.O.H. Chrome-Vanadium Steel (100×).

C 0.45%; S 0.026%; Mn 0.65%; Si 0.15%; P 0.017%; Cr 1.05%; V 0.18%.

Unetched. The white surface represents the polished, unetched

metal. The halftone streak is manganese sulfide and the black areas are non-metallic inclusions of silicates, etc. This photomicrograph shows a typical inclusion. It is excessive in size for crankshaft material. Several small inclusions can also be noted.

Fig. 8 — Steel — Propeller Shaft (100×).

C 0.38%; S 0.032%; Mn 0.64%; Si 0.324%; P 0.027%; Ni 3.51%.

Etched in picric acid. Structure shows ferrite, pearlite and non-metallic inclusions. Much slag and sulfide are visible.

Fig. 9 — Steel Crankshaft (100×).

Etched in nitric acid solution. Structure shows ferrite, pearlite and crack in the metal. Note evidence of ingotism near the crack.

Fig. 10 — Steel Boiler Tube (100×).

C 0.26%; S 0.024%; Mn 0.64%; Si 0.005%.

Etched in picric acid. Structure shows ferrite and sorbitic pearlite. This specimen was taken from a seamless steel boiler tube that had failed. The photomicrograph shows that this tube had been heated above 1600° F. and cooled rapidly. The structure is entirely different from that of an annealed seamless boiler tube. Evidently this tube has been overheated in service.

Fig. 11 — Boiler Steel (100×).

Etched in picric acid. Structure shows ferrite and pearlite. In this photomicrograph, manganese sulfide particles are shown imbedded in a broad ferrite "ghost."

Fig. 12 — Boiler Steel (100×).

Etched in picric acid. Structure shows ferrite and pearlite. The ferrite bands dominate the greater portion of the field. The bands are very narrow and are evenly interspersed with pearlite layers.

Fig. 13 — Nickel Steel — Propeller Shaft (100×).

C 0.49%; S 0.074%; P 0.056%; Ni 3.4%.

Etched in picric acid. Structure shows ferrite, sorbitic pearlite and non-metallic inclusions. Though the grain structure is good for this class of material, this material is defective on account of the excessive amount of non-metallic inclusions.

Fig. 14 — Chrome-Vanadium Steel — Crankshaft (100×).

C 0.41%; S 0.025%; Mn 0.55%; Si 0.210%; P 0.014%; Ni 0.04%; Cr 0.79%; V 0.15%.

This polished, unetched surface shows the presence of an excessive quantity of non-metallic impurities.

Fig. 15 — Acid Open Hearth Steel — Propeller Shaft (100×).

C 0.32%; S 0.031%; P 0.029%.

Etched in nitric acid. Structure shows ferrite and pearlite banding. The forging was annealed by heating for 12 hours to 1650° F.,

maintaining at 1650° F. for 10 hours, cooling in air, reheating for 12 hours to 1480° F., maintaining at 1480° F. for $3\frac{1}{2}$ hours and cooling in air. The ferrite streaks render the forging unsuitable for use as shafting.

Fig. 16 — Steel — Head of Steam Drum (100×).

C 0.263%; S 0.022%; Mn 0.443%; Si 0.01%; P 0.029%.

Etched in picric acid. This specimen was taken from the after head of the steam drum of a boiler which was discovered to be defective. An area of about 48 sq. in. having a honeycombed appearance was observed. The structure shows coarse ferrite and sorbitic-pearlite. Evidently the metal has been much overheated at this point. Analysis of the metal in this region shows the carbon content to be higher than the average. The combination of high-carbon content and high temperature have produced " burning " of the metal in this region. The very large grain size and some of the cavities due to " burning " are here shown.

Fig. 17 — Steel Boiler Tube (100×).

Etched in nitric and picric acids. Structure shows ferrite with a few small specks of non-metallic inclusions. This photomicrograph shows several enormous ferrite grains which are evidence of overheating.

Fig. 18 — Cast Steel (100×).

C 0.266%; S 0.028%; Mn 0.633%; Si 0.236%; P 0.041%.

Etched in picric acid. This specimen was taken from a broken web of the spider of a submarine main motor which failed in service. The structure shows ferrite and pearlite. The ferrite masses mark the outlines of the crystallite or dendrites that first solidified when the casting was poured. Such dendritic cores, as formed from solidifying steel, are regions of lower than average carbon content. This casting has evidently not received a heat-treatment adapted to render such a structure uniform.

Fig. 19 — Steel Boiler Plate (100×).

C 0.32%; S 0.014%; Mn 0.38%; Si 0.014%; P 0.024%.

Unetched metal. The photomicrograph shows a position on a transverse section near the widest part of the crack. Masses of oxides are visible in this region. The crack developed in the sheet when the edges were being brought together in the hydraulic riveting machine. The upper black area represents the edge of the crack.

Fig. 20 — Steel Boiler Tube (100×).

C 0.11%; S 0.025%; Mn 0.38%; P 0.012%.

Etched in picric acid. Structure shows ferrite, sorbitic pearlite and cavities due to the burning and distortion of the metal. This specimen shows the structure of the tube near the crack. The metal has evidently been raised to a very high temperature, approaching the burn-

ing temperature, and then rapidly cooled. The black areas are the cavities due to the burning and distortion of the metal.

Fig. 21 — Admiralty Metal Condenser Tube (100×).

Cu 70.75%; Sn 1.03%; Zn 27.90%; Fe 0.01%; Pb 0.03%.

Etched with chromic acid. Structure shows large grains of alpha brass with pits at grain-boundaries. This condenser tube after service was found to be heavily pitted. The photomicrograph shows the typical structure in the vicinity of one of the pits. The enormous grain size and the intercrystalline character of the corrosion are apparent.

Fig. 22 — Admiralty Metal Condenser Tube (100×).

Cu 70.58%; Sn 1.27%; Pb 0.03%; Fe 0.18%; Zn 27.92%.

Etched in chromic acid. The specimen was taken from a condenser tube which split after six months' service. This photomicrograph shows the structure of the tube at the base of a crack. The structure is rather coarse and shows many twins, but little distortion. The nonmetallic inclusions are present in large quantity in the form of streaks. The intercrystalline nature of the crack is evident.

Fig. 23 — Brass Distilling Condenser Tube (100×).

Cu 64.66%; Sn 0.27%; Zn 34.64%; Fe 0.01%; Pb 0.50%.

Etched in chromic acid. The structure shows a corrosion pit in the failed distilling condenser tube. The dezincification began at the central core and grew radially.

Fig. 24 — Tool Steel (100×).

This photomicrograph shows the decarburization of a tool steel. The upper edge of the tool shows long grains of ferrite with no trace of pearlite. The other end of the tool showed a fine structure of ferrite plus sorbitic pearlite.

Fig. 25 — Armor Plate (1000×).

C 0.40%; S 0.024%; Mn 0.38%; Si 0.08%; P 0.017%; Ni 3.361%; Cr 1.25%.

Etched in 5% HNO_3 in alcohol solution. The structure is martensitic. But it is a bad structure due to its brittleness.

Fig. 26 — Wrought Iron Safety Valve Stud (50×).

C 0.033%; S 0.036%; Mn 0.078%; Si 0.196%; P 0.022%.

Etched in picric acid. Structure shows slag in nearly pure ferrite in lower part of the photomicrograph, and ferrite and pearlite in the upper part. This photomicrograph shows a longitudinal section of a stud from a boiler main stop valve. In the upper part of the photograph, the structure is that of low carbon steel, while in the lower part the structure is that of wrought iron. Sometimes steel scrap is piled with " muck bar " for final rolling. It is probable that the variation in structure of this material was caused in this way. This wrought iron

had a tensile strength of 78,750 lb. per sq. in., an elastic limit of 39,500 lb. per sq. in., an elongation of 29.0% in 2 in. and a reduction in area of 47.5%.

Fig. 27 — Burned Steel (100×).

This steel was burned on heat-treatment for hardening. Structure shows coarse grains of austenite completely enveloped by the cavities (black).

Fig. 28 — Aluminum Alloy Propeller Blade (200×).

Structure shows the forging cracks and surface corrosion in an aluminum alloy propeller blade.

Fig. 29 — Aluminum Alloy Propeller Blade (500×).

Structure shows segregated impurities in an aluminum alloy propeller blade.

Fig. 30 — Duralumin (400×).

Structure shows intercrystalline corrosion of duralumin.

Fig. 31 — Duralumin (200×).

Photomicrograph shows structure of duralumin overheated in heat-treatment.

Fig. 32 — Aero-Valve Steel (100×).

C 0.32%; Si 1.11%; S 0.031%; Mn 0.61%; Ni 19.90%; Cr 6.96%.

Etched in ferric chloride solution. Photomicrograph shows grain distortion and flow of metal due to the ductile fracture on failure of the valve.

Fig. 33 — Stainless Iron (500×).

Photomicrograph shows banded, segregated structure of stainless iron as received from the manufacturer.

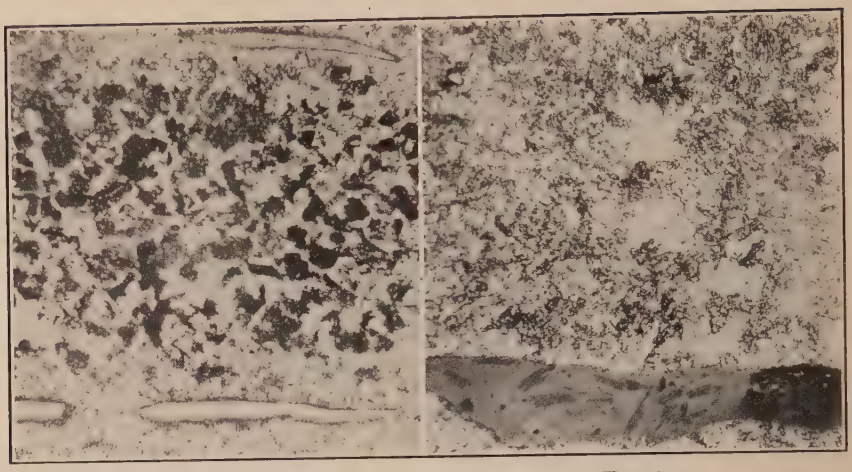

FIG. 1 FIG. 2

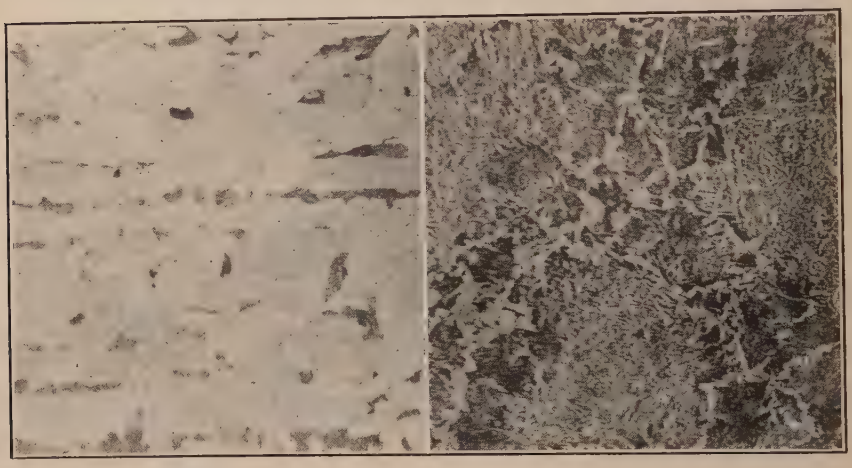

FIG. 3 FIG. 4

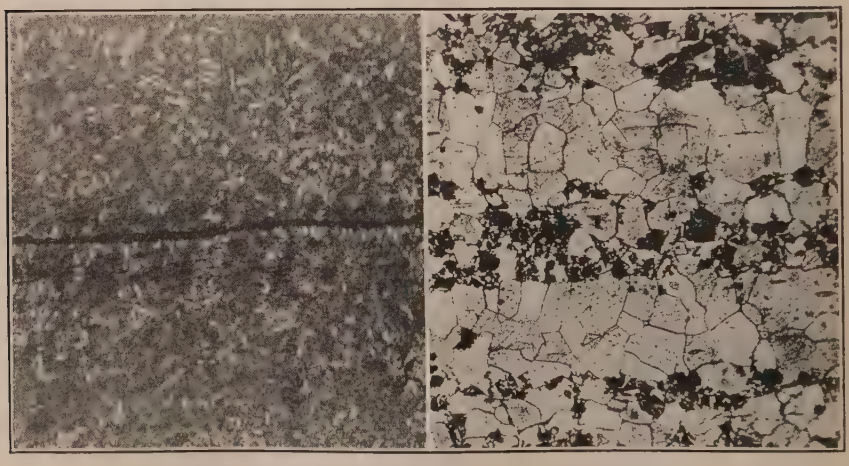

FIG. 5 FIG. 6

FIG. 7 FIG. 8

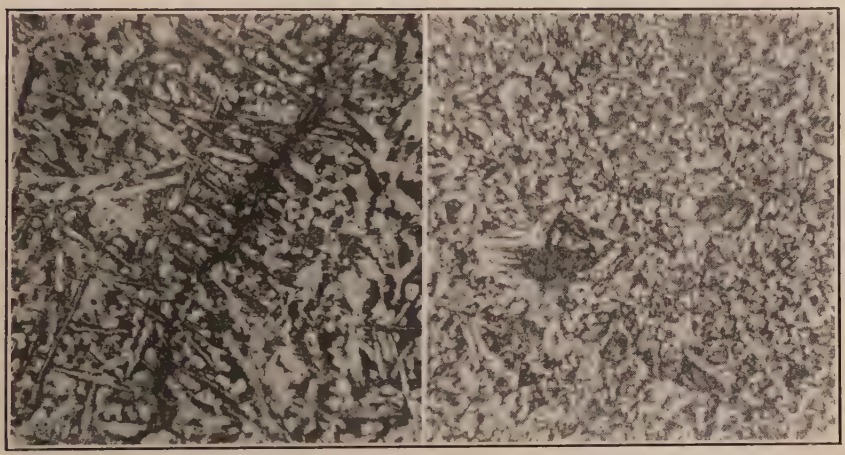

FIG. 9 FIG. 10

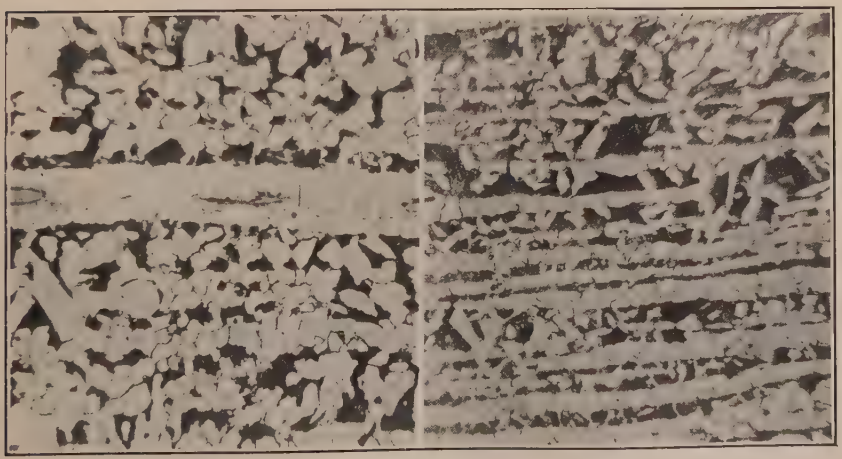

FIG. 11 FIG. 12

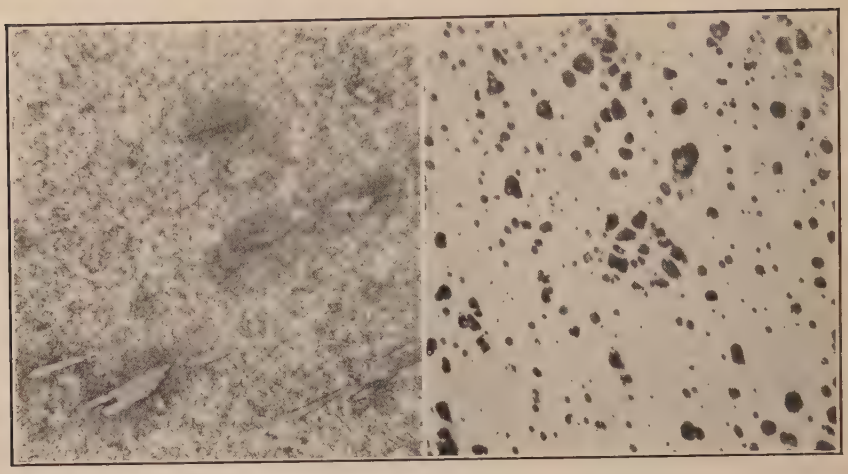

FIG. 13 FIG. 14

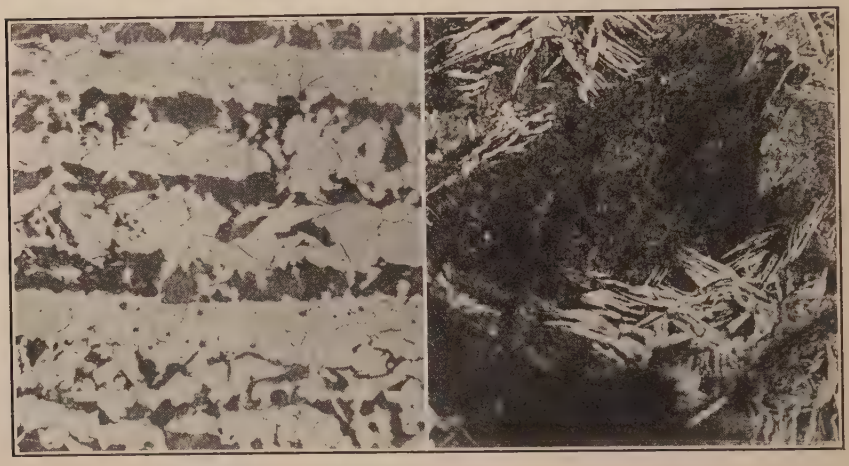

FIG. 15 FIG. 16

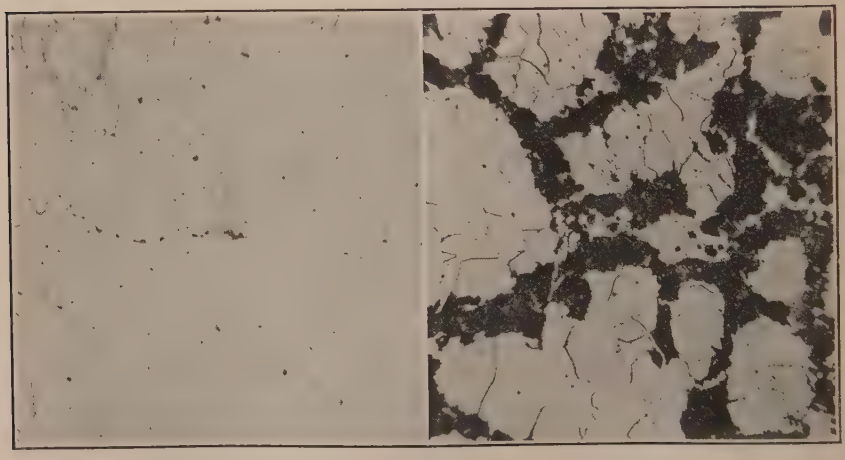

FIG. 17 FIG. 18

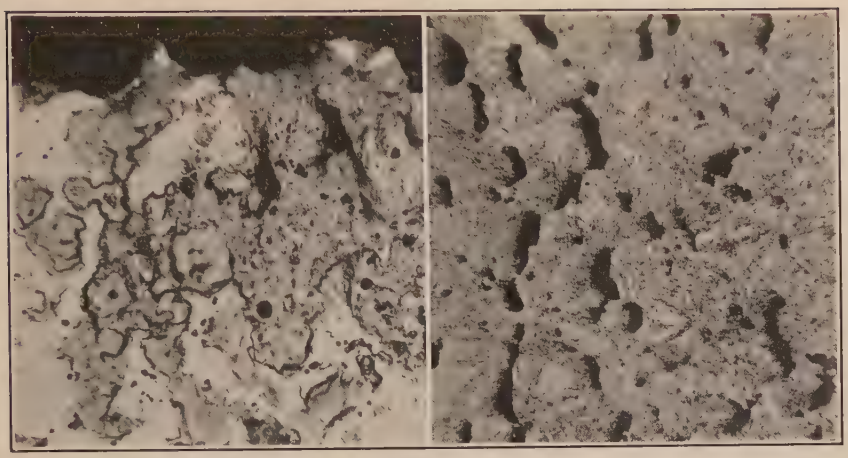

FIG. 19 FIG. 20

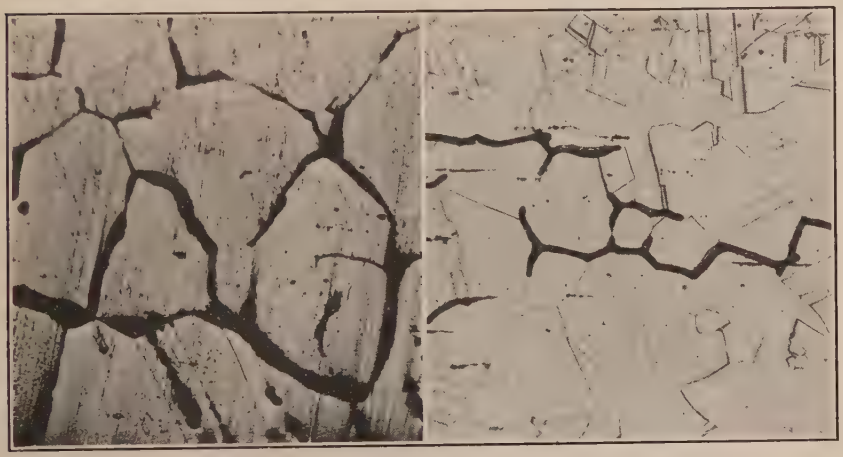

FIG. 21 FIG. 22

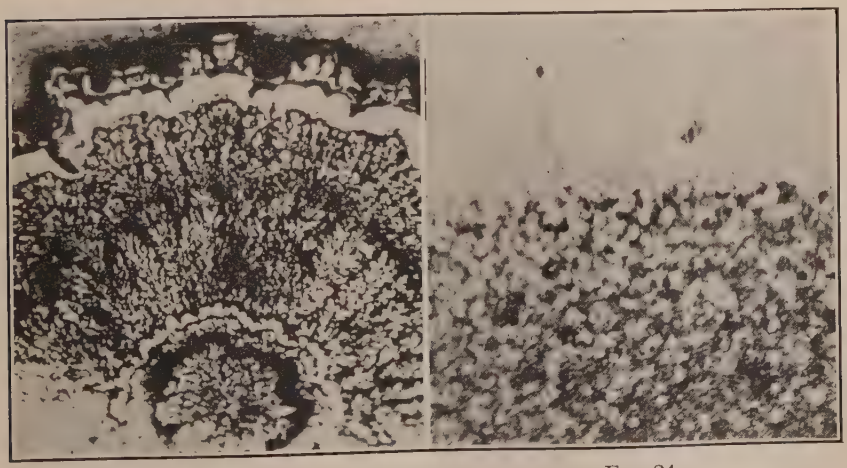

FIG. 23 FIG. 24

PLATE LXV

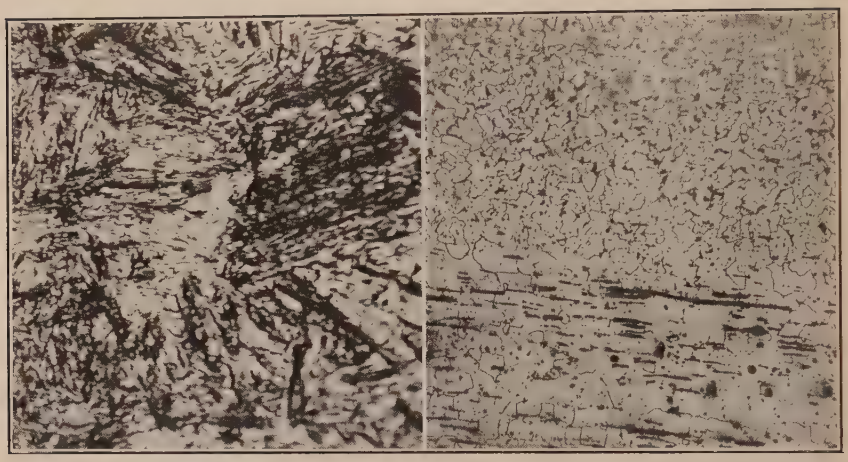

FIG. 25 FIG. 26

FIG. 27

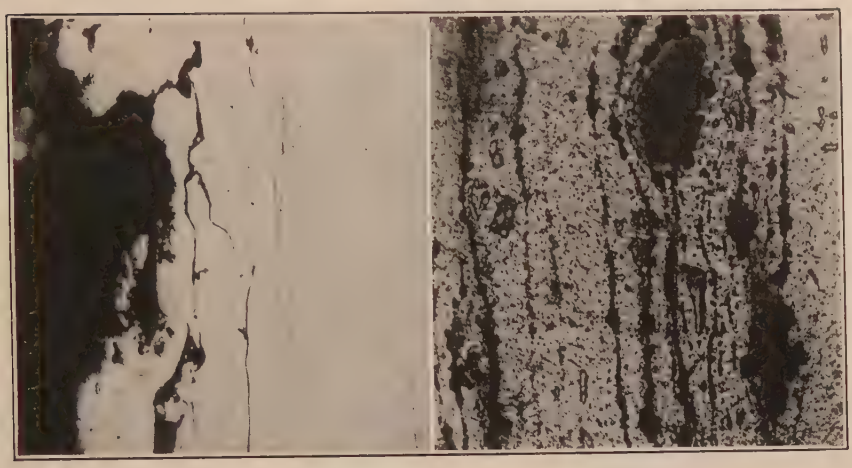

FIG. 28 FIG. 29

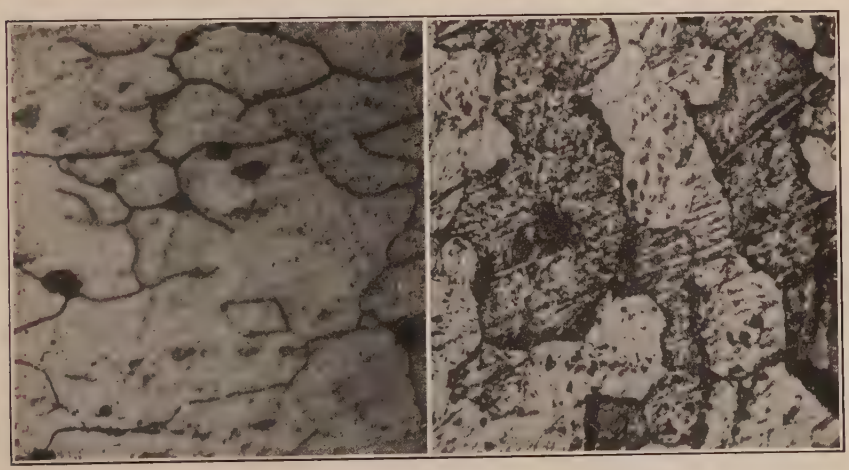

FIG. 30 FIG. 31

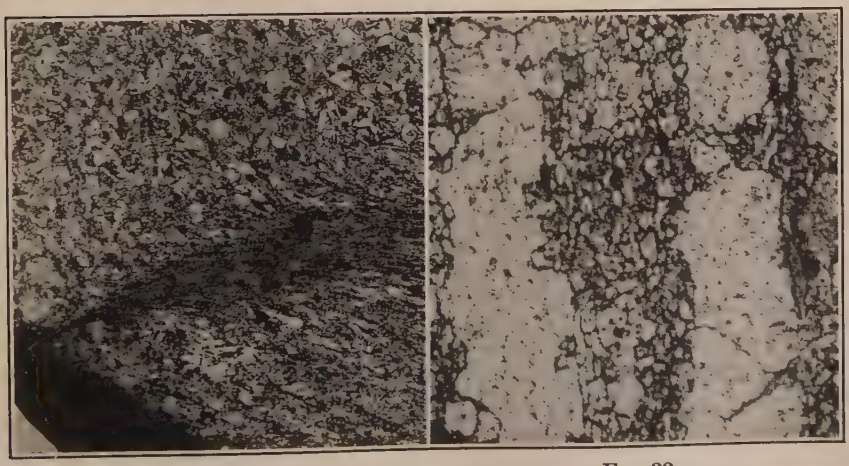

FIG. 32 FIG. 33

EXPERIMENT XXVI

HIGH-POWER METALLOGRAPHY*

Purpose: To study the structural characteristics of austenite and martensite in an iron-carbon alloy at high magnifications.

Reference: F. F. Lucas:* Bell Telephone Laboratories.
Bulletin B–109–1, January, 1925.*
Bulletin B–187–, March, 1926.
Bulletin B–200, July, 1926.
Bulletin B–241, March, 1927.
R. G. Guthrie: Trans. Am. Soc. Steel Treating, March, 1925.
Trans. Am. Soc. Steel Treating, January, 1925.

Theory: Low-power photomicrography may be considered as treating with magnitudes from 1 to about 30 diameters. Medium-power work deals with magnifications from about 30 to about 500 diameters, and high power work extends from 500 diameters upward.

The reason that photomicrography is grouped under three classifications according to magnification is because the apparatus used in each case is quite different and because the preparation of the subject and its treatment also differ. In fact for low-power work the microscope often may be dispensed with entirely, the lens being secured directly to the camera; in other cases, the microscope serves only as a convenient support for the lens.

Medium-power work always requires the use of a microscope, and because rigidity in mounting and accuracy in adjustment are very necessary to correct rendering of the image, some sort of a stand is provided on which the microscope and a suitable illuminating train are mounted.

For high-power work there is an entirely different form of microscopic equipment which reveals the presence of particles beyond reach of all other known means of microscopic vision; reference is made to the ultramicroscope. This instrument is not ordinarily provided with photographic apparatus, although with certain classes of work and under favorable conditions it is possible to reproduce the image photographically.

* Reproduced by permission from Dr. F. F. Lucas.

The ultra-violet microscope takes advantage of the increase in resolving power which accompanies a decrease in the wave length of light employed. This microscope uses ultra-violet light for illumination and quartz objectives corrected for the single wave length 275 uu which lies in the ultra-violet region of the spectrum. Quartz oculars are also used because glass absorbs ultra-violet light almost completely.

Preparation of Specimens: A special iron-carbon alloy was produced by combining carbon with Armco iron. By analysis, this alloy was found to have the following composition:

C	Si	Mn	S	P
2.65	0.01	0.07	0.015	trace

This alloy was hot rolled to a $\frac{3}{8}$-in. rod. A section about 4 ft. in length was heat-treated in the following manner: One end of the rod for a distance of about 14 in. was placed in an electric furnace of the quartz tube type and the other end was allowed to project outside of the furnace, where it could be maintained at approximately atmospheric temperature. The furnace was brought to 1260° C. and maintained at this temperature for a period of about 5 minutes, when the rod was quickly withdrawn and the heated end plunged into an ice and brine solution at a temperature of −10° C. The heated end was used for metallographic study.

PHOTOMICROGRAPHS

Fig. 1 — Magnification 175×. Etched with boiling sodium picrate. Photomicrograph shows the crystallographic relationship between the polyhedral and the dendritic forms of structure. The polyhedral grains of austenite break up along crystallographic planes forming the characteristic dendritic structure. The grains of austenite contain well-defined acicular needles of martensite and are disposed in a black matrix rich in iron carbide. Boiling sodium picrate has the property of staining iron carbide.

Fig. 2 — Magnification 175×. Etched with boiling sodium picrate. Photomicrograph is similar to that of above, but showing an increased breaking up of the grains of austenite forming the characteristic dendritic structure.

Fig. 3 — Magnification 5250×. Etched with picric acid. Photomicrograph shows at high magnification the way in which an austenitic grain breaks up under suitable heat-treatment to form dendrites. The light background is iron-carbide and the small particles austenite. It will be noted that the small particles of austenite are arranged along

straight lines marking a continuation of the crystallographic planes of the large austenitic grain.

Fig. 4 — Magnification 2400×. Etched with picric acid. Photomicrograph shows a large austenitic grain in the process of reverting to the dendritic structure. The same orientation persists in the separated grain particles which are arranged along crystallographic lines. The martensitic structure of one grain shows continuation in the adjoining grain. It is quite evident that a large austenitic grain has divided to form several smaller grains, and these in turn are shown dividing into smaller ones, by separation along crystallographic planes and by segregation and dissolution.

Fig. 5 — Magnification 3230×. Etched with picric acid. Photomicrograph shows development of martensitic needles at the grain-boundary of austenite. Note the fine, granular structure of the martensite. Each needle has an axis or midrib, and these axes are arranged in parallel groups. The axes of adjoining needles meet at a common point.

Fig. 6 — Magnification 2400×. Etched with picric acid. Photomicrograph shows nodular type troostite formed by the direct decomposition of austenite to troostite. Specimen was heated to 1100° C. and quenched in brine. Structure shows white austenite, gray needles of martensite and black nodular troostite.

Fig. 7 — Magnification 2400×. Etched with picric acid. Photomicrograph shows development of troostite along the boundary of the austenitic grain. Here the presence of intercrystalline eutectic is apparent. The austenitic grains contain acicular crystals, which are unmistakably martensite.

Fig. 8 — Magnification 1800×. Etched with boiling sodium picrate. Photomicrograph shows austenite unstained and the martensite deeply stained. Here the early development stages of a " fir tree " or dendrite from a polyhedral austenitic grain is shown. The axis of the martensitic needle is stained slightly darker than the rest of the needle. Troostite has developed near the grain-boundary and is only faintly etched. The intercrystalline eutectic or dendritic mass is also to be noted. It is composed of a matrix deeply stained and contains unstained inclusions apparently of the same composition as the austenitic grain. Decomposition along parallel crystallographic planes has made inroads into the crystal, forming material rich in iron carbide.

Fig. 9 — Magnification 5600×. Etched with boiling sodium picrate. Photomicrograph shows the intercrystalline eutectic composed of a black matrix, iron carbide, containing particles of an unstained constituent, austenite.

Fig. 10 — Magnification 2400×. Etched with picric acid. This photomicrograph shows two sets of lines developed in the austenitic grain and thus the section is parallel to the surface of a cube. In like manner, the development of three sets of lines can be shown. The development of the line traces the crystallographic planes of austenite to the regular system, octahedral form. These lines are known as the Widmanstätten structure and denote the inner symmetry of the crystalline matter, of which the grain is composed. Thus it is seen that the crystallographic planes of the metal have been revealed by a decomposition which has taken place along these planes. The decomposition is troostite, in which the excess constituent of carbide has formed along the crystallographic axis.

Fig. 11 — Magnification 2100×. Etched with picric acid. Photomicrograph shows martensite in austenite. If lines are drawn parallel to the axes of the needles, four sets of parallel lines will result. If the needles are likened to feathers it will be noted that some are lying flat, others are on edge and some are intermediate in position. Martensite is probably a decomposition in the form of thin acicular flakes or plates parallel to the crystallographic planes of austenite. Note the striated appearance of the needles.

Fig. 12 — Magnification 5250×. Etched with picric acid. Photomicrograph shows quite clearly the lack of uniformity of structure of martensite and the development of the three needles from a large needle. It should be noted that the three needles are parallel to each other, and in a measure substantiate what has been inferred that the development of martensite is along crystallographic planes. The surface of the parent needle is quite mottled, which seems to indicate that more than one constituent is present.

Fig. 13 — Magnification 5250×. Etched with picric acid. Photomicrograph shows the martensitic needle traversed by a number of parallel bands which etch to the same degree as the central axis of the needles. This plate was measured and the average thickness of these cross bands was found to be $\frac{1}{100{,}000}$ inch.

Fig. 14 — Magnification 5250×. Etched with picric acid. Photomicrograph shows that the mother-of-pearl appearance of properly prepared martensite when seen visually at high magnifications appears due to a fine lamellar structure.

Fig. 15 — Magnification 3230×. Etched with picric acid. Photomicrograph shows the appearance of tiny cubic pits (white) of alpha iron, suggesting that some transformation had probably preceded the formation of martensite or progressed with it. By careful manipulation,

it was found possible to develop this characteristic where heretofore it had remained obscured. Some tempering action appears to favor their development.

Fig. 16 — Magnification 3230×. Etched with picric acid. Photomicrograph is similar to that of Fig. 15.

Fig. 17 — Magnification 3230×. Etched with boiling sodium picrate. Since the white pits develop with picric acid and do not stain with boiling sodium picrate, the conclusion seems justified that the austenite has precipitated ferrite (or alpha iron) in perfect cubic crystals.

Fig. 18 — Magnification 3230×. Photomicrograph shows a view of a specimen of commercial 1.10–1.20% C. steel heated in such a way as to develop small cubic figures in a matrix of austenite and martensite. The dark blotches are troostite and the tiny cubes are ferrite.

Fig. 19 — Magnification 3230×. Very lightly etched to show the twin formation of martensite common with a twinning plane of austenite. Note the lamellar structure of the martensite and variations in shading. Deeper etching would have obliterated the finer details. This offers substantial evidence of itself that martensite is a decomposition along crystallographic planes of austenite and, therefore, must possess certain crystallographic planes in common with austenite.

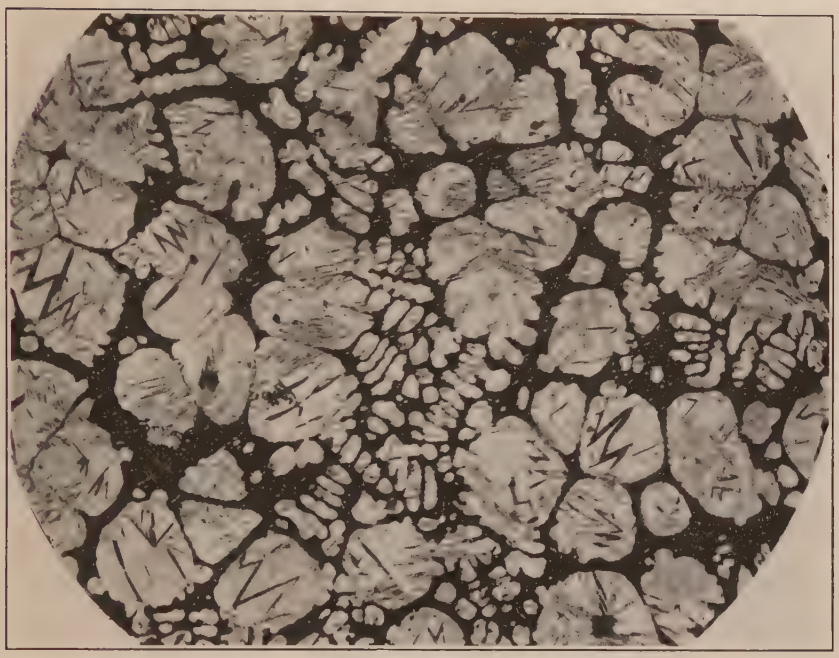

FIG. 1

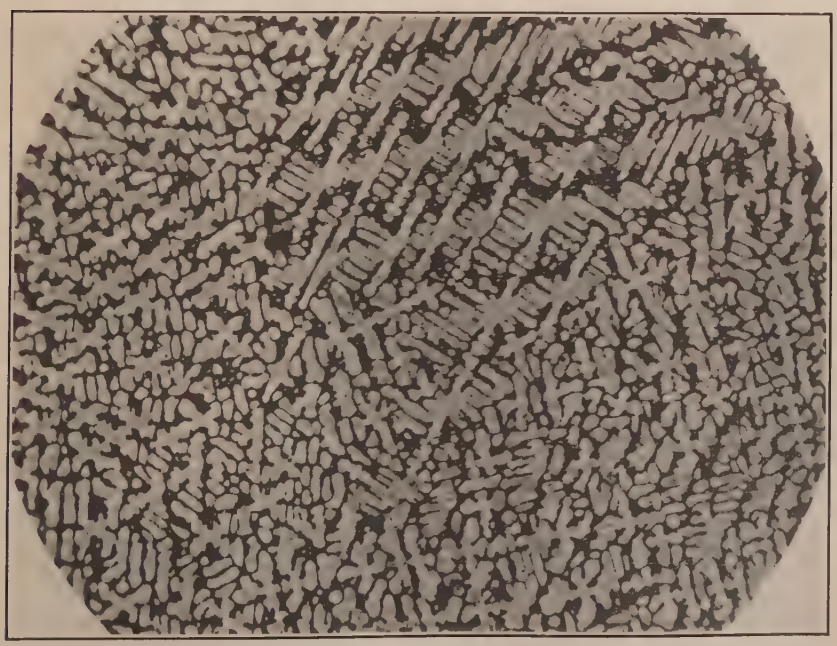

FIG. 2

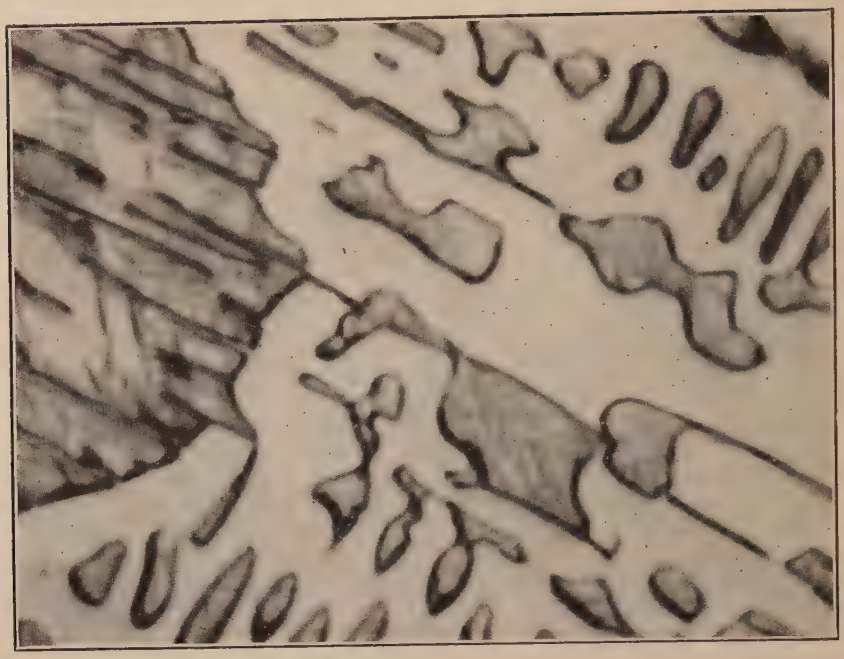

FIG. 3

FIG. 4

PLATE LXIX

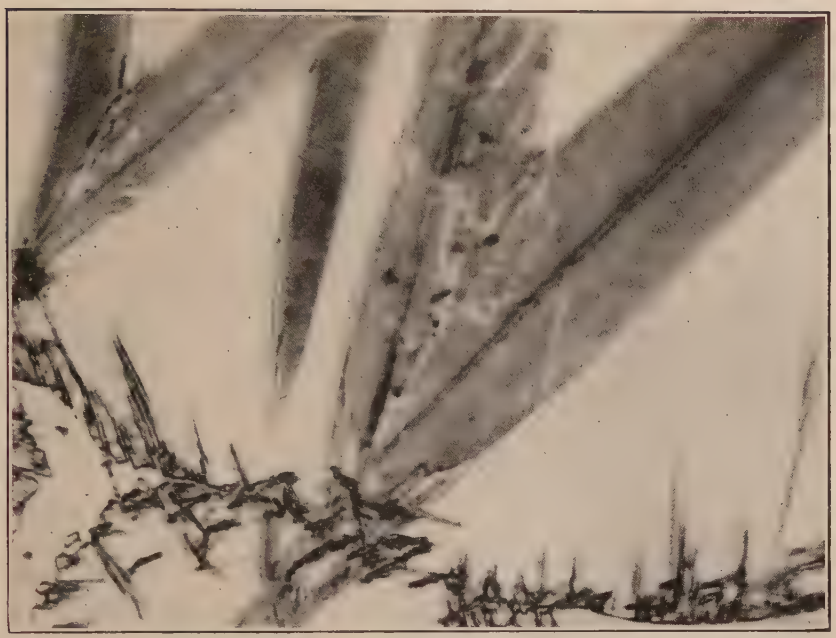

FIG. 5

FIG. 6

FIG. 7

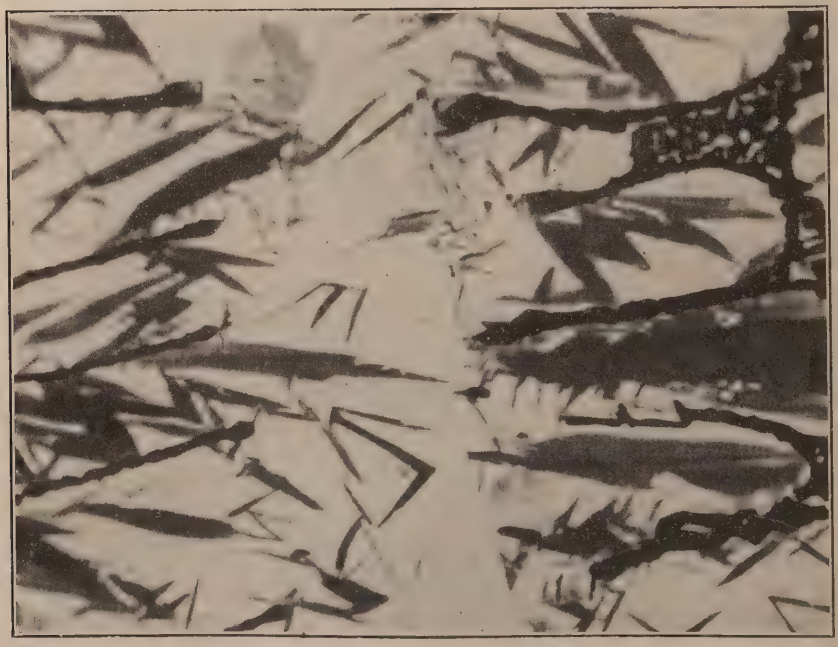

FIG. 8

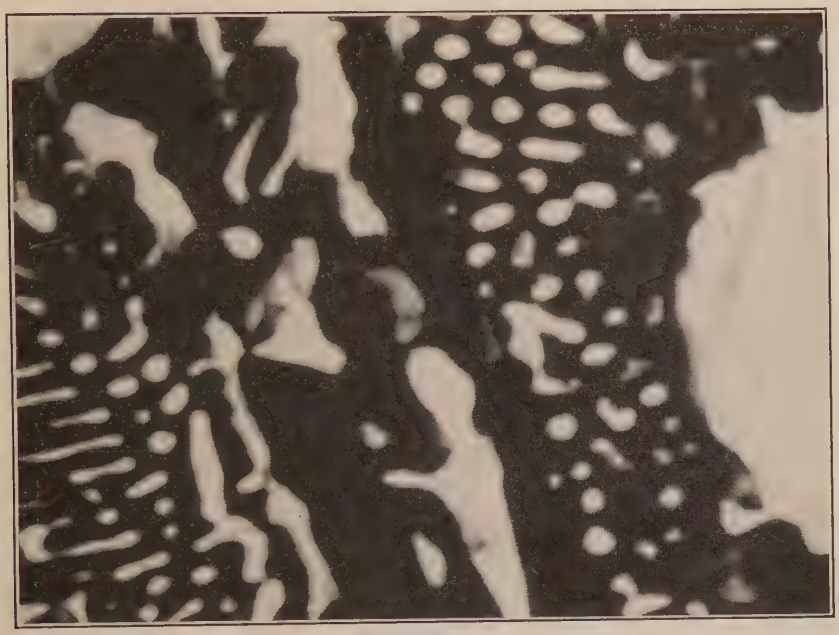

FIG. 9

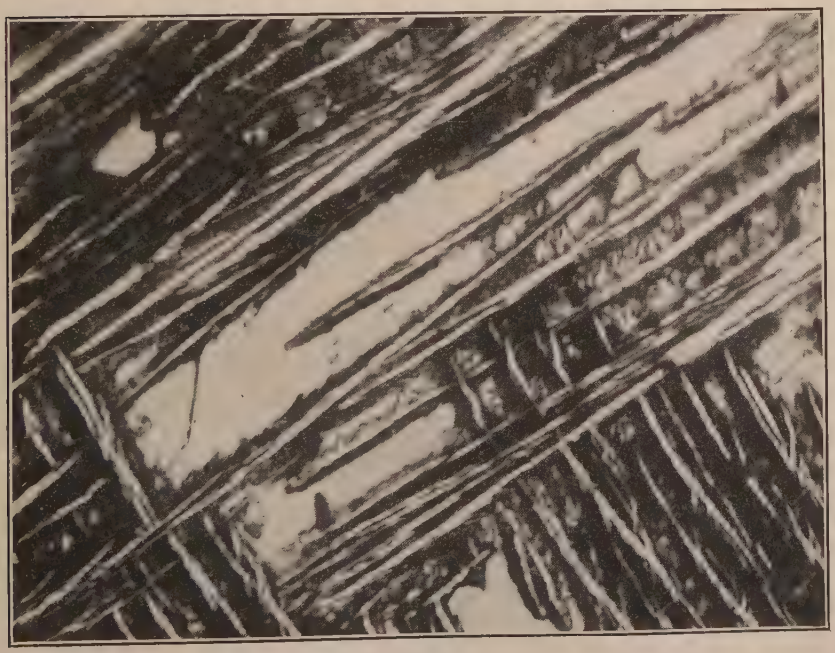

FIG. 10

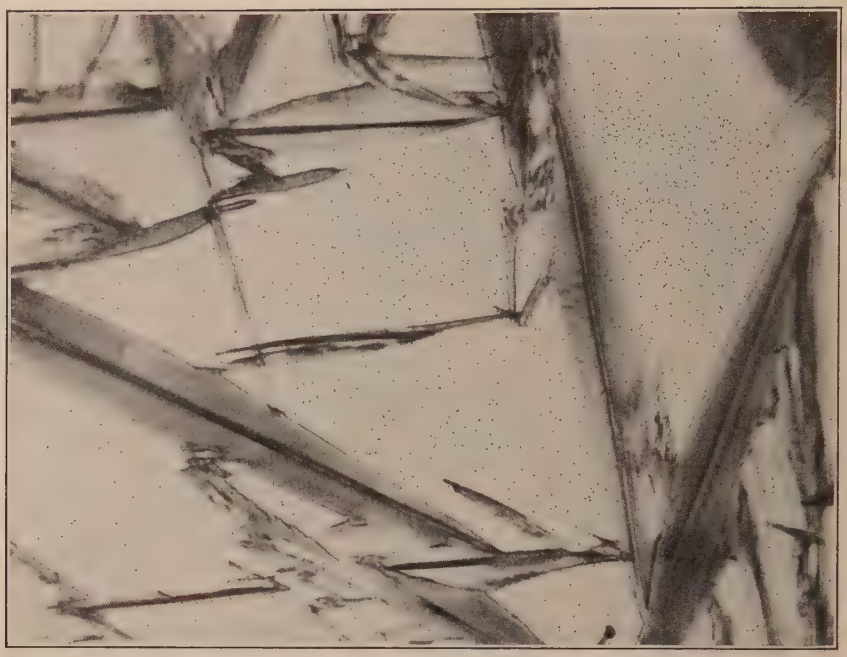

FIG. 11

FIG. 12

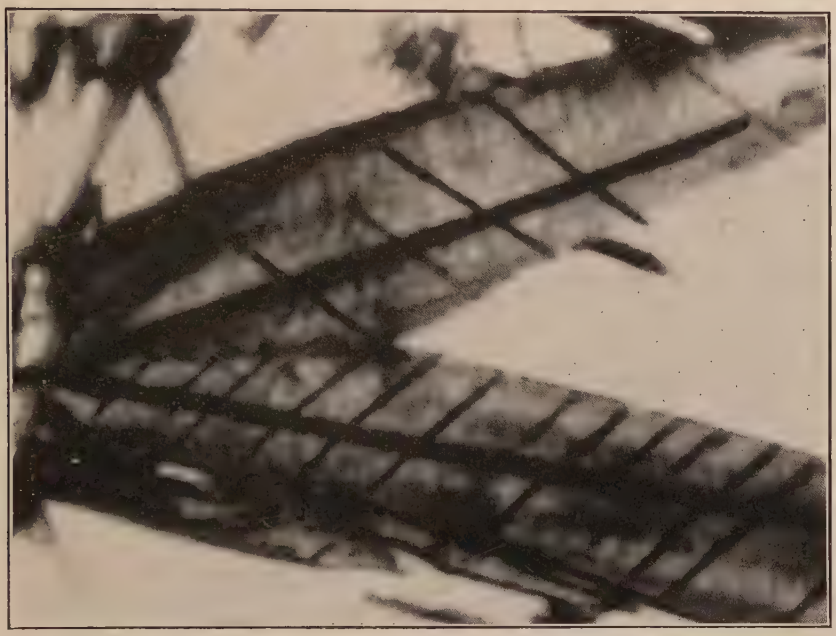

FIG. 13

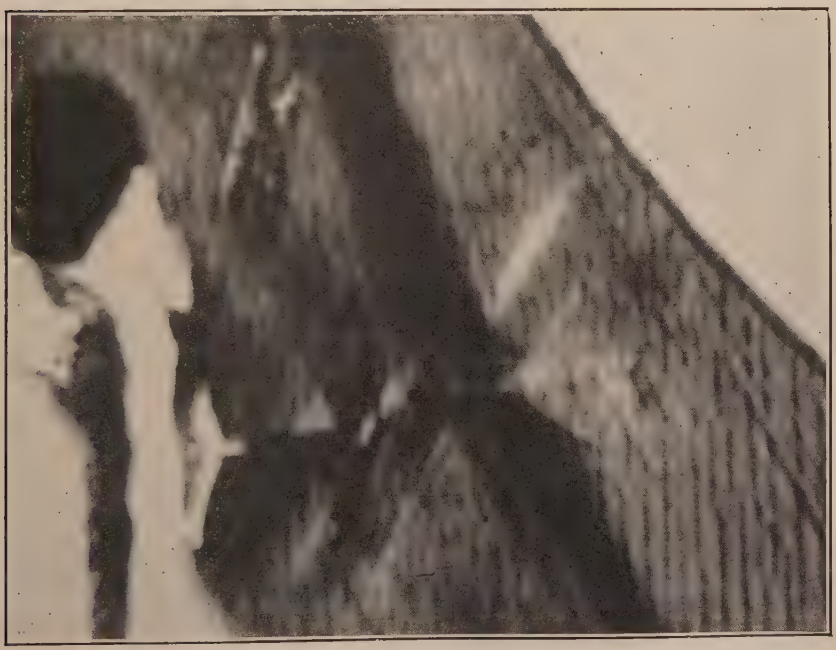

FIG. 14

PLATE LXXIV

Fig. 15

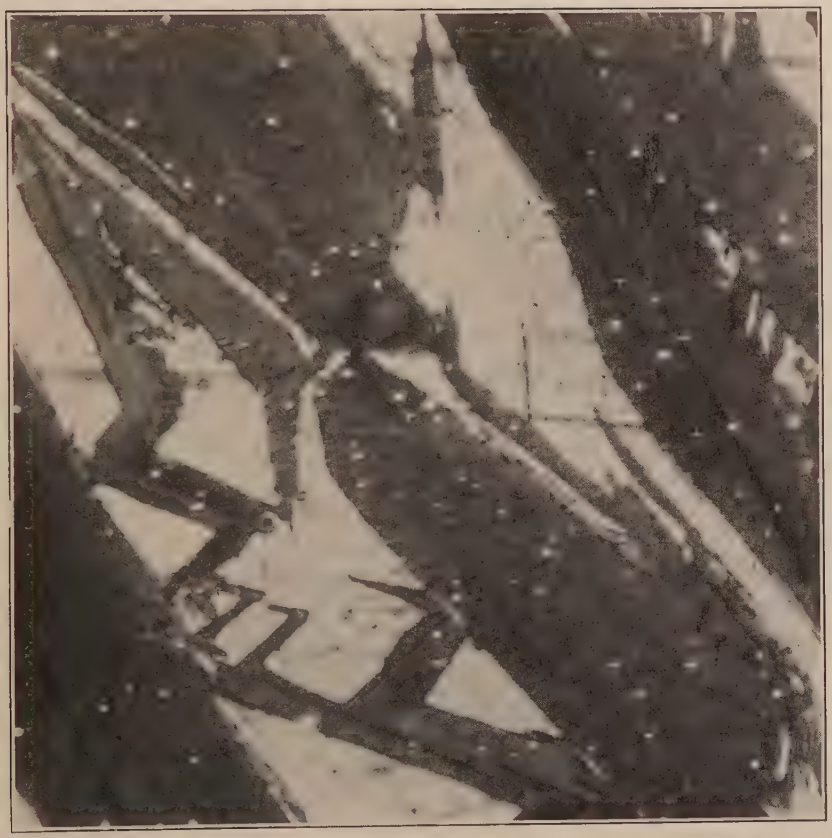

Fig. 16

PLATE LXXV

Fig. 17

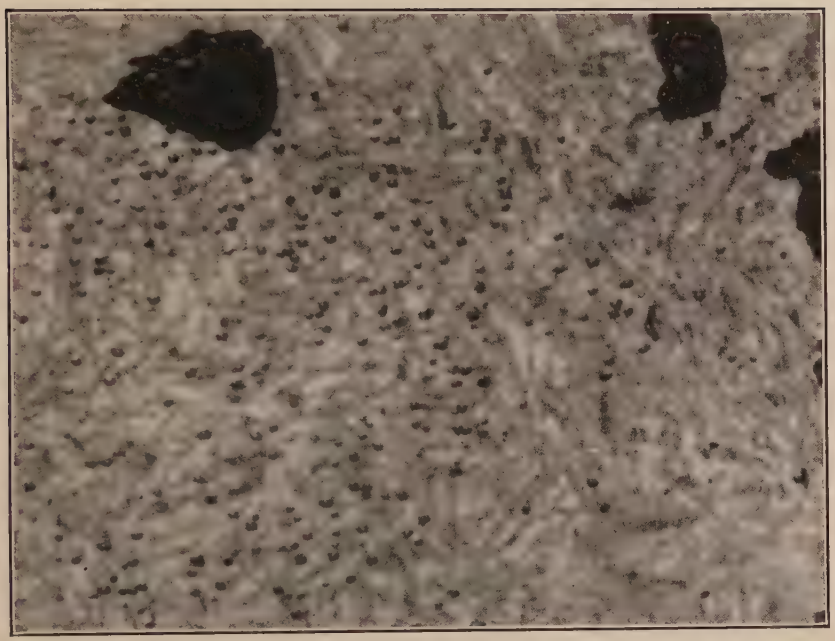

Fig. 18

PLATE LXXVI

FIG. 19

EXPERIMENT XXVII

X-RAY METALLOGRAPHY

Purpose: To study the principles of X-ray metallography and to become acquainted with the photographs of metals and alloys obtained by radiograph and diffraction methods.

References: Clark: Applied X-rays.
Lester: J. Society Automotive Engineers, Aug. 1927.
Lester: Trans. Am. Soc. Steel Treating, Nov. 1924.
Killefer: Ind. and Eng. Chemistry J., June, 1926.
Clark, Aborn and Brugman: J. Society Automotive Engineers, Feb. 1927.
Norton: Tech. Engineering News-Record, October, 1926.

Theory: The microscope discloses characteristic details of fine structure and subsequently gives remarkably complete information regarding the structure of metals and alloys down to the limit of the microscope and of visible light. Recently the adoption of quartz lens microscopes with ultra-violet light of shorter wave-length than visible light led to the disclosure of finer structure that appeared homogeneous under visible light rays, but here again a limit is reached. Now X-rays of very short wave-lengths are found to penetrate matter opaque to ordinary light and are associated with a far finer state of subdivisions of matter than is apparent by microscopic examination in visible or ultra-violet light. The phenomena of selective absorption of X-rays has become one of the greatest practical importance in the field of metallurgy. The use of X-rays for the study of the gross interior structure of opaque materials is known as "radiography."

X-ray metallography or radiography rests upon the fact that X-radiation penetrates matter opaque to visible light and is differentially absorbed depending upon the kind of material in the path. When a beam of X-rays passes through a material, part of the energy is absorbed and the emergent beam has been decreased in intensity. The amount of absorption depends upon the quality of the X-ray beam, the thickness of the object and the nature of the material through which it is passing. Thus a thick object will absorb more than a thin one and a material of high density such as lead or copper, will absorb more than aluminum or wood. Metals absorb the radiation very rapidly but if there is a blow-

hole, a crack or a sand inclusion in the metal, the radiation that goes through the defect will be absorbed to a less extent than the radiation that goes through the adjacent sound metal. Consequently if a photographic film is interposed to intercept the emergent beam after it has passed through the metal, regions of greater photographic density will appear on the negative after development. These black spots on the film are the images of the defects.

The experimental technique in radiography consists in passing a beam of X-rays through the object to be examined and, by a fluorescent screen or photographic plate, recording the varying intensities of the emergent beam and thus obtaining a shadow picture of the interior of the object. The fluorescent screen glows with visible light when X-rays fall upon it, and the brightness of the glow is, under proper conditions, proportional to the intensity of the X-rays. In this way the shadows may be observed directly. The photographic film, however, gives a permanent record of the X-ray picture.

The factors which are involved in a radiograph are, therefore, as follows:

(1) The percentage of energy absorbed depends on the wave-length of the radiation, the thickness of the material, its density and atomic weight. For a given wave-length or voltage the absorption will increase, or the penetration decrease, with the thickness of material and with its atomic weight.

(2) If an object made of materials of different densities, or containing unhomogeneities, or a homogeneous material of varying thickness, is subjected to radiographic examination the film will show upon development densities corresponding to the transparency of the various thicknesses.

The limit of penetrability based on a 30-minute exposure with commercial apparatus is approximately $3\frac{1}{2}$ in. of steel. Potentials of 200,000 to 300,000 volts are required to obtain radiation of sufficient penetrating power.

Metals may be examined with X-rays, first, for radiographic tests in which photographic images of internal details of the gross structure are obtained; second, for diffraction tests in which images are obtained that may be interpreted to give information regarding details of microstructure of the constituents in the metal, that is, detection and estimation of the effects of mechanical and heat-treatment, grain size, and their attributes; and third, for diffraction tests in which images are obtained that may be interpreted to give the fundamental lattice structures and atomic arrangements of the crystals of which all metals and alloys are constituted.

X-ray diffraction of metals is based on the following facts. The atoms of which a material is exposed possess the property of scattering X-rays, thus acting as a diffraction grating to the X-ray beam. This is due to the fact that in solid crystalline matter the spacings of the atoms are in the same order of magnitude as the wave-length of the X-rays, namely, 10^{-8} cm. (1 cm. = 0.3987 in.). When a beam of X-rays, defined by a small pin-hole, is allowed to pass through a thin crystal and to fall upon a photographic film, and after a suitable exposure the film is developed, it will be found that the film has a black spot in the center which is the same shape as the pin-hole, and around it a number of other much fainter spots arranged in a symmetrical fashion. These are due to the scattered X-rays from the regularly arranged atoms of the crystal. This pattern of spots depends upon the particular crystal and upon the orientation of the crystal with respect to the X-ray beam. An object which is not crystalline will not produce a regular pattern of spots in this fashion, but will cause only a slight fogging over the surface of the film in addition to the central spot.

There are two general types of X-ray diffraction technique: first, the Laue method depends upon the diffraction of a pin-hole beam of X-rays of various wave-lengths by a single crystal variously oriented; and, second, the powder method utilizes a monochromatic beam of rays from a slit and crystal powder in which there is opportunity for particles in every possible orientation.

From an X-ray diffraction pattern it is easily possible to determine the exact positions in space of each of the atoms making up metallic crystals. Each metal has its own characteristic spacings and thus it is possible easily to determine what metals are present in a mixture. If two metals are present as such, the diffraction pattern will show two series of characteristic lines, but if they should be in a completely homogeneous solid solution only one series of lines will show. In the simplest cases these lines are intermediate between the positions of those of the metals composing the solution. From the relative displacement of these lines it is easy to reach a close approximation to the constitution of the mixture. If the two metals form an intermetallic compound, an entirely new set of lines characteristic of that compound will be found. This technique is leading to very important facts as to the nature of alloys and the reasons for their changes in properties with changes in composition.

The information obtainable from X-ray data regarding structural composition includes whether it is crystalline or amorphous; single crystal or aggregate; its crystal lattice-structure and dimensions; purity; chemical identity as to whether compound, mixture, adsorption

complex, or solid solution. The data obtainable also apply to grain size, internal strain, uniformity of composition, chemical changes, and the differentiation of good and bad materials.

Apparatus and Procedure: A tungsten target X-ray tube of the Coolidge hot-filament type is ordinarily employed. The filament is heated to incandescence by a separate circuit and this constitutes the cathode in the high-tension circuit, with the target as the anode. A closed-core, oil-immersed, high-tension transformer which may produce up to 300 kilovolts is almost invariably employed. The alternating high-tension current is rectified by mechanically rotating disks or by vacuum-tube Kenotrons. The object which is to be radiographed is placed at some distance from the tube so that the rays proceeding from the focal spot on the target are essentially from a point source. Radiographs are merely shadowgraphs produced by radiation traveling in straight lines from a point source. It is essential to place the photographic film as near to the object as possible in order to prevent distortion. The film is enclosed in a cassette with intensifying screens of calcium tungstate. On account of the fact that some of the radiation is scattered and reflected, as well as passing through or being absorbed in the object, thorough protection with sheet lead on the back and edges of the film is required. The intensifying screens or fluorescent screens are pressed close against both sides of the double coated film and give off visible light which increases the image on the film. In this way the exposures may be greatly reduced.

ILLUSTRATIONS

Fig. 1 is a diagrammatic sketch of the Coolidge X-ray tube and electrical connections.

Fig. 2 is a sketch of the X-ray spectrometer for X-ray surface reflection patterns.

Fig. 3 is a diagrammatic sketch of apparatus used to obtain pin-hole X-ray diffraction patterns.

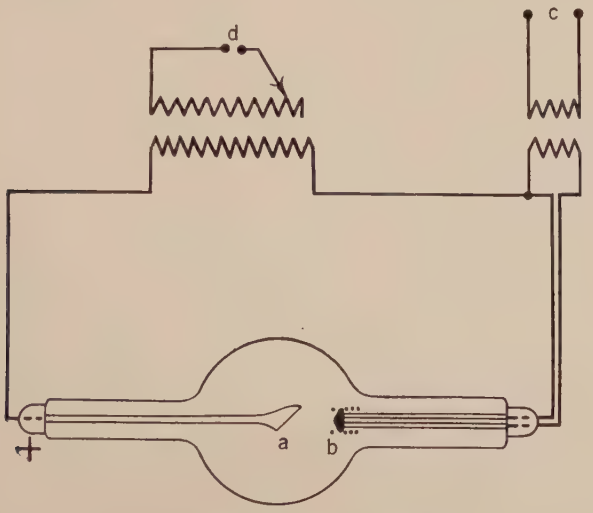

X-Ray Tube and Electrical Connections

a - Tungsten anode
b - Tungsten filament cathode
c - Filament transformer
d - Transformer for rectified current

FIG. 1

Fig. 4 is a diagrammatic sketch of apparatus used to obtain X-ray surface reflection patterns, similar to that of Fig. 2.

Fig. 5 is a series of curves showing the relation between the thickness of steel penetrated, time of exposure, voltage and current through the X-ray tube. Curves *A* and *B* are calculated from the theory to check the observed values.

Fig. 6 is a photograph of the macrostructure of a section through a commercial steel casting showing numerous types of defects which may

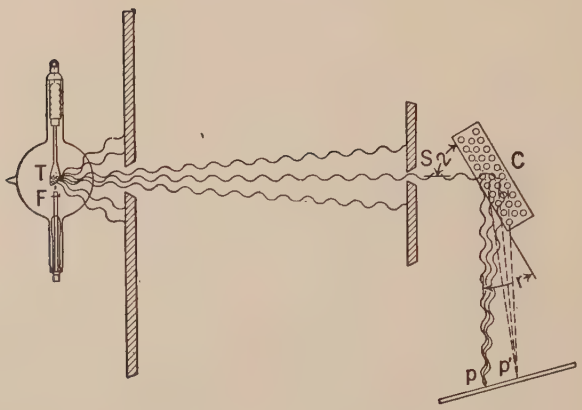

FIG. 2. X-ray Spectrometer

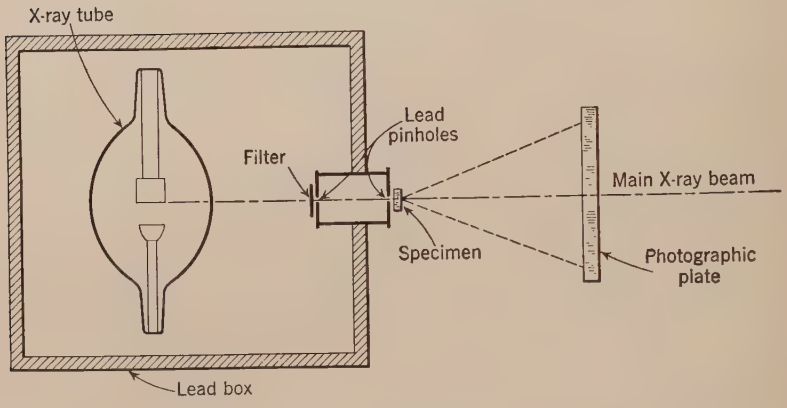

FIG. 3 (Clark)

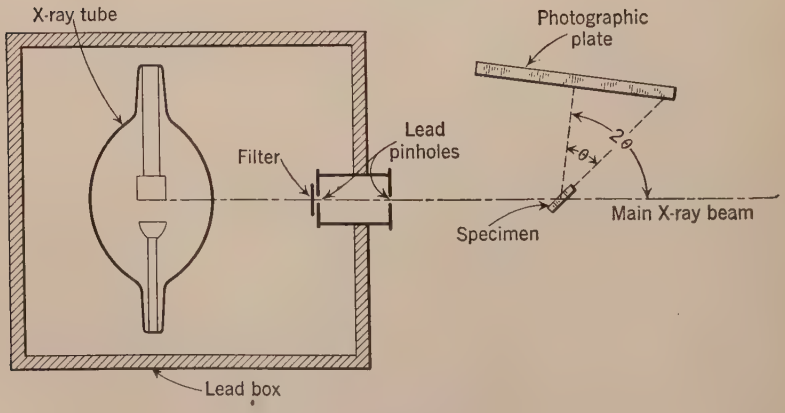

FIG. 4 (Clark)

occur in such steel castings. This casting had passed inspection and had been accepted for service. It was supposed to be a good casting, yet there are numerous defects, very few of which could have been detected by ordinary test methods.

Fig. 7 is a radiograph of a heavy casting made for a 400-lb. air bomb. It shows the defects in the section through the nose. The film was placed horizontally inside the shell and exposed to rays traveling along

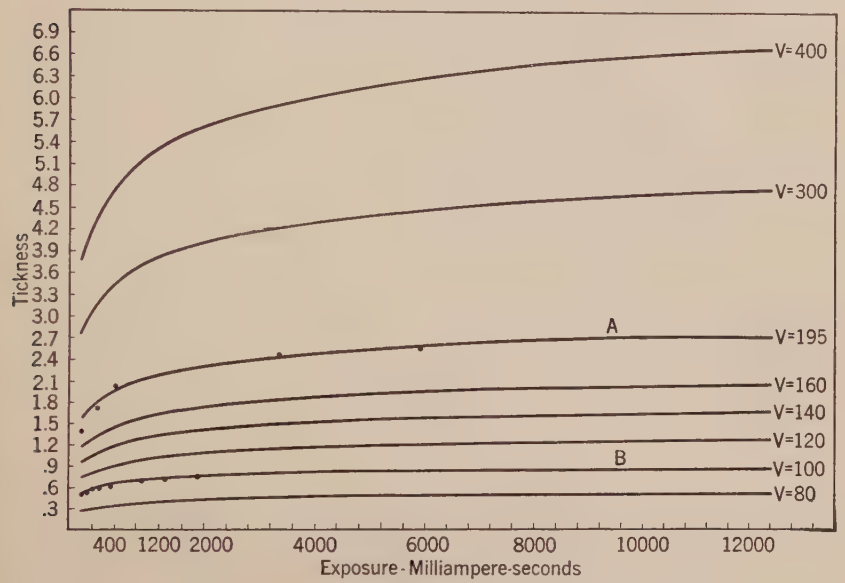

Fig. 5 (Lester)

the axis of the casting through slightly more than 2 in. of metal. The three dark areas are shadows of the columnar risers. The white spots are holes in the casting.

Fig. 8 is a photograph of the above casting which was cut up for study and shows some of the holes represented by the spots shown in Fig. 7.

Fig. 9 is a radiograph of a steel casting showing cavities due to steam injected from a damp mold. The dark spots are the cavities. Occasionally gas pockets are caused by damp molds.

Fig. 10 is a radiograph of a cross-sectioned piece of steel casting, and shows capillary pipes somewhat enlarged by the presence of gas.

Fig. 11 is a radiograph of a steel casting showing dirt and gas trapped in horizontal cross-section where there was no flow of metal toward the riser. The dark areas are either voids or inclusions.

Fig. 12 is a radiograph of a casting for a 10-ton army tank (metal $\frac{1}{2}$ to $\frac{3}{4}$ in. thick) showing sand inclusions (white).

Fig. 13 is a radiograph of a gun-mount steel casting ($1\frac{1}{4}$ in. thick) showing cracks (white) in the metal.

Fig. 14 is a radiograph of a gun-mount steel casting (metal about 1 in. thick) showing gas cavities (white).

Fig. 15 is a radiograph showing pipes in bolt flange of a steel casting. The mottled areas (black) at the white figure (1) is the image of a large cavity, or pipe, caused by shrinking of the metal while solidifying. Smaller cavities are shown at the lower center. Such defects are commonly due to incorrect dimensions or placing of heads of risers intended to supply additional molten metal to the interior of the casting as it cools.

Fig. 16 is a radiograph of a steel casting showing sand inclusions (black).

Fig. 17 is a photograph of section of casting taken near region shown in Fig. 16. The dark mottled areas are the sand inclusions. Here a portion of the mold seems to have collapsed, due to severe erosion. The casting from which Figs. 16 and 17 were taken weighed 1400 lbs. It was estimated that fully 15% of the total metal volume was sand, although the surface indications were so slight that the inspector has passed the casting as acceptable for service.

Fig. 18 is a radiograph of cross-section of steel casting taken through cracks. It will be noted that practically none of the cracks appear on the outside surface. A number of them open through to the inside surface, but some of them do not open to the surface at all. These cracks are shrinkage cracks.

(*Note:* In the radiographs above, if the blow-holes, cavities, cracks and inclusions appear black, they are negative reproductions of the original film. If they appear white, the pictures are positive prints from the original radiographic films.)

Fig. 19 — When a beam of X-rays defined by small pin-holes passes through a single crystal grain of iron, the result is a pattern of sharp spots on a photographic film behind the crystal. This diffraction pattern upon analysis proves that the smallest subdivision which is still crystalline iron is a cube with an atom of iron at each corner and one at the center.

Fig. 20 — Superimposed grains, and aggregates; effect of grain size: a metal specimen which consists of one crystal grain is distinguished by a regular pin-hole pattern of diffraction spots, showing a symmetry of number and arrangement on zone ellipses which cannot be obscured, even though the X-ray beam does not pass through the grain parallel

to a principal axis. If the X-ray beam passes through two grains, the patterns on the plate are superposed; as the number of grains lying side by side or under one another in the path of the beam increases, the spots become more numerous and smaller, all traces of the zone ellipses for one grain being obscured. At the same time the intensity decreases, and longer times of exposure are required. A condition of minute size is finally reached where on a Laue diagram there appears an almost continuous darkened ring, and in the monochromatic pin-hole method the concentric rings of uniform intensity. Fig. 20 gives the patterns for the 1–2–5–120–2,000 and 1,000,000 grains of aluminum in the path of the beam.

Fig. 21 shows the typical concentric ring pattern for iron with a particle size between 10^{-3} and 10^{6} cm. This pattern is a special modification of the straight line spectra obtained by the familiar Hull-powder method in which the monochromatic beam is defined by slits instead of pin-holes.

Fig. 22 — Although it is commonly thought that cast metals generally exhibit a random orientation of grains, an examination of Fig. 22 will show the great practical importance of the pin-hole method in this field. The coarse non-uniform grain mass of steel as ordinarily cast, shown at the top of Fig. 22, is by no means obliterated in the standard annealing processes as the middle view shows. The removal of internal stresses is not impossible under proper annealing conditions. The bottom view of Fig. 22, for the same casting, shows the ideal structure of small equi-axed crystals with neither directed orientation or intensity maxima nor internal strain or radial asterism striations.

Fig. 23 shows the diffraction patterns of a series of silicon-steel samples, differing essentially in the annealing only. The upper left view indicates a partial or unsatisfactory anneal showing a high hysteresis loss of 0.8636 watts per pound; the lower right, a controlled anneal showing a low hysteresis loss of 0.5535 watts per pound; the others show progression in pattern and hysteresis losses between the limits. It is at once apparent that, as the hysteresis losses decrease, the diffraction spots become larger and fewer in number, culminating for minimum loss and best magnetic properties in the diagram of a single-crystal grain extending through the sheet, as indicated in the lower right view. The faulty annealing of the poorest specimen is further shown by the four clustered intensity maxima symmetrically placed around the direct-beam spot; these are residual evidence of the fibering originally produced by the rolling of the sheets before heat-treatment.

Fig. 24 — Fiber Structure: There is an intermediate state between the single crystal and a chaotic aggregate of small crystals; namely, one in which the small crystals are oriented in a definite fashion with

respect to a common direction. "Fibering" in various degrees can be artificially produced, most notably in metals, by mechanical working a chaotic aggregate, that is, rolling into a sheet, drawing into a wire, twisting, compressing, etc.

The study of mechanical deformation in metals represents, therefore, one of the great achievements of the pin-hole method. The entire diagram 360 degree in azimuth is obviously highly desirable and consequently the method is superior in ascertaining this type of information to any other. The behavior of any metal, even after heat-treatment, is dependent on the mechanical work which induces fibering and directional properties. In many of the studies of commercial metals, unsatisfactory behavior is to be attributed to faulty mechanical working and to faulty annealing designed to remove directional properties.

Fig. 25 — Internal Strain: In an uninjured crystal lattice, the planes are in fact plane and act like very good little mirrors towards X-rays, so that images of the narrow aperture produced by the planes are sharp elliptical spots on the photographic plate. If, however, the crystal is stressed beyond the elastic limit, either through external forces or through thermal stresses, translation on slip planes occurs, which as a rule is accompanied by simultaneous bending around crystallographic directions. As a result of this, the planes are curved approximately in the shape of a cylinder, so that the reflection images become distorted into streaks or asterism striations as they do in a cylindrical mirror. Conversely, it may be concluded from the occurrence of such asterism striations that the space lattice has been stressed beyond the elastic limit and that there are residual inner elastic stresses as a result of translation and bending in the lattice, which can be equalized only by suitable heat-treatment. Not only do asterism striations indicate distortion in single crystals but they also appear for aggregates in a state of strain. Fig. 25 shows irregular radial asterism striations produced by internal strain in a metal aggregate (steel casting) due to severe quenching.

Fig. 26 — Welds: The determination of the structure of welds from the X-ray diffraction diagram has been very illuminating, particularly when these results are combined with photomicrographs and tensile-strength tests. The specimens were various butt and lap welds produced by the arc method in air, shown in the upper pair of Fig. 26 and by the General Electric Company's method of welding in hydrogen, shown in the lower pair. The variations in particle size and strains in the various zones between the weld metal and the original bar-metal were clearly disclosed by the X-ray photographs. The maximum strain as judged by asterism is observed in the top of the weld metal, where the last metal has been added and the cooling has been most rapid; while

the smallest particle size is in the refined zone of the original metal adjoining the weld. The hydrogen-atmosphere welds are distinguished from the ordinary type by larger grain-size but a far more uniform grain-size throughout all the zones, even in the refined zone, and a much greater freedom from strain, as if the composite structure were annealed. The oxide impurities at grain-boundaries in the ordinary welds are clearly absent in the hydrogen welds so that there is no interference with grain growth. In spite of large grains in random orientation, these welds are fairly ductile, illustrating an important metallurgical fact that large grains do not necessarily mean brittleness of the specimen.

Discussion: Metal castings is the most important application of X-ray radiographic diagnosis simply because of the wide use of castings and because of the uncertainty of gross structure with empirically developed foundry practice. Cast-steel ingots are too large for study by X-ray methods, and forgings are not suited to these tests because the rolling reduces the defects in the ingot to too small a size for detection. It is more important to understand the nature of defects in castings than in forgings, because it is in the casting that the defect is first formed. If the casting can be made free from defects, the forging will be free from most of its defects. Radiography is very important in the study of welding. There is no positive assurance by the usual methods that a weld has been properly made. Radiographs disclose imperfections of union and inclusions in the welded metals. Visual inspection with a fluorescent screen can be used for thin sections while the pieces move along on a belt or container.

The following defects may be radiographed: gas cavities from metal or mold, sand inclusions, slag inclusions, pipe or shrinkage cavities, porosity, cracks, metal segregation, etc.

The application of X-ray crystallography to the study of metals and alloys has made available information of considerable value in the field of physical metallurgy and metallography. It reveals the atomic arrangement, including the identification of and discrimination between constituents, determination of allotropy, mechanism of solid solution formation, coring, coefficient of thermal expansion, and stress-strain relations. It also enables studies on grain size effects, establishment of preferred orientation by extreme cold work or by electro-deposition, etc.

PLATE LXXVIII

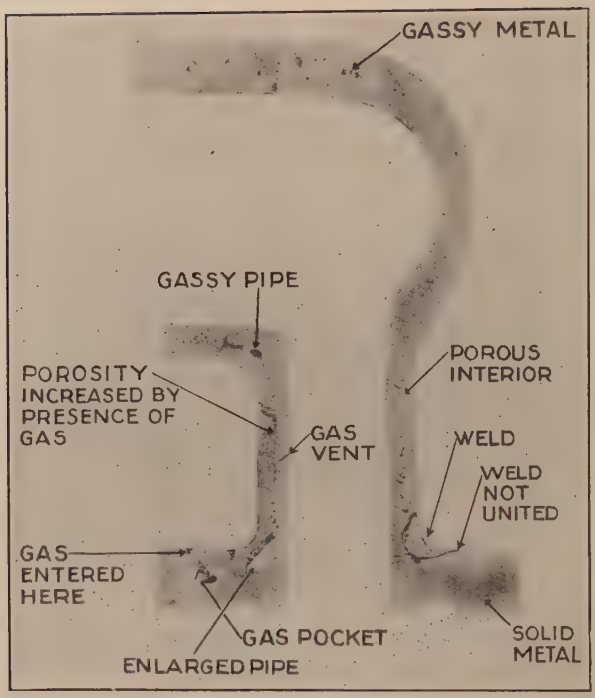

Fig. 6 (Lester)

PLATE LXXIX

Fig. 7 (Lester)

PLATE LXXX

FIG. 8 (Lester)

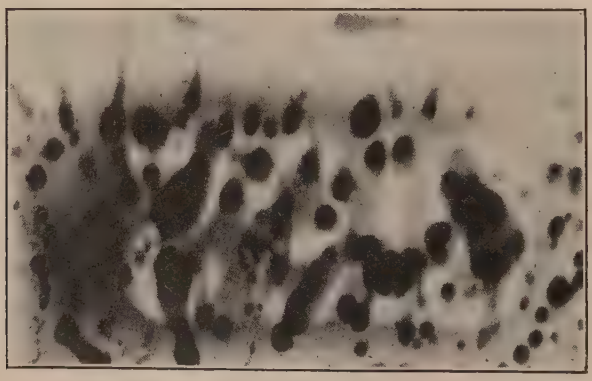

FIG. 9 (Lester)

FIG. 10 (Lester)

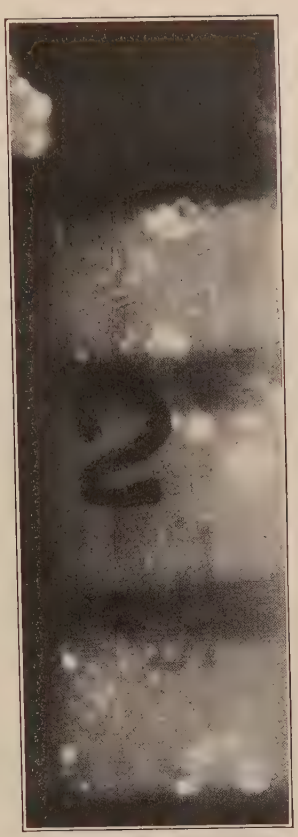

FIG. 12 (Lester)

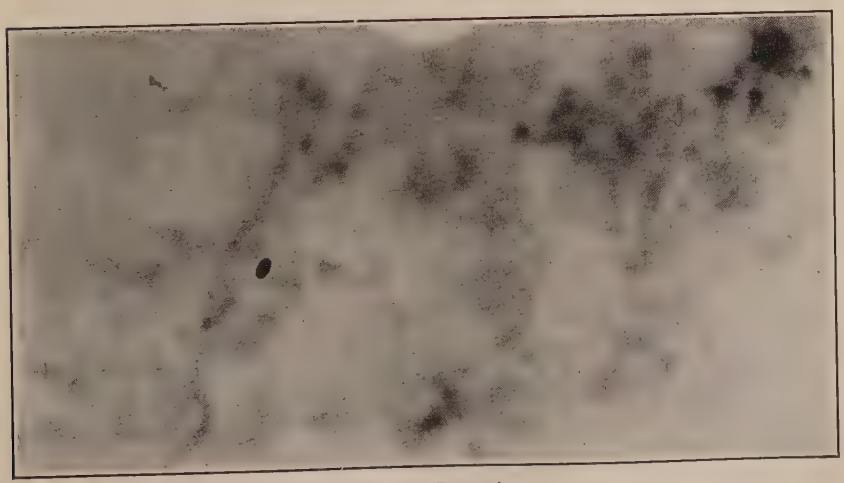

FIG. 11 (Lester)

PLATE LXXXII

FIG. 13 (Lester)

FIG. 14 (Lester)

PLATE LXXXVI

Fig. 15. Lesion.

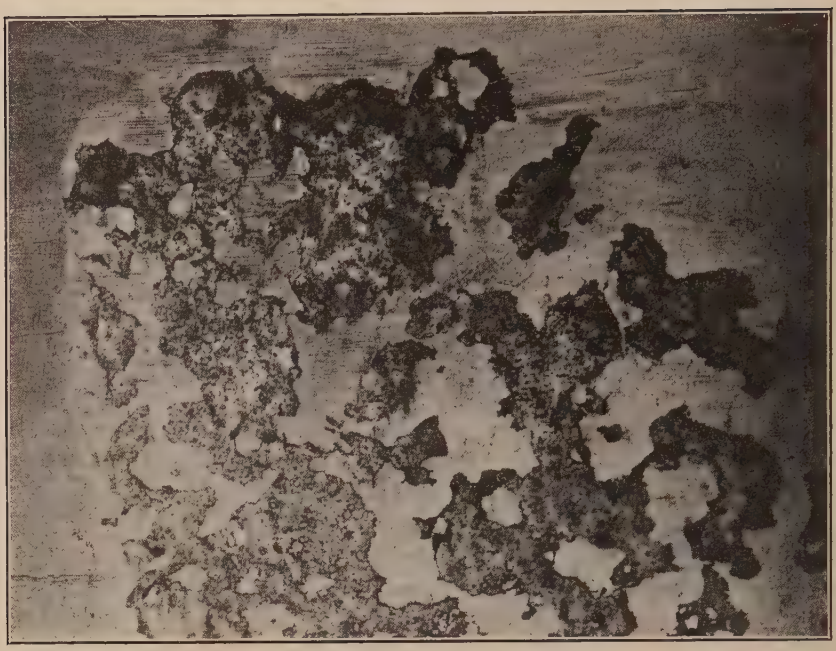

FIG. 17 (Lester)

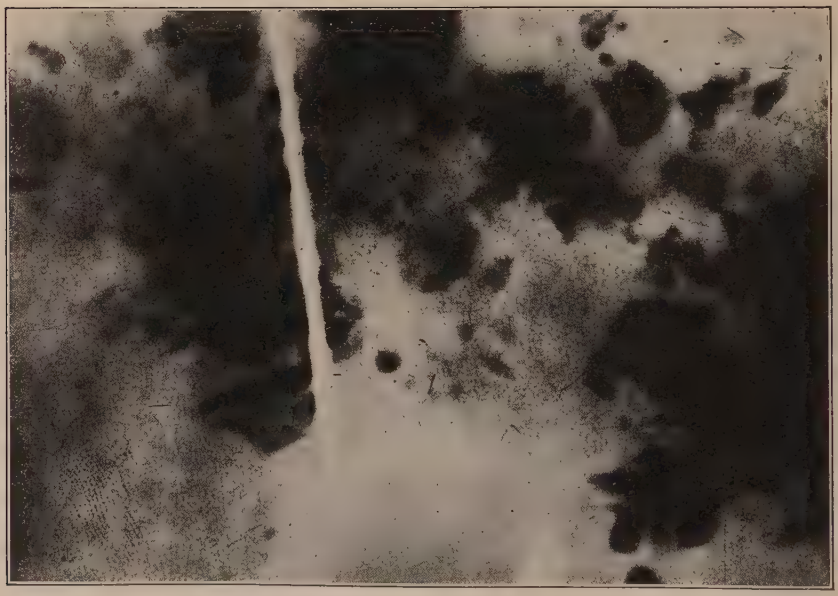

FIG. 16 (Lester)

PLATE LXXXV

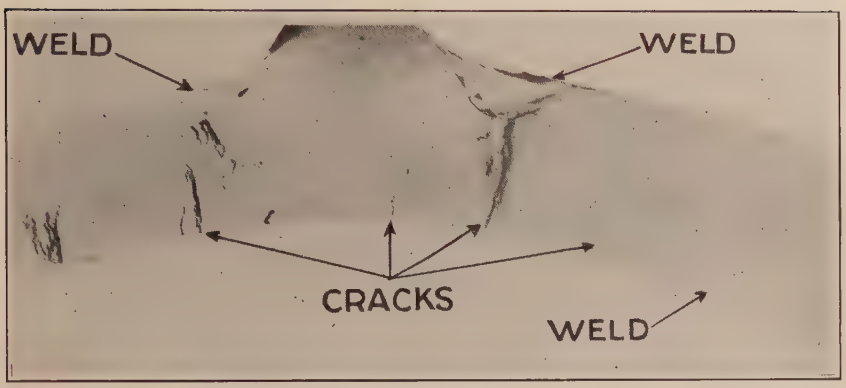

FIG. 18 (Lester)

FIG. 19 (Clark)

Typical Pattern for a Single Crystal of Iron
(Beam Parallel to a [110] Direction)

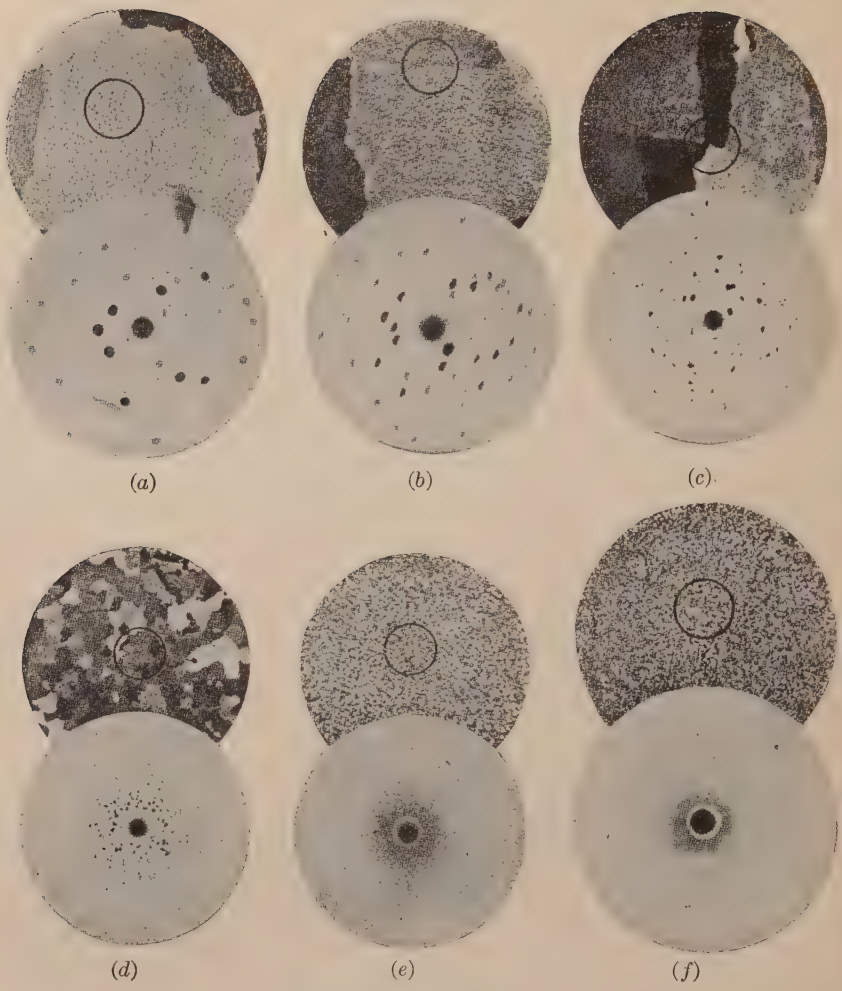

FIG. 20 (Clark)

Patterns for Simultaneous Diffraction of X-rays by Aluminum

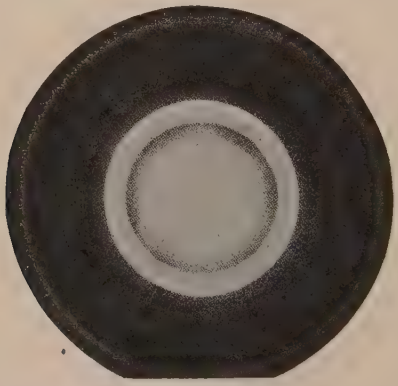

FIG. 21 (Clark)

Pinhole Diagram of Small-Grained Random Aggregate of α-Iron

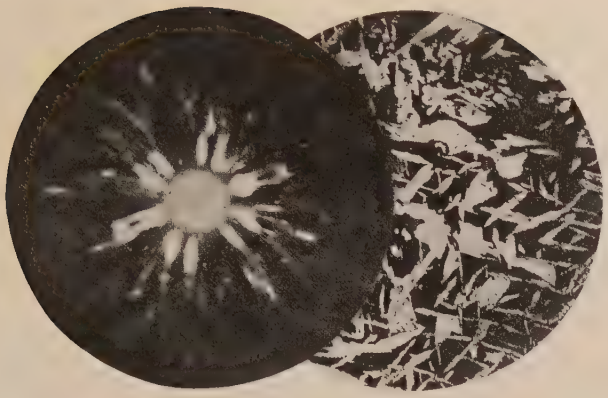

(*a*) As Cast

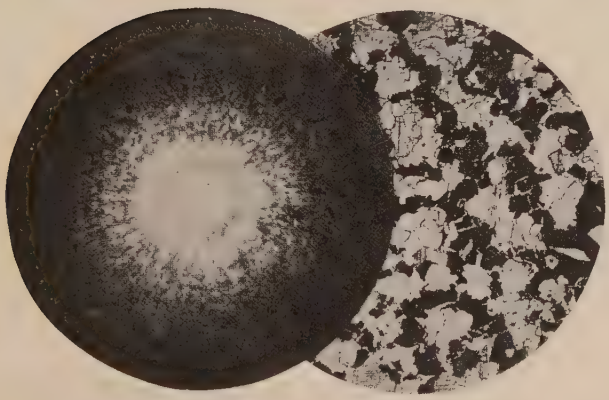

(*b*) After 5-hour Anneal

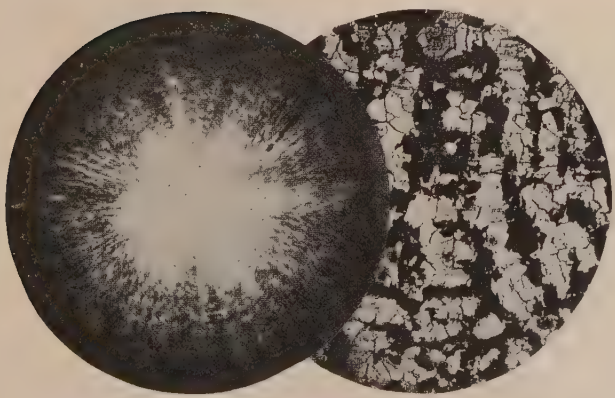

(*c*) After four 5-hour Anneals, Showing Ideal Structure

FIG. 22 (Clark)

Diffraction Patterns and Photomicrographs of Cast Steel, Illustrating Value of X-ray Method in Controlling Heat-Treatment.

FIG. 23 (Clark)

Structures of Silicon Electric Steel after Various Anneals, Showing Progression in Pattern with Decreasing Magnetic Hysteresis Losses in watts per pound as follows:

(*a*) (Poorest) 0.8636; (*b*) 0.8181; (*c*) 8068; (*d*) 0.7727; (*e*) 0.6931; (*f*) (Best) 0.5535.

(*a*) Pattern for Cold-Drawn Aluminum Wire, Showing High Degree of Fibering.

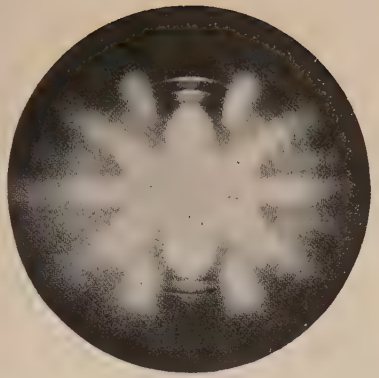

(*b*) Fiber Pattern for Cast-Steel Bar at Point of Rupture in a Tension-Testing Machine.

FIG. 24 (Clark)

Irregular Radial Asterism Striations Produced by Internal Strain in a Metal Aggregate (Steel-Casting).

FIG. 25 (Clark)

PLATE XC

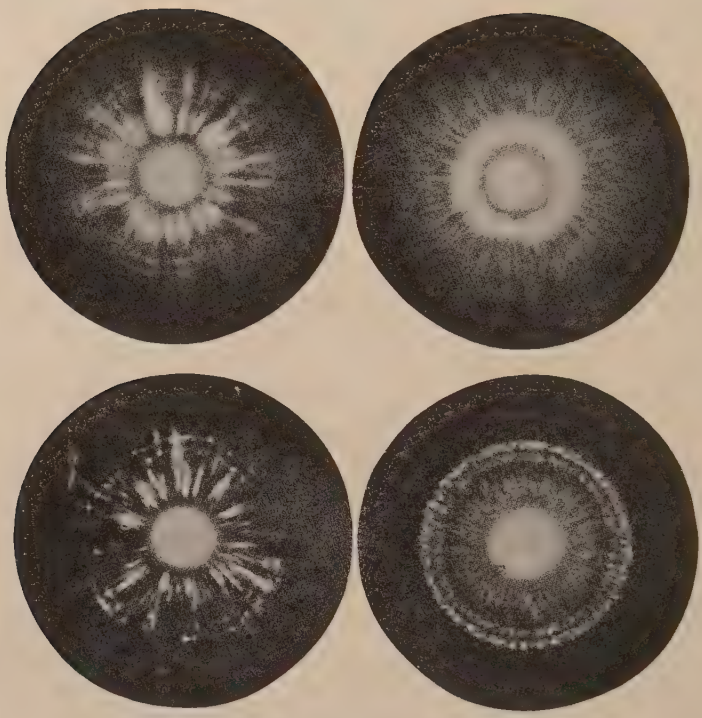

X-ray Determination of Weld Structure

Fig. 26 (Clark)

APPENDIX I

ETCHING REAGENTS

The structure of a metal or alloy may usually be developed by etching a polished surface. This is accomplished by either immersing the specimen in a suitable chemical reagent or applying the solution with a swab or a medicine dropper. After etching for the proper time which is determined by experience, the specimen is washed in running water and then in absolute alcohol and dried either in a warm air-blast or with cotton or soft paper toweling. To bring out the proper structure, considerable care and some skill are required. *Do not over-etch.* If over-etched, the specimen must be repolished and re-etched. The most suitable etching reagent varies with the material to be etched. Some of those that have proved to be very satisfactory are listed below.

(1) Iron and Steel:

(a) **Nitric acid** — 5% or 10% solution of HNO_3 in absolute ethyl alcohol.
(b) **Picric acid** — 5% solution of picric acid in absolute ethyl alcohol.
(c) **Iodine solution** — 1.2 grams I + 1.2 grams KI + 1.2 cc. H_2O + 97 cc. alcohol.
(d) **Nital** — 5 cc. conc. HNO_3 in 95 cc. absolute methyl alcohol.

(2) Copper and its Alloys (Brasses and Bronzes):

(a) **Ammonium hydroxide and hydrogen peroxide** — 75% conc. NH_4OH + 25% H_2O_2.
(b) **Grard's Solution (Acid Ferric Chloride)** — 19 grams $FeCl_3$ + 6 cc. HCl + 100 cc. H_2O.
(c) **Ammonium Persulfate Solution** — 1 gram $(NH_4)_2S_2O_8$ + 90 cc. H_2O.
(d) **Alcohol Ferric Chloride** — 34 grams $FeCl_3$ + 250 cc. conc. HCl + 750 cc. alcohol.
(e) **Chromic Acid** — Saturated solution. Emphasizes the grain boundaries and also the oxide inclusions.

(3) Aluminum and its Alloys:

(a) **Sodium Hydroxide Solution** — 50% NaOH + 50% H_2O.
(b) **Hydrochloric Acid** — 10 cc. conc. HCl in 90 cc. H_2O.
(c) **Hydrofluoric Acid** — 5% solution.

(4) Lead and its Alloys:

(a) **Hydrochloric Acid** — Concentrated or 50% solution.
(b) **Nitric Acid** — 10% solution.
(c) **Picric Acid** — 5% solution in alcohol.

(5) Nickel and its Alloys:

(a) **Nitric and Acetic Acid Solution** (Merica) — 50 cc. conc. HNO_3 + 25 cc. glacial $HC_2H_3O_2$ + 25 cc. H_2O.
(b) **Ferric Chloride Solution** — 1 gram $FeCl_3$ + 2 cc. conc. HCl + 3 cc. H_2O.

(6) Tin and its Alloys:

(a) **Nitric Acid** — 10% solution in H_2O.
(b) **Hydrochloric Acid** — concentrated.

(7) Zinc and its Alloys:

(a) **Iodine Solution** — 1 part iodine + 3 parts KI + 10 parts H_2O.
(b) **Chromic Acid** — Solution contains 94% conc. HNO_3 and 6% chromic acid. A few drops of this solution are added to 100 cc. H_2O just before using.
(c) **Nitric Acid** — 10% solution.

(8) Magnesium and its Alloys:

(a) **Nitric Acid** — 2% aqueous solution.

(9) Gold-Silver-Platinum and their Alloys:

(a) **Aqua Regia** — 1 part conc. HNO_3 + 5 parts conc. HCl + 6 parts water.

APPENDIX II

THEORY OF THE POTENTIOMETER PYROMETER*

The Potentiometer. — The potentiometer provides, first, a means for securing a known variable potential, and, second, suitable electrical

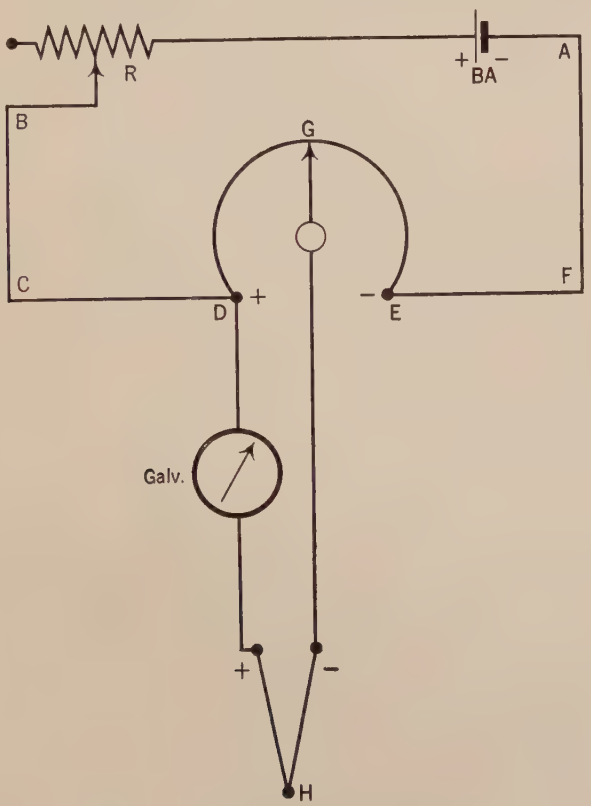

Fig. 1

connections for opposing that potential to the unknown electromotive force of the thermocouple. The two are connected electrically, so that they oppose one another. So long as one is stronger than the other, a current will flow through the thermocouple; when the two are equal, no current will flow.

* Printed with permission of the Leeds & Northrup Co.

Fig. 1 shows the wiring of the potentiometer in its simplest form. The thermocouple is at *H*, with its polarity as shown by the symbols + and −. It is connected with the main circuit of the potentiometer at the fixed point *D* and the movable point *G*.

A current from the dry cell *BA* is constantly flowing through the main, or so-called potentiometer circuit, *ABCDGEF*. The section

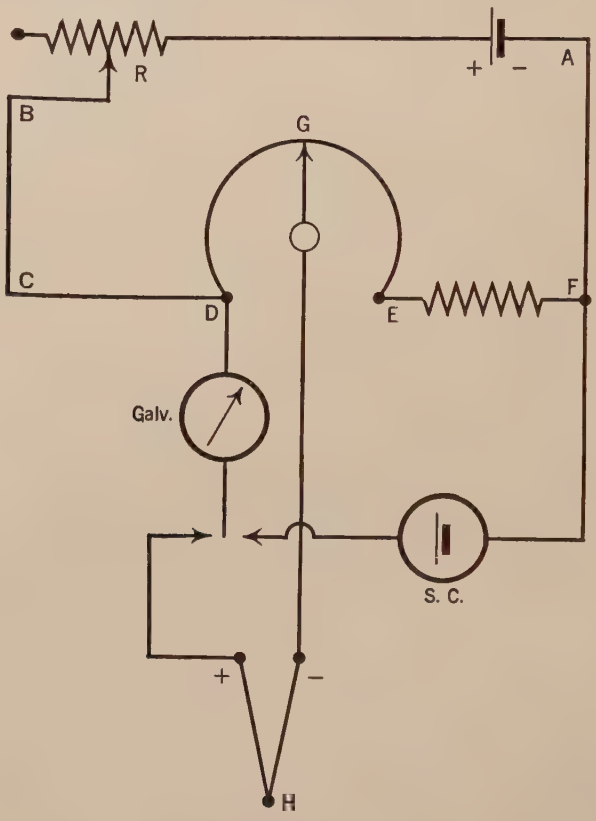

Fig. 2

DGE of this circuit is a slide wire, uniform in resistance throughout its length. The temperature scale is fixed to this slide wire. The current from the cell *BA* as it flows through *DGE* sets up a difference in potential between *D* and *E*. There will also be a difference in potential between *D* and all other points on the slide wire. The polarity of this is in opposition to the polarity of the electromotive force of the thermocouple which connects into the potentiometer at *D* and at *G*. By moving *G* along the slide wire a point is found where the potential between *D* and

G in the slide wire is just equal to the electromotive force generated by the thermocouple. A galvanometer in the thermocouple circuit indicates when the balance point is reached, since at this point the galvanometer needle will show no deflection.

The potential in the slide wire will vary with the current flowing through it from the cell BA and a means for standardizing this is pro-

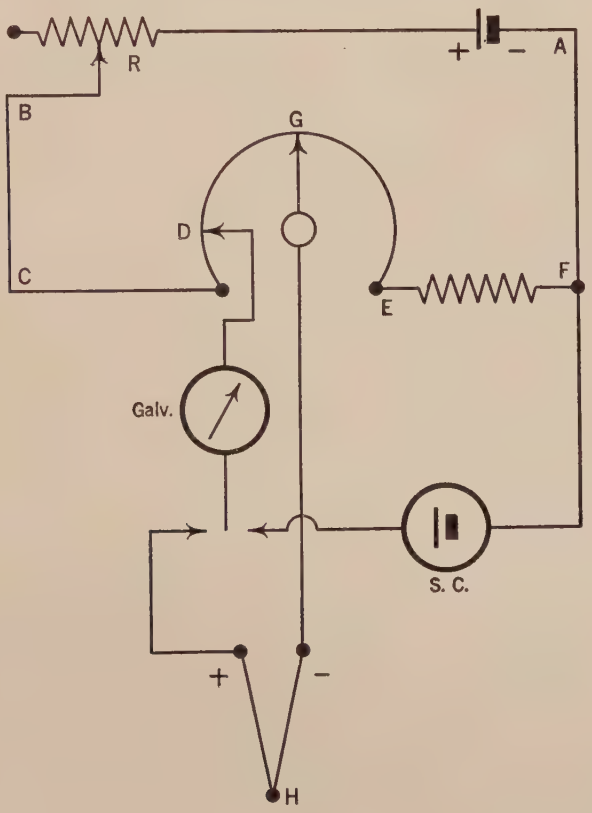

Fig. 3

vided. S.C., Fig. 2, is a Weston type standard cell whose voltage is constant. It is connected to the potentiometer circuit at two points D and F by closing the contact shown between S.C. and Galv., whenever the potentiometer current is to be standardized. The galvanometer is then in series with S.C. The variable rheostat R is then adjusted until the current flowing is such that, as it flows through the slide wire DGE and the standard resistance EF, the fall in potential between D and F is just equal to the voltage of the standard cell S.C. At this time the

galvanometer will indicate a balance in the same way as when it was used with a thermocouple. By this operation the current in the slide wire *DGE* has been standardized. The standard cell is then disconnected and the thermocouple connected by closing the contact shown between Galv. and the + side of *H*.

Automatic Cold Junction Compensator. — The net electromotive force generated by a thermocouple depends upon the temperature of the hot

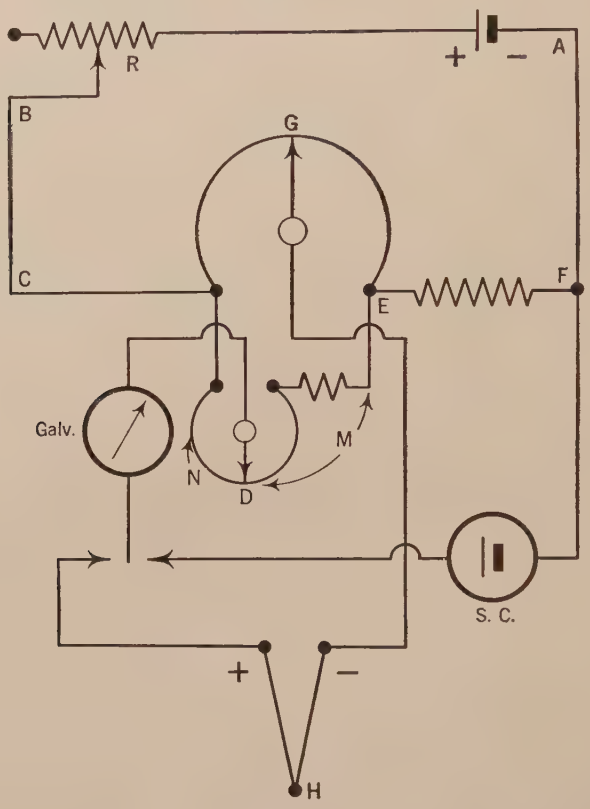

Fig. 4

junction and the temperature of the cold junction. Any method adopted for reading temperatures by means of thermocouples must in some way provide a means of correcting for the temperature of the cold end. For this purpose, the potentiometer may have either of two very simple devices. In one form the operator is required to set a small index to a point on a scale corresponding to the known cold junction temperature. In the other form, an even more simple automatic compensator is em-

ployed. The principle of each is described in the following paragraphs.

As previously explained, the electromotive force of the thermocouple is measured by balancing it against the potential DG in the slide wire of the potentiometer. As shown in Fig. 2, the magnitude of the bal-

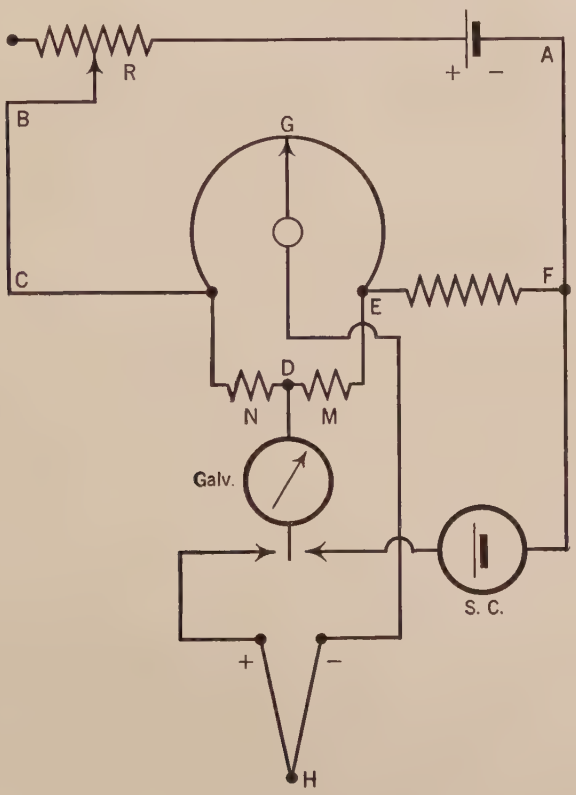

Fig. 5

ancing potential is controlled by the position of G. Make D movable as shown in Fig. 3, and the magnitude of the potential DG may be varied either from the point D or the point G. This gives a means for compensating for cold junction changes by setting the slider D. As the cold junction temperature rises, the net electromotive force generated by the thermocouple decreases, assuming the hot junction temperature to be constant. To balance this decreased electromotive force the slider D is moved along its scale to a new point nearer G. In other words, the slider D is moved along its scale until it corresponds to the

known temperature of the cold junction, and then the potentiometer is balanced by moving the slider G. The readings of G will then give the temperature of the hot junction directly.

The same results will be obtained if another slide wire upon which D bears is placed in parallel with the slide wire of G, as shown in Fig. 4. It is such a slider wire, with a temperature scale fixed upon it, that forms the manually operated cold junction compensator.

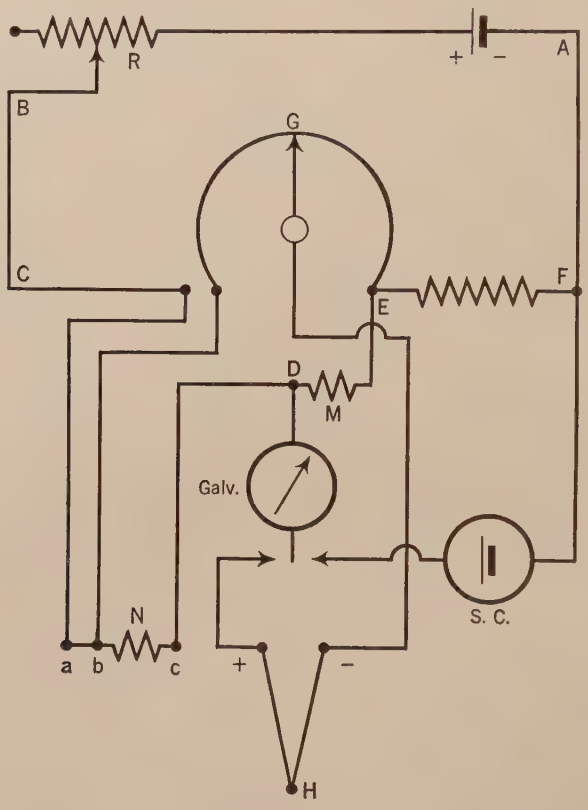

Fig. 6

It should be noted that the effect of moving the contact D, Fig. 4, is either to increase N and decrease M, or to decrease N and increase M; in other words, the ratio between N and M is varied. In Leeds & Northrup indicators and recorders employing the automatic cold junction compensator, the ratio of N to M is varied automatically, in the following manner:

The point D, Fig. 5, is mechanically fixed; on one side of D is the

constant resistance coil M, on the other the nickel coil N. N is placed at or near the cold junction of the thermocouple. Nickel has a high temperature coefficient (that is, its resistance changes about 0.25% for every degree F.) and the electrical proportions of M and N are such that the resistance change of N, as it varies with the temperature of the cold junction, has practically the same effect upon the balancing potential between D and G that the movement of the point D has in the hand-operated compensator of Fig. 5.

Fig. 6 shows a modification of Fig. 5 to meet the condition where the cold junction of the thermocouple is to be located at some point distant from the measuring instrument.

APPENDIX III

SOME PROPERTIES OF COMMON METALS

Metal	Color	Atomic Weight	Specific Gravity	Specific Heat at 0 deg. Cent.	Electrical Conductivity (Silver at 0 deg. Cent. = 100)	Melting Point, °C.
Aluminum	Tin-white	27.0	2.70	0.222	57	659
Antimony	Silver-white	120.2	6.697	0.04864	4	630
Arsenic	Steel-gray	74.96	5.727	0.083	5	850
Barium	Yellow-white	137.37	3.78	0.05	.....	850
Beryllium	Steel-colored	9.08	1.85	0.3756	.....	1280
Bismuth	White	209.0	9.759	0.0285	1.3	271
Cadmium	Blue-white	112.4	8.65	0.0546	20	321
Calcium	Silver-white	40.07	1.54	0.1704	18	810
Cerium	Steel-gray	140.25	6.82	0.04479	.....	640
Chromium	Grayish-white	52.0	6.92	0.1053	.....	1615
Cobalt	Steel-gray	58.97	8.71	0.1084	15	1480
Copper	Reddish-yellow	63.57	8.93	0.0939	94	1083
Gold	Yellow	197.2	19.3	0.0316	67	1063
Iridium	Gray	193.1	22.42	0.0317	.....	2350
Iron	Grayish-white	55.84	7.88	0.11012	17	1530
Lead	Blue-gray	207.2	11.34	0.02925	7.2	327.4
Magnesium	Silver-white	24.32	1.75	0.25	34	651
Manganese	White-gray	54.93	7.42	0.1217	.....	1230
Mercury	White-gray	200.6	13.6	0.0333	1.5	−39
Molybdenum	Dull Silver	96.0	10.3	0.0659	26.8	2620
Nickel	White	58.68	8.9	0.10836	20.5	1452
Palladium	White	106.7	11.4	0.0582	.....	1550
Platinum	White	195.2	21.5	0.0317	13.5	1755
Rhodium	Bluish-white	102.9	12.4	0.05803	.....	1950
Selenium	Steel-gray	79.2	4.8	0.08	Varies	218.5
Silver	White	107.88	10.53	0.0555	100	960.5
Tantalum	Iron-gray	181.5	16.64	0.035	.....	2850
Thorium	Grayish-white	232.4	12.16	0.0276	.....	1700
Tin	Silver-white	118.7	7.3	0.056	11.3	232
Titanium	Dark-gray	48.1	4.5	0.0978	.....	1800
Tungsten	Steel-gray	184.0	19.3	0.035	30.1	3370
Vanadium	Light-gray	51.0	6.0	0.125	.....	1720
Zinc	Bluish-white	65.37	7.14	0.0906	25.5	419.4
Zirconium	Gray	90.6	6.4	0.0662	.....	1700

REFERENCE INDEX

Aluminum Company of America, 152
American Society for Steel Treating, Trans. Nov. 1929, 113
Anderson: The Metallurgy of Aluminum and its Alloys, 152, 161

Bausch & Lomb Optical Co. Catalogues, 3
Bell Telephone Laboratories, Bull. B-109-1, Jan. 1925, 196
Bull. B-187, March 1926, 196
Bull. B-200, July 1926, 196
Bull. B-241, May 1927, 196
Brady: Journal Institute Metals, 28; 369 (1922), 48
Bullens: Steel and its Heat Treatment, 64, 81, 96, 106
Bureau of Aeronautics, Navy Dept., Tech. Note. 136, Properties and Heat Treatment of Duralumin in the Construction of Aircraft, 161
Bureau of Standards Circular 7, Pyrometer Testing and Heat Measurements, 53
Bureau of Standards Bull. 76, Aluminum and its Light Alloys, 161
Bureau of Standards Bull. Scientific Paper 347, Heat Treatment of Duralumin, 161
Bureau of Standards, Tech. Paper 170, Pyrometric Practice, 53
Burgess: High Temperature Measurements, 53

Campbell, Columbia University, 2
Clark: Applied X-rays, 213

Desch: Metallography, 29

Fry: Krupp Co. of Germany, 113

Greaves and Wrighton: Practical Microscopical Metallography, 3, 118, 131, 135, 146, 173
Green: American Institute Min. and Met. Eng. J., Feb. 1925, 48
Guillet and Portevin: Metallography and Macrography, 29, 64, 75, 118, 131, 143, 167, 173
Gulliver: Metallic Alloys, 14, 23, 29, 118, 131, 135, 143, 146, 167, 173, 178
Guthrie: Trans. American Society Steel Treating, Jan. 1925, 196
Guthrie: Trans. American Society Steel Treating, March 1925, 196

Jeffries and Archer: The Science of Metals, 48, 118, 126, 135, 173
Johnson: Materials of Construction, 118, 126

Killefer: Ind. and Eng. Chemistry J., June 1926, 213

Leeds & Northrup: Bulletin 866-A, 57
Leitz & Co. Catalogues, 3, 14
Lester: J. Society Automotive Engineers, Aug. 1927, 213
Lester: Trans. American Society Steel Treating, Nov. 1924, 213

Machlet: American Gas Furnace Co., 113

Norton: Tech. Eng. News-Record, October 1926

Portevin: J. Institute of Metals 29, 239 (1923), 48
Price and Davidson: American Institute Metals, Sept. 1916

Rosenhain: Introduction to Physical Metallurgy, 184

Sauveur: Metallography and Heat Treatment of Iron and Steel, 3, 14, 19, 57, 64, 75, 81, 96, 106

Williams and Homerberg: Principles of Metallography, 14, 19, 23, 75, 96, 113, 126, 131, 135, 146, 152, 173

ILLUSTRATION INDEX

A

Admiralty metal, 134, 193
Aero valve steel, 195
Alclad 17ST, 160
Alcumite, 151
Aluminum, 35, 157
  X-ray pattern of, 232, 235
Aluminum alloys
  Al-bronze, 150
  Al-bronze eutectic, 52
  Al-manganese, 159
  Al-manganese-magnesium, 177
  Al-silicon, 159
  Al-Si eutectic, 52
  Al-Zn bronze, 52
  17ST, 158
  No. 12, 159
  No. 43, 159
  No. 122, 158
  No. 195, 160
Aluminum alloy propeller blade, 195
Antimony, 34, 37,
Antimony lead eutectic, 51
Antifriction metal, 172
Armco iron, 70
Armor plate, 194

B

Babbitt, 171
Bausch & Lomb
  binocular microscope, 10
  metallurgical microscope, 10
  objectives, 5
Bearing
  babbitt, 171
  Frary, 171
  Navy antifriction, 172
  plastic bronze, 171
  steel roller, 172
  Cu-Pb, 171
  Cu-Sn, 170
  Pb-Sb, 170
  Pb-Sn, 170
  Sb-Sn, 170
Binocular microscope, 10
Bismuth, 33
Bismuth-lead eutectic, 51
Bismuth-tin eutectic, 51
Boiler steel, 191, 192, 193
Boiler tube, 191, 192, 193
Boiler plate, welded joint, 38
Bolt head, 46
Brass,
  10% Zn, 122
  20% Zn, 122
  30% Zn, 122
  40% Zn, 123
  48% Zn, 123
  55% Zn, 123
  annealed, 128
  brazed joint, 38
  cast, 37
  common, 134
  Muntz metal, 134
  Naval, 134
  properties of, 125
  rolled, 128, 130
Brass distilling condenser tube, 181
Brazed joint
  in brass, 38
  in boiler plate, 38
  in condenser tube, 181
  in steel, 183
Bronze
  5% Sn, 139
  15% Sn, 139
  27% Sn, 139
  30% Sn, 139
  80% Sn, 139
  aluminum, 150
  Al-Zn, 52
  composition "G," 150
  delta eutectoid, 52, 140
  effect of heat treatment, 145
  manganese, 134
  phosphorus, 150, 151
  plastic, 171
  V-Mn, 151
  zinc, 150

C

Cadmium-tin eutectic, 51
Calibration curve, thermocouple, 56
Case-hardening, 108, 110, 112
Cast iron, 79, 80
  nickel, 105
  Ni-Cr, 105
Cast steel, 95
Charcoal iron, 102
Chromium-nickel-steel turbine blade, 190
Chromium-vanadium-steel crankshaft, 192
Common brass, 34
Compensating eyepiece, 5
Composition "G" bronze, 150
Condenser tube, brass, 193
Condenser tube, brazed, 181
Constantan, 176
Cooling curves, 26
  eutectic, 26
  pure metal, 26
  pure metal plus eutectic, 26
Copper, 122
Copper, Dawson, 150
Copper-magnesium casting, 177
Copper-tin alloys, properties of, 142
Copper-tin equilibrium diagram, 141
Copper-zinc alloys, 122, 123
Copper-zinc equilibrium diagram, 124
Crankshaft, Cr-V, 192
Crankshaft, airplane engine, 191
Crankshaft, steel, 191

D

Dawson hardened copper, 150
Delta eutectoid, bronze, 140
Diffraction apparatus, X-ray, 218
Duralumin, 157, 158, 176, 195
  physical properties of, 165
Duriron, 105

E

Electrolytic iron, 70
Eutectic, 52
  Al-bronze, 52
  Al-Si, 52
  Bi-Pb, 51
  Bi-Sn, 51
Eutectic, Cd-Sn, 51
  iron phosphide, 51
  Pb-Sb, 51
  Sn-Pb, 51
  Sn-Zn, 51
Eutectoid,
  delta bronze, 52, 140
  pearlite, 52
Everdur, 150
Eyepiece, 5
  Huygenian, 5
  compensating, 5

F

Frary metal, 171

G

Gray cast iron, 79
Gun metal, 151

H

Huygenian eyepiece, 5

I

Illuminator, 4, 8
  vertical, 4, 8
  oblique, 4
Iron, Armco, 70
  charcoal, 102
  electrolytic, 70
  gray cast, 79
  iron-carbon, properties of, 74
  iron-carbon thermal equilibrium diagram, 73
  iron-nickel, cast, 105
  iron-nickel-chromium, cast, 105
  iron-silicon alloy, 102
  malleable cast, 80
  phosphide eutectic, 51
  pig, 79
  stainless, 104
  white cast, 80
  wrought, 17, 69
  X-ray pattern of, 231, 232

L

Lead-antimony eutectic, 27, 51
Lead-antimony series of alloys, 27, 28
  100% Pb, 27
  92% Pb, 27
  87½% Pb, 27
  75% Pb, 27
  50% Pb, 28
  25% Pb, 28
  10% Pb, 28
  0% Pb, 28
Lead-bismuth eutectic, 51
Lead-dendrite, 33
Lead-tin eutectic, 51
Lead-zinc ingot, 42
Leeds & Northrup potentiometer circuit, 63
Leeds & Northrup sample holder, 63
Leitz micrometallograph, 11, 12
Leitz microscope, 9
Leitz objectives, 5

M

Magnolia metal, 43
Malleable cast iron, 80
Manganese bronze, 134
Micrometallograph, 11, 12
Microscope
  Bausch & Lomb, 10
  binocular, 10
  Leitz, 9
Monel metal, 176

N

Naval brass, 134
Navy antifriction metal, 72
Nickel, 76
Nickel iron, 102
Nickel steel propeller shaft, 190, 192
Nickel steel stern tube shaft, 190
Nitralloy, 117
Nitrided steels, 115, 116, 117

O

Objectives
  achromatic, 5
  apochromatic, 5
Objectives
  Bausch & Lomb, 5
  Leitz, 5

P

Pearlite eutectoid, 52
Phono-electric trolley wire, 150
Phosphor bronze, 150, 151
Photomicrography, high power, 201, 212
Pig iron, 79
Potentiometer, 239, 240, 241, 242, 243, 244
Potentiometer circuit, Leeds & Northrup, 63
Propeller shaft, 191, 192

R

Radiograph
  of air bomb casting, 225
  of steel castings, 226, 227, 228, 229, 230, 231

S

Silicon electric steel, X-ray pattern of, 234
Silicon zirconium steel, 105
Slag in wrought iron, 69
Solder, Sn-Pb, 177
Soldered iron joint, 183
Spectrometer, X-ray, 218
Stainless iron, 104
Stainless steel, 104
Steel,
  aero-valve, 104, 195
  airplane engine crankshaft, 190
  boiler, 191
  B.O.H., Cr-V, 191
  burnt, 194
  case-hardened, 43, 108, 110, 112
  casting, 95, 192, 224
  corrosion-resisting, 104
  crankshaft, 191
  Cu-Mo, 102
  extra hard, 71
  fracture, 84, 85, 93
  fiber pattern, 235
  hard, 71

Steel,
hardened, 88, 89
heat-treated, 88, 89, 92
I-beam, 47
manganese, 103
medium, 71
mild, 71
Ni-Cr, Mo, 103
Ni-Mn, 103
Ni-V, 103
nitralloy, 117
nitrided, 115, 116, 117
propeller shaft, 191
radiographs of, 226, 227, 228, 229, 230, 231, 233
rivet, 190
S.A.E. 1025, 190
semi-hard, 71
sheared, 44
Si-Zr, 105
soft, 70
stainless, 104
tool, 193
twisted, 45
very hard, 71, 72
Stainless iron, 105
Stainless steel, 104
Strain in metal, 235

T

Tensilite, 151
Thermal equilibrium diagrams, 26
of Cu-Sn, 124
of Cu-Zn, 124
of Fe-C, 73
of Pb-Sb, 26
Thermocouple, calibration curve, 56
Tin, 37, 117
Tin-bismuth eutectic, 51
Tin-cadmium eutectic, 51
Tin-lead eutectic, 51
Tin-zinc eutectic, 51
Tobin bronz, 134
Tool steel, 193
Transformation point curves, 61, 62
Transformer iron, 102
Turbine blade, 190

W

Welded joint in boiler plate, 38
Welded link of chain, 38
Welded Pb-Sb alloy, 181
Welded steel plate, 181, 182
Welded wrought iron joint, 38
Welds, X-ray patterns, 236
White cast iron, 80
White metal, 176
Wrought iron, 18, 69
Wrought iron bent, 43
Wrought iron safety valve stud, 194
Wrought iron, slag in, 69

X

X-ray penetration curves, 219
X-rays, 216
pattern of aluminum, 232, 235
pattern of cast steel, 233
pattern of iron, 231, 232
pattern of Si-electric steel, 234
pattern of welds, 236
spectrometer, 218
tube, 217

Y

Y-alloy, 177

Z

Zinc, 36, 37, 122
Zinc, copper alloys, 122, 123
Zinc ingot, 41
Zinc-lead ingot, 42
Zinc-tin eutectic, 51

SUBJECT INDEX

A

Abrasives, 14
Achromatic objectives, 4
Acicular needles, 197
Admiralty metal, 119, 132
Admiralty metal condenser tube, 188
Aero valve steel, 99, 100, 189
Aging, 162
Airplane engine crankshaft, 185
Alclad, 155
Alcumite, 148
Allotriomorphic, 65
Alloys, 1
  compounds, 1
  eutectics, 1
  eutectoids, 1
  examination of, 14
  pure metal, 1
  solid solutions, 1
  structural elements, 1
  structure of, 2
Alpha brass, 119
Alpha iron, 64
Alumina, 15
Aluminum, 31, 152, 153
Aluminum alloy propeller blade, 189
Aluminum alloys,
  Alclad 17ST, 155
  duralumin, 153, 161, 174, 189
  manganese-magnesium, 174
  manganese, 154
  silicon, 155
  17ST, 154
  No. 12, 154
  No. 43, 155
  No. 122, 154
  No. 156, 195
  Y-alloy, 177
Aluminum bronze, 148
Aluminum bronze eutectoid, 49
Aluminum-silicon eutectic, 50
Aluminum-zinc bronze, 49
American ingot iron, 65
Ammonia, 113
Ammonium hydroxide, 15
Amorphous carbon, 76
Antimony, 23, 31
Apochromatic objectives, 4
Arc lamp, 13
Arc light, 10
Armco iron, 65, 197
Armor plate, 188
Atomic weights, 246
Austenite, 82, 83, 90, 94, 197
Automatic cold junction compensator, 242
Axles, 66
Azo, 20

B

Barium carbonate, 39, 106
Base metal thermocouple, 53
Bausch & Lomb objectives, 5
Bearing metals, 167, 168, 169
  Cu-Sn, 167
  Cu-Pb, 169
  Pb-Sb, 167
  Pb-Sn, 168
  Sb-Sn, 167
  babbitt, 168
  Frary metal, 169
  Navy antifriction, 168
  plastic bronze, 169
  steel roller bearing, 169
  theory of, 167
Bismuth, 30, 48
Bismuth-lead, 48
Bismuth-tin, 48
Black heart malleable cast iron, 77
Blowholes, 15
Boiler plates, 66, 187
Boiler steel, 186
Boiler tube steel, 186
Boiler tubes, 66, 187
Bolts, 66
Bomb, air, 219
Brass, 16, 31
  character of, 118

Brass, effect of cold rolling, 129
effect of composition, 118
effect of heat treatment, 126
effect of mechanical working, 126
properties of rolled brass, 129
Cu-Zn alloys, 118
10% Zn, 119
20% Zn, 119
30% Zn, 119
40% Zn, 119
48% Zn, 119
50% Zn, 119
55% Zn, 119
Brass alloys, 131, 132
aluminum in, 131
common, 132
iron in, 131
lead in, 131
manganese in, 131
Muntz metal, 132
Naval, 132
nickel in, 131
pipe, 132
spring temper, 129
theory of, 131
tin in, 131
Tobin, 132
Brass distilling condenser tube, 188
Brass pipe, 132
Brazed joint in boiler plate, 31
Brazed joint in brass, 31
Brazing, theory of, 178
Brinell hardness testing machine, 106
Broadcloth, 15
Bromide, 20
Bronze, 118, 135, 136, 137, 138
alpha, 137
beta, 138
delta, 138
epsilon, 138
gamma, 138
5% Sn, 135
15% Sn, 135, 136
27% Sn, 136
30% Sn, 136
80% Sn, 136
effect of composition, 135
effect of heat treatment, 143
pipe fittings, 135
theory of, 135
Bronze alloys, 146, 147
aluminum in, 146
antimony in, 146
arsenic in, 146
manganese in, 146
nickel in, 146
phosphorus in, 146
silicon in, 146
zinc in, 146
Bronze, composition "G," 147
Bronze delta eutectoid, 137
Burned steel, 189

C

Cadmium-tin eutectic, 49
Calibration of thermocouple, 53
Camera, 9, 10
Car wheels, 67
Carbon, 13
Carburization, 106
theory of, 106
Carburizing steel, 106, 107, 108, 109, 110, 111
Case, 106
Case-hardening, 106
Cassette, 216
Cast irons, 68, 75, 76
Gray cast iron, 75
malleable cast iron, 75
mottled cast iron, 75
white cast iron, 75
Casting molds, 23
Cast steel, 187
Cavities, 15
Cedar wood oil, 7
Cementation, 106
Cementite, 15, 66, 67, 68
Charcoal, 39, 106
Charcoal iron, 97
Chemical compounds, 1
Chemical heterogeneity, 29
Chromatic aberration, 4
Chrome-vanadium crankshaft, 186
Chromium, 96
Chromium steels, 96
Chromium-vanadium steels, 185
Cold junction, 53
Collimator lens, 10
Color fringes, 5

Color of metals, 246
Combined carbon, 76
Common brass, 132
Condenser, 7
Constantan, 173
Coolidge X-ray tube, 216
Cooling curves, 23, 26
  of eutectic, 26
  of metal plus eutectic, 26
  of pure metal, 26
Copper, 97, 118
Copper-manganese casting, 175
Copper-molybdenum steel, 97
Copper steels, 97
Core, 106
Cored crystals, 2
Cored structure, 119
Corrosion-resisting steel, 99
Cracks, 15
Critical points, 57
Critical range, 82
Crystal skeletons, 30
Crystallites, 30
Crystalline heterogeneity, 30
Cyco paper, 21

D

Dawson hardened copper, 148
Decalescence, 57
Defects in metals, 184
Delta eutectoid, 49
Delta eutectoid in bronze, 137
Dendrite, 2, 30
Dendritic structure, 119
Developer, 19
Dies, 66, 67
Difference couple, 58
Difference method, 58
Direct-time-temperature method, 57
Double thermocouple holder, 57
Drills, 67
Dry plates, 19
Duralumin, 153, 161, 174, 189
  analysis of, 161
  character of, 161
  effect of heat treatment, 161
  properties of, 166
  special duralumins, 161
  zinc duralumins, 161
Duriron, 100

E

Electric resistance furnace, 53
Electrical conductivity of metals, 246
Electrolytic iron, 65
Etching, 14, 237
Etching reagents, 237, 238
  for aluminum and its alloys, 237
  for Au, Ag, Pt and their alloys, 238
  for copper and its alloys, 237
  for iron and steel, 237
  for lead and its alloys, 237
  for magnesium and its alloys, 238
  for nickel and its alloys, 237
  for tin and its alloys, 238
  for zinc and its alloys, 238
Etching reagents, chemicals, 237, 238
Eutectic, 1, 23, 48
Euctectoid, 1, 48, 66
Eutectoid steels, 68
  hyper-euctoid, 68
  hypo-eutectoid, 68
Everdur metal, 147
Extra hard steels, 67
Eyepieces, 5, 6
  compensating, 5, 6
  Huygenian, 5, 6

F

Failure in metals, 184
Ferric chloride, 15
Ferrite, 15, 64, 68
Fiber structure, 221
Fibering, 221
Filter, 10
Flaws, 15
Flourescent screen, 214
Flourite apochromatic objective, 4
Focusing glass, 10
Fusion welding, 178
  electric, 178
  gas, 178
  thermit, 178

G

Galvanometer, 57
Gears, 66, 135
Germination, 184
Glycerol, 100

Grain, 30
Graphite, 15, 76, 77
Graphitic cast iron, 75
Gray cast iron, 75, 76
Grinding, 14
Gun castings, 132, 220
Gun jackets, 66
Gun metal, 148

H

Hard steels, 67
Hardened steels, 86
Heat-treated steels, 81
High power metallography, 196
  theory of, 196
Hot junction, thermocouple, 53
Hull powder method, 221
Hydrogen peroxide, 15
Hyper-eutectoid, 67
Hypo-eutectoid, 66
Hypo fixer, 19
Hysteresis, 59

I

I-beam, 44
Illuminator, vertical, 7, 8
Internal strain, 222
Inverse rate method, 57
Iodine, 32
Iris-diaphragm, 12, 13
Iron, 68
Iron, pig, 65
Iron-carbon, thermal equilibrium diagram, 68
Iron-carbon alloys, physical properties of, 68
Iron phosphide eutectic, 49
Iron silicate, 100
Iron sulfide, 77

J

Junctions, 53
  cold, 53
  hot, 53

K

Kenotrons, 216

L

Laminated pearlite, 82
Lantern slides, 20
Lathes, 67
Laue method, 215
Lead, 23, 30
Lead-antimony eutectic, 49
Lead-bismuth, 48
Lead-tin, 48
Leitz & Co., 5
Lens, 5
Lens, collimator, 10
Lens, plano-convex, 5
Light, 10
  arc, 10
  monochromatic, 10
Light filter, 10
Liquid hardener, 20

M

Macroscopic examination, 29
Magnolia metal, 39
Malleable cast iron, 66, 76, 77
Manganese, 97
Manganese bronze, 132
Manganese nickel, 174
Manganese steel, 97, 98
Manganese sulfide, 77
Martensite, 82, 83, 86, 90, 94, 197
Mechanical heterogeneity, 44
Medium steel, 66
Melting points of metals, 54
Metals, properties of, 246
Metallography, 1
Metallography, X-ray, 213
Metalloid, 48
Microscope, 3
  Bausch & Lomb, 8
  binocular, 11
  Le Chatelier, 10
  Leitz, 8
  use of, 3
Micrometallograph,
  description of, 3, 9, 10
  Leitz, 10, 11, 12
Molybdenum, 47
Molybdenum steels, 97
Monel metal, 73
Muntz metal, 14, 132

N

Naval brass, 132
Negatives, 20
Neuman lines, 98
Neutral body, 57
Nickel, 58, 96, 173, 245
Nickel cast iron, 101
Nickel-chrome cast iron, 101
Nickel-chromium-molybdenum steel, 98
Nickel iron, 97
Nickel manganese steel, 98
Nickel steels, 96
Nickel-vanadium steel, 98
Nitralloy, 113
Nitric acid, 15
Nitriding, 113
  microstructure of, 113, 114
  theory of, 113
Noble metal thermocouple, 53
Non-ferrous alloys, 173

O

Objective, 4, 7
Ocular, 4, 5
Oil immersed objective, 7
Open-hearth furnace, 65
Oxides, 15, 64
Oxy-acetylene, 32

P

Pearlite, 16, 64, 66, 67, 68, 87, 90, 91
Pearlite eutectoid, 49
Phonoelectric trolley wire, 146
Phosphor-bronze, 147, 148
Phosphorus, 49, 68, 76
Photography, 19
  azo, 20
  bromide, 20
  cyko, 21
  developer, 19
  dry plates, 19
  hypo fixer, 19
  velox, 20
Photomicrography, 4, 196
Picric acid, 15
Pig iron, 49, 65, 76
Pipe, 39
Plano-convex lens, 5
Platinum-iridium thermocouple, 58
Platinum-rhodium thermocouple, 56
Polishing, 4
Potentiometer, 23, 53, 239
Powder method, 215
Propeller shaft, 184, 186
Properties of common metals, 246
Pure iron, 64
Punches, 67
Pyrometer, 53
Pyrometer potentiometer, 215

Q

Quartz objectives, 197
Quartz oculars, 197

R

Radiography, 213, 214
Rails, 66
Reamers, 67
Recalescence, 57
Reflecting glass plate, 13
Reflecting prism, 13
Reinforcing bars, 66
Retardations, 57
Rivet head, 44
Rivet steel, 185
Rivets, 66
Rockwell hardness, 86, 87

S

Semi-hard steel, 67
Shafts, 66
Sheared steel, 44
Shore scleroscope, 106
Silicates, 15
Silicon, 68, 76, 97
Silicon steels, 97
Silicon-zirconium steels, 100
Slag, 15, 64
  oxide, 64
  phosphide, 64
  silicates, 64
Slip planes, 98
Sodium picrate, 77
Sodium thiosulfate, 20
Soft steel, 66
Soldering, theory of, 178

Solid solutions, 1
  definition of, 1
  properties of, 1
Sorbite, 82, 83, 86, 87, 90, 94
Sorbitic pearlite, 82, 166
Specific gravity of metals, 246
Specific heat of metals, 246
Spherical aberration, 4
Spheroidal cementite, 67
Spring steel, 67
Spring temper brass, 129
Springs, 67
Stainless iron, 99, 189
Stainless steel, 99
Steam drum, 187
Steel, 64, 65, 68, 81, 82, 86
  drawn, 86
  fracture of, 81
  hardened, 86
    drawn, 86
  metallography of heat treated, 81, 82
  microscopic examination of, 81
  tempered, 86
Steel crankshaft, 186
Stern tube shaft, 185
Structure, 5, 30
  chemical heterogeneity, 39
  crystalline heterogeneity, 30
  mechanical heterogeneity, 44
Sulfides, 15

T

Tensilite, 148
Thermal critical points, 57
Thermal equilibrium diagrams, 23, 26
Thermocouple, 23, 56, 240
  Pt, Pt-Ir, 58
  Pt, Pt-Rh, 56
Thermocouple, calibration of, 53
Tin, 31, 174
Tin base bearing metal, 137
Tin-bismuth, 48
Tin-lead, 48
Tin-zinc eutectic, 48
Tobin bronze, 132
Tool steel, 67, 188
Tools, 66, 67
Torpedo tube casting, 132
Transformation points, 57
Transformer iron-silicon alloy, 98
Troostite, 82, 83, 86, 87, 90, 94, 198
Tungsten, 97
Tungsten steels, 97
Turbine blade, 185

U

Ultra microscope, 196
Ultra-violet light, 197
Ultra-violet microscope, 197

V

Vanadium, 97
Vanadium-manganese bronze, 148
Vanadium steels, 97
Very hard steels, 67

W

Welding, 178
  forge, 178
  fusion, 178
  pressure, 178
  theory of, 178
Welds, 32, 222
  joint in boiler plate, 32
  link in chain, 32
  wrought iron joint, 32
Weston standard cell, 241
White cast iron, 75, 77
White metal, 174
Wire, 66
Wood charcoal, 39
Wratten filter, 19
Wratten safe light, 20
Wrought iron, 14, 32, 39, 64, 188

X

X-radiation, 213
X-ray diffraction tests, 214, 215
X-ray diffraction patterns, 217
X-ray crystallography, 223
X-ray metallography, 213
X-ray spectrometer, 217

X-ray tube, 216
X-rays, 213, 214

Y

Y-alloy, 177

Z

Zinc, 31, 39, 118
Zinc bronze, 147
Zinc-lead ingot, 39
Zirconium nitride, 100
Zirconium sulfide, 100